Protecting the environment from contamination with barrier systems: advances and challenges

Protéger l'environnement de la contamination avec des systèmes de barrière : avancées et défis

R. Kerry Rowe
Geoengineering Centre and Queen's-RMC, Dept. of Civil Engineering, Queen's University, Kingston, Ontario, Canada.

Stephan Jefferis
Environmental Geotechnics, Banbury, UK and Dept. of Engineering Science, University Oxford, UK.

With sections contributed by:

Fady B. Abdelaal
Geoengineering Centre and Queen's-RMC, Dept. of Civil Engineering, Queen's University, Kingston, Ontario, Canada

Andrea Dominijanni
Department of Structural, Geotechnical and Building Engineering, Politecnico di Torino, Torino, Italy

Kelvin Legge
Department of Water and Sanitation, Pretoria, South Africa

Ennio M. Palmeira
University of Brasília, Brasília, Brazil

John Scheirs
ExcelPlas, Highett, Victoria, Australia

Charles D. Shackelford & Joseph Scalia IV
Department of Civil and Environmental Engineering, Colorado State University, Fort Collins, Colorado, USA

Tony L.T. Zhan
Department of Civil Engineering, Zhejiang University, Hangzhou, China

Craig H. Benson
School of Engineering, University of Virginia, Charlottesville, Virginia, USA

Abdelmalek Bouazza
Monash University, Clayton, Victoria, Australia

Gemmina Di Emidio
Ghent University and Pollux Consulting, Ghent, Belgium

Jeffrey C. Evans
Bucknell University, Lewisburg, Pennsylvania, United States

Evelina Fratalocchi
Facoltà di Ingegneria, Università Politecnica delle Marche via Brecce Bianche Ancona

Maria G. Gardoni,
Federal University of Minas Gerais, Belo Horizonte, Brazil

Takeshi Katsumi
Graduate School of Global Environmental Studies, Kyoto University, Kyoto, Japan

Mario Manassero
Department of Structural, Geotechnical and Building Engineering, Politecnico di Torino, Torino, Italy

Denys Parra
Anddes Perú and National University of Engineering, Lima, Peru

ABSTRACT: The state-of-the-art for barriers systems control of pollution migration and hydraulic structures including liner systems for landfills, mine waste, and dams/lagoons are discussed along with some comments on current significant environmental issues. Recent research on geomembranes, geosynthetic clay liners, and composite liners and the practical implications are discussed. The need to design taking account of the interactions between the liner system components is highlighted. Regional differences relating to environmental geotechnics of municipal solid waste and mining waste and the implications of differences in regulations and climate are discussed. Vertical barrier systems may be regarded as mature technologies and research funding is much more limited. A bibliography of key papers on cut-off walls has been compiled. It is recognized that major changes to cement-bentonite formulations will be necessitated by the drive to reduce carbon footprints together with the dwindling availability of pulverised fuel ash and blastfurnace slag. The implications for environmental geotechnics associated with recycled materials, waste minimization, and some overarching issues are discussed. The paper finishes with some thoughts about the future of environmental geotechnics and some concluding comments.

RÉSUMÉ : L'état de l'art des barrières pour le contrôle de la migration de la pollution et des structures hydrauliques, y compris les barrières pour les installations de stockage de déchets, les déchets miniers et les barrages / lagunes, est discuté avec quelques commentaires sur les problèmes environnementaux actuels importants. Des recherches récentes sur les géomembranes, les géosynthétiques bentonitiques et les étanchéités composites ainsi que les implications pratiques sont discutées. La nécessité de concevoir en tenant compte des interactions entre les composants de la barrière est soulignée. Les différences régionales relatives à la géotechnique environnementale des déchets solides municipaux et des déchets miniers sont discutées. Les systèmes de barrières verticales peuvent être considérés comme des technologies matures. Une bibliographie des principaux articles sur les murs d'étanchéité a été synthétisée. Il est reconnu que des changements majeurs dans les formulations ciment-bentonite seront rendus nécessaires par la volonté de réduire l'empreinte carbone. Les implications pour la géotechnique environnementale associées aux matériaux recyclés, à la minimisation des déchets et à certaines questions globales sont discutées. L'article se termine par quelques réflexions sur l'avenir de la géotechnique environnementale et quelques commentaires conclusifs.

KEYWORDS: GCLs, geomembranes, barrier systems, cut-off walls, slurry systems, cement- and soil-bentonite, recycled materials

1 INTRODUCTION

The last quarter of the 20th century saw a growing concern in many countries with the previous thoughtless "out of sight, out of mind" approach to waste disposal. This approach frequently involved the co-disposal of liquid hazardous waste, heavy metals, and municipal solid waste. To make matters worse, waste had often been disposed in worked-out sand and gravel pits without any liner with the mantra "dilution is the solution to pollution". After many decades of inappropriate waste disposal, the consequent impacts on the environment and human health became apparent. Awareness eventually triggered highly publicized removal of people from their homes and the closure of schools such as occurred in response to President Carter's declaration of two states of emergency at the infamous Love Canal site located in Niagara Falls, New York State, USA (Cohen et al. 1987; Colten and Skinner 1996; Phillips et al. 2007) and at Lekkerkerk in the Netherlands (Brinkmann 1981). Situations such as these and the identification of many "Superfund sites" in the USA prompted governments to develop regulations for waste management (e.g., The Resource Conservation and Recovery Act, RCRA, passed in October 1976 to address the increasing problems faced by the USA from the growing volume of municipal and industrial waste). Four primary consequences of the recognition of the potentially harmful effects of waste disposal practices were the recognition of the need to:

(i) classify and separate different types of waste (e.g., construction and demolition, municipal solid waste, hazardous waste, radioactive waste etc.);
(ii) design waste disposal facilities to minimize the risk of contaminant escape to the environment and remove past nuisances (e.g., fires, vector rodents, birds) associated with facility operations; and
(iii) contain and remediate past problems,
(iv) proactively consider and address potential future problems.

The last three of these four consequences fall within the realm of environmental geotechnics. Thus, this paper is divided into three parts. Part A deals with preventative environmental geotechnics (i.e., actions to prevent future pollution and addresses the second consequence above). Part B deals with remedial environmental geotechnics (actions to minimize the impact of past contamination) and addresses the third consequence above. Finally, Part C deals with some over-arching issues relating to future developments in environmental geotechnics and begins to address the fourth consequence above. Contributions on these three topics were sought from leading research groups across the World and their input has been integrated into this paper.

Preventative environmental geotechnics for waste management emerged from the need to develop better landfills for the disposal of hazardous and municipal solid waste. Since the early 1980s landfills have been at the forefront of the development of what we now know as geoenvironmental engineering and the more geotechnically focused area of environmental geotechnics. Regulations that were developed generally banned the disposal of liquid hazardous waste and required its solidification and stabilization in some manner before disposal in an engineered landfill. Early liner systems focused initially on the use of natural or compacted low permeability clay liners but soon also incorporated geomembranes to form composite liners. The development of geosynthetic clay liners (GCLs) and the paucity of suitable natural clays for compacted clay liners in many areas saw the adoption of GCLs as an alternative to compacted clay in composite liners.

With recognition of the risks of relying on only a single, albeit composite liner, for the disposal of hazardous wastes, the use of double composite liners with a leak detection/secondary leachate collection system became enshrined in many regulations.

Experience in the operation of these facilities and their monitoring, academic research, and innovations by manufacturers have substantially advanced the development of geomembranes and GCLs in the 21st century. Today's high density polyethylene (HDPE) geomembranes (GMBs) are much more sophisticated than those of the 1970s to late 1990s. The use of geomembranes has expanded to a range of products broadly defined as HDPE but with different resins and additive packages suitable for different applications. A similar situation applies with respect to linear low density polyethylene (LLDPE) and polyvinyl chloride (PVC). Thus, for important projects, the geomembrane needs to be selected for the specific end-use. Key issues and advancements concerning HDPE geomembranes are reviewed in §2.

In parallel with the growth in HDPE use in landfill applications, there was a growth in the use of bituminous geomembranes (BGMs) for lining canals. Success in this application has prompted consideration of their use in a range of other applications such as landfill covers, pond liners, and covers for mine waste. §3 explores BGMs 20 years into the 21st century.

Like HDPE geomembranes and BGMs, GCLs have advanced significantly, as has the range of applications for GCLs. Of the many types of GCL available, needle-punched GCLs with a layer of bentonite sandwiched between two geotextiles and held together by needle-punching have become dominant. However, they have also evolved with an extensive range of different products (one manufacturer alone produces 50 different GCLs). Differences include standard sodium bentonite and polymer amended bentonite, mass of bentonite, geotextile characteristics and mass, amount of needle-punching, and the presence or absence of a polyolefin layer (anything from 200 g/m² to 2000 g/m²) either applied in a molten state to form a coating or glued to the GCL to enhance the performance of the GCL. §4 discusses these advances with a particular focus on the use of enhanced bentonites.

Initially, leachate collection systems involved relatively primitive toe drains and French drains to allow leachate collection and minimize the escape of contaminated fluids to the environment. However, it was soon found that these systems experienced significant clogging and build-up in the leachate head (Rowe and Yu 2012). This prompted a movement to have blanket drains initially of pea gravel but clogging of these leachate collection systems still occurred (Fleming et al. 1999; Rowe and Yu 2010). The solution to this problem was the use of relatively coarse uniform gravel as a drainage layer. However, initial applications of the solution began to compromise the service life of geomembranes by increasing punctures and, arguably of more importance, inducing tensile strains that can become stress cracks in the future. Issues such as this began to raise awareness of the interactions between the barrier system components themselves, and between the components and the environment. §5 seeks to raise awareness of the importance of designing barriers as a system, carefully considering the many interactions and how they affect the system's overall performance.

Key contaminants of concern in developing most landfill regulations last century were chlorinated solvents, heavy metals, and metalloids. Regulations and modern waste management practices have substantially reduced the concentrations of these contaminants in the waste stream. Consequently, the predominant contaminants in modern municipal waste leachate are volatile fatty acids (from the biodegradation of organic waste) and salts (such as sodium chloride) with relatively trace amounts of the contaminants of primary concern in the last century.

Generally, people did not concern themselves with salt as a contaminant of concern. Very few regulations explicitly list chloride as a critical contaminant to be controlled by the landfill design. A notable exception is Regulation 232/98 (MOE 1998) in Ontario, Canada, which prescribes chloride as a significant critical contaminant. The technical experts formulating MOE regulations at the time were aware of the potential for both known unknowns and unknown unknowns. They recognized that chloride is one of the most mobile contaminants in landfill leachate and present at concentrations far above drinking water objectives. Thus, it was an excellent tracer and by keeping chloride release very low, we were also keeping other releases low. In 2022 we now recognize that landfill leachate contains many contaminants of emerging concern. These are predominantly very useful and widely used manufactured chemicals that were subsequently found to have potential health implications. These contaminants include per- and polyfluoroalkyl substances (PFAS), bisphenol-A (BPA), polybrominated diphenyl ether (PBDE), polychlorinated biphenyls (PCBs), and carbon nanoparticles. §6 discusses the implications of these contaminants for existing landfills and future landfills. Even with the banning or restriction on the production of many of these chemicals, they can be expected to be entering landfills and in landfill leachate for many decades to come.

While highly developed countries are struggling to deal with contaminants of emerging concern, a substantial proportion of the human population lives in less-developed countries, particularly in Asia, Africa, and South America. While there are some examples of well-developed regulations and practices in these regions, in large part in this century, they are still struggling with issues that more developed countries addressed last century. §7 explores these issues from the perspective of those living in Asia, Africa, and South America.

While landfills have been the focus of the developments and applications for barrier systems, the volume of waste generated by mining is enormous compared to the waste contained in landfills. Although there are notable exceptions, the mining industry has generally been far less concerned with environmental impact or even the risks to human life and property from mine waste than has been the case for municipal and hazardous waste facilities. This is particularly true in the less-developed parts of the world. For example, South America is a significant source of minerals. However, several recent tragic failures have forced insurance companies to pressure mining companies to pay more attention to the risks to human life and property and there is growing concern regarding their environmental impact.

The use of geosynthetics generally, and especially in barrier systems, has grown substantially this century even with the absence of appropriate regulations and/or the enforcement of regulations in many countries. §8 examines geosynthetic applications in mining. It notes the lack of regulations and standards relevant to the many facilities at high altitudes with steep side slopes and tailings storage facilities that pose a risk from liquefaction.

Remedial environmental geotechnics emerged from the need to clean up the problems such as those triggered by investigations of the landfilling of chemical waste at Love Canal (see the analysis of the social and technical issues set out in Mazur (1998)). Remediation of contaminated land has been and remains a preeminent issue in some areas/countries on which massive sums have been and are yet to be expended. However, although inputs for this state-of-the-art review were sought from researchers and practitioners from around the world, a notable gap in the responses received was on the clean-up of contaminated land. As a result, the lead authors are left with the impression that from an academic research perspective, contaminated land clean-up is either (a) regarded as a mature discipline where innovation is primarily by consultants and clean-up contractors and managed by regulators who, in many countries, now have substantial experience and powers under environmental regulations (though not always the necessary funding), or (b) research funding is largely limited to areas such as biomediated and bioinspired geotechnics.

Part B then considers the present state of research and practice for:

- vapour barriers used to minimize the impact of residual volatile organic compounds when redeveloping brownfield sites (§9).
- vertical barrier walls (cut-off walls) formed by slurry trench techniques. These are mature technologies with very few reported problems in service. The approach, therefore, has been to seek input from experts to identify significant issues on which a fuller listing of papers complements a brief discussion (§10).

It is unlikely that 40 years ago anyone would have predicted the path that has been taken by what is now the subdiscipline of preventative environmental geotechnics. Thus, it would seem foolish to try and predict where we will be in another 40 years. However, we can look forward a decade and Part C considers:

- increased pressures to recycle materials and some unintended consequences (§11),
- waste minimization (§12),
- other emerging issues (§13), and
- finally, some thoughts on the future of preventative environmental geotechnics as a discipline (§14).

Just as Covid-19 may change hard land use, global warming, and the current drive to eat less meat and become more vegetarian may significantly impact the use of greenspace. For example, about 70% of the land is managed by farming in the UK, and less than 10% is urban development. Reduction in the numbers of grazing animals may allow tracts of land to be returned to 'nature' (re-wilding) if not used for crops or unless someone is paid to manage them. Therefore, we must expect the growth of scrubland with a return to climax vegetation over a timescale measured in centuries. We must plan for this, and in particular, we need to be undertaking back-casting studies. If the future impacts of current plans seem unacceptable, then change is needed now and should not be deferred to when problems arise.

1.1 *Contaminating lifespan and service life*

An important consideration in this paper is the service life of the components of barrier systems and the overall service life of the system. Barrier systems should be designed to control contaminant escape to a negligible level or the ingress and egress of water or gases to an acceptable level. The contaminating lifespan of a waste disposal facility is, by definition, the period during which the barrier system must control contaminant escape to a negligible level (MOE 1998; Rowe et al. 2004).

The service life of a component of the barrier system depends on the material properties of that component and the environmental conditions that will cause it to fail. For example, for an HDPE geomembrane the critical property for containment is the stress crack resistance (SCR). When the geomembrane cracks extensively, it no longer serves its containment function and can be said to have reached its service life. However, whether the stress cracks occur depends both on the stress crack resistance that is remaining (a material property) and the tensile stresses applied to the geomembrane. Consequently, a geomembrane with a given stress crack resistance may have reached its service life in one application and not in another depending on the design and the consequent tensile stresses and strains within the geomembrane. Thus, when talking about a material characteristic in isolation it is better to use the term *time to nominal failure* to define when the material has reached a critical time in its life.

Often the *time to nominal failure* is taken to be the time when some engineering property of significance has reduced to 50% of the original or specified value. As the critical property (e.g., stress crack resistance for a geomembrane or hydraulic resistance for a GCL) reduces below its design value the likelihood of it reaching its service life increases. Thus, the service life of a component in a barrier system is related to the time to nominal failure but, in general, is not equal to the time to nominal failure.

For a good design, the service life will generally be longer than the time to nominal failure. For poor design and/or construction and/or operations the service life could be less than the time to nominal failure. It is important to keep this distinction in mind in discussions of material behaviour and service life.

Barrier systems are often designed recognizing that components may reach their service life before the contaminating lifespan of the facility is reached. A good design is one in which the other components of the system will then control the release of contaminants to an acceptable level. Thus, the service life of the system is when the barrier system can no longer control the release of contaminants to a negligible level.

1.2 *Notation*

This paper contains many symbols and terms that may be new to the reader. Key symbols are defined in the appendix "Notation". References in one part of this paper to a section another part of the paper are indicated by §.

PART A: PREVENTATIVE ENVIRONMENTAL GEOTECHNICS

2 EVOLVING HDPE FORMULATIONS AND MULTILAYERED GEOMEMBRANES

Over the past decade, there has been a substantial increase in the range of what are generically called 'HDPE geomembranes'. This includes new tailored resins developed to address issues and shortcomings identified with standard HDPE and multilayered geomembranes with white and conductive layers. This section seeks to make the reader aware of some of the materials presently available on the market as well as some of the challenges and insights that have been developed this century, notwithstanding the fact that most regulations or guidelines relating to HDPE geomembranes are still heavily rooted in what was known and available in the last century.

This sub-section will discuss the various polymers and additives used in the manufacture of HDPE geomembranes and the functional performance properties they confer.

2.1 *Polymers and additives used for manufacturing state-of-the-art HDPE geomembranes*

High density polyethylene (HDPE) geomembranes are the most widely manufactured and the most widely used polymeric liners in the geosynthetics industry. To ensure their long-term stability and durability (service life), HDPE geomembranes contain proprietary blends of specialized additives: antioxidants, stabilizers, carbon black, and chemicals to improve the base polymer's processing stability, welding stability.

The long-term service lifetime of HDPE liners is mainly dependent on the level and effectiveness of the additive package. The manufacturers do not disclose the additives they employ in their different HDPE geomembranes to the end-user. However, there is a body of technical knowledge regarding what constitutes good practice and best practice in the formulation of HDPE geomembranes.

2.1.1 *The Base Resin*

There is a large range of potential candidate base resins for manufacturing HDPE geomembranes. Over 100 different polyethylene resins are purported to be suitable for HDPE geomembrane production. However, prudent selection of the base polymer is required to achieve the correct balance of processability, mechanical properties, and perhaps most importantly the outstanding stress crack resistance (SCR) required for HDPE geomembrane long-term durability.

HDPE resin gain favour with the early use of geomembranes in landfill liners because its high crystallinity gave it very good chemical resistance. However, the Achilles heel of the high crystallinity of HDPE resin was its propensity to stress crack, which is cracking failure at a level of stress lower than the yield stress. For this reason, there has been a move away from the use of HDPE resin and the base resins used today for HDPE geomembranes are generally medium-density polyethylene (MDPE) with a fractional melt index (i.e., an MFI of less than 1 g/10 mins under 2.16 kg mass). The term HDPE is retained not because of the resin but because the density of the geomembrane once the carbon black is added to the resin falls into the category defined by ASTM as HDPE.

The designer needs to be judicious in the selection of the geomembrane resin to ensure long-term resistance to stress cracking which is an inherent property of the base resin and not the additive package. Table 1 shows some typical PE base resins used for HDPE geomembranes as well as some newer higher temperature capable polyethylene for raised temperature (PERT) resin grades.

In recent developments, there are some new additives such as diene terpolymer (DTP) from Exxon Mobil where just 3% by weight of DTP added to a geomembrane increases the NCTL-SCR from 1500 hours for additive-free resin to greater than to 3000 hours for the DTP blend.

2.1.1.1 *PERT Resins*

For higher temperature applications such as brine ponds or solar heating ponds, the base polymer chosen for the HDPE geomembrane should be a Polyethylene of Raised Temperature (PERT) resin that optimizes tie-chain concentration through the introduction of co-monomers. Example PERTs include Dowlex, Dow's Intrepid 2498 or Dowlex 2344 or LyondellBasell's Hostalen 4731B (a new-generation PERT resin).

2.1.1.2 *Recycled Polyethylene*

The virgin geomembrane base resin is often supplied to the geomembrane manufacturer in a pellet form which is then mixed with carbon black, antioxidants, and stabilizers in a carrier resin and "let down" into the formulation.

Regrind or rework flake/pellets (previously processed by the same manufacturer in-house but never used in the field) may be added to the extruder during melt processing without adverse effects. However, this contrasts with reclaimed, recycled, or post-consumer recycled material which should not, under any circumstances, be allowed in the geomembrane formulation.

Table 1. Typical PE base resins used for "HDPE" geomembranes

Name of Resin	Manufacturer	Comments
Marlex K306/K307	Chevron Phillips	Linear MDPE; Unimodal and broad MWD; the most widely used geomembrane resin worldwide
Borstar FB1350	Borealis	Linear MDPE; bimodal and broad MWD
Enable 3505	Exxon Mobil	Metallocene linear MDPE; Unimodal and narrow MWD
Daelim XP9000	Daelim, South Korea	Metallocene bimodal MDPE
Intrepid 2498 NT/2499 NT	Dow	Bimodal HDPE PERT resin
Dowlex 2344	Dow	New Generation PERT HDPE resin Ethylene-octene copolymer, produced in the proprietary solution process. It has a unique molecular structure with a controlled side-chain distribution, which provides excellent stress crack resistance properties
Total XRT70	Total, France	Hexene-based PERT copolymer resin
Eltex TUB220-RT	Ineos, Switzerland	Hexene-based PERT copolymer resin with narrow MWD
Hostalen 4731B	Lyondell Basell	New Generation PERT HDPE resin

2.1.2 *The Additive Package*

The additive package that is mixed with the geomembrane base resin is usually delivered to the processing extruder via a concentrate called a masterbatch. The masterbatch for an HDPE geomembrane application generally comprises the following essential ingredients:

- a resin carrier (usually a matched flow index MDPE or a higher flow linear low density polyethylene, LLDPE);
- a carbon black pigment of the correct particle size (typically 22-25 nm);
- a titanium dioxide pigment (for white geomembranes);
- a processing stabilizer such as a hindered phosphite
- a thermal stabilizer which comprises a primary antioxidant such as a hindered phenolic antioxidant;
- a ultra-violet radiation, UV, stabilizer such as a hindered amine stabilizer (HAS, formerly HALS) which also serves as a long-term thermal stabilizer;
- an acid neutralizer (to scavenge acidic residues from the PE catalyst); and
- a polymer processing aid (PPA) such as a fluorinated elastomer.

2.1.2.1 *Carbon Black*

Carbon black is added into geomembrane formulation for general stabilization purposes, particularly for ultraviolet-radiation screening, but it also has some free radical trapping capabilities. Therefore, it is generally added as a preformulated concentrate in pellet form. The "masterbatch" comprises a carrier resin with carbon black and possibly the antioxidants/stabilizers. The carrier resin should be the same as the host resin insofar as density and melt flow are concerned. However, sometimes higher flow carrier resins are used to ensure good mixing with the geomembrane base resin.

The acceptable level of carbon black content in an HDPE geomembrane is 2-3% of the total weight of the formulation.

It is critical that, in addition to the amount of carbon black used, the particle size is also carefully chosen and specified. Carbon blacks are classified by the primary size as classified in ASTM D1765. For instance, the commonly used N330, N550, and N660 grades have particle size ranges of 26-30 nm, 40-48 nm, and 49-60 nm, respectively.

The choice of carbon black matters! For example, the 60 nm N660 carbon black used in some geomembranes made in Asia is too coarse for optimum UV screening. N660 carbon black has been associated with failures from UV-related degradation. However, as carbon black particle size decreases, the specific surface area increases substantially. The smaller carbon blacks require more antioxidants/stabilizers to be added to the resin to compensate for the proportion of additives adsorbed by carbon black particles' high surface area. Since the carbon black for geomembranes needs to be of the correct particle size to impart optimum UV protection, the N330 grade is the most preferred for geomembranes. However, given the very small primary particle size of this carbon black, it is prone to agglomeration (Fig. 2.1), and thus, the extruder must provide good dispersive and distributive mixing capabilities to break down carbon black agglomerates, which can act as stress concentration points and initiate cracking (Fig. 2.2).

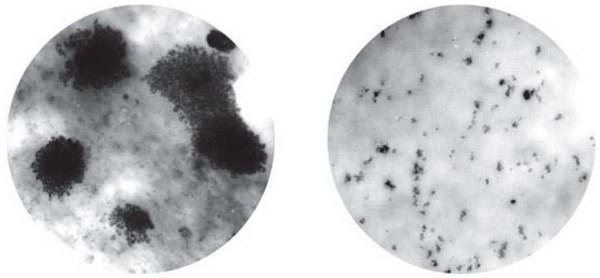

POOR DISPERSION OF CARBON BLACK IN HDPE NOTE AGGLOMERATES OF CARBON BLACK PRIMARY PARTICLES

WELL DISPERSED CARBON BLACK IN POLYETHYLENE

Figure 2.1 Photomicrographs showing poor carbon black dispersion on the left and good carbon black dispersion in HDPE on the right.

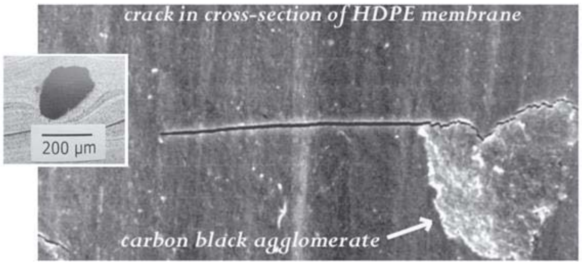

Figure 2.2 Stress crack initiated at a carbon black agglomerate in an HDPE geomembrane (inset with scale bar showing the size of the carbon black agglomerate).

2.1.2.2 *Titanium Dioxide*

White-surfaced HDPE geomembranes contain a concentrated titanium dioxide white pigment known as coated rutile. Since rutile has semi-conductor properties that can produce free radicals that can degrade the geomembrane when exposed to UV light, titanium dioxide particles are coated with a passivating barrier layer of alumina, silica, and/or zirconium. The better the coating, the lower the propensity to produce free radicals, reducing photoinduced degradation in the geomembrane. Thus, the titanium dioxide pigments of choice, known as 'durable' grade, have coherent passivating layers. The importance of using a durable grade of titanium dioxide in HDPE geomembranes is highlighted in Figure 2.3.

Since titanium dioxide is not as effective a UV screen as carbon black and not all the photocatalytic activity of titanium dioxide can be suppressed by the passivating coatings, white surface geomembranes generally contain very high levels of HAS up to twice that required in black HDPE.

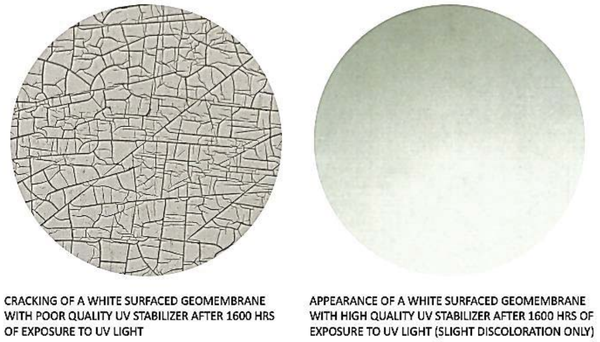
CRACKING OF A WHITE SURFACED GEOMEMBRANE WITH POOR QUALITY UV STABILIZER AFTER 1600 HRS OF EXPOSURE TO UV LIGHT

APPEARANCE OF A WHITE SURFACED GEOMEMBRANE WITH HIGH QUALITY UV STABILIZER AFTER 1600 HRS OF EXPOSURE TO UV LIGHT (SLIGHT DISCOLORATION ONLY)

Figure 2.3 Photomicrograph showing the surface of a white HDPE geomembrane on the left with the incorrect type of white pigment (not a properly coated rutile) and on the right HDPE with a well-selected durable coated rutile after exposed to 1600 hours UV.

2.1.2.3 *Primary Antioxidant*

A primary antioxidant protects the HDPE from high-temperature thermal oxidation during extrusion and welding and contributes some long-term thermal stabilization.

A primary antioxidant commonly selected for geomembranes is Irganox 1010 (BASF), a tetrafunctional phenolic antioxidant (i.e., four active sites per molecule). The higher the loading of Irganox 1010, the longer the Oxidative Induction Times (OIT), as shown in Figure 2.4. However, the ester bridges in Irganox 1010 (Figure 2.5) renders it susceptible to hydrolysis (i.e., hydrolytic breakdown), particularly at higher temperatures in the presence of water and high pH. The products of hydrolysis of Irganox 1010 are of a lower molecular mass and higher polarity than Irganox 1010 and are therefore readily leached-out of a geomembrane in contact with water or an aqueous solution, and to a lesser extent out of a geomembrane in contact with moist or saturated soil.

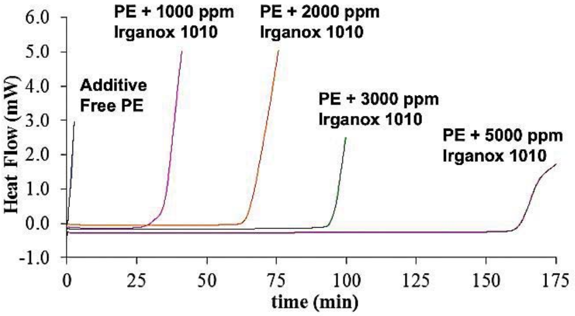

Figure 2.4 OIT curves obtained by DSC show that the OIT increases proportionally with Irganox 1010 added to the HDPE geomembrane.

A more preferred antioxidant is the trifunctional Irganox 1330, which does not contain ester groups in its structure (Figure 2.6) and hence is resistant to hydrolysis. A recent study by Wang et al. (2020) has shown that Irganox 1330 has excellent long-term ageing resistance compared to other non-ester-based alternatives like Irganox 3114 and Irganox 1024. Since Irganox 1330 does not contain ester groups in its structure, it is ideally suited to act as a long-term heat stabilizer in HDPE liners in applications with long-term water contact such as full or partial immersion and moderate to high temperatures such as exposed applications on crests and batters. Furthermore, since Irganox 1330 has no polar ester linkage, it is significantly more hydrophobic than Irganox 1010 and hence less easily extracted by water.

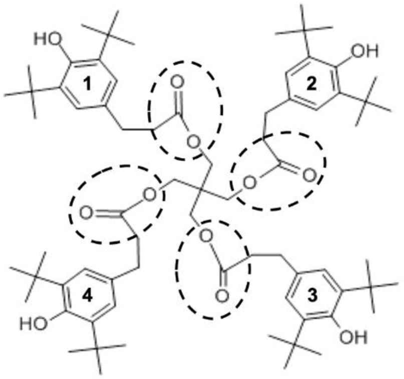

Figure 2.5 Tetrafunctional chemical structure of the Irganox 1010 molecule with four active hindered phenolic sites (numbered) and the four ester groups outlined by dotted ovals.

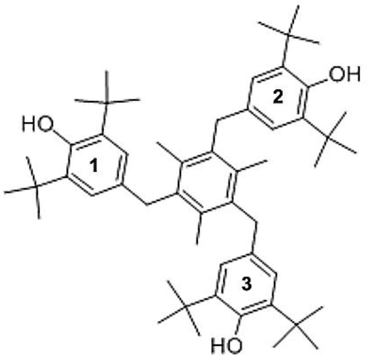

Figure 2.6 Trifunctional chemical structure of Irganox 1330 molecule with three active hindered phenolic sites (numbered).

In contrast to Irganox 1010 there are no ester groups in this Irganox 1330 molecule. Careful selection of the primary antioxidant is required to optimize both functionality (i.e., activity) and resistance to hydrolysis, as shown schematically in Figure 2.7.

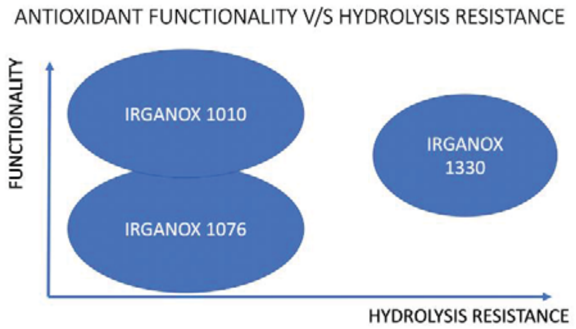

Figure 2.7 Functionality and resistance to hydrolysis of common antioxidants used in HDPE geomembranes.

2.1.2.4 *Hindered Amine Stabilizer (HAS/HALS)*

Hindered Amine Light Stabilizers (HALS/HAS) have active sites based on the radical trapping ability of the 2,2,6,6-tetramethylpiperidine group in their structure. The efficacy of HAS in HDPE is a function of the number of active sites per HAS molecule. The permanence and resistance to extraction of HAS is a function of the size and bulkiness of the HAS molecules (a combination of their molecular weight and molecular volume). A well-known HAS additive used in early geomembrane formulations was Tinuvin 770 (Figure 2.8).

Tinuvin 770 has rather limited stabilizer activity compared to more modern HAS additives, and the ester groups in its structure make it susceptible to hydrolytic degradation and rapid extraction. In contrast, Chimassorb 119 has eight active sites per molecule, and each active site is a methylated piperidinyl active site with a nitrogen atom at its centre. There are no ester groups susceptible to hydrolysis (see Figure 2.9). The methyl group protects the 'basic' nitrogen atom of the active site from protonation (i.e., adding a hydrogen atom) by acids (H^+ donors). Therefore, the methylated HAS such as Chimassorb 119 exhibit excellent resistance to acids, and they are not deactivated (i.e., neutralized) in acidic environments. For this reason, methylated HAS (also referred to as N-methyl HAS) such as Chimassorb 119 are the stabilizers of choice for HDPE geomembranes intended for use in aggressive acidic environments such as acidic pregnant liquor ponds, acid heap leach pads, and acidic tailings dams such as those used in copper and uranium ore extraction. Furthermore, Chimassorb 119 has a very bulky molecular structure (Figure 2.9) with a high molecular weight (2285.6 g/mol), significantly decreasing the propensity to be extracted from the HDPE matrix by liquid media.

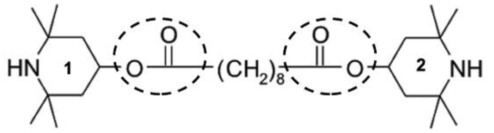

Figure 2.8 Difunctional chemical structure of Tinuvin 770 molecule with two active piperidinyl sites (numbered). Ester groups in this molecule are shown in dotted ovals.

By comparison, Chimassorb 944, which is a regular N-H HAS with eight to ten active sites per molecule and excellent resistance to extraction, has a molecular weight of 2000-3100 g/mol (Figure 2.10). However, the active sites of Chimassorb 944 are relatively basic and thus are susceptible to acid attack and neutralization (i.e., deactivation) in acidic media. Therefore, careful selection of the HAS is required to optimize both functionality (i.e., activity) and hydrolysis resistance, as shown schematically in Figure 2.11.

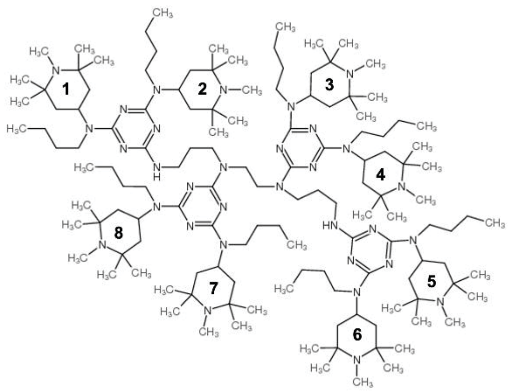

Figure 2.9 Chimassorb 119 molecular structure with 8 active methylated piperidinyl sites (numbered) and no susceptible ester groups in this stabilizer molecule.

2.1.2.5 *Acid Neutralizer*

An acid neutralizer such as hydrotalcite DHT-4A (Kisuma Chemicals) is generally added to neutralize acidic catalyst residues and by-products of the catalytic polymerization processes used to produce polyethylene. These acidic residues can reduce the effectiveness of basic HAS stabilizers and can lead to corrosion of steel processing equipment. Thus, the hydrotalcite additive is added to 'mop up' these acidic residues.

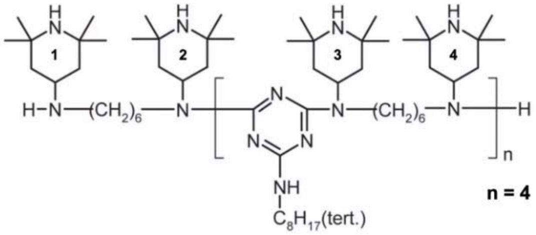

Figure 2.10 Chimassorb 944 molecular structure with two numbered active piperidinyl sites within the repeat unit in the main structure and two terminal active sites, making the total number of active sites around 10 per molecule.

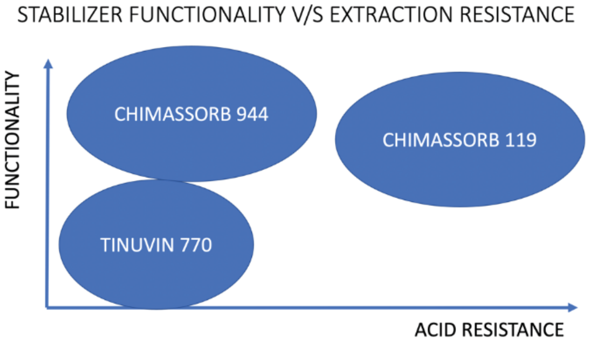

Figure 2.11 Functionality and acid resistance of common HAS stabilizers used in HDPE geomembranes.

2.1.2.6 *Polymer Processing Aid*

A fluorinated elastomer (fluoropolymer) is the most common type of polymer processing aid used in geomembrane resins. Very small levels of a fluoro elastomer such as Dynamar FX 5911X substantially improve the melt processing of high-molecular weight HDPE resins by establishing a low surface energy between the polymer melt and the metal die surface of the extruder. This means that the HDPE can be processed by extrusion at high speeds without melt fracture and avoid die build-up that can otherwise lead to lacings, defects, and pin holes in the geomembrane, such as those shown in Figures 2.12 and 2.13.

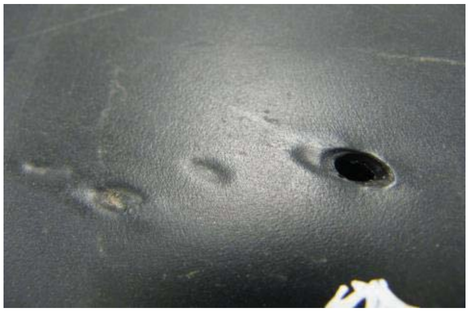

Figure 2.12 Lacing hole defect in an HDPE geomembrane caused by die build-up.

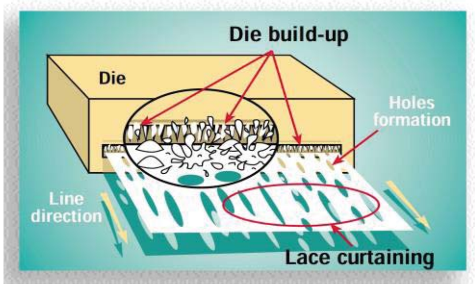

Figure 2.13 Schematic of die build-up causing lacing hole defects in an HDPE geomembrane

Another advantage of a polymer processing aid in HDPE extrusion is that it greatly reduces polymer build-up in dead spots in the extruder, such as on the screw and barrel. Such dead spots create polymer hang-ups that degrade and become carbonized due to their excessive residence time in the extruder. Periodically these degraded particles get swept back in the mainstream flow of the melt and become embedded in the final geomembrane as hard nodular defects such as the carbonized lump defect shown in a microtomed section of HDPE geomembrane in Figure 2.14.

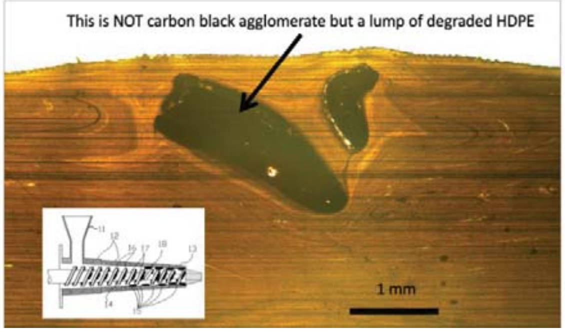

Figure 2.14 Carbonized polymer defects in an HDPE geomembrane.

2.1.3 *Loss of Additives During Service*

Different HDPE geomembrane manufacturers use different blends, ratios and levels of antioxidants and stabilizers. The antioxidants are based on different hindered phenolic antioxidants, hindered phosphites and thioesters, while the stabilizers are based on hindered amines (HAS). These protective stabilizing additives are depleted by five main mechanisms, namely:

(i) leaching (by liquids),
(ii) migration (to interface),
(iii) consumption (by free radicals),
(iv) deactivation (by chemicals),
(v) and neutralisation (by acid/base interactions).

A geomembrane's *time to nominal failure* (see §1.1) and ultimately, it's service life depends on the specific resin and the composition and amount of their antioxidant/stabilizer package added. The potential for oxidative degradation of polymers is most pronounced during the high-temperature, high-shear conversion processes (e.g., extrusion, internal mixing, milling, calendaring) of the polymer to a finished product.

Antioxidants are used to prevent accelerated oxidative degradation (i.e., autooxidation) of the polymers during processing. The antioxidants retained after manufacturing protect the geomembrane for much of the subsequent service life. The Std-OIT (sometimes simply referred to as OIT) and HP-OIT index tests provide complementary information regarding the antioxidant and stabilizer systems in the post-manufactured geomembrane. A standard OIT (Std-OIT) at 200°C (ASTM D3895) measures the effectiveness of retained antioxidant levels. To detect the retained stabilizer content, an HP-OIT at 150°C (ASTM D5885) is performed.

Std-OIT can only detect antioxidants that are effective at the 200°C test temperature, such as hindered phenolic and hindered phosphites that are used to inhibit oxidation of the geomembrane during the extrusion processing of the liner, welding of the liner, and the geomembrane service life. However, stabilizers such as hindered amines stabilizers (HAS) and thiosynergists are not active at these test temperatures (i.e., around 200°C) and therefore cannot be detected by the Std-OIT test. For this reason, the HP-OIT test run at 150°C to detect these stabilizers (Scheirs 2009).

2.1.4 *Specifications for Additives in HDPE Geomembranes*

It is difficult to write a specification for HDPE geomembranes around a particular additive or group of additives, because the additive package recipes used by manufacturers are proprietary. Moreover, due to the cost or availability of additives together with ongoing R&D in geomembrane formulations, the additives are subject to change on a regular basis. Also, for reasons such as those discussed in the previous subsections, a geomembrane that performs well in one environment may perform badly in a quite different environment depending on the compatibility of the resin and additives to the two environments. Standard *de facto* minimum requirements such as GRI-GM13 serve as a useful guide in noncritical situations. However, since the end-user is generally unaware of what additives are used in any geomembrane, the only way of assessing the compatibility of a geomembrane with a given environment or suitability for applications where a long service life is essential is by accelerated testing. For example, the selection of a geomembrane for a 550-year service life in a low-level radioactive disposal facility is described by Rowe et al. (2020) and that for a 20-year service life in a pond for a highly acid liquid subject to high temperature and UV exposure is described by Folwell et al. (2021).

2.2 *Geomembrane manufacture and design implications*

HDPE geomembranes have good barrier properties due to their relatively high degree of crystallinity, where the crystalline regions retard the diffusion of molecules significantly more than the amorphous regions. For this reason, HDPE is favoured as a landfill barrier over LLDPE which has a lower degree of crystallinity. To achieve high crystallinity and high strength, HDPE or MDPE resin of relatively high molecular weight is used. The melt flow index (MFI also known as the melt flow rate, MFR) is an index for the average molecular weight of the polymers in the resin. Lower MFI implies higher average molecular weight. The flow rate ratio (FRR) of the MFI obtained under two different pressures (e.g., extruded with an applied load due to a mass of 21.6 and 2.16 kg) is an indirect measure of the breadth of the molecular weight distribution.

The two main processing techniques for manufacturing HDPE geomembranes are flat bed (slot die) extrusion (FBE) and vertical blown film extrusion (BFE). The two processes require resin with different rheology, as reflected by the MFI and FRR requirements. Both processes can produce high-quality geomembranes. However, different defects and challenges can arise for the two processes, and these should be understood by the design engineer.

Flat bed extrusion (FBE) involves the molten mix of resin and additives being forced to spread laterally from the injection points through two horizontal die lips. The die lip gap controls the thickness. Therefore, the rheology of the mix must be such that it is spread uniformly (without segregation) across the die width from the injection points. This typically implies a lower average molecular weight and narrower molecular weight distribution (i.e., higher MFI and lower FRR) than a BFE geomembrane. If the mix does not spread uniformly without segregation, it can differ in properties across the roll width.

Blown film extrusion (BFE) is one of the most used methods of manufacturing HDPE geomembranes. The resin is first melted by subjecting it to heat and pressure inside the barrel of an extruder and then forced through a narrow annular slit in the die to control its thickness. Immediately after being extruded, the BFE process material must be pulled upwards from the die. The resin requires a higher molecular weight (lower MFI) and broader molecular weight distribution (higher FRR) than the FBE process to support the weight of the vertical bubble. The quality of the BFE product is controlled by the following:

- Output rate: In blown film extrusion, screw speed most controls the output. Generally, higher screw speed implies higher output.
- Blow-up ratio: The blow-up ratio is described as the ratio of bubble diameter per die diameter. It defines how much the bubble expands in the transverse direction.
- Neck-point height: Neck-point height is usually expressed by the distance from the die surface to the point where the necked diameter of the bubble becomes the shortest.
- Thickness is controlled by the take-up speed, which is controlled by rotational speed primary nip rollers at the top of the blown film column since the lip opening is fixed.

This BFE process may result in greater strength anisotropy than the FBE process. However, this is usually not an issue for design since HDPE must be designed for very small strains (well below the yield strength) and break strength is a quality control and not a design parameter.

A change in take-up speed and the consequent change in the cooling rate also affects crystallinity, yield strength, and internal stresses in the geomembrane post-manufacture. Thus, changing take-up speed can result in different initial stress crack resistance, SCR_o, for the same resin. For example, four HDPE geomembranes made sequentially from the same resin with only the take-up speed changing to change thickness had SCR_o of 680 hours (1 mm), 800 hours (1.5 mm), 950 hours (2 mm) and 1100 hours (2.4 mm) (Ewais and Rowe 2014). Rowe et al. (2019) attributed the differences in SCR_o in part to morphological differences but primarily due to different residual stresses – a result of the different cooling rates. When the residual stresses were allowed to relax to the representative value, there was no statistically significant difference in the representative stress crack resistance, SCR_m, of the four geomembranes with $SCR_m \sim 290$ hours (giving a ratio of $0.26 < SCR_m/SCR_o < 0.43$). Based on a study of many HDPE geomembranes, Rowe et al. (2019) found that generally the initial SCR_o does not provide a meaningful representation of the materials representative stress crack resistance, SCR_m. From this study, the representative stress crack resistance is between 17 and 52% of the initial post-manufacture value SCR_o (i.e., $0.17 \leq SCR_m/SCR_o \leq 0.52$ with an average of 0.37). This is consistent with observations of a decrease in SCR with time for a geomembrane stored away from sunlight at 20^{o}C. Rowe and Ewais (2015) reported that the SCR of an HDPE geomembrane reduced from SCR_o=550 hours to SCR=330 hours after 4 years of storage in the laboratory, and 190-195 hours after 6 years of field exposure without any evidence of degradation in either case.

The decrease in SCR from SCR_o to SCR_m is not degradation. Instead, it is the geomembrane transitioning from an unstable thermodynamic state after its manufacture and shipping to the site to a stable state representing the real material property available to the designer before degradation. It is the value of SCR_m that is relevant to the design. A reasonable estimate of SCR_m can often be obtained by ageing the geomembrane for 3 months at 55 to 65°C. For some geomembranes, the SCR after 3 months of ageing at this temperature will exceed SCR_m. However, it is still a much better estimate of the representative SCR than SCR_o.

Although most of the geomembranes examined by Rowe et al. (2019) were blown film, the one flat bed geomembrane examined also experienced a significant decrease from SCR_o to SCR_m. The geomembranes tested had an average SCR_m/SCR_o =0.37±0.1 (i.e., a standard deviation of 0.1; 70% of geomembranes tested had $0.27 < SCR_m/SCR_o < 0.47$) .

Another feature of the BFE process is the folding of the geomembrane between the nip rollers before it is cut and placed on the roll for delivery to the site. This fold, located at the quarter points with half-a-roll-width between them, serves as a location for the formation of Λ shape wrinkles when the geomembrane is heated by solar radiation in the field (Figure 2.15). FBE geomembranes do not have this preferred location for wrinkling. However, the coefficient of thermal expansion is essentially the same for both BFE and FBE geomembranes, and hence the total amount of wrinkling is also essentially the same. Therefore, there is no advantage to either one or the other method of manufacture from the perspective of wrinkles. In both cases, the geomembrane must be covered at a time when the wrinkles are minimal (e.g., evening or very early morning).

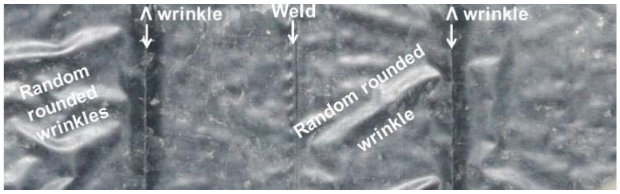

Figure 2.15 Aerial photo of Λ wrinkles arising at quarter points from fold in blown film geomembrane running parallel to the roll

2.3 *Problems with high levels of additives*

The ever-increasing drive to reach greater durability with HDPE geomembranes has meant increased loadings of antioxidants and stabilizers are being incorporated into the polymer. While this leads to very high Std-OIT values and HP-OIT values and >90% retention of HP-OIT after oven ageing it has also resulted in increased problems with waxy surface layers and additive blooming and, consequently, with fusion welding.

Blooming, or exudation as it is technically known, is the diffusion of the additives from the HDPE to the surface of the liner to form a greasy/waxy layer on the liner surface. Such surface residues can interfere with welding of the geomembrane. During welding, the additives and polymer waxes that have bloomed from the HDPE accumulate on the hot wedges of the welding machines and then are pushed laterally to give excess squeeze-out and abnormally large squeeze-out areas.

Excess blooming of HDPE geomembranes can be detected by:

(i) the appearance of a whitish visible line on upon dragging a fingernail along the surface of the liner.
(ii) observing excessive smoking and blackening of the brass wedges of the welding machine.
(iii) an abnormally wide and/or thick squeeze-out zone.
(iv) a more prominent than normal amine peak in the FTIR at 1560 cm^{-1}.

The Blooming of HAS is due to their relatively low solubility in polyolefin matrices and the HAS reaching their saturation solubility in HDPE starting when levels exceed 0.5 wt.% (5000 ppm) and approach 1 wt.% (10,000 ppm). Also, a base polymer with high levels of cyclohexane extractables can contribute to the excess squeeze-out problem by increasing the level of oligomers and waxes in the polymer.

Blooming and exudation are most prevalent with geomembranes that are highly stabilized with AO and HAS. Their limited solubility in the PE means that the excess diffuses (blooms) to the surface of the geomembrane, particularly with hot storage. During wedge welding, the excess molten polymer mixed with waxes and additives is laterally extruded and deposited on the liner adjacent to the weld tracks. When blooming causes excess squeeze-out, the squeeze-out may retain high Std-OIT and HP-OIT values due to its excess additives despite more heating than the parent polymer. Regular cleaning of the wedges reduces the incidence of excessive squeeze-out due to blooming but at the expense of reduced welder productivity.

Possible preventative measures to reduce excess squeeze-out arising from excess wax/additive migration include:

- Testing the geomembrane before welding for the presence of waxy layers of bloomed additives and waxes (see ATR-IR method below).
- Using an ethyl acetate solvent to clean the flaps and remove excess bloom and waxes before welding.
- Regularly cleaning of the brass hot wedges but this is at the expense of welder productivity.
- Setting a specification for the maximum acceptable level of exuded polymer/additives for a geomembrane.

Figure 2.16 shows the various infra-red absorption bands of typical additives used in HDPE geomembranes. Since all these additives have characteristic and distinct IR absorption peaks, the surface-sensitive analysis technique of ATR-IR can be used to identify the presence and levels of migratory additives in HDPE that have exuded from the geomembrane.

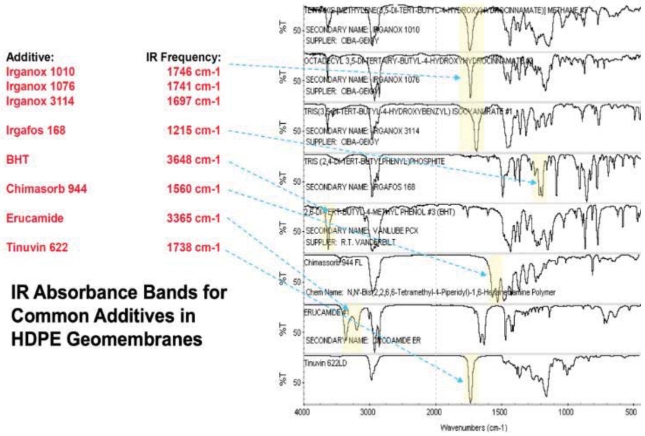

Figure 2.16 IR Absorbance bands are detectable for blooming additives from HDPE geomembranes (courtesy of ThermoFischer Scientific).

2.4 *Testing of multilayered geomembranes*

These layers have the potential to complicate traditional methods of monitoring material behaviour. For example, standard oxidative induction time (Std-OIT; ASTM D 3895) and high pressure oxidative induction time (HP-OIT; ASTM D 5885) tests are typically used to assess the initial OIT values and antioxidants/stabilizer depletion time for the aged geomembrane specimens. For white and/or conductive geomembranes, assessment of the OIT values can be more challenging relative to traditional black geomembranes. Rowe et al. (2020) showed a notable variation of the OIT values between the textured white and conductive geomembranes and their smooth edges provided for welding purposes in the field. In addition, multiple exothermic peaks are typically observed during the thermal oxidation in the Std-OIT test of conductive geomembranes (Figure 2.17, presumably due to the conductive layer that may not be homogenously distributed across the entire geomembrane surface area). To minimize such local variations of stabilizer concentration and the difference in the formulation of the different layers of these geomembranes, ASTM D5885 and D8117 recommend homogenization of the sample before OIT analysis. Alternatively, individual layers may be separated from the sample using thick microtomes to remove or separate a particular layer as a whole and analysed for OIT separately.

Mechanical properties, especially tensile break strength/elongation (ASTM D6693) and stress crack resistance (ASTM D5397) are typically used to assess the initial properties of a given geomembrane and for assessing the degradation beyond antioxidant depletion.

The variable thickness resulting from the texturing in coextruded nitrogen textured BFE geomembranes or the variation of formulation in multilayered geomembranes can give a large coefficient of variation in break properties.

The SCR test involves preparing specimens with a prescribed notch that should produce a ligament thickness equal to 80% of the nominal thickness of the specimen (ASTM D5397). However, this procedure cannot be used to assess the SCR of textured geomembranes due to the variation of the ligaments obtained when notching the textured part of the roll. Alternatively, the SCR of textured geomembranes manufactured with a single base resin in all layers is assessed using the roll's smooth edge to minimize the SCR's variability. However, in this case, the skin will be minimal or missing in the smooth edge sample relative to the textured geomembrane.

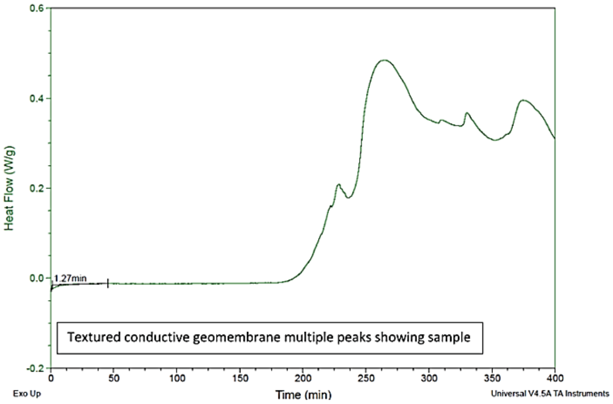

Figure 2.17 Differential scanning calorimetry thermogram showing the multiple exothermic peaks in textured conductive geomembrane

.

For multilayered geomembranes coextruded with different polymer formulations, the direction of the notch (top or bottom surface) can affect the SCR since the notch can eliminate one or more layers of the geomembrane, leaving the crack to propagate through the other layers of the geomembrane. Therefore, ASTM D5397 test method recommends that the geomembrane be notched on the functionalized side in case of geomembranes formulated with a single functionalized external layer or notched on the side exposed to the sun in the field in case of geomembranes with two functionalized external layers (Appendix X2 in ASTM D5397).

An alternative method to assess the SCR, especially for textured multilayered geomembranes, without eliminating any skin layers is using plaques to homogenize the different layers according to ASTM D4703 Procedure C. In this method, two specimens of the geomembrane are faced together, then heated to above the normal melt temperature of the geomembrane, and finally squeezed together under pressure. The plaque is then cooled and removed from the mould. Rowe et al. (2020)

compared SCR of samples taken directly from the roll to plaques of a smooth white using ASTM D5397. They found that the SCR was more than 70% greater for the plaque specimens (>1000 hours) than the 590 hours obtained by the standard method by the same laboratory. Such difference in the SCR can be attributed to the annealing of the geomembrane during the preparation of the plaques that may increase their SCR (Abdelaal et al. 2015). This suggests that the plaque method does not give a representative SCR of the material taken directly from the roll and tested (Rowe et al. 2020).

While multilayered geomembranes can provide designers with many desirable characteristics, assessing their properties (especially due to ageing) is an issue requiring further research.

3 BITUMINIOUS GEOMEMBRANES

3.1 *Introduction*

Bituminous geomembranes (BGMs) comprise a thick nonwoven geotextile impregnated with bitumen to give an essentially impervious yet flexible sheet (Figure 3.1). The bitumen used in the production of BGMs is either oxidized or, more recently, stabilized with elastomers such as styrene-butadiene-styrene (SBS). These bitumen modifications reduce its temperature sensitivity and make it suitable for geomembrane applications (Peggs 2008; Touze-Folz and Farcas 2017). In some BGM products, a layer of glass fibre fleece is used to provide dimensional stability during manufacturing and can increase the strength and puncture resistance (e.g., Bannour et al. 2013; Blond and Breul 2014). The surface layer of the BGM is usually sanded to increase the interface shear strength of BGMs to improve stability on side slopes (El-Dana and Breul 2010). The bottom layer of the geotextile usually has an anti-root polyethylene backing film. BGMs are relatively thick (3–5 mm) and are claimed to withstand installation-related mechanical damage. They have also been used for cold regions applications (e.g., lining Diavik Diamond Mine in Canada's Northwest Territories).

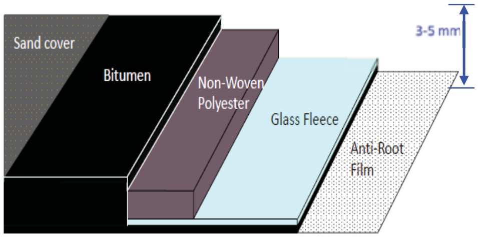

Figure 3.1 BGM different layers (AXTER COLETANCHE, 2009)

Historically the use of BGMs has been largely limited to use in dams, canals, potable water reservoirs, and other low risk environmental applications. Due to their ease of field seaming and suitable mechanical and physical properties (such as high mass per unit area, high puncture resistance, relatively high density, and low coefficient of thermal expansion; Peggs 2008), BGMs are often considered as a strong candidate for the liner materials in different geoenvironmental applications. Today, BGMs have been used, or introduced as candidates, to line municipal solid waste (MSW), low-level radioactive waste (LLRW) landfills (Breul et al. 2006), and more recently mine tailing ponds and heap leach pads (Peggs 2008; Lazaro and Breul 2014).

3.2 *Puncture resistance of BGMs*

The short-term puncture resistance is a key aspect of the BGM properties that governs the BGM performance as a hydraulic barrier in high stress applications. The cylinder test is typically performed to assess gravel induced short-term damage in the geomembranes (e.g., ASTM D5514; Shercliff 1998; Rowe et al. 2013; Lupo and Morrison 2007). Previous investigators (e.g., Blond and Breul 2014; Lazaro and Bruel 2014; Clinton and Rowe 2017) used a similar setup to assess the compatibility of BGMs with the site-specific materials such as the gravel drainage layer or subgrade by assessing their puncture resistance and/or the tensile strains induced under excessive overburden pressures simulating different applications (Figure 3.2).

Blond and Breul (2014) examined different BGMs with different thicknesses under both hydrostatic stresses (stresses induced due to high water heads) and mechanical stresses (drainage layer is installed on top of the geomembrane with low hydraulic heads). Depending on the BGM material, they observed failure in the BGM under mechanical stresses between 2.7 MPa and 5.2 MPa while failure of the different BGMs took place under hydraulic stresses between 0.64 MPa and 1.0 MPa only. They concluded that puncture resistance of the BGM is significantly higher under mechanical stress than hydrostatic pressures. Another study by Clinton and Rowe (2017) examined punctures and strains for a 4 mm BGM under an overburden pressure of 2.0 MPa using overliner and underliner materials simulating heap leaching applications. A direct comparison was made between the BGM and a 1.5 mm HDPE and showed more physical damage to the BGM than the HDPE (in the form of holes). Under these conditions under these conditions, they observed hundred and 15 holes in the 60 cm diameter sample (Figure 3.3). However, a subsequent leakage test showed that even though the BGM had more holes than the HDPE, its leakage was lower, suggesting that the gravel may have sealed many of the holes in the BGM.

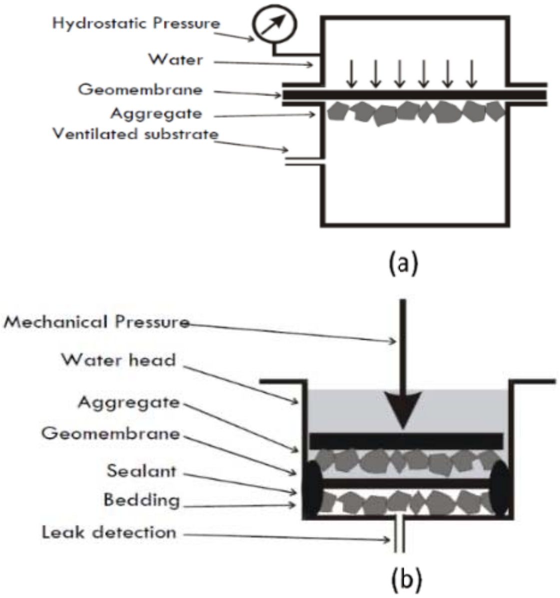

Figure 3.2 BGM puncture tests; (a) application of hydrostatic stresses; (b) Mechanical stresses (modified from Blonde and Breul 2014).

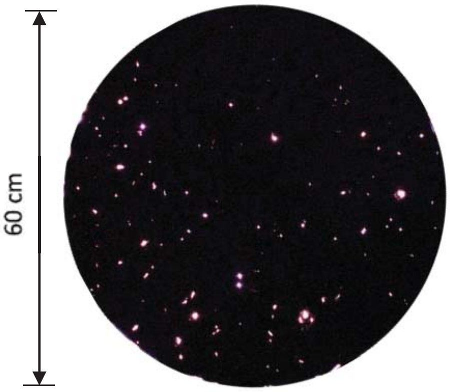

Figure 3.3 BGM sample after a cylindrical test at 2 MPa showing 115 holes in the 60 cm diameter sample (modified from Clinton and Rowe 2017).

3.3 *Chemical durability of BGMs*

In the long-term, examining the chemical compatibility of BGMs with the service conditions in different applications is essential to ensure their longevity to meet the long service life requirement of waste containment applications. Ageing of the bitumen has been extensively studied as the key factor to determine the lifetime of asphalt pavement and showed that oxidation can happen as the result of photo-oxidation (UV) and/or thermal oxidation (Hofford 2015). However, the ageing of a BGM is more complex since its different components may interact differently with ageing conditions. This may have different implications on the different properties of the geomembrane (i.e., mechanical versus waterproofing properties). This was shown in a study by Touze-Foltz and Farcas (2017) when investigating the performance of aged elastomeric BGMs exhumed from two ponds 6, 10, 15, 20, and 30 years after installation. While the tensile test results indicated that the mechanical properties of the core reinforcement were not affected after 30 years, specimensaged over 15 years showed complete consumption of the polymer and oxidation of the bitumen within the first few microns from the surface of the BGM. Esford and Janssens (2014) incubated BGMs in a diluted acidic solution (20% sulfuric acid +100 ppm kerosene) for 3 years at room temperature which was a much more aggressive chemical exposure. The results showed that the BGM maintained its properties within acceptable limits, and hence they concluded that BGM could be suitable to be used as a primary geomembrane for ponds. However, at the elevated temperatures (like those recorded for the geomembrane liners in some geoenvironmental applications), bitumen as a viscoelastic material is expected to exhibit significant changes in its properties (Touze-Folz and Farcas 2017) while all components of the BGMs may exhibit thermal degradation affecting the overall properties of the BGM. This was shown by Addis et al. (2016), reporting a large-scale failure of the BGM liner in a copper/gold mine disposal facility occurring several months after installation. The thermal Imaging showed that the surface temperature of the exposed BGM reached 86°C and the tensile tests conducted on exhumed specimens showed a decrease in the tensile strength, especially at the seams. It was concluded that a combination of the elevated temperatures and tensile stresses caused BGM degradation and failure. Combining the effect of elevated temperatures and chemical exposure, Samea and Abdelaal (2019) examined the performance of BGMs using immersion tests in synthetic mining solutions at pH=0.5 and pH=13.5, simulating the pregnant leach solution (PLS) from heap leaching applications, and 55°C. They showed that the BGMs exhibited more degradation in the high pH solution compared to the low pH solution. However, further research is still needed to investigate the long-term performance of BGMs to ensure their proper use in many different applications to provide the desired environmental protection.

4 ENHANCED BENTONITE GEOSYNTHETIC CLAY LINERS

4.1 *Conventional geosynthetic clay liners*

Geosynthetic clay liners (GCLs) are thin (~4- to 10-mm thick), factory manufactured barriers commonly used for hydraulic and chemical containment applications, including municipal and hazardous solid waste landfills, surface impoundments (e.g., ponds and lakes, aeration lagoons, fly ash lagoons, tailings impoundments), canals, storage tanks, and secondary containment of above-grade fuel storage tanks (e.g., Petrov et al. 1997a,b; Rowe 1998, 2005; EPA 2001; Bouazza 2002; Koerner 2005; Shackelford 2008; Bouazza and Bowders 2010; Scalia et al. 2018a; Norris et al. 2020). GCLs often are used in lieu of compacted clay liners (CCLs) due to lower cost, ease of installation, and minimal consumption of airspace (e.g., Koerner and Daniel 1995; Daniel et al. 1997; Bouazza 2002). The low hydraulic conductivity of conventional GCLs to water, which typically is on the order of ~1×10^{-11} to 3×10^{-11} m/s, yields a barrier with a leakage rate that is equal to or lower than that of CCLs. The low hydraulic conductivity of conventional GCLs that do not include a geomembrane component is attributed exclusively to the natural bentonite within the GCL.

4.1.1 *Swelling behaviour, of natural (unenhanced) bentonite*

Swelling of the montmorillonite mineral fraction of the bentonite upon hydration is the primary mechanism controlling the hydraulic conductivity of bentonite in GCLs. The bentonite granules (or particles for GCLs with powdered bentonite) swell, filling the intergranular pores that conduct the bulk of the flow (Tian et al. 2016b, 2019). Bentonites in GCLs that are hydrated with liquids that promote swelling have narrow and tortuous pathways that yield low hydraulic conductivity (A in Figure 4.1), whereas hydrating liquids that suppress swelling lead to larger and less tortuous flow paths and much higher hydraulic conductivity (B in Figure 4.1) (Jo et al. 2001; Kolstad et al. 2004; Scalia and Benson 2011; Tian et al. 2016a, 2019; Chen et al. 2018).

The swelling of bentonite is intimately tied to interlayer swelling in the montmorillonite mineral (Norrish 1954). Montmorillonite is a 2:1 aluminosilicate clay mineral, meaning that the crystalline structure of the mineral comprises sequential layers, also referred to as lamellae or platelets, comprising a single sheet of aluminium (Al) octahedra sandwich between and chemically bonded to adjacent sheets of silica (Si) tetrahedra, often referred to as the TOT structure. As illustrated in Figure 4.2, these TOT layers stack to form individual particles or tactoids. Although the schematic depiction in Figure 4.2 implies that an individual clay particle comprises only two layers, the number of layers for any given particle varies and can be substantially greater than two (as will be demonstrated subsequently). For example, based on the fabric boundary surface (FBS) theory that considers the microstructure of smectite-rich clay soils to be a dual-porosity medium comprising both interlayer, inaccessible nanometer-size pores and intertactoid, accessible micropores, the average number of layers or lamellae per tactoid, $N_{l,AV}$, is given by the following expression (Manassero et al. 2018; Manassero 2020):

$$N_{l,AV} = N_{l,AV0} + \frac{\alpha}{e_m}\left(\frac{c_s}{c_0}+1\right) + \beta e_m\left[1-\exp\left(-\frac{c_s}{c_0}\right)\right] \qquad (4.1)$$

where c_s is the salt concentration of the equilibrium bulk solutio n (pore water), c_0 is the reference salt concentration (= 1 eq/L), e_m is the bentonite micro-void ratio. The dimensionless parameters $N_{l,AV0}$ ($\geq$ 1), α ($\geq$ 0) and β ($\geq$ 0) have to be adjusted based on a given set of test results for the same clay soil. The FBS theory (Eq. 4.1) provides an assessment of the microstructure under different chemico-mechanical boundary conditions and illustrates the primary parameters affecting $N_{l,AV}$. Individual clay particles also can accumulate or aggregate to form larger granules or aggregates of clay particles. Note that the terminology used to describe the various components of individual montmorillonite particles and aggregates of particles as well as the associated pore spaces between the layers, particles, and aggregates can vary significantly in the literature (e.g., compare Jo et al. 2006; Likos and Lu 2006; Likos and Wayllace 2010; Acikel et al. 2018; Manassero 2020).

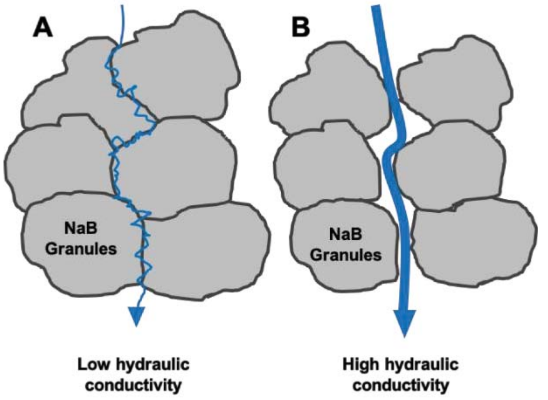

Figure 4.1. Swelling of sodium bentonite (NaB) granules and corresponding hydraulic conductivity.

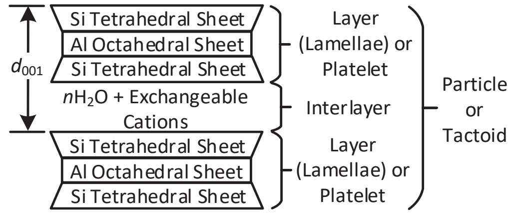

Figure 4.2. Schematic illustration of 2:1 layered crystalline structure of natural montmorillonite.

The interlayer space between consecutive layers is occupied by both water molecules (H_2O) and exchangeable cations, which typically include sodium (Na^+), potassium (K^+), calcium (Ca^{2+}), and magnesium (Mg^{2+}) to varying extents. The cations are held or bound electrostatically to the surfaces of the layers due to a net negative charge located within the Al octahedra sheet as a result of the process of isomorphic substitution, whereby the Al^{3+} within an aluminium octahedron is replaced by a lower charged cation, such as Mg^{2+}, during crystalline formation of the montmorillonite. The magnitude of the negative charge or surface charge deficiency increases with the number of substituted Al^{3+} in the Al octahedra comprising the sheet, and generally, it varies on the order of 0.5 to 1.2 equivalents of charge (eq) per unit cell, with an overall average of 0.66 eq per unit cell (Mitchell and Soga 2005; Lee and Shackelford 2005), which correlates to about 1.1 to 1.9 eq/m^2 of surface area (Jury et al. 1991). The magnitude of this negative charge dictates the number of equivalent positive charges associated with the exchangeable cations external to the crystalline structure required for electroneutrality. The total number of equivalents associated with the sum of all exchangeable cations is commonly referred to as the cation exchange capacity (CEC).

Because isomorphic substitution occurs in the Al octahedral sheet, the distance between the source of the negative charge and the location of the exchangeable cations is relatively large, such that the bound cations are free to exchange with those in the bulk pore water always provided that electroneutrality is maintained. For example, two initially bound Na^+ ions can be replaced by one Ca^{2+} ion, which is the reason these electrostatically bound cations are referred to as exchangeable cations. Also, the cation that dominates the exchange complex of the montmorillonite dictates the type of montmorillonite and, therefore, the type of bentonite (e.g., Gleason et al. 1997). For example, when the predominant exchangeable cation is Na^+, the montmorillonite is referred to as sodium montmorillonite (Na-montmorillonite) and the associated bentonite is referred to as sodium bentonite (Na-bentonite). Conversely, when the predominant exchangeable cation is Ca^{2+}, the montmorillonite is referred to as calcium montmorillonite (Ca-montmorillonite), and the associated bentonite is referred to as calcium bentonite (CaB).

In addition to the exchangeable cations, immobile water molecules also are bound to the surfaces of the mineral solid phase in the interlayer zone. Although the water molecule, H_2O, is charge neutral, the polar nature of H_2O imparts charged behaviour. The volume of the bound water molecules dictates the thickness of the interlayer space and, therefore, the basal spacing, d_{001}, between successive layers (see Figure 4.2). The hydration or crystalline swelling phase, the extent of which is directly related to the magnitude of d_{001} (Norrish 1954; Jo et al. 2001), occurs as the montmorillonite is initially hydrated from a dry state and continues until there are several monolayers of bound water molecules. The osmotic swelling phase occurs subsequently and depends on the cation concentration in the bulk pore water, provided that the exchangeable cations are predominantly monovalent. When the bulk pore water comprises a relatively low concentration of monovalent cations, and the exchangeable cations are monovalent, osmotic swell occurs such that the fraction of immobile, bound water and the corresponding swell volume is relatively high, resulting in relatively low hydraulic conductivity because the conductive interparticle (intertactoid) and intergranular pores are smaller, and the flow paths are more tortuous. This situation occurs, for example, when Na-bentonite is hydrated and permeated with deionized water (DW).

Conversely, only the crystalline or hydration swelling phase occurs when the bulk pore water comprises a relatively high concentration of cations, and the exchangeable cations are multivalent. As a result, swelling is minimized, and the resulting hydraulic conductivity is relatively high. This situation occurs when CaB is hydrated and/or permeated with electrolyte solutions with significant concentrations of multivalent cations. For example, the free swell of CaB upon hydration with DW typically is on the order of three millilitres per two grams of dry bentonite (3 mL/2 g), whereas the free swell of Na-bentonite hydrated with DW typically is on the order of 30 mL/2 g (Jo et al. 2001; Kolstad et al. 2004).

4.1.2 *Chemical compatibility issue with bentonite*

The aforementioned crystalline swelling occurs within the tactoids (i.e., within the interlayer pore space), and is mostly controlled by the hydration potential energy of the interlayer cations, which is insensitive to the salt concentration of the equilibrium bulk solution. In contrast, osmotic or double-layer swelling occurs between the tactoids (i.e., in the intertactoid pore space). This is driven by a difference in the osmotic pressure between the mobile pore water and the external bulk solution, the magnitude of which depends on the concentration and valence of the cations in the mobile pore water (e.g., Laird 2006). Thus, when Na-bentonite is hydrated or permeated with a liquid containing a high concentration of ions, osmotic swelling of the montmorillonite is suppressed, increasing *k*. The increase in *k* can range from one to several orders of magnitude depending on several factors, including the ionic strength, I ($=\frac{1}{2}\sum c_i z_i^2$, where c_i and z_i are the molar concentration and associated charge of ionic species, i, summed over all ionic species in solution), the ratio of monovalent-to-multivalent cations of the hydrating/permeant liquid, and the confining stress or void ratio, e, of the bentonite, where $e = n/(1 - n)$ and n is the total porosity (Jo et al. 2001; Kolstad et al. 2004).

For example, consider the hydraulic conductivity ratio, k/k_w, shown in Figure 4.3 for two conventional GCLs permeated with calcium chloride ($CaCl_2$) solutions. As indicated, the ratio k/k_w, defined as the ratio of k when the GCL is permeated by a particular chemical solution to that when permeated by water, k_w, increases with increasing $CaCl_2$ concentration for both GCLs, with k/k_w eventually reaching a value based on permeation with a 500 mM $CaCl_2$ solution ranging from 2.7 orders of magnitude for GCL1 to 4.9 orders of magnitude for GCL2. Note that k_w for GCL1 and GCL2 were 2.4×10^{-11} m/s and 7.0×10^{-12} m/s, respectively, such that the respective k values based on permeation with 500 mM $CaCl_2$ were $\sim1.2\times10^{-8}$ m/s and $\sim5.7\times10^{-7}$ m/s.

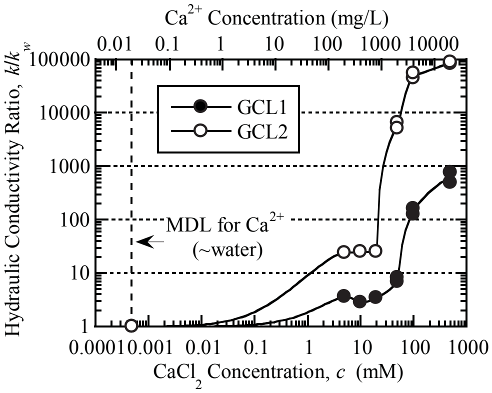

Figure 4.3. Ratio of the hydraulic conductivity based on permeation with calcium chloride ($CaCl_2$) solutions, k, relative to that based on permeation with water, k_w, as a function of the $CaCl_2$ concentration for the permeant solution for two GCLs [MDL = Method Detection Limit] (data from Lee and Shackelford 2005).

The k values shown in Figure 4.3 are based on a low effective stress (35 kPa) that may not represent the stresses encountered in many applications. Lower k values are anticipated at higher effective stresses (e.g., see Petrov et al. 1997a,b; Petrov and Rowe 1997; Rowe 1998; Shackelford et al. 2000; Katsumi and Fukagawa 2005; Thiel and Criley 2005; Bradshaw et al. 2013; Norris et al. 2020). Nonetheless, the results shown in Figure 4.3 indicate that the k of GCLs can be altered when permeated with aqueous solutions of moderate to high ionic strength and going beyond Figure 4.3 the effect has been found to vary with the chemical species in the solution as well as concentration (e.g., Fehervari et al. 2016a,b; Chen et al. 2018; Xu et al. 2018; AbdelRazek and Rowe 2019) and/or pH (e.g., Shackelford et al. 2000, 2010; Benson et al. 2010b; Bouazza and Gates 2014; Athanassopoulos et al. 2015; Liu et al. 2015; Ghazizadeh et al. 2018; Scalia et al. 2018a; Prongmanee and Chai 2019; Norris et al. 2020; Li et al. 2021). This limitation of conventional GCLs comprising Na-bentonite has led to the development and use of GCLs comprising enhanced bentonites that have been modified to resist the potential for chemical attack resulting in hydraulic incompatibility (e.g., Di Emidio et al. 2011; Bohnhoff et al. 2013; Bohnhoff and Shackelford 2014; Scalia et al. 2014, Scalia and Benson 2016, Di Emidio et al. 2017; Scalia et al. 2018a).

4.2 *Polymer modified and enhanced bentonites*

The terms "polymer modified bentonite", "polymer enhanced bentonite", or simply "enhanced bentonite" are sometimes used interchangeably and sometimes "polymer modified" is used as a broad category to cover all modified bentonites, whereas "enhanced bentonite" represents a special category of modified bentonites. The latter approach is adopted in this paper because the role of the modification or enhancement may differ. In some cases, low-quality bentonites are chemically modified by the addition of polymers simply to improve the swell capacity or k_w such that they perform similarly to higher quality natural Na-bentonite in standard index tests such as ASTM D 5890 and D 5887 (e.g., Haug and Boldt-Leppin 1994) and may be regarded as "substitution bentonites" since the primary objective is to meet the standard specification for Na-bentonite. The term enhanced bentonites as used herein excludes these bentonites. Enhanced bentonites are defined herein as natural bentonites that are chemically modified to achieve low k to solutions that alter the hydraulic conductivity of natural Na-bentonites.

4.2.1 *Enhanced bentonites*

Chemicals that commonly have been used for bentonite enhancement include anionic polymers such as polyacrylate and polyacrylamide (e.g., Heller and Keren 2002; Scalia et al. 2011; Bohnhoff 2012; Scalia 2012; Bohnhoff and Shackelford 2013; Bohnhoff et al. 2014; Chen et al. 2019; Prongmanee et al. 2018a,b; Scalia et al. 2018a,b; Prongmanee and Chai 2019; Chai and Prongmanee 2020; Li et al. 2021), and carboxymethylcellulose (e.g., Di Emidio 2010; Di Emidio et al. 2015; De Camillis et al. 2014, 2016; Fan et al. 2020), cyclic organic carbonates such as propylene carbonate (Onikata et al. 1999; Katsumi et al. 2008; Mazzieri et al. 2010) and glycerol carbonate (Fehervari et al. 2016a,b; Gates et al. 2016), and other organic compounds such as ethylene glycol (Szczerba and Kalinichev 2016) and quaternary ammonium cations (QACs) such as hexadecyltrimethylammonium and benzyltriethylammonium (Soule and Burns 2001; Burns et al. 2006).

Bentonites modified with QACs, known as organobentonites or organoclays, are used primarily as a sorptive medium for organic compounds (e.g., Lee et al. 2012; Di Emidio et al. 2017) or as hydraulic barriers in GCLs or other configurations specifically to contain nonaqueous phase liquids (Lee et al. 2012; Benson et al. 2015). These enhanced organobentonites will not be discussed further herein.

A summary of some of the more commonly studied enhanced bentonites is provided in Table 4.1. However, the general category of contaminant-resistant clays (CRCs) pertains to commercial products of which the modifying or chemical enhancement agent and process are proprietary and, therefore, unknown. As a result, although CRCs are considered herein, little detail of these enhanced bentonites can be provided.

Table 4.1. Some enhanced bentonites (modified from Scalia et al. 2018a)

Name of bentonite	*Additive(s) or modification*
Bentonite polymer composite (BPC)	Sodium polyacrylic acid (Na-PAA) and other dry mixtures of bentonite and hydrophilic polymers
Dense prehydrated (DPH)	Sodium carboxymethylcellulose (Na-CMC) plus Na-PAA
HYPER clay (HC)	Na-CMC
Multiswellable bentonite (MSB)	Propylene carbonate (PC) or glycerol carbonate (GC)
Contaminant resistance clay (CRC)	Unknown (proprietary)

The concept supporting the use of enhanced bentonites for hydraulic and chemical containment applications is illustrated conceptually in Figure 4.4. As previously noted concerning Figure

4.3, the *k* of natural bentonite tends to increase with increasing concentration of dissolved chemicals, *c*, particularly multivalent cations such as the metals. The objective of using enhanced bentonites is to provide greater resistance to hydraulic incompatibility, such that the relationship between *k* and *c* is shifted to maintain the lower *k* at a much higher *c*. Ideally, this improved chemical resistance offered by the enhanced bentonite would be sustainable such that *k* is independent of *c*. However, in reality, there is an upper limit on the ability of the enhanced bentonite to sustain chemical resistance and maintain a suitably low *k* (e.g., see Scalia et al. 2014; Chen et al. 2019; Li et al. 2021). Given the variability in the chemistries of liquids to be contained, as well as the variability in bentonites and associated chemical enhancements, the key practical consideration is to match a specific type of enhanced bentonite to a specific liquid to be contained such that the desired performance of the enhanced bentonite GCL (EB-GCL) is achieved.

For example, consider the *k* values shown in Figure 4.5 for a conventional GCL, a natural Na-bentonite, and a polymerized bentonite. The *k* values for the conventional GCL are the same as those for GCL2 shown in Figure 4.3 from Lee and Shackelford (2005), whereas the results for the bentonite and polymerized bentonite are from Scalia et al. (2014). As indicated in Figure 4.5, the trend in the *k* of the Na-bentonite with increasing $CaCl_2$ concentration of the permeant liquid is like that of the conventual GCL, with significantly higher *k* resulting from $CaCl_2$ concentrations ≥ 50 mM. In contrast, the polymerized bentonite maintained a low *k* over the entire range in $CaCl_2$ concentrations examined.

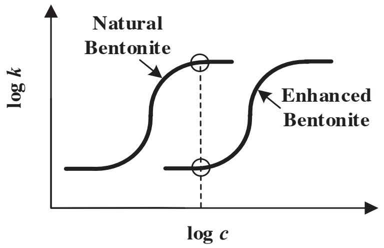

Figure 4.4 Concept of improved resistance to chemical incompatibility in hydraulic conductivity, *k*, with respect to the solute concentration, *c*, resulting from the use of enhanced bentonite relative to a natural (unenhanced) bentonite.

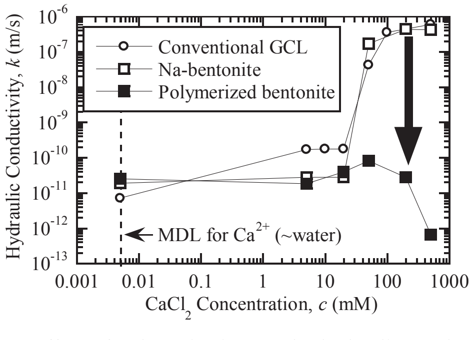

Figure 4.5. Effect of polymerization on the hydraulic conductivity of bentonite [MDL = Method Detection Limit] (data from Lee and Shackelford 2005; Scalia et al. 2014).

4.2.2 *Mechanisms for enhanced bentonites*

Scalia et al. (2018a) identified three potential mechanisms in polymer enhanced GCLs that can prevent alterations in *k*, viz., (i) prevention of cation exchange, (ii) intercalation or insertion of a chemical additive within the interlayer space of the montmorillonite mineral, and (iii) polymer clogging of interparticle, intraparticle, and/or intergranular (interaggregate) pores (see also Jo et al. 2006; Likos and Lu 2006; Salles et al. 2009; Acikel et al. 2018; Tian et al. 2019; Norris 2021). The use of chemical additives to prevent cation exchange was hypothesized early in the development of some enhanced bentonites (e.g., Flynn and Carter 1998; Trauger and Darlington 2000), but has not been supported in recent studies (Benson et al. 2014; Scalia et al. 2014; Tian et al. 2016a,b; Chen et al. 2019). Therefore, no further consideration of the prevention of cation exchange as the mechanism underlying the hydraulic compatibility of EB-GCLs is provided.

The concept of intercalation within the interlayer space of the montmorillonite mineral is illustrated schematically in Figure 4.6. Intercalation has been evaluated through determination of the basal spacing, d_{001}, via x-ray diffraction (XRD), spectroscopic techniques such as nuclear magnetic resonance (NMR) and Fourier-transform infrared (FTIR) (Gates et al. 2016; Bokobza 2018), and scanning electron microscopy (SEM) (Gates et al. 2016; Prongmanee et al. 2018b). Multiswellable bentonites (MSBs) amended with propylene carbonate (Onikata et al. 1999; Katsumi et al. 2008; Mazzieri et al. 2010) and glycerol carbonate (Fehervari et al. 2016a,b; Gates et al. 2016) have been shown to exhibit crystalline swelling over a wider range of solute concentrations. Crystalline swell enhancement via intercalation is described in detail in Onikata et al. (1999). Gates et al. (2016) note that other cyclic organic carbonates may provide similar crystalline swell enhancement. However, Onikata et al. (1999) showed that, in NaCl solutions with *I* greater than 0.75 M, crystalline swell did not occur despite enhancement. This hydraulic compatibility enhancement is consistent with the conceptual behaviour, shown in Figure 4.4.

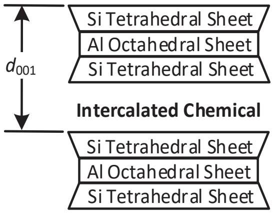

Figure 4.6. Schematic illustration of chemical intercalation of montmorillonite crystalline structure.

Polymer clogging of interparticle, intraparticle, and/or intergranular (interaggregate) pores, as illustrated schematically in Figure 4.7, has been demonstrated to be a dominant mechanism underlying improved hydraulic compatibility of some polymer enhanced bentonites in GCLs (Scalia and Benson 2016; Scalia et al. 2018a; Tian et al. 2019; Li et al. 2021; Norris 2021). The polymer occupies the most conductive pores within the enhanced bentonite, forcing flow to more narrow and tortuous flow paths, resulting in lower *k*.

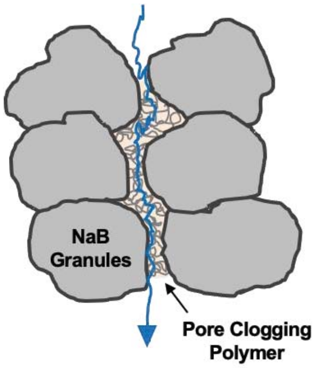

Figure 4.7. Polymer gel clogs pores between sodium bentonite (NaB) granules in a BPC-GCL (adapted from Gustitus et al. 2020).

Pore clogging was initially hypothesized as the mechanism underlying improved hydraulic compatibility of BPC by Scalia et al. (2014) based on observations of clogging of permeameter tubing by hydrogel and the lack of correlation between swelling and *k*. Lack of correlation between swelling and *k* also has been observed by Tian et al. (2016a,b) and others. Further support of this pore-clogging mechanism was provided by Tian et al. (2016b) via SEM images of dehydrated polymer within the interparticle pore space of BPC permeated with DW (see Figure 4.8). Recent pore-scale Imaging of BPC-GCLs permeated with high ionic strength bauxite liquor solutions also indicates that the *k* of the BPC-GCLs was controlled by pore-blocking with the polymer hydrogel (Li et al. 2021).

A topic of current research is the degree of permanence of pore-clogging polymer hydrogel within enhanced bentonites. Specifically, under what conditions does pore-clogging polymer hydrogel occur and attach to the mineral surface to render the enhancement effectively permanent. Elution of polymer enhancements (both linear polymers observed as high viscosity effluent and hydrogels) has been reported for numerous enhanced bentonites, including BPCs and CRCs (Scalia et al. 2014; Scalia and Benson 2016; Tian et al. 2016a,b; Chen et al. 2019; Tian et al. 2019). However, in some cases, this elution has only delayed the eventual onset of high *k*. In contrast, in other cases, the polymer enhanced bentonite has maintained a low *k* after polymer elution has ceased. It is important to recognize that the rate of polymer elution may be controlled by the apparent viscosity of the polymer at the shear rate imposed by the test conditions. This viscosity may be orders of magnitude greater than water, giving a polymer conductivity orders of magnitude lower than the hydraulic conductivity (to water) until water breakthrough occurs (Ejezie et al., 2018). Understanding elution behaviour is critical to forecasting the long-term stability of polymer-enhanced bentonites. Based on several sources, Norris (2021) summarizes the three potential mechanisms for anionic polymer adsorption to clay platelets as (i) complexation via anion exchange, (ii) hydrogen bonding or ligand exchange, and (iii) cation bridging. A detailed explanation of the adsorptive mechanisms between anionic polymers and Na-bentonite, and hydrogel formation and stability, is provided by Norris (2021).

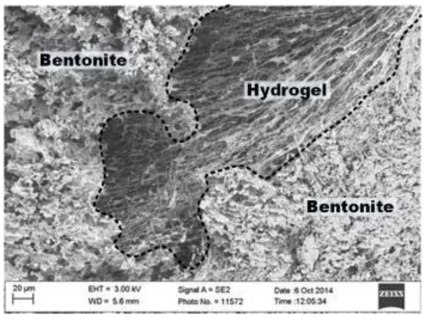

Figure 4.8. Scanning electron microscope image shows polymer hydrogel formation between bentonite particles/aggregates (from Scalia et al. 2018a).

4.3 *Enhancement chemicals*

4.3.1 *Polymers*

Polymerization is the process whereby small molecules referred to as monomers are combined chemically to form much larger, chainlike molecules or macromolecules. Polymers may be categorized as electrically neutral or nonionic and charged or ionic depending on the polymerization process. Charged polymers include cationic (positively charged), anionic (negatively charged) (e.g., Ashmawy et al. 2002; McRory and Ashmawy 2005; Ozhan 2018a,b), and zwitterionic (both positively and negatively charged). Cationic polymers and anionic polymers also are referred to as polycations and polyanions, respectively (e.g., Breen 1999). Polyanions are currently the most prevalent polymers used in enhanced bentonites (Scalia et al. 2018a), although polycations also have been used (e.g., Razakamanantsoa et al. 2012). In a polyanion, a negatively charged ionic group on the polymer repeating unit (e.g., negative carboxylate (COO^-) and negative sulfonate (SO_3^-)) is satisfied by a cation to maintain electroneutrality, similar to how bound cations satisfy the net negative structural charge of the montmorillonite crystal. The water solubility or degree of swelling of a polymer is attributed to the solvation of these ionic groups and associated counterions (Buchholz and Graham 1998).

Polymers can be linear, branched, or crosslinked. Linear polymers comprise single chains of repeated monomers. Branched polymers comprise branches of repeated monomer chains. Crosslinked polymers contain numerous repeated polymer chains linked together at multiple crossing points. These crosslinks can be physical (electrostatic interactions) and chemical (covalent), and can be incorporated in the polymer during synthesis or may result when, for example, the negative charge from two anionic groups are satisfied by a single divalent cation (termed cation bridging). Linear polycation and polyanion polymers will dissolve into water. Sufficient concentrations of dissolved polymers will increase the viscosity of the hydrating solution. Crosslinked polymers do not dissolve, but instead form hydrogels, which are three-dimensional networks of polymers that swell when hydrated and hold large quantities of water (Wichterle and Lím 1960; Bahram et al. 2016) via osmotic forces similar to montmorillonite, except that the montmorillonite platelets would be linked together into flexible networks that then respond to the same swell-controlling stimuli.

An example of a polyanion is polyacrylic acid (PAA) with negatively charged carboxyl groups. These carboxy groups are typically satisfied by protons or sodium ions during synthesis. PAA can be linear and aqueous miscible, and function as a flocculent (among numerous applications) that accumulates numerous clay platelets via cation bridging until a floc of sufficient size is formed to settle. PAA also can be crosslinked, often termed polyacrylate (PA), and used as a superabsorbent in baby diapers and other applications (Buchholz and Graham 1998).

As indicated in Table 4.1, two principle polyanions used to produce enhanced bentonites in EB-GCLs are sodium polyacrylic acid (Na-PAA) and sodium carboxymethylcellulos (Na-CMC). As noted earlier, Na-PAA can be linear or crosslinked, although Scalia et al. (2014) showed that the use of crosslinked Na-PAA was not effective for enhancing the hydraulic compatibility of Na-bentonite to high ionic strength $CaCl_2$ solutions. These and many other polymers have been evaluated for use in CRCs. Given the range of different polymers available, the number of potential polymers for use in enhanced bentonites is practically unlimited. However, a matter that always must be considered is the potential for degradation of the polymer, for example, by biodegradation. Many naturally derived polymers (e.g., xanthan and carboxymethyl-cellulose) are readily biodegradable. The chemicals used and species released by elution and/or degradation must be environmentally acceptable (for example, the release of acrylamide will be unacceptable in many jurisdictions).

4.3.2 *Cyclic organic compounds*

Cyclic organic carbonate (COC) compounds, such as propylene carbonate (PC) and glycerol carbonate (GC), have been proposed as swelling activation compounds capable of being intercalated and maintaining high swell in the presence of highly saline or otherwise high ionic strength solutions (Onikata et al. 1996; Gates et al. 2016), and PC is the chemical used for MSB (Onikata et al. 1999; Katsumi et al. 2008), whereas GC has been used to resist alterations in the *k* of bentonite permeated with hypersaline solutions (Fehervari et al. 2016a,b). Unlike the large polymer macromolecules, there is considerable evidence that COCs are intercalated and, through activation of crystalline swelling, maintain low *k* when subjected to permeation with chemical solutions of extreme chemistry. However, as previously noted, Onikata et al. (1999) showed that MSB did not maintain osmotic swell when subject to NaCl solutions with $I > 0.75$ M. Thus, COCs appear to be promising organic compounds for enhanced bentonites but may not necessarily provide unlimited enhanced performance as illustrated conceptually in Figure 4.4.

4.4 *Mixtures and processing*

The characteristics and properties of enhanced bentonites are a complex function of several factors, including but not limited to whether the constituent materials are mixed in a dry state or a wet state, the control exercised on the temperature and pH in the processing, and any resulting milling or other post mixing procedures that are implemented to control such factors as the particle (tactoid) and/or aggregate (granule) size of the final product for use in the GCL. To illustrate some of these factors, the general preparation procedures for the enhanced bentonites listed in Table 4.1 are described.

BPC (Table 4.1) was created by vigorously mixing dry Na-bentonite with an aqueous solution containing acrylic acid monomer and sodium persulfate as the thermal polymerization initiator, leading to the formation of sodium polyacrylate (SAP). Based on the analogies between the powder XRD patterns of sodium bentonite and BPC, Scalia et al. (2014) and Scalia and Benson (2017) concluded that the long-chain molecules of SAP do not intercalate between the montmorillonite platelets. They hypothesized that the low hydraulic conductivity of BPCs against concentrated solutions of multivalent cations should be ascribed to the partial occlusion of the conductive pores between montmorillonite tactoids rather than an improved crystalline swelling. This finding has led to the commercial BPCs manufactured today, which comprise a dry mixture of granular sodium bentonite and dry polymer particulate (Tian et al. 2016a,b, 2019; Chen et al. 2019; Gustitus et al. 2020). When contacted by the permeant solutions, the bentonite and polymer particulate hydrate, the latter forming a polymer gel that blocks the pores between the bentonite granules. SEMs presented by Tian et al. (2016b, 2019) illustrate how the polymer gel fills the intergranular pore space.

DPH-GCL (Table 4.1) is manufactured by vigorously mixing dry sodium bentonite with an aqueous solution containing the SAP, Na-CMC, and methanol to promote montmorillonite exfoliation and extrusion under vacuum until a bentonite sheet of reduced thickness and high bulk dry density is obtained. Although the exact mechanisms by which Na-CMC is adsorbed on the surface of montmorillonite crystals are still the subject of debate (Theng 2012), a consensus is that the aforementioned polymer can intercalate between the montmorillonite platelets, thus acting as a prop to hold open the interlayer pore space and to prevent flocculation or aggregation in the presence of aggressive liquids (Kolstad et al. 2004; Qiu and Yu 2008; Mazzieri and Di Emidio 2015).

HCs (Table 4.1) are bentonites modified with the anionic polymer, Na-CMC. However, instead of being vacuum-extruded as with DPH-GCL, the slurry of the bentonite, polymer, and water is oven-dried at 105°C. As a consequence of oven drying, the polymer is irreversibly adsorbed through the fixed cations to the negative surface of the clay, thereby promoting a dispersed structure of the clay lamellae resulting in more tortuous flow paths and lower hydraulic conductivity (Di Emidio 2010). This dehydration at high temperatures is hypothesized to improve the long-term containment performance against aggressive permeant solutions due to the reduced tendency of the polymer to be eluted. XRD analyses performed by Di Emidio et al. (2015) show an increase (i.e., 0.006 nm) in the basal spacing, d_{001}, of HCs with increasing polymer dosage. The characteristic peak of the enhanced montmorillonite broadened, shifting to the left, which corresponds to greater basal spacings and indicates that the polymer intercalated in the interlayer region between the platelets. Also, the interplatelet spacings increased with increasing polymer dosage. Similar results were obtained by Di Emidio (2010) for the DPH-GCL (i.e., 0.016 nm). Qiu and Yu (2008) demonstrated that CMC intercalated into the montmorillonite interlayer, expanding the interlayer distance from 1.25 nm to 1.47 nm as evidenced from the XRD pattern of the enhanced montmorillonite. This shift was greater and, therefore, more evident compared to that of the HC, probably due to the higher dosage of CMC in the study by Qiu and Yu (2008), which was 2-to-1 CMC-to-montmorillonite weight ratio or 100 times greater than that for HYPER clay with 2% polymer modification. Qiu and Yu (2008) also show results of a peak broadening that, according to the authors, most likely indicated a disordered intercalated structure. However, further research is needed to validate these assumptions, namely the adsorption of Na-CMC within the interlayer pore space based on a measured increase in the basal spacing of less than 0.1 Å and the improvement in the resistance against polymer elution as a result of oven-drying at 105 °C.

MSB (Table 4.1) is produced by mixing dry Na-bentonite with liquid propylene carbonate (PC), an aprotic polar organic solvent with a relative permittivity ranging from 66 to 71 at temperatures between 20 and 0 °C, respectively (Simeral and Amey 1970). Although relatively high if compared to the typical values measured for non-polar and other polar organic solvents, these values of the relative permittivity for PC are lower than the range of 80 to 88 associated with pure H_2O. Based on the powder XRD patterns presented by Onikata et al. (1999), PC is believed to intercalate between individual montmorillonite platelets and promote crystalline swelling as a result of increased solvation energy of the exchangeable cations (Mazzieri et a. 2010; Di Emidio et al. 2017; Scalia et al. 2018a).

As previously noted, commercially produced CRCs have been used extensively in practice for EB-GCLs (e.g., Ashwamy et al. 2002; Scalia et al. 2018a). However, as proprietary materials, CRCs are generally produced by unknown methods and/or materials, including in-situ polymerization, wet mixing, or dry mixing. Therefore, the proprietary nature of these materials precludes the ability to provide further details as to how these materials are produced.

4.5 *Properties of enhanced bentonites*

4.5.1 *Hydraulic conductivity*

The k of EB-GCLs versus conventional GCLs containing natural Na-bentonite is compared in Figure 4.9 as a function of *I* (Figure 4.9a) and pH (Figure 4.9b). Sources and screening methodology for the data shown in Figure 4.9 are provided in Scalia et al. (2018a). Enhanced bentonit and EB-GCLs generally exhibit lower *k* than natural Na-bentonite to permeant solutions with *I* greater than about 20 mM following the conceptual trend illustrated in Figure 4.4. In contrast, CRCs generally exhibit *k* similar to those for Na-bentonite over the same range in *I*. However, some CRCs exhibit lower *k* than Na-bentonite, similar to other enhanced bentonites. Of note, greater than 95% of the data shown in Figure 4.9 are from *k* tests performed at low effective stresses (<100 kPa). In general, the detrimental effect of hydraulic incompatibility is reduced or eliminated with an increase in effective stress, depending on the magnitude of the effective stress and the chemistry of the permeant liquid (Shackelford et al. 2000). Scalia et al. (2018a) provide additional discussion on the influence of effective stress on the *k* of enhanced bentonites based on limited available data.

Although data for the *k* of polymer EB-GCLs to extremely high and low pH solutions are limited, most of the available data are plotted in Figure 4.9b. At relatively neutral pH ($4 \leq pH \leq 10$), the *k* is primarily controlled by *I*. Low *k* at both low pH (< 1) and high pH (>13) are shown for BPC, illustrating the potential for enhanced bentonites to provide enhanced hydraulic compatibility in extreme pH environments. DPH-GCLs, BPC-GCLs, and some CRCs also show promise in hyperalkaline solutions (pH >12) (Tian and Benson 2019; Li et al. 2021). Additionally, linear and cross-linked polymers are well-known to be pH sensitive. However, the results of a recent study reported by Norris et al. (2020) indicated that a CRC permeated with a copper mining process solution with a pH of 1.2 resulted in a high k ($>1.0\times10^{-8}$ m/s). These results highlight the need for site-specific compatibility testing and additional research on the effects of pH on the hydraulic compatibility of different enhanced bentonites.

The significant variability in the data for CRCs and Na-bentonite shown in Figure 4.9 illustrates the need for k testing for specific combinations of CRCs and conventional GCLs with the actual liquids to be contained. Recent findings have shown that the current generation of enhanced bentonites that have been designed for specific applications (e.g., containment of coal combustion residuals) can provide necessary hydraulic compatibility for containment of high I leachates (e.g., Chen et al. 2019). However, given current limitations on screening methods for enhanced bentonite hydraulic compatibility, hydraulic compatibility testing using the actual liquids to be contained as permeant liquids is required for CRCs. In addition, compatibility testing must continue until all reaction fronts have passed through the test sample (Jefferis 1992).

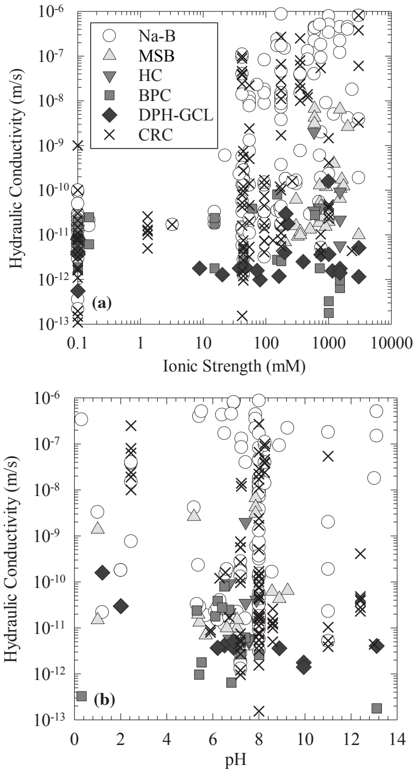

Figure 4.9. Hydraulic conductivity of natural Na-bentonite (Na-B), multiswellable bentonite (MSB), and polymer enhanced bentonites, including HYPER clay (HC), bentonite-polyacrylic-acid composite (BPC), dense prehydrated geosynthetic clay liner (DPH-GCL), and proprietary contaminant resistant clays (CRCs) versus (a) ionic strength and (b) pH of permeant liquid for all stress and prehydration conditions (from Scalia et al. 2018a,b).

4.5.2 *Membrane behaviour and solute diffusion*

Malusis and Shackelford (2002a) reported that GCLs containing natural Na-bentonite could perform as semipermeable barriers that restrict the migration of solutes via the process commonly known as anion exclusion (or negative adsorption). Kang and Shackelford (2011) showed that consolidation of GCLs (e.g., due to waste loading) could significantly enhance solute restriction and semipermeable membrane behaviour. Since solute restriction enhances the containment function of GCLs used as barriers, semipermeable membrane behaviour can have important practical implications (Scalia et al. 2018a,b).

Malusis and Shackelford (2002a) measured the chemico-osmotic or membrane efficiency coefficient, ω, as a function of the salt (KCl) concentration difference established across specimens of a conventional GCL using the closed-system apparatus described by Malusis et al. (2001). Values of ω represent the degree or extent of solute restriction and generally range from zero for a porous medium that does not exhibit solute restriction to unity for a porous medium that exhibits complete solute restriction (i.e., $0 \leq \omega \leq 1$). The results from Malusis and Shackelford (2002a) for the case where the porosity of the GCL specimen, n, was 0.74 are shown in Figure 4.10 in the form of ω as a function of the average KCl concentration established across the specimen, c_{ave}. As indicated by these results, the GCL specimen exhibited significant solute restricting capability (i.e., $0.14 \leq \omega \leq 0.68$) even at a relatively high n of 0.74, although ω decreased approximately semilogarithmic linearly with an increasing c_{ave}. The reason for this resulting trend is that, as c_{ave} decreases, the distributions in the negative electrostatic surface potentials or diffuse double layers (DDLs) associated with the surfaces of the individual clay particles (tactoids) are extended and overlap, resulting in a net negative potential between the particles such that anions are prohibited from entering the micropore. The associated cations are also prohibited from entering the micropore due to electroneutrality in the pore water. However, as c_{ave} increases, the negative electrostatic surface potentials become increasingly more compressed, such that the overlap is increasingly reduced and eventually eliminated to the extent that the micropores become accessible to the anions and the associated cations. This trend of decreasing ω with increasing c_{ave} reflects chemical incompatibility of the natural Na-bentonite within the GCL with respect to semipermeable membrane behaviour.

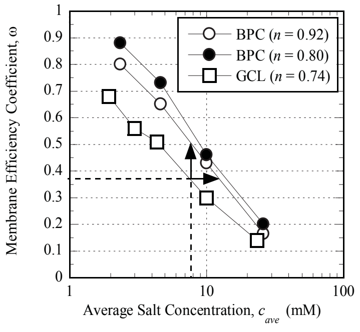

Figure 4.10. Improvement in semipermeable membrane behaviour of bentonite polymer composite (BPC) relative to that for a GCL containing Na-bentonite as a function of specimen porosity, n (data from Malusis and Shackelford 2002a and Bohnhoff and Shackelford 2013).

Bohnhoff and Shackelford (2013) used the same apparatus as that employed by Malusis and Shackelford (2002a) to measure ω for two specimens of BPC subjected to differences in KCl concentrations over a similar range in c_{ave}. Their results, also shown in Figure 4.10, indicated that both BPC specimens generally resulted in improved membrane behaviour, relative to that exhibited by the GCL specimen with natural Na-bentonite, even though the porosity of the two BPC specimens was greater than that for the GCL specimen. Thus, the BPC specimens reflected greater resistance to chemical incompatibility than the conventional GCL tested by Malusis and Shackelford (2002a), showing the advantage of using BPC in GCLs for chemical containment applications (e.g., also see Shackelford and Scalia 2016). However, Bohnhoff and Shackelford (2013) also noted that the trend of decreasing ω with an increasing c_{ave} for the two BPC specimens was similar to that for the GCL, indicating that the improved resistance to chemical incompatibility for the BPC was limited.

The semipermeable membrane behaviour of bentonites resulting from solute restriction affects the transport of solutes (ions) following three different mechanisms, i.e., hyperfiltration, chemico-osmotic counter advection, and restricted solute diffusion (Malusis et al. 2013, 2015, 2021). All three of these mechanisms work to reduce the solute mass flux relative to the case where there is no solute restriction (i.e., ω = 0), with restricted diffusion being the most relevant flux reduction mechanism when the hydraulic conductivity is sufficiently low such that diffusion is the dominant transport process. In this case, an osmotic effective diffusion coefficient, D^*_ω, can be defined for a given diffusing solute as follows (Dominijanni et al. 2018):

$$D^*_\omega = \left(1-\omega\right)\tau_m D_{s,0} \tag{4.2}$$

where τ_m is the dimensionless matrix tortuosity factor, which accounts for the tortuous nature of the solute diffusive pathways through the porous medium, and $D_{s,0}$ is the free-solution (aqueous-phase) diffusion coefficient of the salt as defined by Shackelford and Daniel (1991). For a given τ_m and $D_{s,0}$, the relationship between D^*_ω and ω given by Eq. 4.2 is linear as first postulated by Manassero and Dominijanni (2003).

For example, Mazzieri et al. (2010), Malusis and Daniyarov (2016), Di Emidio et al. (2015), and Bohnhoff and Shackelford (2015) conducted laboratory tests for the simultaneous measurement of ω and D^*_ω on specimens of MSB, DPH-GCL, HC and BPC, respectively, subjected to single salt aqueous solutions (i.e., solutions of KCl or $CaCl_2$). The experimental results of these studies have been re-evaluated herein in accordance with Eq. 4.2 based on a single value of τ_m for each enhanced bentonite and in terms of the restrictive tortuosity factor $\tau_r = D^*_\omega / \tau_m D_{s,0}$, which accounts for the effect of anion exclusion in semipermeable clays (Malusis and Shackelford 2002b), and the resulting values of τ_r are shown as a function of ω in Figure 4.11. The generally good agreement between the experimental data and the relationship given by Eq. 4.2 suggests that the proposed theoretical framework upon which Eq. 4.2 is based is reasonable for interpreting the influence of the pore-scale electrical interactions on solute diffusion in enhanced bentonites.

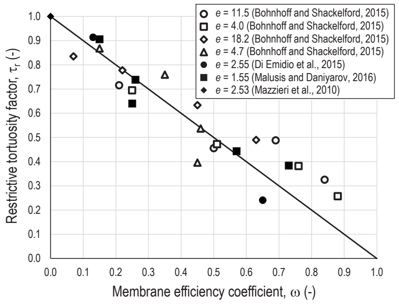

Figure 4.11. Measured values of the restrictive tortuosity factor versus measured membrane efficiency coefficient, ω, compared with the theoretical interpretation based on Eq. 4.2 (continuous line) [*e* = void ratio].

The aforementioned values of τ_m determined for the enhanced bentonites are compared with the corresponding values that were determined for natural Na-bentonite and conventional GCL specimens by Dominijanni et al. (2018) and Manassero (2020) in Figure 4.12. Also shown in Figure 4.12 is the empirical relationship between τ_m and n based on the following exponential function adopted by Olsen and Kemper (1968), among others, to investigate the changes in diffusive tortuosity for both saturated and unsaturated porous media:

$$\tau_m = \frac{\chi}{n} \cdot 10^{\left(\lambda \cdot n\right)} \tag{4.3}$$

where the dimensionless parameters χ and λ were calibrated using the aforementioned experimental data. Regardless of the type of testing apparatus and solutes contained in the solutions, the values of τ_m follow a non-linear trend versus porosity, suggesting that the degree of interconnectivity of the conductive pores in the enhanced bentonites is similar to that of unenhanced bentonites at a given porosity. However, the τ_m values determined for the BPC tested by Bohnhoff and Shackelford (2015) tend to be lower than the those based on the overall trend for the other bentonite specimens, suggesting that the enhancement mechanism for the BPC can be attributed to partial clogging of the conductive pores such as previously indicated in Figure 4.8 and, therefore, to more meandering channels, greater tortuosity (lower τ_m), and lesser solute diffusion.

Even though the fitting parameters used for the trends described in Figure 4.12 based on Eq. 4.3 were derived from the results of diffusion measurements, Al-Tarawneh et al. (2009) observed that the differences in the geometric tortuosity factors estimated either via diffusion or *k* tests are negligible when the uniformity coefficient, C_u, is close to unity (i.e., narrow grain-size distribution), as typically is the case with bentonites used in geoenvironmental containment applications. Thus, Eq. 4.3 likely can be extended to provide an estimate of the matrix tortuosity factor to be used in the Kozeny-Carman equation (Kozeny 1927; Carman 1956) for the evaluation of the bentonite *k*.

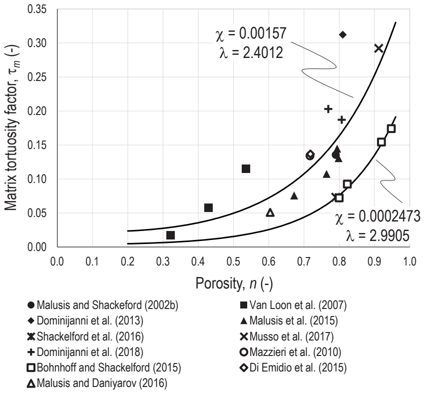

Figure 4.12. Matrix tortuosity factor, τ_m, as a function of the porosity, *n*, for natural Na-bentonite (closed symbols) and enhanced bentonites (open symbols) (note: the continuous lines represent the interpolation curves based on Eq. 4.3).

4.6 *Current and future directions*

The current and future directions of the study of enhanced bentonites are focused on resolving questions and potential issues related to using these materials in GCLs and optimizing materials and methods for production. These directions include providing a better understanding of the mechanisms associated with the long-term performance of EB-GCLs and resolving potential issues related to polymer elution, wet-dry cycling, and non-standard temperatures (Scalia et al. 2018a). Also, there is a need to develop screening methods for enhanced bentonites that provide a quick and reliable indication of the expected performance of a specific enhanced bentonite for a specific containment liquid. Some discussion of ongoing efforts to address these issues follows.

4.6.1 *Mechanisms*

Critical to predicting the long-term hydraulic behaviour of enhanced bentonites and EB-GCLs is understanding the mechanisms governing the hydraulic compatibility of these materials (e.g., see Norris 2021). For example, the long-term *k* tests performed by Katsumi et al. (2008) using single-salt permeant solutions with specimens of MSB and DPH-GCL, by Di Emidio et al. (2015) with a HYPER clay (HC) specimen, and by Scalia et al. (2014) with BPC specimens are interpreted herein to gain insight into the microstructural arrangement of these enhanced bentonites and EB-GCL using a modified Kozeny-Carman equation as described by Guarena et al. (2020) and Manassero (2020). In this case, except for the HC specimen, a value of $N_{l,AV}$ was determined from each measured value of *k* based on the known values for the CEC, *e*, and the specific gravity (G_s) for the tested enhanced bentonites, and τ_m was assessed via Eq. 4.3. For the HC specimen that was tested to determine both the chemico-osmotic and diffusion properties, a τ_m of 0.137 was obtained via extrapolation of the apparent tortuosity factor $\tau_a = \tau_r \tau_m$ to $\omega = 0$ corresponding to $\tau_r = 1$ (Malusis and Shackelford 2002b; Shackelford and Moore 2013; Dominijanni et al. 2018).

The resulting experimental values of $N_{l,AV}$ are shown in Figure 4.13 versus the micro-void ratio (e_m) and are compared to the corresponding iso-concentration curves based on the FBS represented by Eq. 4.1 ($N_{l,AV0}$ = 1.56; α = 8.82; β =10.01) as calibrated by Manassero (2020) using the experimental results provided by Petrov and Rowe (1997) for *k* of a conventional needle-punched GCL prehydrated with distilled water. Note that the salt concentration used in Eq. 4.1 was expressed as millinormality (mN) instead of millimolarity (mM) (e.g., 50 mM = 100 mN for $CaCl_2$ whereas 50 mM = 50 mN for NaCl).

As shown in Figure 4.13a, all of the calculated $N_{l,AV}$ values for the MSB specimens based on permeation with the concentrated electrolyte solutions are greater than the model predictions based on Eq. 4.1 as calibrated with respect to the results from Petrov and Rowe (1997), likely due to the absence of prehydration by exposure or permeation with DW prior to permeation with the electrolyte solutions (e.g., Shackelford et al. 2000) in the case of the MSB specimens tested by Katsumi et al. (2008). The reduction in *k* for the MSB specimens permeated with electrolyte solutions containing NaCl at intermediate concentrations (200 < c_s < 1000 meq/L) relative to that of the natural Na-bentonite can be attributed to the influence of the PC on the extent of osmotic swelling. Even though crystalline swelling (i.e., increased basal spacing) due to the PC cannot be excluded, the reduction in *k* also may be attributed to the lower relative permittivity of PC compared to that of molecular water (H_2O), which can be effective in blocking the negative electric charge carried by the associated montmorillonite crystals resulting in a closer intertactoid distance under the same effective confining stress. This postulated decrease in intertactoid distance is reflected by the low e_m values in Figure 4.13a, which correlate with the low *k* values based on the modified Kozeny-Carman equation.

Unlike MSB, the ability of DPH-GCL to maintain a dispersed bentonite fabric and, hence, a low *k* upon permeation with concentrated $CaCl_2$ solutions, as demonstrated by $N_{l,AV}$ values that are close to the iso-concentration curve for DW (Figure 4.13b), is attributed to the treatment procedure for DPH-GCL, which involves prehydration with the aqueous solution of Na-PAA and Na-CMC followed by preconsolidation (densification) through vacuum-extrusion. In this regard, low hydraulic conductivity also was evident for the HC specimen, which again is consistent with low $N_{l,AV}$ values (Figure 4.13c). However, unlike the tests performed with DPH-GCL by Katsumi et al. (2008), the salt solutions used by Di Emidio et al. (2015) for HC were not sufficiently concentrated to indicate the effectiveness of Na-CMC in favouring a dispersed microstructure upon exposure to harsh chemical environments. Furthermore, although the preparation of HC involves a polymeric solution similar to that used for DPH-GCLs, HCs are oven-dried. As such, the contribution of densification to the long-term barrier performance is negated.

As the contribution due to densification may be significant (Kolstad et al. 2004), further study is needed to investigate whether treatment with Na-CMC is adequate for aggressive leachates in the absence of the preconsolidation effect. In this regard, Fan et al. (2022) have shown recently that the *k* of HC is 1-2 orders-of-magnitude lower relative to that of natural Na-bentonite when permeated with landfill leachate laden with heavy metals. Di Emidio et al. (2019) showed that the *k* of HC (non-prehydrated) to seawater (*I* = 0.77M) under low confining stress (14 kPa) remained on the order of 10^{-11} m/s (2 orders-of-magnitude lower than untreated clay) in the long-term after 80 pore volumes of flow over about 8.5 years of permeation.

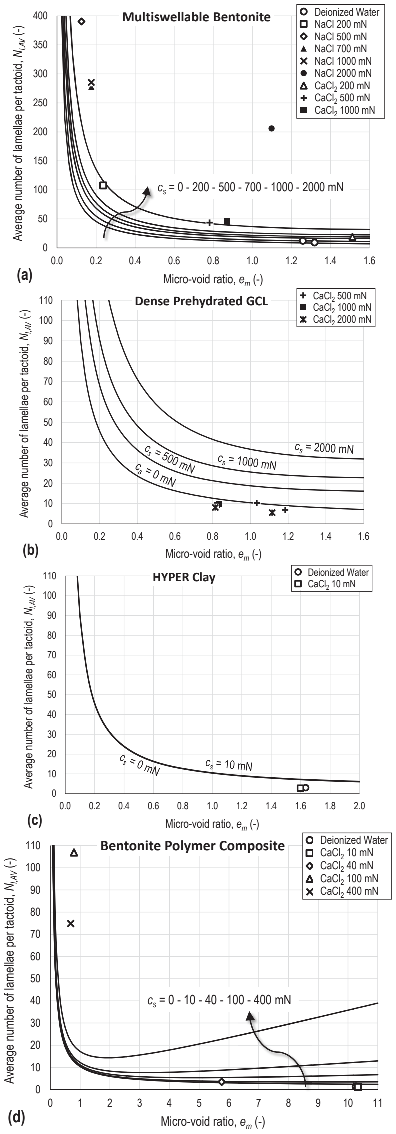

Figure 4.13. Comparison between the iso-concentration curves given by Eq. 4.1 (continuous lines), as calibrated on the hydraulic conductivity test results by Petrov and Rowe (1997), and the values of the average number of lamellae per tactoid, $N_{l,AV}$, obtained for: (a) the MSB tested by Katsumi et al. (2008); (b) the DPH-GCL tested by Katsumi et al. (2008); (c) the HYPER clay tested by Di Emidio et al. (2015); (d) the BPC tested by Scalia et al. (2014).

The relatively high $N_{l,AV}$ values observed for the BPC specimens tested at the highest $CaCl_2$ concentrations (Figure 4.13d) can be attributed, similar to the MSB specimens, to direct permeation with the chemical solutions, i.e., without prehydration. Furthermore, the reduction in k noticed by Scalia et al. (2014) in comparative tests performed on natural Na-bentonite specimens (e.g., see Figure 4.5) is related to the low τ_m values based on Eq. 4.3 and the low e_m values evident in Figure 4.13d. However, in contrast to MSB, the decrease in the pore volumes accessible to the solvent and solute transport with increasing $CaCl_2$ concentration is caused by the polymer hydrogel partially occluding the bentonite pores, as previously noted with respect to Figure 4.8.

Given the wide range of void ratios and salt concentrations of the permeant solutions used by Katsumi et al. (2008), an evaluation of the reliability of the theoretical framework based on the FBS (Eq. 4.1) can be undertaken by adjusting the $N_{l,AV0}$, α and β parameters using the dataset pertaining to the MSB specimens. As shown in Figure 4.14, ordinary least-squares regression of experimental versus theoretical $N_{l,AV}$ values resulted in $N_{l,AV0} = 1.00$, $\alpha = 27.51$, and $\beta = 77.42$ with a coefficient of determination (R^2) of 0.9151, which is considered satisfactory given the complexity of the mechanisms governing bentonite flocculation/dispersion. The resulting good agreement shown in Figure 4.15a suggests that the theoretical framework is reliable for describing the macroscopic effects of the microstructural arrangement of smectitic clays for both prehydrated and non-prehydrated specimens.

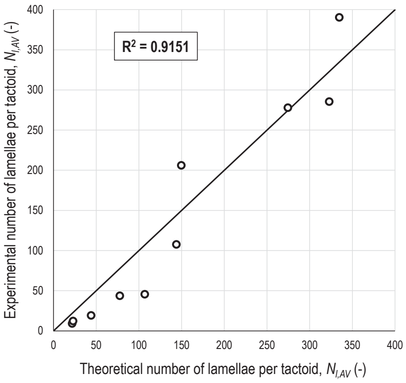

Figure 4.14. Experimental versus the theoretical average number of lamellae per tactoid, $N_{l,AV}$, using the hydraulic conductivity test results provided by Katsumi et al. (2008) for non-prehydrated MSB specimens and the related calibration of the FBS parameters (Eq. 4.1).

As shown in Figure 4.15b, despite the relatively limited available data, interpretation of the hydraulic conductivity tests performed by Scalia et al. (2014) for BPC specimens also yields $N_{l,AV}$ values that agree reasonably well with those from Eq. 4.1 calibrated using the results for the MSB specimens tested by Katsumi et al. (2008). This consistency suggests that the microstructures of both MSB and BPC are not affected significantly by the presence of the PC or the long-chain Na-PAA (Table 4.1), respectively, which impact the accessible pores and/or the degree of interconnectivity of such pores, whereas a more prominent role is likely attributable to the order in which the bentonite specimens are permeated with the electrolyte solutions. Thus, only the treatment procedure developed for HC and DPH-GCLs is effective in maintaining a dispersed fabric regardless of the ionic strength of the permeant solution (Figure 4.13b), thus supporting the hypothesis that Na-CMC is intercalated and acts as a prop between the montmorillonite unit layers.

The detrimental impact on the bentonite barrier performance due to the absence of prehydration is illustrated further in Figure 4.16, wherein the comparison between the iso-concentration curves associated with both the prehydrated GCL tested by Petrov and Rowe (1997) and the non-prehydrated MSB tested by Katsumi et al. (2008) reveals that the most significant differences in the $N_{l,AV}$ parameter occur at medium-to-high salt concentrations. In contrast, less marked differences are observed at low salt concentrations.

The iso-concentration contours (Figure 4.16) from Eq. 4.1 based on the results for the prehydrated GCLs are in good agreement with the data for the enhanced bentonites treated with Na-CMC (i.e., DPH-GCL and HC), and corresponding $N_{l,AV}$ values for DPH-GCL and HC are practically independent of the salt concentration of the permeant solution. This result means that, from a practical perspective, the α and β parameters in Eq. 4.1 are close to zero. Therefore, for this kind of polymeric additive (i.e., Na-CMC), the related physico-chemical mechanism likely is intercalation that maintains separation between the individual lamellae resulting in a dispersed microfabric. Thus, the MSB and BPC maintain low values of k at a high salt concentration (Figure 4.15) due to pore clogging and/or a reduction in the intertactoid pore volume (microscopic pores) even with flocculation, whereas the Na-CMC polymer apparently maintains a dispersed fabric of the enhanced bentonite, which is characterized by low values of $N_{l,AV}$.

As a practical consequence, in the case of MSB and BPC, even if a low k can be maintained in the long-term in the presence of concentrated (high I) permeant solutions, the persistence of osmotic efficiency and the related membrane behaviour is doubtful, as reflected by the results in Figure 4.10. In contrast, the Na-CMC enhanced bentonites appear to maintain a low k in the presence of concentrated permeant solutions and a significant osmotic efficiency when exposed to solutions with up to the medium salt concentrations. Nonetheless, further experimental and theoretical studies are needed to validate these preliminary conclusions.

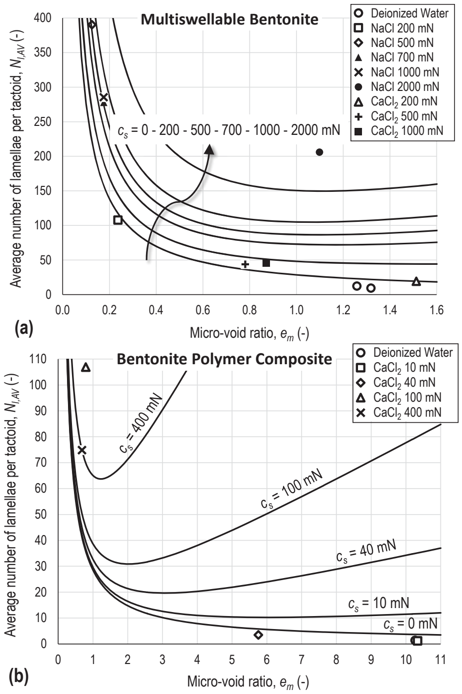

Figure 4.15. Comparison between the iso-concentration curves of the FBS given by Eq. 4.1 (continuous lines), as calibrated using the results of the hydraulic conductivity tests performed on MSB specimens by Katsumi et al. (2008), and the values of the average number of lamellae per tactoid, $N_{l,AV}$, for (a) the MSB tested by Katsumi et al. (2008), and (b) the BPC tested by Scalia et al. (2014).

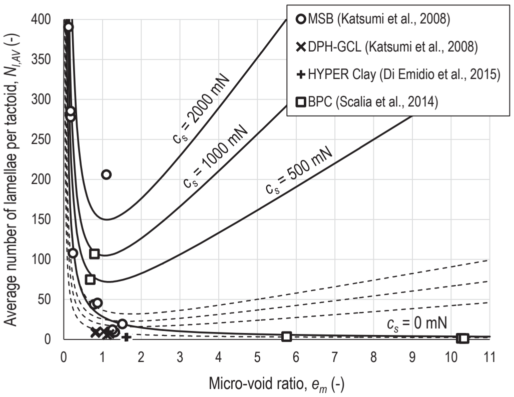

Figure 4.16. Iso-concentration curves based on Eq. 4.1 calibrated using the results of the hydraulic conductivity tests performed by Katsumi et al. (2008) on non-prehydrated MSB specimens (continuous lines) and by Petrov and Rowe (1997) on prehydrated GCL specimens (dashed lines).

4.6.2 *Polymer elution*

Clogging of conductive intergranular or interaggregate pores by polymer hydrogel is the mechanism responsible for the low k of BPC-GCLs, and the reason k of these materials is not directly related to swelling (Scalia et al. 2014; Scalia and Benson 2017; Tian et al. 2019; Li et al. 2021). Scalia et al. (2014) observed elution of polymer hydrogel from k tests performed on BPC with high polymer loading, viz. 28.5% by mass (Figure 4.17). This eluted polymer clogged the small (3.2 mm) inside diameter effluent tubing of the flexible-wall permeameter such that the apparent *k* was observed to decrease to a value on the order of 1.0×10^{-13} m/s (see Figure 4.5). Upon cleaning the permeameter tubing, the apparent *k* increased approximately 2-3 orders of magnitude, and after multiple cleaning cycles, eventually stabilized. Similar observations have been made by Scalia and Benson (2017), Chen et al. (2019), Tian et al. (2019), and Li et al. (2021), albeit generally to a lesser extent, commensurate with the lower polymer loading of the later generation polymer EB-GCLs that were tested. Scalia et al. (2014) hypothesized that the same clogging effect observed in the flexible-wall permeameter tubing also was occurring within the BPC pores. When permeant liquids with high *I* prevent osmotic swelling of the bentonite, the polymer hydrogel may migrate to occupy intergranular pores yielding low *k*.

Figure 4.17. Mobile polyacrylate hydrogel crosslinked with Ca^{2+} eluted from flexible-wall permeameter (note: scale is in mm).

As previously noted, the presence of polymer hydrogel within polymer EB-GCL pores was documented using SEM images by Tian et al. (2016, 2019) (see Figure 4.8). Recent studies have shown that: (i) elution behaviour, is sensitive to the chemical nature of the permeant liquid (Scalia et al. 2014; Tian et al. 2019); (ii) elution of a greater fraction of the polymer from an EB-GCL correlates with a higher *k* (Chen et al. 2019; Tian et al. 2019); and (iii) retention of a greater fraction of polymer corresponds to a greater discrepancy between swelling and *k*, i.e., low *k* associated with low swelling. Lower *k* also has been shown to correlate to higher initial polymer loading (Zainab and Tian 2020; Li et al. 2021). These observations illustrate that, for the polymer to reach intergranular pores and affect *k*, sufficient polymer must be present, the polymer must be evenly distributed, and the polymer must be retained in the bentonite pores. Additional study is needed to understand the mechanisms that lead to polymer redistribution and retention within polymer EB-GCL pores and to understand better the mechanisms governing hydraulic compatibility of polymer EB-GCLs. Methods to measure polymer loading in EB-GCLs are described by Gustitus et al. (2020) and Norris et al. (2022).

The eluted polymer may be in the form of the crosslinked hydrogel (e.g., Figure 4.17) or high viscosity (sticky) effluent from linear polymer. Unfortunately, current standard methods for hydraulic compatibility tests (e.g., ASTM D6766) do not consider polymer elution. Thus, additional care should be taken to ensure that the measured *k* is not the result of clogged porous stones or tubing. This possibility can be evaluated by reassembling the permeameter and passing the permeant liquid through the tubing under the same differential head between the platens. Tian et al. (2019) used total organic carbon analysis (ASTM D4839) to measure effluent polymer content, although the study of additional methods is ongoing. The necessity to continue permeation until no further polymer is eluted (mobile) requires further research. Understanding polymer elution behaviour is critical to understanding the long-term behaviour of EB-GCLs and ensuring that laboratory hydraulic compatibility results are accurate (Gustitus and Benson 2020).

4.6.3 *Wet-dry cycles in polymerized clays*

Conventional GCLs used as containment barriers can be exposed to changes in the degree of hydration, such as periodic precipitation events (e.g., daily, weekly, monthly, seasonal) as well as seasonal temperature variations, especially when the GCL is placed close to the ground surface as in the case of cover systems. For these reasons, several studies have evaluated the effects of wet-and-dry cycling on the hydraulic performance of conventional GCLs (e.g., Lin and Benson 2000; Bouazza et al. 2007; Rowe et al. 2011; Hoai and Mukunoki 2020).

Although natural Na-bentonite used in GCLs has exhibited considerable self-healing capability upon rehydration after being subjected to defects (e.g., Sari and Chai 2013; Rowe and Li 2020), several studies have indicated significant detrimental impacts resulting from wet-dry cycling (e.g., Hoai and Mukunoki 2020), especially in the case where hydration or wet-dry cycling is accompanied by cation exchange of divalent cations (e.g., Ca^{2+}) in the pore water for initially bound monovalent cations, primarily the Na^{+} associated with the Na-bentonite, in the GCL (e.g., Lin and Benson 2000; Bouazza et al. 2006, 2007; Thiel et al. 2006; Benson and Meer 2009; Rowe and Abdelatty 2011; Tang et al. 2011; Bradshaw et al. 2013; Rowe and Hosney 2013; De Camillis et al. 2014; Mukunoki et al. 2014; De Camillis et al. 2016, 2017; Yu and El-Zein 2019; Yu et al. 2020; Lieske et al. 2020; Rowe and Hamdan 2021; Khan et al. 2021). In this latter case, the effect of the cation exchange is to reduce osmotic swell such that upon rehydration, the *k* can be detrimentally impacted, resulting in poor performance on the GCL (e.g., James et al. 1997; Meer and Benson 2007; Benson and Meer 2009; Benson et al. 2010a). In particular, thermal cycles combined with cation exchange have been shown to significantly affect the hydraulic performance and k_w of some NaB-GCLs due to the loss of swell capacity and ability to seal needle-punched bundles (Rowe et al. 2017, 2019, 2021).

The use of EB-GCLs for increased resistance to downslope erosion of GCLs in exposed composite liners and chemical attack and improved hydraulic performance in situations where the barrier is subjected to wet-dry cycling has been suggested.

However, only a limited number of studies have evaluated the impact of wet-dry cycling on the hydraulic performance of EB-GCLs.

De Camillis et al. (2016, 2017) studied the performance of polymer modified GCLs when cation exchange was combined with wet-and-dry cycling. The performance of untreated Na-bentonite after wet-and-dry cycling in seawater (SW) was compared to that of a polymer treated Na-bentonite. The clay was treated with 2% and 8% by dry mass of Na-CMC anionic polymer following the HYPER clay (HC) procedure (Di Emidio 2010). In De Camillis et al. (2016), the results of swell index tests indicated that the swelling ability increased as the polymer content increased. Similar results were obtained from one-dimensional swell tests. As shown in Figure 4.18, the swelling of HC with 8% polymer (HC+8%) after the 6th wet-dry cycle was still considerably greater relative to that for the Na-bentonite under the same conditions and surprisingly similar to the swell of the Na-bentonite in contact with DW. Also, as shown in Figure 4.19, the *k* of the untreated Na-bentonite increased sharply within three wet-dry cycles. Cracks formed in the Na-bentonite by drying remained intact, resulting in preferential flow paths and high *k*. In contrast, the HC specimens maintained a *k* to seawater lower than 1.0×10^{-9} m/s. During the 4th wet-dry cycle, the *k* of untreated bentonite was three orders-of-magnitude higher than that of the HC with 2% polymer (HC+2%).

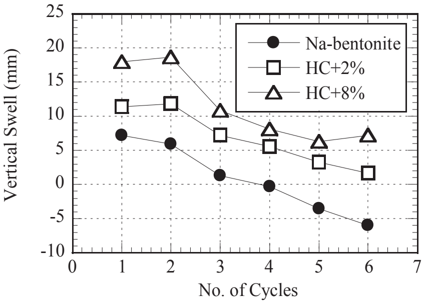

Figure 4.18. Swell of untreated Na-bentonite and HYPER clay with 2% or 8% Na-CMC anionic polymer (HC+2% and HC+8%) at the end of each wetting cycle (De Camillis et al. 2016).

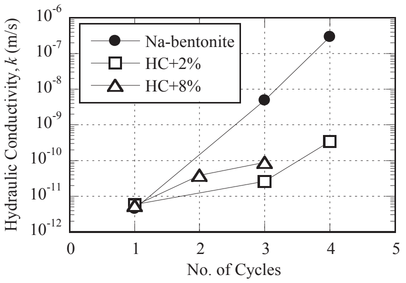

Figure 4.19. Hydraulic conductivity of untreated Na-bentonite and Hyper clay with 2% or 8% Na-CMC anionic polymer (HC+2% and HC+8%) permeated with seawater after each wetting cycle.

De Camillis et al. (2017) evaluated cracks by means of micro computed tomography (µCT) scanning analysis on untreated Na-bentonite and the HC+2% and HC+8% after six wet-dry cycles with seawater. µCT is a non-destructive three-dimensional (3D) Imaging and analysis technique, which is frequently used in the study of geomaterials (Cnudde and Boone 2013). The µCT analysis demonstrated a better self-healing capacity (smaller volume of cracks) generated on the HC specimens relative to the untreated Na-bentonite.

The 3D visual results of the µCT scans for the different samples (Na-bentonite, HC+2% and HC+8%) after the 3rd drying stage and during the 4th wetting stage are shown in Figure 4.20. The analysis also allowed determining the volume percentage of the cracks compared to the coherent zone of the samples. Visually, the difference between the different samples is clear, i.e., the cracks in the untreated Na-bentonite are larger compared to those for the HC specimens. The cracks in the HC specimens occur mainly in the upper parts of the chosen subsection and did not propagate downwards. During the wetting cycle, the bentonites swell, thereby closing the drying cracks. The µCT scans revealed more unhealed cracks for the untreated Na-bentonite relative to the HC specimens. This observation is more evident for the HC+8% specimen, wherein almost all cracks are closed.

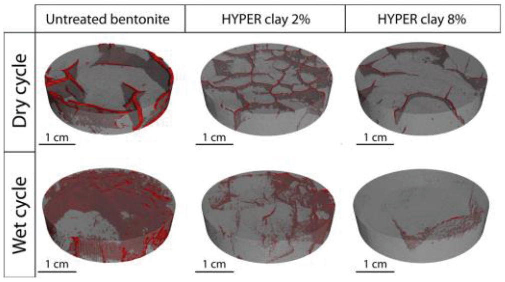

Figure 4.20. 3D rendered results of the µCT scan of untreated bentonite, HYPER clay with 2% or 8% Na-CMC anionic polymer after the 3rd dry cycle and during the 4th wet cycle (note: cracks are displayed in red).

The untreated Na-bentonite developed cracks up to 6.0% of the total initial volume. In contrast, the volume of cracks in the HC+2% and HC+8% specimens were lower than 1.0% of the initial volume, i.e., 0.94% and 0.12%, respectively (Figure 4.21). During the wetting cycle, the volume of the cracks decreased for all clays. After wetting, the volume of the cracks in the untreated Na-bentonite specimen was 1.2% of the total volume, whereas those for the HC+2% and HC+8% specimens were 0.45% and 0.05%, respectively.

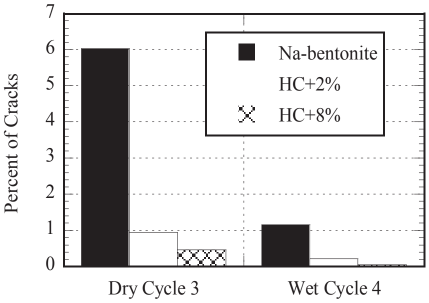

Figure 4.21. Percent volume of cracking in untreated Na-bentonite and HYPER clay with 2% or 8% Na-CMC anionic polymer (HC+2% and HC+8%) at the end of the 3rd dry and 4th wet cycles.

Results of several studies involving enhanced bentonites or EB-GCLs subjected to wet-and-dry cycling using electrolyte solutions are shown in Figure 4.22. Mazzieri and Pasqualini (2008) and Mazzieri et al. (2016) reported the performance of DPH-GCL and MSB subjected to wet-and-dry cycling with a $CaCl_2$ solution and seawater (SW). The DPH-GCL tested by Mazzieri and Pasqualini (2008) was subjected to four wet-dry cycles with 0.0125 M $CaCl_2$ ($I = 0.075$ M) and dried at 35°C until the weight was constant. The DPH-GCL and MSB tested by Mazzieri et al. (2016) were subjected to five wet-dry cycles with SW ($I = 0.71$ M) and dried at 35°C until the weight was constant. The GCL with HC (GCL w/HC) is the needle-punched GCL prototype with HC tested by De Camillis et al. (2016, 2017) and De Camillis (2017), which was subjected to four wet-dry cycles first and then permeated with SW ($I = 0.77$ M). The hydration was either first with DW and then for three cycles with SW or simply with four wet-dry cycles using SW. The GCL w/HC specimens were dried at 60°C until the weight was constant.

The GCLs tested by De Camillis (2017) were exposed to the worst conditions, as the hydrating liquid was the most aggressive (i.e., $I = 0.77$ M vs. $I = 0.075$ M and $I = 0.71$ M) and the drying temperature was the highest (60ºC vs. 35ºC), resulting in severe desiccation. In addition, the needle-punched GCL produced more cracks relative to the MSB and DPH-GCL. Overall, the GCL w/HC specimens provided the lowest k values, suggesting a good hydraulic performance in contact with SW.

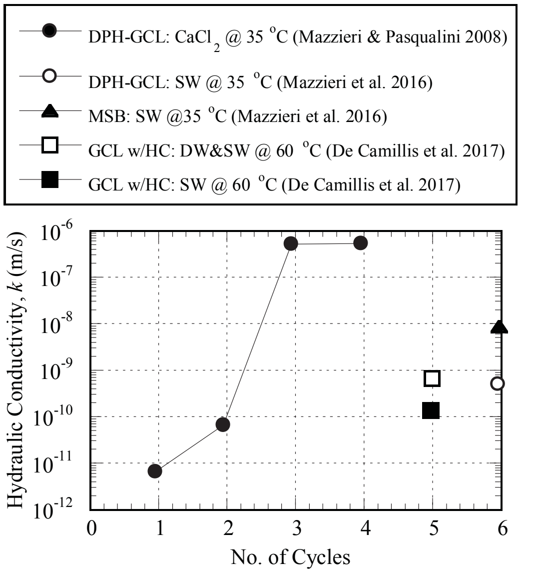

Figure 4.22. Hydraulic conductivity of several enhanced bentonites permeated with different liquids at different temperatures as a function of the number of wet-dry cycles (DW = deionized water; SW = seawater).

Lieske et al. (2020) addressed the cracking and self-healing capacity of GCLs subjected to drying and wetting in $CaCl_2$ salt solutions. The evolution of cracks and the cracking patterns were evaluated via X-ray Imaging, and soil-water retention behaviour was tested on the raw bentonite using micro-cells and a chilled-mirror hygrometer. The morphology of the crack patterns in the GCLs was highly affected by the pore fluid, which was attributed to reduced tensile strength caused by the salt induced aggregation.

Khan et al. (2021) investigated the suction of GCLs prototypes containing HC+8% compared to untreated GCLs. The matric suction of the GCLs was measured by filter paper test and humidity sensors. Different electrolytic solutions were used as the permeant liquids. The soil-water retention capacity was greater for the GCL with HC+8% relative to the GCL with the untreated Na-bentonite.

The aforementioned studies suggest that enhanced bentonites, particularly HC, can provide improved resistance to the detrimental impacts resulting from wet-and-dry cycling in the presence of electrolyte solutions relative to that for unenhanced Na-bentonites. However, the unanswered questions from all of these studies are: (a) for how long does the enhancement of the bentonite provide positive effects, and (b) what are the consequences of elution of the polymer? There is a paucity of data addressing these questions; however, the available data, discussed subsequently, raises some questions about long-term performance of at least three enhanced bentonites.

Leaving a composite liner comprising a geomembrane over a GCL exposed to solar radiation will subject the GCL to repeated hydration and dehydration (i.e., wet-dry) cycles. This is known to induce significant shrinkage of some Na-bentonite GCLs (Thiel and Richardson 2005; Thiel et al. 2006; Bostwick et al. 2010; Rowe et al. 2011, 2013b, 2018; Brachman et al. 2018) as well as downslope erosion of the bentonite in the GCL (Rowe et al. 2014, 2016; Ashe et al. 2015; Brachman et al. 2015; Rentz et al. 2016a,b).

Enhanced bentonite in an EB-GCL has been hypothesized to prevent downslope erosion. However, this hypothesis and associated laboratory testing have not explored the effects of cation exchange and polymer elution with repeated wet-dry cycles in the field. To test this hypothesis, in 2011, Rowe et al. (2016b) constructed one section of a full-scale field liner at the Queen's University Environmental Liner Test Site (QUELTS II) with an EB-GCL containing a polyacrylamide enhanced bentonite.

After 15 months of field exposure, there was significant evidence of polymer elution to the surface of the EB-GCL, which had become very slick and slippery. In addition, there was evidence that evaporated, and subsequently, condensed water had been flowing down the slope in rivulets. As a result, there was 132 mm of panel overlap shrinkage (35% greater than the comparable NaB-GCL with traditional Na-bentonite), although no downslope erosion was observed. Thus, the EB delayed downslope erosion relative to the companion product with NaB. However, 15 to 28 months of flow over the GCL washed the eluted polymer away and, after 28 months of exposure, downslope erosion was observed for the EB-GCL. This erosion included both irrecoverable and extreme erosion features (e.g., an eroded zone 130 mm wide, as shown in Figure 4.23).

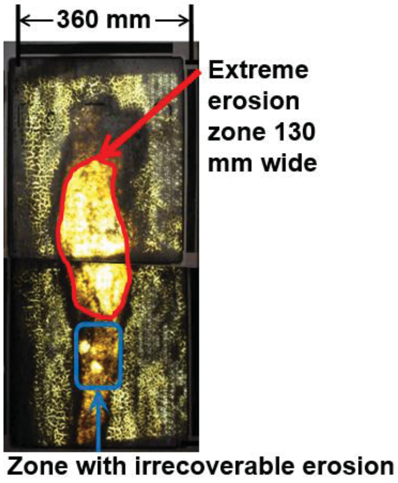

Figure 4.23. Extreme downslope bentonite erosion and irrecoverable erosion in a 720-mm-long segment of an EB-GCL after 28 months in field exposure at the QUELTS. Composite of two photographs taken in the field using a thin portable light table slid below the GCL and taken in a lightweight (cardboard) field "darkroom". The band in the middle is the edge of the portable light table. Other black areas are hydrated bentonite, and the leopard-skin areas are highly desiccated bentonite with light shining through the desiccation cracks (modified from Rowe et al. 2016b)

The aforementioned full-scale field study only examined one EB-GCL. However, the findings initiated several studies (e.g., Rowe and Hamdan 2021a,b) involving periodic water flow over five commercially available GCL products from three continents, including three EB-GCLs (one of which was used at QUELTS as a control for which the field behaviour was known). All five GCLs were hydrated with a simulated porewater comprising 10 mmol/L $CaCl_2$ to induce the cation exchange commonly observed with hydration from natural soils, including at QUELTS. All five GCLs were subjected to similar wetting periods but daily, weekly, and fortnightly interludes between wetting cycles at room temperature. The EB-GCLs initially had a slightly lower hydraulic conductivity to tap water than that for the NaB-GCLs. However, over time, the NaB-GCL performed far better than the EB-GCLs. For example, one NaB-GCL with a scrim-reinforced nonwoven carrier experienced an order-of-magnitude increase in hydraulic conductivity, k_w, that was expected based on cation exchange and a low at 15 kPa stress. The second NaB-GCL with a woven carrier experienced an up to a two orders-of-magnitude increase in k_w. The increase was partially due to cation exchange and partially due to mini-wrinkles that developed due to GCL shrinkage during the wet-dry cycles. In contrast, the three EB-GCLs experienced up to

3 to 4 orders-of-magnitude increases in $k_{w.}$

4.6.4 *Temperature effects*

Organic materials associated with solid waste containment facilities decompose biologically, resulting in increases in the temperatures of the waste (Rowe 2005, 2012). GCLs used as barriers in mining, variant, and industrial applications may be exposed to elevated temperatures ranging from 60 °C to 80 °C when the GCL has been in contact with the wastes for more than five years (Thiel and Smith 2004; Bouazza et al. 2014). Also, containment facilities that expose GCLs to high temperatures and aggressive organic and/or inorganic chemicals (e.g., landfills, solar ponds, brine ponds) present a challenge (Ghavam-Nasiri et al. 2019; Rowe 2020; Yu and El-Zein 2019). In facilities such as brine ponds and solar ponds where temperatures up to 90 °C have been reported during daytime (El-Sebaii et al. 2011; Bouazza et al. 2014), the lower overburden stresses on the liner system, compared to solid waste landfill systems, correlate with greater risks of desiccation (Southen and Rowe 2005; Rowe and Verge 2013; Hoor and Rowe 2013). For these and other reasons, evaluating the potential effects of elevated temperatures on the properties and performance of conventional GCLs and EB-GCLs may be important.

Ratkievicius et al. (2016) and Geng et al. (2016) performed viscosity tests on specimens of bentonite mixed with cationic and anionic polymers. Polymer addition increased the viscosity of the mixtures. Low viscosity was associated with a contracted polymer conformation, whereas high viscosity was attributed to the formation of an extended polymer conformation. Contracted polymers (low viscosity) prevent the formation of effective bridging between bentonite particles and polymer chains (Lage et al. 2009).

Ozhan (2018b) investigated the effects of temperature on the hydraulic conductivity of polymer EB-GCLs. Hydraulic conductivity tests were performed on specimens of EB-GCLs that were treated with either 1% or 2% by mass of an anionic polymer (AP) or a cationic polymer (CP) and an unenhanced GCL at temperatures of 20°C, 40°C and 60°C using 0.1 M and 0.5 M $MgCl_2$ solutions as the permeant liquids. The results, shown in Figure 4.24, indicated that the *k* increased with increasing temperature, which was attributed to a decrease in the viscosity of the permeant liquids with increasing temperature (Rowe 2005; Bouazza et al. 2014; Vryzas et al. 2017). However, the hydraulic conductivity of the polymer EB-GCLs was up to two orders-of-magnitude lower than that of the unenhanced GCL, which suggests that the dry polymer mixing procedure used for the EB-GCLs may have partially clogged the pores of the EB-GCLs and/or reduced the sizes of the conductive pores (Li and Zhang 2009; Haase and Schanz 2016). Generally, the EB-GCL with 2% CP resulted in the lowest *k*. Also, as indicated in Figure 4.25, the ratio of the hydraulic conductivity based on permeation with the 0.5 M $MgCl_2$ solution, $k_{0.5}$, to that based on permeation with the 0.1 M $MgCl_2$ solution, $k_{0.1}$, or $k_{0.5}/k_{0.1}$, was greater than unity in all cases, indicating some degree of hydraulic incompatibility with all specimens at all temperatures. Overall, the values ranged from 6.3 for the 2% AP GCL at 60 ºC to 232 for the 1% CP GCL at 60 ºC. However, unlike the *k* results shown in Figure 4.24, the 2% AP GCL performed the best with respect to $k_{0.5}/k_{0.1}$, with values in the range $6.3 \leq k_{0.5}/k_{0.1} \leq 13.4$.

Yu et al. (2020) assessed the desiccation and healing potential of GCLs with and without polymer modification when exposed to thermal gradients and then permeated with distilled or highly saline water. Two types of GCLs were subjected to thermal gradients in a series of instrumented column tests that replicated conditions like those found in brine ponds with low overburden pressure, high thermal gradients, and subsequent permeation with a salt solution (brine). These were the same GCLs as used in the field study reported by Rowe et al. (2016a,b) and the laboratory study by Rowe and Hamdan (2021a,b), with one GCL (denoted GCL2 in Rowe et al. 2016a,b) being a conventional GCL with unenhanced Na-bentonite whereas the other GCL was a polyacrylamide EB-GCL (GCL7 in Rowe et al. 2016a,b). The influence of temperature on the desiccation of the two types of GCLs was investigated by monitoring water loss and desiccation cracking. Some desiccated specimens were subjected to direct *k* tests with distilled water, while others were permeated with synthetic brine. With a moderate temperature of 40 °C applied to the top of the liner, the EB-GCL experienced less cracking than the unenhanced GCL, but this advantage disappeared when temperatures increased. Both desiccated specimens of the unenhanced GCL and the EB-GCL exhibited significant self-healing when permeated with distilled water.

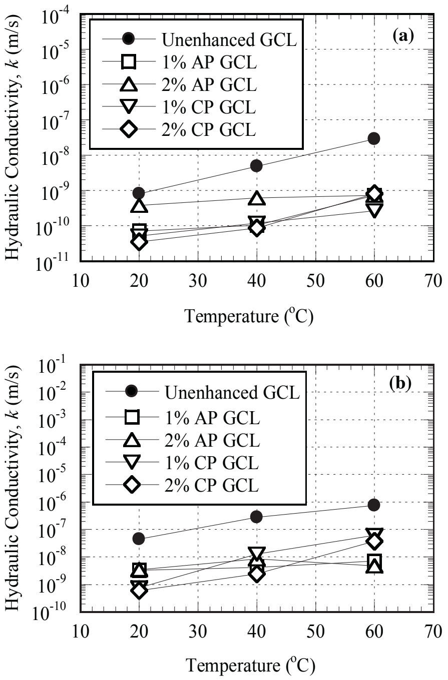

Figure 4.24. Effect of temperature on the hydraulic conductivity of unenhanced GCL and GCLs enhanced with an anionic polymer (AP) or a cationic polymer (CP) based on permeation with $MgCl_2$ solutions: (a) 0.1 M $MgCl_2$; (b) 0.5 M $MgCl_2$ (data from Ozhan 2018b).

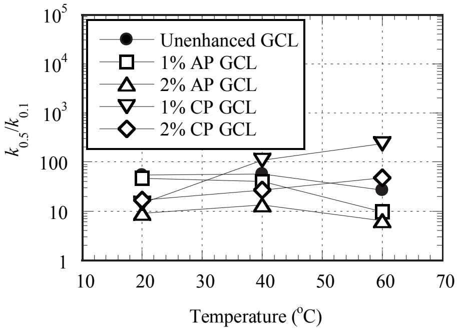

Figure 4.25. Effect of temperature on the hydraulic conductivity of unenhanced GCL and GCLs enhanced with an anionic polymer (AP) or a cationic polymer (CP) based on permeation with a 0.5 M $MgCl_2$ solution, $k_{0.5}$, relative to that based on permeation with a 0.1 M $MgCl_2$ solution, $k_{0.1}$, or $k_{0.5}/ k_{0.1}$ (data from Ozhan 2018b).

The soil-water retention characteristics of the unenhanced GCL and the EB-GCL were tested along the drying path by filter paper and a vapour sorption analyser. The experimental results are shown in Figure 4.26. For volumetric water contents greater than about 10%, the total suction for the EB-GCL is noticeably greater than that for the unenhanced GCL. The inflection point, air entry suction, and the slope of the curve also were greater for the EB-GCL. Yu et al. (2020) concluded that the addition of polyacrylamide appears to have enhanced the water retention properties of the GCL.

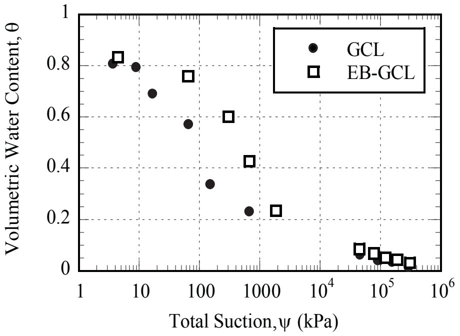

Figure 4.26. Soil-water retention curves of conventional (untreated) GCL and enhanced bentonite GCL (EB-GCL) treated with polyacrylamide polymer (Yu et al. 2020).

Also, in the study by Yu et al. (2020), the crack patterns of the unenhanced GCL and EB-GCL specimens were evaluated after the specimens were subjected to different temperatures, and the results from the quantitative image analysis are shown in Figure 4.27. The results indicated that the cracks became denser at higher temperatures for both specimens, consistent with the water content variations, which was expected since higher temperatures lead to faster and more severe desiccation. However, the cracks in the EB-GCL were less significant for heating temperatures of 40 °C and 50 °C. For almost all results shown in Figure 4.27, the EB-GCL experienced less desiccation than the unenhanced GCL. Also, the average crack width for the EB-GCL specimen at 40 °C heating was considerably smaller than that for the unenhanced GCL, which could result in a better self-healing potential for the EB-GCL upon rehydration of distilled water (Yu and El-Zein, 2019). The critical unanswered question of this study, as with other similar research showing positive results for EB-GCLs relative to NaB-GCLs, is for how long will this benefit persist, and what will be the performance over the longer term?

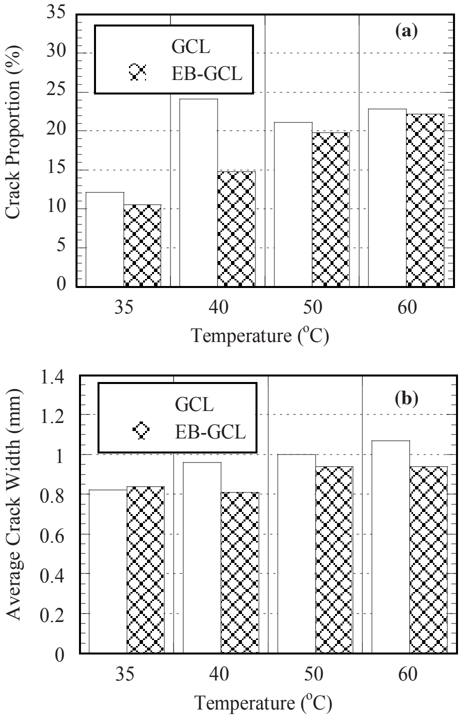

Figure 4.27. Effect of temperature on cracking from tests on specimens of unenhanced GCL and enhanced bentonite GCL (EB-GCL) treated with polyacrylamide polymer: (a) crack proportion; (b) average crack width (data from Yu et al. 2020).

As previously noted, De Camillis et al. (2016, 2017) studied the effect of wet-and-dry ageing on untreated, and polymer treated HYPER clays. The HYPER clays exhibited three orders-of-magnitude lower hydraulic conductivity relative to the untreated clays after four wet-dry cycles in seawater. Khan et al. (2021) postulated that a possible reason for this improved behaviour is due to the improved soil-water retention capacity of HYPER clay (HC) compared to the untreated clay (UC). As a result, Khan et al. (2021) evaluated the matric suction of prototype GCLs containing HC and UC using the filter paper technique under both wetting and drying conditions in the presence of different electrolytic solutions. The filter paper technique is suitable to measure the suction due to its low cost, and the ability to measure a wide range of matric suctions, typically from 10 to 10^5 kPa (Acikel et al. 2015; Hanson et al. 2013; Barroso et al. 2006). The resulting measured soil-water retention curves (SWRCs) for specimens of both UC and HC are shown in Figure 4.28.

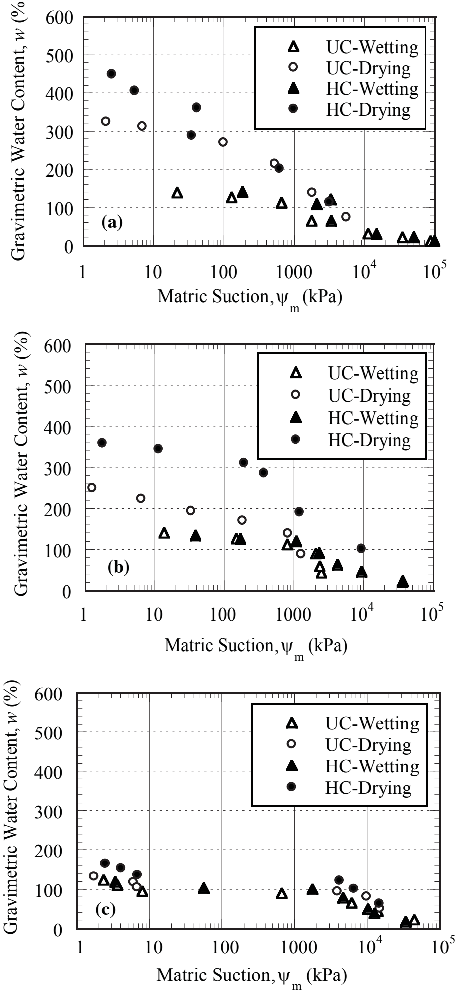

Figure 4.28. Soil-water retention curves of untreated clay (UC) and HYPER clay (HC): (a) distilled water; (b) 10 mM $CaCl_2$; (c) seawater.

For all liquids, the gravimetric water content for the HC at a given suction for both wetting and drying SWRCs was greater than that for the UC. In the case of distilled water (Figure 4.28a), the HC demonstrated higher suction for the same water content suggesting the presence of more microvoids (intra-aggregate pores), resulting in increased matric suction. The intercalation of the Na-CMC polymers within the montmorillonite platelets in HC (Di Emidio 2010) results in a decrease in pore diameter, which correlates with an increase in the matric suction (Khan et al. 2021). In addition, the increase in gravimetric water content also can be attributed to the absorption of water by the Na-CMC anionic polymer. In the case of the wetting SWRC curve, the decrease in gravimetric water content with increasing electrolyte concentration (i.e., distilled water <10 mM $CaCl_2$ < SW) was sharper for the UC relative to the HC, which can be attributed to a compression of the DDLs in the UC (Khan et al. 2021). The typical hysteresis effect between wetting and drying curves is also apparent for HC and UC specimens. The hysteresis effect decreases with an increase in the ionic strength of the solution. However, the hysteresis effect was more distinct in the HC specimens, which was attributed to the possibility that polymer intercalation decreased the contact angle and diameter of conducted pores, thereby increasing the capillary pressure and water retention (Khan et al. 2021).

4.6.5 *Screening methods*

Lee et al. (2005) showed that the k of unenhanced GCLs permeated with DW and CaCl2 solutions could be correlated with the index properties of the bentonite portion of the GCL, including the liquid limit (*LL*) test (ASTM D4318), sedimentation volume, and swell index (*SI*) test (ASTM D5890), when performed using the same permeant liquids. Thus, these index properties may help provide a quicker and less time-consuming but preliminary indication of the potential for a specific GCL to achieve a suitably low *k* for a specific liquid. However, Scalia et al. (2018a) demonstrated that indicator tests used for conventional GCLs generally are not effective for predicting the *k* of polymer EB-GCLs. Tests shown to be ineffective include *LL*, *SI*, and fluid loss conducted with the permeant liquids. This lack of correlation results from the different mechanisms underlying hydraulic compatibility of polymer enhanced bentonites relative to natural NaB-GCLs (viz., swelling). More recently, Gustitus and Benson (2021) introduced the flow-swell index test for BPC-GCLs that addresses the swelling of bentonite granules and retention of polymer gel in the pore space of a BPC. They illustrate that the flow-swell index can differentiate between BPC-GCLs with low and high *k* and indicate that more extensive testing is needed to develop a threshold flow-swell index that applies to a broad range of BPC-GCLs and permeant solutions.

Also, Christian et al. (2020) have recently shown that one of the reasons the *SI* of polymer-enhanced bentonites does not correlate with *k* is because the standard specimen preparation procedure for the *SI* test based on ASTM D5890 requires sieving of the material, such that a portion of the polymer component of the enhanced bentonite can be removed before the *SI* is measured. They hypothesize that the correlation can be improved when the standard swell index testing procedure is modified such that the polymer component is not removed via sieving.

Due to these limitations with the *SI* test, Di Emidio et al. (2013) recommended using one-dimensional (1D) swell pressure tests because the mechanisms governing swell pressure are different from those governing swell index. Hydrated bentonite adsorbs a large amount of water. Because of this water entering the interparticle pores and the interlayers in individual montmorillonite crystals comprising the bentonite particles, a swell pressure is developed, leading to an increase in volume and accompanying stress on the surrounding materials that are manifested as the swell pressure. In contrast, the macropore formation in the *SI* test leads to an increase in volume but does not increase the interstitial stress between clay particles or the stress on the surrounding materials. Furthermore, because of the hydrophilic nature of polymers used for polymer enhanced bentonites, the measured swell pressures for these bentonites are higher than those for the unenhanced bentonites, which overcomes the aforementioned technical limitations of the *SI* test.

However, the testing procedures and equipment for the 1D swell pressure test are more complex than those for the standard index tests. Also, the testing durations for the swell pressure test typically are longer than testing durations for the standard index tests. For example, the testing durations of the swell pressure tests conducted by Di Emidio et al. (2013) lasted from 5 to 10.5 days. In contrast, those for the *SI* testing procedure, including the preparation of the specimen, typically are ≤ 1 day. Thus, there is still a need to develop rapid and simple screening tests relevant to EB-GCLs and reflect the unique mechanisms underlying the hydraulic behaviour of this class of materials.

4.7 *Summary of current status and remaining questions*

This section of the paper presents a state-of-the-art review of the development and evaluation of enhanced bentonites in geosynthetic clay liners (GCLs), referred to as enhanced-bentonite GCLs (EB-GCLs), for use as barriers in chemical containment applications. Enhanced bentonites (EBs) are natural bentonites that are chemically modified to achieve greater resistance to hydraulic incompatibility and low hydraulic conductivity when permeated with liquids of extreme chemistry, including high ionic strength liquids as hypersaline solutions and/or highly acidic or highly alkaline solutions. Chemicals commonly used for the enhancement of natural bentonites include anionic polymers such as polyacrylic acid (PAA) and carboxymethylcellulose (CMC), cyclic organic carbonates such as propylene carbonate (PC) and glycerol carbonate (GC), and other organic compounds such as ethylene glycol (EG). Prevalent EBs include bentonite polymer composite (BPC), dense prehydrated (DPH) bentonite, HYPER clay (HC), multiswellable bentonite (MSB), and a wide variety of commercially available EBs with proprietary (unknown) enhancements collectively referred to as contaminant resistant clays (CRCs). These enhancements may be grouped into three categories, viz. polymer enhancements (e.g., PAA and CMC), organic compound enhancements (e.g., PC, GC, and EG), and unknown enhancements (i.e., CRCs). Low-quality bentonites that are beneficiated to perform similarly to higher quality bentonites and bentonites modified with quaternary ammonium cations known as organobentonites or organoclays have been excluded from consideration because these modifications typically are performed for purposes other than the achievement of hydraulic compatibility when permeated by liquids of extreme chemistry.

Two primary mechanisms have been postulated for improved chemical resistance and hydraulic compatibility of EBs and EB-GCLs based on permeation with liquids of extreme chemistry, viz. polymer clogging of interparticle, intraparticle, and/or intergranular (interaggregate) pores, and intercalation of polymers or organic compounds within the interlayers of the montmorillonite crystals comprising the montmorillonite mineral component of bentonite particles. Preliminary evidence based on XRD analysis and theoretical evidence based on the fabric boundary surface (FBS) theory supports intercalation as the primary mechanism for MSB and HC, whereas both SEM Imaging and the FBS theory support pore-clogging as the primary mechanism for BPC. In the case of DPH-GCL, both intercalation of CMC and densification via vacuum preconsolidation likely contribute to improved chemical resistance, although the relative effect of each contribution remains unknown. Overall, further experimental and theoretical studies are required to confirm these preliminary conclusions for wider range of conditions, including variations in the degree of pre-hydration of these EBs, effective stresses, and permeant liquid chemistries. Also, since the long-term persistence of these mechanisms is largely unknown, longer-term experimental studies should be conducted considering these broader ranges of conditions. Finally, for polymer enhanced EBs and EB-GCLs such as BPC, additional study is needed to understand the mechanisms that lead to polymer redistribution and retention within the pores of these materials and better understand the mechanisms governing hydraulic compatibility for polymer EB-GCLs.

The polymer clogging mechanism for BPC has been attributed to the formation of polymer hydrogel within the pores of the BPC, which is largely a function of the polymer loading and the pore water chemistry during permeation. Under certain conditions, such as relatively high polymer loadings, the hydrogel may be eluted from the BPC, resulting in inaccurate laboratory measurement of the hydraulic conductivity, especially for long-term behaviour. Thus, understanding polymer elution behaviour is critical to understanding the long-term behaviour of polymer EB-GCLs and ensuring that laboratory hydraulic compatibility results are accurate. Also, the necessity to continue permeation until no further polymer is eluted (mobile) requires further research.

The evidence to date suggests that EBs and EB-GCLs can offer improved resistance to hydraulic incompatibility and improved performance with respect to solute transport via diffusion and semipermeable membrane behaviour, relative to that of natural bentonites when exposed to relatively high ionic strength liquids. However, hydraulic conductivity test results based on permeation with extreme pH liquids (acidic or alkaline solutions) are limited and mixed. Also, the results of hydraulic compatibility tests for CRCs are generally more variable than those for the more standard EBs and EB-GCLs, likely due to the variability in, and the unknown nature of, the enhancement materials and procedures for CRCs. Thus, for practical applications, prudence dictates that hydraulic conductivity, membrane, and/or diffusion testing be conducted using the specific EB or EB-GCL with the specific liquid(s) to be contained.

The results of limited studies performed using HCs and HC-GCLs, DPH-GCL, and MSB indicate that EBs and EB-GCLs are more resistant than natural bentonites to the detrimental effects of wet-and-dry cycling with medium-to-high ionic strength liquids and elevated temperatures. However, additional studies to evaluate these effects for broader ranges of EBs and EB-GCLs and testing conditions are needed.

Reliable and accurate screening methods are needed to provide more rapid and less costly assessments of the potential for chemical compatibility between site-specific EBs and EB-GCLs and containment liquids. In this regard, the recently developed flow-swell index test shows promise.

Most of the research described in this section has been based on well-conceived and conducted laboratory experiments that have largely focused on the fundamental behaviour of the material under essentially ideal conditions. The typical type of studies as described herein, while extremely valuable at providing insight into the material behaviour under the conditions examined, need to be viewed with considerable caution in terms of providing recommendations or comments regarding their likely good performance in the field. Performance in the field depends on many variables that are difficult to simulate under laboratory conditions but may significantly impact the performance in the field. Even the performance of traditional NaB-GCLs commonly used as low permeability liners is complex, as will be illustrated in §5. EB-GCLs are at least one additional step more complex. While there is still plenty of good laboratory-scale research that can be conducted, the future major insights into EB-GCL behaviour and performance likely will come from well-documented, full-scale field trials of EB-GCLs in applications for which there are currently being marketed and used.

The long-term performance of enhanced GCLs will depend on how much polymer can be bound to the bentonite. The unbound polymer will be sensitive to elution, especially as, over time, the polymer is diluted by influent permeating liquid. It will be vulnerable to degradation (both anaerobic and aerobic) though bound polymer will not be immune. Laboratories may be relatively sterile with little opportunity to initiate biodegradation. The second author of this paper has observed biodegradation of a polymer claimed by the supplier to be firmly bound when stored under moist, anaerobic conditions. Polymer degradation is well recognized as a problem for drilling fluids and other excavation support fluids – especially for naturally derived polymers. For polymer enhanced GCLs, relatively little research has been reported on the amount of polymer that can be bound. This may be very small compared to the amounts used in some enhanced GCLs (Lam and Jefferis, 2019). If the polymer is not bound but merely provides a viscous pore blocker (Ejezie et al. 2020), an appropriate question to ask is why use clays such as bentonite with their intraparticle porosity. Could silts or sands give similar (if equally time-limited) performance? Also, what are the properties of the polymer-porewater system (solution?) when prepared at the expected in-GCL concentration?

---

5 GEOMEMBRANE AND GCL IN A BARRIER SYSTEM

5.1 *Design life*

Barrier systems should be designed to control contaminant escape to a negligible level or the ingress and egress of water or gases to an acceptable level. The contaminating lifespan of a waste disposal facility is, by definition, the period during which the barrier system must control contaminant escape to a negligible level (MOE 1998; Rowe et al. 2004). Thus, the design life for a facility containing contaminants will be either when the source of contaminant is removed (e.g., for a leachate lagoon) or the facility reaches its contaminating lifespan (e.g., a MSW landfill). The design life for a lagoon, pond, or dam is the time the barrier system needs to control the escape of fluids to an acceptable level. While the design life of the cover is the length of time the cover is required to control the ingress and egress of liquids and gases to an acceptable level. The design life of ponds and lagoons may be a few decades. The design life of a liner for a dam is commonly about a century. The contaminating lifespan of a waste disposal facility depends on its size (predominantly the thickness of waste) and the nature of the waste. It typically ranges from about 100 to 300 years for municipal solid waste, to over 500 years for low-level radioactive waste, and to millennia for mine waste and long-lived low-level radioactive waste. Thus, the service life of the barrier system components is a critical consideration since the system requires service life greater than the contaminating lifespan or design life as appropriate.

5.2 *Designing liners as part of a system*

5.2.1 *Geomembrane-clay composite liners*

The previous sections have primarily considered the performance of geomembranes and GCLs alone. However, there are many applications where HDPE geomembranes and GCLs are used together to form a single composite liner. In these applications, the strength of one component offsets the weaknesses of the other. In particular, while intact HDPE is practically impermeable to aqueous solutions and many gases, the leakage through even relatively small holes can be significant. On the other hand, the GCL, while still having a relatively high hydraulic resistance, cannot match the intact geomembrane for resistance to fluid flow but is highly effective in limiting the leakage through holes in the geomembrane (e.g., Giroud and Bonaparte 1989; Rowe 1998, 2006, 2012, 2018, 2020). Therefore, the geomembrane and GCL form a single composite liner (Figure 5.1a). Similarly, a geomembrane in intimate contact with a compacted clay liner (CCL) is a single composite liner.

The importance of the hydraulic conductivity, *k*, of a GCL and the effect of permeant and stress on *k* are well-recognized, as highlighted in §4. However, it is generally not well recognized that combining a geomembrane and GCL (or CCL) to form a composite liner introduces a new and important parameter: the GMB-GCL interface transmissivity. This interface transmissivity controls the ability of fluid to spread laterally at the interface contact between the GMB and GCL (or CCL). With a few notable exceptions, relatively little attention has been paid to the importance of the interface transmissivity between the geomembrane and GCL. It is often implicitly and incorrectly assumed that the interface transmissivity is proportional to the *k*. However, there is little correlation between the GCL *k* and GMB-GCL interface transmissivity (Rowe 2012, Abdelrazek and Rowe 2019). The interface transmissivity can be affected by bentonite, but it is controlled by the geometry and the path of least resistance at the GMB-GCL or GMB-CCL interface.

Rowe (2020a) provides a recent overview of GMB-GCL interface transmissivity. Rowe (2018) discusses the effect of leaving a geomembrane exposed over compacted clay and the significant impact the desiccation of even a few millimetres of the clay at the clay surface can have on interface transmissivity. Design calculations should consider the potential implications of desiccation of the clay surface because it can effectively decouple the performance of the geomembrane from the CCL to the point that it no longer acts as a composite liner but they act as two separate liners. One approach to addressing this concern is to have a composite liner comprised of a GMB/GCL/CCL, as shown in Figures 5.1 and 5.2b. In this scenario, the self-healing capacity of the GCL minimizes the effect of desiccation of the clay liner surface (Rowe 2018). Thus, when controlling leakage is a critical consideration, and the advantages of the thickness of the CCL are desired, the composite liner system may be comprised of an HDPE geomembrane over a GCL over a CCL (Figure 5.2b; Priyanto et al. 2019; Rowe et al. 2020). Here, the GCL is less prone to cracking and has self-heal capacity even if it does crack. The use of the GCL provides a geomembrane-GCL interface transmissivity orders of magnitude lower than that of the compacted clay (Rowe 2012).

5.2.2 *Geomembrane-tailings composite behaviour*

Another example of how adjacent materials can interact to perform better than either material alone by forming a composite liner arises when silty sand or finer tailings are placed over a geomembrane in a tailings storage facility (Figure 5.3). The leakage through a geomembrane hole is substantially reduced by the head loss that occurs in the tailings within about 5 hole-diameters of the hole (Joshi et al. 2017; Rowe et al. 2017; Chou et al. 2018, 2021; Rowe and Fan 2021; Fan and Rowe 2021, 2022a). The subgrade also plays a critical role with respect to the potential for piping in the shorter-term and tensile strains that control the service life of the geomembrane in the longer-term (Fan and Rowe 2022).

5.2.3 *Barrier system component interactions*

Rowe (2011) emphasized that while consideration of the characteristics of the individual components of the design (e.g., geomembrane or GCL) is necessary, it is not sufficient to ensure a good design. Liners do not operate in isolation. They are part of a larger barrier system (Figures 5.1 and 5.2). Therefore, it is essential to consider the potential interactions between different system components and how they may affect the entire system's performance. It is particularly critical when seeking to "improve" or optimize a system component that one also looks carefully for the potential unintended consequences of that optimization. Rowe (2011) demonstrated how an action that may enhance the performance of one part of the system might negatively affect other parts of the system. The design objective should be to ensure optimal performance of the entire system, not the components in isolation.

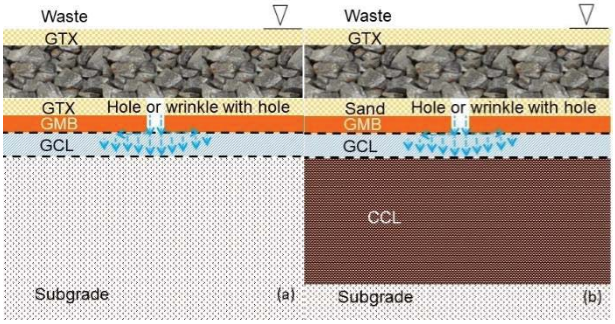

Figure 5.1. Barrier system with a single composite liner: (a) GTX filter over coarse granular drainage layer over GTX protection layer over HDPE GMB with a hole over GCL over subgrade (b) GTX filter over coarse granular drainage layer over sand protection layer over HDPE GMB with a hole over GCL over CCL over subgrade.

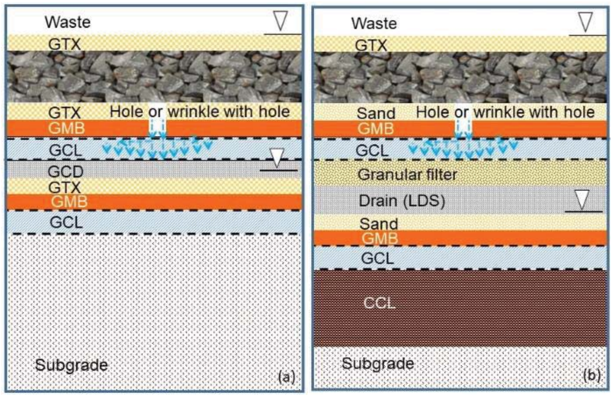

Figure 5.2. Barrier system with a double composite liner: (a) GTX filter over coarse granular drainage layer over GTX protection layer over HDPE GMB with a hole over GCL over granular drainage layer over GTX protection layer over HDPE GMB over GCL over subgrade (b) GTX filter over coarse granular drainage layer over sand protection layer over HDPE GMB with a hole over GCL over granular filter over granular drain over sand protection layer over GMB over GCL over CCL over subgrade.

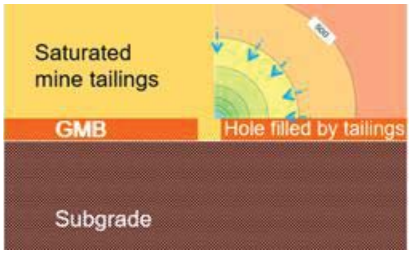

Figure 5.3. A single geomembrane covered by silty sand tailings forms a composite system with the tailings above and within the hole, substantially reducing leakage through the hole. The nature of the subgrade can also control the service life of the geomembrane.

For example, it is now well established that coarse uniform gravel provides the best drainage system for leachate in a municipal solid waste landfill (Rowe 2005; Rowe and Yu 2010, 2013). However, that excellent drainage layer may compromise the service life of the barrier system if the strains induced in the underlying geomembrane give rise to premature stress cracking (Abdelaal et al. 2014; Ewais et al. 2014b). Thus, in addition to improving the leachate collection system, one must also introduce a system to adequately minimize the strains in the geomembrane (Rowe et al. 2013; Rowe and Yu 2019; Rowe et al. 2019c). More generally, the potential interaction between the soils or other materials above or below a component in a liner system must be considered in any design.

5.3 *Impact of the environment on barrier system performance*

When designing a barrier system, consideration must also be given to the environment in which it is constructed and the environment in which it will serve its design function. For example, when a protection/drainage layer is placed, the weather conditions will significantly influence subsequent leakage through a composite liner. This is because the weather conditions influence the liner temperature. The hotter the geomembrane when covered relative to when it was placed and welded, the greater the thermal expansion and, consequently, the number of wrinkles and the area beneath interconnected wrinkles in the geomembrane. The height of wrinkles and area beneath wrinkles directly affect the probability that a hole intersects a wrinkle and the area over which leachate can spread once it flows through that hole (Figure 2.15; Giroud and Morel 1992; Chappel et al. 2012a,b; Rowe et al. 2012a,b; Rentz et al. 2017). Wrinkles can have a detrimental impact on system performance for multiple reasons. These include the facts that:

(i) the wrinkle acts as a target for damage. A wrinkle is more likely to have a hole than a flat geomembrane sheet (Gilson-Beck 2019; Rowe 2020),

(ii) a hole in the wrinkle would allow leakage orders of magnitude greater than the hole alone if it were in direct contact with the clay liner (Rowe 1998; 2005; 2012; 2020),

(iii) the local tensile strain in the geomembrane at a wrinkle makes the wrinkle a location for early stress cracking, especially when a weld passes over a wrinkle, and

(iv) the wrinkle acts as a point for the accumulation of humid air beneath an exposed geomembrane and subsequently a point for condensation of the water vapour i. focusing the flow beneath the wrinkle as the geomembrane cools in the evening after a warm day (thereby potentially contributing to downslope erosion; §5.5.2.2).

(v) the wrinkle creates an area of reduced stress into which bentonite in an underlying GCL could migrate,

(vi) GCL below a wrinkle will have a higher k than the GCL in direct contact with the geomembrane.

(vii) the wrinkle increases the risk of internal erosion when the GCL is above a drainage layer in double liners (Figure 5.2; §5.5.2.2 (ii)).

Thus, the cumulative effect of a transient event, such as the rise and fall of the sun each day with the consequent rise and fall of geomembrane temperature throughout the period that the composite liner is left exposed, can cause permanent damage to the GCL beneath the geomembrane.

Similarly, the wrinkles that were present when the cover soil will be placed will be locked into the system. While the locked-in wrinkles may get smaller with loading, they generally do not disappear (Stone 1984; Soong and Koerner 1998; Brachman and Gudina 2008). Wrinkles provide a conduit for enhanced leakage through any hole in the geomembrane on or near a wrinkle (Rowe 1998, 2012). In both cases, transient events not considered in design can have a permanent and substantial impact on the leakage through a barrier system and, consequently, on the surrounding environment.

5.4 *Need for Construction Quality Assurance (CQA)*

In barrier system construction: '*you get what you inspect, not what you expect*' (see §15.17). For every important project, an effort should be made to minimize the effect that construction activities will have on leakage through the liner. This should include minimizing the number of holes in the geomembrane when it goes into service and minimizing leakage through any undetected holes or holes that subsequently develop. Doing so will require high-quality, full-time and knowledgeable observation of every step of liner installation and covering as part of the construction quality assurance (CQA) program. The CQA should be conducted by an appropriately qualified expert independent of the contractor. The critical importance of appropriate CQA has been well-recognized for more than 35 years, as highlighted in the classic paper by Giroud and Fluet (1986). These days CQA should include a leak location survey before and after cover soil is placed on the geomembrane (Giroud 2016; Gilson-Beck 2019; Rowe 2020).

5.5 *Barrier system Service life*

5.5.1 *Geomembrane service life*

When landfills were first being built with geomembrane liners 50 years ago and for the next 40 years, the effect of leachate on the service life could have been regarded as a known unknown. Research over the last 20 years has changed that, and now the service life of a geomembrane liner can be reasonably estimated and regarded as known if one simply asks the question (Rowe 2020). Service-life of a modern geomembrane depends on

1. geomembrane used – (polymer and additive package), and
2. The exposure conditions:
   - Elements (UV; rapid changes in temperature),
   - Chemical composition of fluid in contact with a geomembrane,
   - Temperature,
   - Nature of exposure,
   - Sustained tensile strains in geomembrane, and
   - Seams (welds)

HDPE geomembranes have evolved substantially over the last 30 years. Today's high-quality HDPE geomembranes are highly engineered materials, and one can select a geomembrane with an appropriate resin and additive package for a given application (§2). With appropriate testing to confirm the compatibility of the geomembrane with the fluid to be contained, appropriate design to minimize tensile strain in the geomembrane, and appropriate construction and CQA to ensure that it is constructed following the design, a modern HDPE geomembrane used as a landfill liner could have a service-life of many hundreds of years and in some cases millennia (Rowe 2020, Rowe et al. 2020).

Unfortunately, the level of attention being paid to providing premium geomembranes with a long service life has not been paid to the other geosynthetic components of the barrier systems such as the geotextiles shown in Figures 5.1 and 5.2. Unlike modern HDPE geomembranes, geotextiles and geocomposite drains are generally not well stabilized against thermo-oxidative degradation. While they may have service lives up to decades, there is a paucity of data on longer-term performance. This should be an essential consideration in designing facilities with a century or more design life. This is especially relevant to landfills and mine waste.

5.5.2 *GCL service life*

5.5.2.1 *Factors affecting the service life of a GCL*

The majority of GCLs on the market comprise a layer of bentonite sandwiched between two geotextiles and needle-punched together. However, the description is deceptively simple. The Canadian GCL manufacturer produces 50 different GCLs that meet this basic definition and, except for the multicomponent GCLs, they all have the same $k \leq 5 \times 10^{-11}$ m/s (ASTM D5887) given on the manufacturer's product sheets, However, they have significant variance in price and field performance. The factors affecting the field performance of the GCL include:

- the type and granularity of the bentonite,
- the mass of bentonite per unit area,
- the amount of needle-punching,
- the mass of the nonwoven needle-punched cover geotextile (upper during manufacture),
- the type and mass of the carrier geotextile (lower during manufacture),
- whether the needle-punched fibres are thermally bonded to the carrier geotextile,

- whether there has been a plastic layer and if so
  - was the layer a coating applied in a molten state so that it is impregnated into and onto carrier geotextile (known as a coated GCL), or
  - was it produced separately and glued to the carrier geotextile (a laminated GCL),
  - what polymer is used for the coated/laminated layer, and
  - what is the mass per unit area of the coated/laminated layer?

The needle-punched structure of these GCLs serves three potential purposes:

i. keeping the bentonite contained between the geotextiles following GCL manufacture through to and after it is installed,
ii. providing restraint to the GCL during hydration at low stress levels, thereby reducing the swelling and improving the hydraulic characteristics of the GCL at low effective stress.
iii. providing internal shear strength. The needle-punched fibres increase the apparent friction angle from about 8-10° for hydrated bentonite alone to a higher value. The magnitude of the increased friction angle and apparent cohesion will depend upon the amount of needle-punching and how the needle-punched fibres are anchored to the carrier geotextile.

A coating or laminate applied to GCL reduces the *k* by about an order of magnitude from less than $5x10^{-11}$ m/s (ASTM D5887) to typically less than $5x10^{-12}$ m/s (ASTM D5887) for multicomponent GCLs with either a coating or laminated plastic layer. In addition to reducing *k*, the coating can also protect the GCL from hydrating or losing moisture in a manner that could impact its ultimate performance.

Although GCLs have a typical ASTM D5887 hydraulic conductivity, as stated in the previous paragraph, the actual *k* in the field can vary from an order of magnitude lower than that indicated above to 4 to 5 orders of magnitude higher depending on the factors listed above together with the exposure conditions. A discussion of how these factors affect GCL field performance is provided by Rowe (2020).

5.5.2.2 *Discussion of factors affecting the service life of a GCL*

The following discussion of GCL service life is primarily based on Section 12.10.2 of Rowe et al. (2004) but has been updated.

The primary active component of a GCL is bentonite. Bentonite is a naturally occurring swelling clay formed by the deposition of volcanic ash that was consolidated into shale/mudstone. The nature of the bentonite may depend on whether the ash settled in saltwater or freshwater. The lowest permeability bentonite is natural sodium bentonite deposited in saltwater and was first discovered in the Cretaceous Benton shale found at Fort Benton in Montana but subsequently found in Wyoming, North Dakota, South Dakota, Colorado, Kansas, and Nebraska, USA. Most of the bentonite used in high-quality GCLs manufactured in North America is natural sodium bentonite obtained by mining the shale and grinding it into either coarse grains (coarse sand size), fine grains (medium to fine sand size), or powdered form (silt size). Most high-grade sodium bentonite is Wyoming bentonite, with Turkey also having deposits of high-quality sodium bentonite. Mixed sodium/calcium bentonite is mined in Australia, Greece, India, Russia, and Ukraine. Calcium bentonite is mined in southern USA, China, Germany, Greece, India, New Zealand, and Turkey. China is now the world's largest producer of bentonite, followed by the USA and India.

The minerals in bentonite (predominantly montmorillonite) have been around for millennia and are likely to remain for millennia under typical field applications. However, its *k* can be affected by many factors, particularly the chemistry of the water with which it is hydrated and permeated and the effective stress under operating conditions. Thus, in design, consideration must be given to the operative *k* under the expected field conditions. This *k* will, as noted above, depend both on the details of the GCL manufacturer itself and the exposure conditions. Within this context, the bentonite in the GCL may be expected to have a very long service life (thousands of years) provided that:

(i) there is no significant loss of bentonite during installation of the liner,
(ii) there is no significant lateral movement (thinning) of bentonite or gaps/holes post-installation,
(iii) there is no significant internal erosion,
(iv) there is no change in macrostructure due to wet-dry or freeze-thaw cycles or this is accounted for in the design *k*,
(v) the *k* was selected based on a realistic assessment of the field conditions (chemistry of fluid to be contained, pore fluid adjacent to the GCL, effective stress etc.), and
(vi) it is installed with appropriate seams.

It follows from the preceding that the service life of a GCL will also be of the order of millennia provided the six factors above have been addressed in design and construction and provided that the GCLs long-term performance is not contingent on the service life of the geosynthetic components.

The factors affecting the bentonite above, together with the dependence of the GCLs service life on the long-term performance of the geosynthetics, will be discussed in the following subsections.

(i) Avoiding loss of bentonite during installation of the liner

Good CQA is essential to ensure that appropriate measures are taken in moving and placing the GCL while avoiding loss of bentonite or significant movement during installation.

(ii) Avoiding significant lateral movement (thinning) of bentonite or gaps/holes post-installation

Potential causes of zones with inadequate bentonite post-installation include:

- voids in subgrade that are bridged by the GCL,
- traffic (human or machine) over the GCL, especially if permitted to hydrate prematurely,
- protrusions in the subgrade,
- stones that are not initially in contact with the liner but migrate into contact post-installation due to the consolidation of compacted till or movement of stones due to freeze-thaw,
- gravel/stone in the cover soil directly above the liner,
- significant internal erosion (see (iii) below),
- wrinkles in a geomembrane (see below),
- premature wetting and shrinkage of the GCL, and/or
- downslope erosion (see below).

The foregoing can all be mitigated by good construction quality assurance. The last four can also be mitigated, to some extent, by appropriate design, as discussed subsequently.

Wrinkles in the geomembrane should be minimized for the reasons given in §5.3. Wrinkles can be mitigated by the designer specifying that the protection geotextile and granular layer shall only be placed over the geomembrane when:

- The area beneath wrinkles is less than 6% of the geomembrane area covered when the overlying material is placed (i.e., no visually interconnected wrinkles and any wrinkles present are hydraulically isolated from other wrinkles).
- All wrinkles are less than 50 mm in height.
- The longest wrinkle is less than 10 m in length.

and having good CQA to ensure compliance with the specifications. While minimizing wrinkles is desirable, it is essential that the geomembrane is not covered while in a state of tension either due to thermal contraction on very cold day or due to efforts to avoid wrinkles.

Shrinkage of the GCL due to wet-dry cycles

Manufacturers' installation guidelines recommend covering a GCL with at least 0.3 m of soil shortly after the liner is installed (i.e., before the GCL can hydrate). If this is followed, then shrinkage and downslope erosion is highly unlikely.

Panel shrinkage occurs when GCLs are left exposed without at least 0.3 m of cover soil for a prolonged period if, during this period, they can experience wet-dry cycles with hydration followed by water evaporation. These repeated cycles can result in shrinkage of some GCLs both longitudinally and/or transversely, reducing the overlap and ultimately creating gaps between the overlapped panels (Thiel and Richardson 2005; Koerner and Koerner 2005; Thiel et al. 2006; Bostwick et al. 2010; Rowe et al. 2010, 2011a, 2013, 2018, Brachman et al. 2018).

GCL panel shrinkage can be mitigated by preventing wet-dry cycles when there is negligible ballast soil over the GCL. This can be best achieved using a multicomponent GCL. Encapsulation of the bentonite between the overlying geomembrane and the coating applied to the carrier geotextile can prevent moisture uptake and hence no wet-dry cycles. This will also prevent downslope erosion discussed below. The downside of this approach is that if there is a hole in the geomembrane, either in the shorter- or longer-term, the bentonite will be hydrated by the leachate in the environs of the hole. This is most likely and most critical below a wrinkle where the effective stress is zero. If the leachate-bentonite interaction increases *k* more than the subgrade pore water-bentonite interaction, then an alternative approach for minimizing shrinkage and downslope erosion is to use the multicomponent GCL with the coating facing up in contact with the geomembrane. In this way, the GCL can hydrate from the subsoil.

If a multicomponent GCL is not available or suitable for a given application, the magnitude of the thermal cycles that cause the generation of both wrinkles and the evaporation of moisture from the GCL can be reduced with the use of a white geomembrane (Take et al. 2016; Rentz et a; 2016, 2017). A white geomembrane will reduce the magnitude of, but not prevent, eventual shrinkage and downslope erosion.

If a multicomponent GCL is not available or suitable for a given application, the magnitude of the thermal cycles that cause a generation of both wrinkles and the evaporation of moisture from the GCL can be reduced with the use of a white geomembrane (Take et al. 2016; Rentz et al. 2016, 2017). The white geomembrane will reduce, but not prevent, eventual shrinkage and downslope erosion.

Downslope erosion occurs when a GCL in a composite liner is exposed for a prolonged period without at least 0.3 m of cover soil. Typically, the GCL in the composite liner will uptake moisture from the subgrade, followed by water evaporation from the GCL into the airspace between the GCL and geomembrane, followed by condensation of that moisture and the consequent distilled water running down even a gentle slope (e.g., 3%). The distilled water running over the GCL can cause bentonite erosion to the bottom of the slope. The bentonite can be partially or totally eroded and can leave two layers of geotextile with effectively no bentonite between them (Ashe et al. 2014, 2015; Brachman et al. 2015; Rowe et al. 2016a,b). This mechanism only occurs with distilled water. It does not occur with tap water flowing over the GCL. It has only ever been reported when the composite liner is left exposed for a prolonged period to solar radiation, contrary to the manufacturers' recommendations.

GCL downslope erosion can be mitigated by preventing wet-dry cycles when there is negligible ballast soil over the GCL. The approaches described above on mitigating panel shrinkage will be equally effective at mitigating downslope erosion.

(iii) Avoiding significant internal erosion.

Rowe and Orsini (2003) examined the potential for internal erosion for several subgrades and GCLs. A GCL with a woven carrier over the pea gravel subgrade experienced internal erosion at a head of 27 m. Bentonite erosion caused a two order of magnitude increase in apparent *k* and permittivity by the time of test termination. A GCL with a nonwoven carrier experienced one order of magnitude increase in apparent *k* and permittivity at a head of 28.5 m. A GCL with a scrim-reinforced nonwoven carrier did not experience any internal erosion. It sustained a 41 m head without a change in apparent *k*, which remained at about 1.5×10^{-11} m/s. With a silty sand subgrade having 25% fines, none of the GCLs experienced any internal erosion at a head of up to 49 m. In landfill projects, the service life of the geotextile component is likely to be less than the contaminating lifespan of the landfill. In these situations, a suitable granular filter should be placed between the GCL and any drainage layer unless it can be demonstrated that for the highest reasonable head, no erosion is likely to occur for the proposed GCL with the hydrated bentonite in direct contact with the drainage layer.

(iv) Avoiding or accounting for macrostructure due to wet-dry or freeze-thaw cycles

Wet-dry cycles and freeze-thaw cycles can change the structure of the bentonite and increase *k*. The effect on *k* is a function of the level of cation exchange that has occurred before or during the wet-dry or freeze-thaw cycle. For example, Table 5.1 summarizes the results for two NaB GCLs and three EB-GCLs subject to the same cation exchange from the hydrating simulated pore water prior to being subjected to wet-dry cycles by Rowe and Hamdan (2021a) in the swell index values of 9-12 mL/2g. The *k* values reported were obtained with 8-hour wetting cycles and drying cycles ranging from 16 hours to 14 days for each GCL for one year. Although the exposure conditions were identical, the impact on *k* varied substantially with *k* increasing from $1\text{-}5 \times 10^{-11}$ m/s prior to cation exchange to $0.9\text{-}4 \times 10^{-10}$ m/s with cation exchange. However, after the wet-dry cycles there was no significant change in *k* for the GCL with NaB bentonite and a SRNW carrier geotextile. For the GCL with NaB bentonite and W carrier geotextile, *k* increased tenfold to 4×10^{-9} m/s with this increase due to mini-wrinkles that developed in the woven geotextile caused local thinning of the bentonite. For the three EB-GCLs, the wet-dry cycles increased *k* by between a factor of 10 and 200 relative to that with cation exchange alone (i.e., to between 5×10^{-8} m/s' and 2×10^{-7} m/s). Thus, the natural sodium bentonite was more resistant to wet-dry cycles and freeze-thaw cycles than alternative enhanced bentonites. However, there was still an impact and the first objective of design, where practical, is to avoid wet-dry or freeze-thaw cycles. If this is not possible, the effect of freeze-thaw can be mitigated by minimizing cation exchange before and during the wet-dry or freeze-thaw cycles and adjusting the design *k* to account for the change in macrostructure due to the cycles.

For a composite liner where freeze-thaw or wet-dry cycles can not be avoided, one design approach is to encapsulate the bentonite between the geomembrane above and the coating/laminate bonded to the carrier geotextile below. Provided that the geomembrane is placed without allowing the GCL to hydrate (e.g., from rainfall), these two layers serve to prevent hydration of the GCL. Without hydration, neither wet-dry cycles nor freeze-thaw cycles will have any effect on the hydraulic performance of GCL. If a small hole in the geomembrane or coating permits minor local hydration, the general effect will be no consequence.

Table 5.1. *k* permeated with tap water at 15 kPa after cation exchange and 24-315 wet-dry cycles (modified from Rowe and Hamdan 2021a)

Bentonite granularity	M_a (g/m^2)	Carrier GTX	$k \times 10^{10}$ (m/s)
NaB Fine	5527	NWSR–TT	0.9-3
NaB Powder	4557	W–TT	4-20
EB Fine	5257	NWSR–TT	2-1000
EB Powder	5160	W–TT	20-500
EB Powder	5775	NWSR	2-2000

NWSR= scrim reinforced nonwoven; W= woven, TT= thermally treated

For a GCL used alone, the GCL is protected from hydration from the subgrade and hence cation exchange by the plastic layer and using a clean sand layer with minimal cations as the ballast layer above the GCL. In this scenario, it is likely that the bentonite will be hydrated from above by rainfall or snowmelt. Therefore, at least 0.3 m and preferable 0.6 m thick soil layer should be placed quickly after placement of the GCL and before hydration of the GCL. Generally speaking, since increasing thickness of fill above the GCL minimizes the effect of wet-dry or freeze-thaw cycles, the sooner the soil is placed the better. Even with wet-dry and/or freeze-thaw cycles, GCL *k* of a multicomponent GCL is likely to be less than $5\text{x}10^{-12}$ m/s for the service life of the coating since the coating controls the hydraulic resistance. However, some impact on *k* may be expected once the service life of the coating is reached.

(v) Realistic selection of design hydraulic conductivity, *k*

The design GCL *k* must be selected based on a realistic assessment of the field conditions. Important considerations in selecting the *k* are:

- the choice of the GCL and the factors listed in §5.5.2.1. With respect to these points, consideration should be given to the following when a long service life is required:
  - A scrim reinforced carrier geotextile with a mass per unit area ≥ 200 g/m².
  - A nonwoven cover geotextile with a mass per unit area ≥ 200 g/m².
  - A dry bentonite mass unit area ≥ 4300 g/m² and ≥ 4800 g/m² for critical projects.
  - A multicomponent GCL with the coating having a mass per unit area ≥ 200 g/m² and ≥ 300 g/m² when the coating is particularly important. Serious consideration should be given to using a multicomponent GCL for pond/lagoon applications.
  - No more needle-punching than is essential for internal shear strength (needle-punched bundles can become a pathway for fluid flow when they are large and the GCL subject to cation exchange (e.g., Rowe et al. 2017).
  - Unless the GCL remains perpetually submerged, powdered bentonite generally performs better than fine granular bentonite, which generally performs better than coarse granular bentonite in real field situations.
  - Natural sodium bentonite is preferred for most important applications (see §4 for extreme applications). Sodium bentonite that has been generated from calcium bentonite by processing with soda ash or poor-quality bentonite to which polymers have been added to reduce its *k* and/or increase its swell index are more prone to a substantial increase in *k* (e.g., from $3\text{x}10^{-11}$ nominal to $1\text{x}10^{-7}$ m/s after several years in the field) and decreasing service life under less than ideal field conditions.
    - If polymer EB-GCLs are being considered, wet-dry or freeze-thaw or potential polymer elution represents a limitation to the service life.
- cation exchange due to the adjacent soils and permeation with the fluid to be retained.
- the effective stress. Note that for a GCL in a composite liner, the effective stress on the GCL below a wrinkle is essentially zero. Hence, *k* below a wrinkle will be substantially higher than the *k* where the GMB is in direct contact with the GCL.

Caveat emptor

Unfortunately, it is not uncommon for a designer to specify an appropriate GCL considering all the factors above and then, during construction, the contractor substitutes an alternative GCL to that was specified. The alternative is usually proposed because it is cheaper (i.e., it has less mass per unit area of geotextile, and/or coating, and/or bentonite mass per unit area) and has the same *k* on the manufacturer's product information sheet. This type of decision is usually made without realizing that the *k* on the product information sheet does not represent field conditions. While the quantities listed in §5.5.2.1 may not affect *k* in a standard index test where the GCL is permeated by deionized water under an effective stress ~35 kPa and differential head of ~1.5 m (e.g., ASTM D5887), they have been shown to substantially (by orders of magnitude) affect the long-term performance and service life of the GCL. No substitution of the material that does not fully meet the specifications should be permitted without the expressed written approval of the designer of record.

(vi) GCL is installed with appropriate seams.

To provide appropriate seams, the GCL specification should generally require that (Brachman et al. 2016; Joshi et al 2017, 2018):

- GCL panels be overlapped by 300 mm along the roll length (600 mm at ends) and supplemental bentonite be placed between the panels at a rate of a 400 g/m in a continuous 150 mm wide fillet,
- Alternative seaming using impregnated bentonite or a manufactured groove are not acceptable substitutes for the supplemental bentonite applied as indicated above. These approaches work under ideal conditions but are far more prone to failure in real field situations than appropriately applied supplemental bentonite. Inappropriate bentonite at the overlap leads to excessive leakage at the overlaps.
- Wrinkles and crimps should be avoided at overlaps.

Good CQA will be required to ensure these conditions are met.

5.5.2.3 *Design such that GCLs long-term performance is not contingent on the service life of the geosynthetic components.*

The service life of the GCL is only contingent on the factors affecting the bentonite as itemized above provided that:

- needle-punching (for internal shear strength),
- bonding of the coating/laminate to the carrier geotextile (to provide adequate shear strength),
- coating/laminate (reduce *k* and/or to prevent hydration from subgrade),
- carrier geotextiles (to prevent internal erosion),

are not needed for the design life of the facility.

These four factors are discussed below.

(a) The needle-punching is not required for long-term internal shear strength in the GCL if the design features are such that either the slope is sufficiently small that the shear strength of the bentonite at the applied normal stress provides a sufficient factor of safety or there is a reinforcing layer to carry the shear forces on slopes and prevent excessive shear stress transfer to the GCL on the side slopes. Under either of these circumstances, the service life of needle-punched fibres will not affect the service life of the GCL.

(b) The bonding of the coating/laminate to the carrier geotextile is not required for the long-term to prevent sliding at the interface between the two layers for the same two reasons discussed in (a) above. Under either of these circumstances, the service life of the bonding to the carrier geotextile will not affect the service life of the GCL.

(c) The coating/laminate is not required for the long-term if the coating is not required to maintain a low *k* or to prevent hydration or cation exchange after the liner system is operational. Often the coating may be relied upon to prevent hydration and cation exchange during construction when the GCL could be subjected to wet-dry or freeze-thaw cycles before it is covered with waste or liquid to be contained. Under these circumstances, the service life of the coating/laminate will not affect the service life of the GCL.

(d) The carrier geotextile and coating/laminate are not required to prevent internal erosion of the bentonite for the long-term if the GCL is resting on a filter compatible material.

In situations where the geotextile is required to provide shear strength or to prevent internal erosion or the coating is required to provide a low *k* or isolate the bentonite from an aggressive solution then the service life of the GCL will be controlled by the service life of the geotextile and/or coating.

The service life of the geotextile components of typical GCLs and that of the coating/laminates are presently unknown (although both are currently subject to investigation at Queen's University in

Canada). von Maubeuge and Ehrenberg (2000) have suggested a "conservative" estimate of a service life of 25-50 years for the polypropylene fibres in the GCL. Assuming that this estimate is for normal operating temperatures of about 25°C or below, and in the absence of any other published information, this is probably a reasonable guesstimate for the geotextile and coating in typical applications where the fluid is not aggressive.

5.5.2.4 *GCL service life summary*

Provided that the design *GCL k* is selected considering the potential effects of leachate interaction and low effective stress below wrinkles, and with appropriate consideration to ensure no potential internal erosion, then the bentonite component can be considered to have a service life of millennia provided the performance of the bentonite is not dependent on the longevity of the geosynthetic components of the GCL. However, if the geosynthetic components are critical to performance, then the service life of the GCL is dictated by the service life of the critical geosynthetic component(s).

5.5.3 *Composite liner service life summary*

Subject to appropriate consideration of the issues raised in the foregoing subsections including the effects of exposure conditions in the selection of compatible materials, the service life of a composite liner will be equal to the shorter of the service life of the geomembrane or the GCL. Thus, with appropriate design (including the selection of materials; Rowe et al. 2020; Rowe 2020a, 2020b) and construction, HDPE underlain by a GCL can provide very long service life and is suitable for use in dams, ponds, or lagoons, or in covers for closure of landfills or mine waste facilities, or as a bottom liner for landfills or mine waste facilities. Depending on the exposure conditions, the likely service life may range from decades to millennia.

5.5.4 *Drainage layer service life*

With appropriate design, the gravel drainage layers (leachate collection and leak detection systems) in Figures 5.1 and 5.2 can be designed to have a service life of centuries to millennia (MOE 1998; Rowe et al. 2004; Rowe and Yu 2013). Similarly, sand protection layers and granular filters can be designed to have a service life of centuries to millennia.

There is very little information published on the longevity of geocomposite drains. Unpublished work by Reinert and Rowe has shown that there can be a substantial variability between products with some having an estimated service life of only a few decades while others may have an estimated service life in excess of a century as a liner for a water retaining structure. This topic is subject to considerable ongoing research.

5.6 *Need for Potential Failure Modes and Effects Analysis*

The need for a potential failure modes and effects analysis is well-established in dam engineering. However, this approach could go far beyond dam engineering and extend to any significant geotechnical engineering project. For example, in the field of geoenvironmental engineering, any unacceptable environmental impact arising from a facility intended to prevent that impact may be regarded as a failure. In this context, many failures occur due to known factors whose consequences are known but were not considered in design due to a failure to consider all potential failure modes.

A failure mode that is commonly overlooked in the design of barrier systems is the service life of the components of the system. Consequently, little consideration is given to the potential effects of the service life of the component being reached. For example, consider a design for a construction and demolition waste landfill with a contaminating lifespan of 50 years and a maximum liner temperature of less than 25°C. In this case, the design profiles shown schematically in Figures 5.1a and 5.2a for a single and double composite liner barrier system may be appropriate. Subject to the usual caveats of appropriate design, material selection, and construction, it is reasonable to anticipate that the system in Figures 5.1a and 5.2a will have a service life of more than 50 years and hence be sufficient. However, if the contaminating lifespan and hence design life were 200 years, and one could not rely on the geotextile protection layer to prevent excessive strain in the geomembrane once the protection layer geotextile has reached the end of its service life, which by definition is when it no longer serves its design function of protecting the geomembrane. This would then reduce the service life of the geomembrane to an extent dependent on the resin that was used, and the tensile strains developed when the protection layer is no longer effective. Similarly, the geotextile component of the GCL is unlikely to last 200 years. If stability is dependent on the internal shear strength of the geotextile, the system's capacity to perform effectively is limited by the service life of the needle-punching.

Similarly, if the subgrade is not filter compatible with the bentonite, then there is potential for internal erosion of the bentonite into the subgrade when the lower (carrier) geotextile has reached its service life, thereby reducing the service life of the GCL. These considerations apply to the single and double composite liner systems in Figures 5.1a and 5.2a. If these designs are not appropriate, alternative designs are shown in Figures 5.1b and 5.2b.

5.7 *Monitoring for and managing the unexpected*

A potential failure modes and effects analysis can effectively deal with the known knowns and the known unknowns. The greatest challenge is, of course, the unknown unknowns. The unknown unknowns are unexpected, and monitoring is needed to detect them. When the unknown unknowns manifest themselves and become known, they are usually found to be due to an unanticipated complex interaction of many factors that influence the system's performance. Once known, these issues can be resolved with time and appropriate resources. The following paragraphs discuss one such example of the field revelation of unexpected outcomes and the flow-through consequences.

Following more than 15 years of extensive field use of NaB GCLs and research into their behaviour, Richardson and Thiel (2005) made public the problem of GCL panel shrinkage. This was shortly followed by a more detailed paper (Thiel et al. 2006) documenting several field cases and illustrating the mechanism with laboratory tests. This prompted two field trials at different sites to monitor panel shrinkage. These unpublished trials failed to identify any significant problem. Thus, while field cases had demonstrated significant shrinkage and panel movements of up to 1.2 m, trials designed to emulate this yielded negligible shrinkage, thereby raising the question as to why this unexpected behaviour occurred in some cases and not others? In these circumstances, how could a design engineer know whether there is likely to be a problem with a GCL hidden below the geomembrane? The search for an answer to this question has involved 15 years of coordinated research at several institutions, as outlined below. This case illustrates the complexities of in-field performance and the multiplicity of factors influencing that performance.

The shrinkage reported by Thiel et al. (2006) was predominantly for GCLs from one US manufacturer. Another major manufacturer had no reports of any problems. To understand the mechanisms, the observed variability in the likelihood of shrinkage, and to assess whether it was good luck or good management by the manufacturer with no reported problems, 18 full-scale test sections were constructed using four GCL products at the Queen's University Environmental Liner Test Site (QUELTS) in 2006. Some sections were with a smooth geomembrane, and some with textured to resolve whether the texturing was the cause of the problem. A composite liner was exposed on six relatively flat (3% base) sections and six on a 3:1 (horizontal:vertical) side slope facing south. Another six north facing sections involved GCLs covered by about 0.7 m of silty sand.

During the 5 years monitoring of the QUELTS I sections side-by-side on the same subgrade and exposed to identical climatological conditions, it became apparent that: (a) geomembrane texturing was not an issue, (b) covering a GCL with the silty sand effectively eliminated shrinkage, and (c) there were notable differences in the performance of the four GCLs in terms of the exposed composite liner shrinkage on both the side slope and base (Rowe et al. 2018; Brachman et al. 2018). The maximum shrinkage for the four products in the exposed composite liner over 4.8 years was 30, 75, 415, and 665 mm. These differences could not be fully explained based on laboratory shrinkage tests, although it became apparent that the drying rate was a factor in explaining the magnitude of the shrinkage (Bostwick et al. 2010; Rowe et al. 2010, 2011a). It also became apparent that the uptake and loss of moisture were different for different GCL products with the same bentonite. The shrinkage was affected by the nature of the geotextile component of the GCL. These findings led to a series of studies to evaluate the differences in water retention characteristics of these four GCLs as a function of their geosynthetic structure (Beddoe et al. 2010, 2011). The work was then extended into a broader study of GCL water retention curves for different GCLs (Acikel et al. 2015, 2018a,b, 2020, 2021, 2022; Tincopa et al. 2020).

During the monitoring of panel shrinkage between 2006 and 2011 at QUELTS I, it also became evident that shrinkage was not the only problem. All four GCL products were experiencing downslope erosion (Brachman et al. 2015; Take et al. 2015; Rowe et al. 2016a,b). Laboratory tests designed to examine downslope erosion (Rowe et al. 2014; Ashe et al. 2015) reproduced the downslope erosion observed at QUELTS I. The downslope erosion was only observed for GCLs that had experienced a hydration and drying cycle. Laboratory tests indicated that downslope erosion only occurred with distilled water. About 40 ppm calcium in tap water was sufficient to prevent downslope erosion for at least up to 365 cycles, and it was inferred to be unlikely to occur with leachate leaking through a hole in a wrinkle in a geomembrane.

The QUELTS I field study, combined with growing interest in the hydration and desiccation of GCL under a constant thermal gradient (Southen and Rowe 2004, 2005a,b, 2007, 2011; Azad et al. 2011,2012; Rowe and Verge 2013, Hoor and Rowe 2013; Bouazza et al. 2017b; Ghavam-Nasiri et al. 2017, 2019, 2020) served as the impetus for co-ordinated studies of:

- thermal conductivity of GCLs (Ali et al. 2016).
- gas permeability, water vapour movement and uptake by GCLs (Rouf et al. 2016a,b,c).
- the uptake and loss of moisture from the soil (Rayhani et al. 2011; Siemens et al. 2012; Anderson et al. 2012; Rowe et al. 2011b, 2019b, 2021; Carnero-Guzman et al. 2021).
- the effects on subgrade mineralogy (Bouazza et al. 2014, 2017a).
- subgrade particle size, density and water content, and the role they played in shrinkage (Rowe et al. 2019b, 2021).
- potential for self-healing of holes in GCLs, such as due to downslope erosion (Li and Rowe 2020, 2021; Rowe and Li 2020).

QUELTS I lead to a search for a means of minimizing the risk of downslope erosion. Therefore, based on input available in 2011-2012 from the studies cited above, QUELTS II was constructed in 2012 with a control section identical to one of the sections at QUELTS I and the remaining six sections exploring means of minimizing or eliminating downslope erosion (Rowe et al. 2016a; Rentz et al. 2016,2017).

QUELTS II provided the following new insights and guidance for design (Rowe et al. 2016a and §5.5.2):

- When a geomembrane composite liner is heated by the sun, moisture evaporates from the underlying GCL. The water vapour accumulates at geomembrane wrinkles generated by the sun's heat. At night, the water vapour condenses on the underside of the geomembrane. This distilled water drips onto the GCL and runs down the GCL in rivulets, eroding the bentonite. Repetition of this process creates areas with little or no bentonite. The loss of bentonite is difficult to detect visually.
- Downslope bentonite erosion was more extensive on a 3H:1V slope than a 33H:1V (3%) slope; however, it also occurred on a 3% (2°) base slope.
- The extent of downslope erosion and the time required to occur appeared to be related to the GCL capacity to retain moisture when heated. Two potential factors contributing to the reduced rate of downslope erosion progression were: (i) a higher mass per unit area of bentonite and (ii) the use of powdered bentonite.
- It was confirmed that the best way of avoiding both shrinkage and downslope erosion was to cover the composite liner in a timely manner with a suitable protection geotextile and ≥ 0.3 m of cover soil or gravel.
- A multicomponent GCL with an intact polypropylene coating facing up to minimize moisture loss into the airspace between the geomembrane and GCL prevented downslope erosions and reduced, but did not eliminate, panel shrinkage after 28 months of exposure.
- An EB-GCL with polyacrylamide-based polymer enhanced bentonite experienced widening desiccation cracks in laboratory tests, indicating minor bentonite erosion. No holes had formed in the field at QUELTS II in 15 months of field exposure. However, irrecoverable erosion was observed on the 3:1 slope at QUELTS II after 28 months of field exposure. Thus, the benefits of polymer enhancement may be time-limited for EB-GCLs.
- The EB-GCL experienced the most panel shrinkage of all GCLs at QUELTS II. As discussed in the previous section, even without downslope bentonite erosion, polymer elution and loss with water running down the slope over the GCL combined with drying cycles can increase the *k* of EB-GCLs by 1000-10,000-fold.

The investigations outlined above highlight the value of an integrated, multi-institutional approach that brings together different laboratory techniques and field studies to address a complex issue (an unknown unknow until earlier this century) such as the performance of GCL in real-world applications.

6 CONTAINMENT OF EMERGING CONTAMINANTS OF CONCERN

6.1 *The issue*

Municipal solid waste (MSW) landfill regulations and generic designs commonly in use have been largely developed for the contaminants of concern of the last century. They generally proved very effective at containing those contaminants over the past few decades. However, the situation has become more complex with the recognition that synthetic chemicals used for many decades because of their numerous advantages over existing natural chemicals have three significant drawbacks. First and foremost is recognizing actual or potential health and environmental impacts from these chemicals in the products in which they have been used and are now in landfills. Second, many of these synthetic chemicals are not readily biodegradable by existing bacteria and hence are persistent organic pollutants (POPs) "forever chemicals". Third, many of the chemicals are lipophilic and tend to accumulate in fat and, in doing so in progress through the food chain to be consumed by humans. This creates the need to re-evaluate the safety of our existing landfills. Landfills that adequately contain low concentrations of volatile chlorinated solvents and heavy metals cannot be assumed, a priori, to be adequate for containing the contaminants of emerging concern. Their suitability can only be established, in advance of a problem, by appropriate modelling. Also, the fact that these contaminants

(a) can be in landfill leachate at concentrations well above allowable levels in drinking water, and
(b) do not readily biodegrade

raises questions about the whether service life of the engineered facilities is long enough to contain them for their contaminating lifespan.

Landfill liners are intended to act as barriers to the diffusive advective transport of contaminants present in the waste and leachate (Rowe 1988; Rowe et al. 2004). Therefore, a geomembrane with no holes would provide a complete barrier from advective transport of contaminants resulting in diffusion being the dominant means of transport.

HDPE geomembranes provided an excellent diffusion barrier for most contaminants of concern when regulations were developed. The exceptions were volatile organic compounds such as benzene, toluene, ethylbenzene, and xylenes (BTEX) together with chlorinated compounds such as dichloromethane (DCM), trichloroethylene (TCE), and tetrachloroethylene (PCE) that could easily diffuse through HDPE geomembranes (August and Tatzky 1984; Park and Nibras 1993; Sangam and Rowe 2001; Rowe et al. 2004; Divine and McCray 2004; Joo et al. 2005; McWatters and Rowe 2009a,b, 2010, 2014,2018, McWatters et al. 2019; Park et al. 2012, Shackelford 2014, Jones and Rowe 2016; DiBattista and Rowe 2020a,b, DiBattista et al. 2020). Even these compounds were only likely to be problematic for a barrier system over unsaturated soil underlain by an aquifer where the contaminants could diffuse through the typical composite liner and then migrate in a gaseous phase through the unsaturated soil to an aquifer. This could be mitigated by several metres of saturated or near-saturated attenuation layer below the composite liner.

Advection through a composite liner will be controlled by the number and size of holes in the geomembrane and whether the holes coincide with wrinkles. Studies have shown that even with good construction quality assurance (CQA), 5 holes/ha may be expected and 20 or more holes/ha with casual CQA (Giroud and Bonaparte 1989, Giroud 2016). However, the critical factor controlling leakage is the number of holes coincident with wrinkles that allow the fluid to spread out over a much larger area than would occur had the hole in the geomembrane been in direct with the clay liner.

Based on monitoring data of leakage through the primary liner in double-lined New York State landfills with very good construction quality assurance but no leak location survey, the probability of the leakage exceeding a given value is shown in Table 6.1. This needs to be considered in assessing impact.

6.2 *Per- and polyfluoroalkyl substances (PFAS)*

Per- and PolyFluoroAlkyl Substances (PFAS) are a group of over 4700 synthetic compounds with a carbon chain where fluorine atoms have replaced some or all of the hydrogen atoms. In large part, PFAS are highly stable due to the strong chemical bond developed between the carbon and fluorine atoms. Thus they are very persistent organic pollutants and hard to degrade, being resistant to hydrolysis and different degradation mechanisms (e.g., thermal, microbiological and photolytic; Milinovic et al. 2015, Bouazza 2021). As a result, they have been extensively used in industrial and consumer goods for applications such as treating and protecting textiles including clothes, carpets, coated paper, and coated food and cardboard packageing or leather products (ATSDR 2015, CELA 2019, CONCAWE 2016, EPA 2003, EPA 2017, NTP 2016, Ahrens 2011, Cousins et al. 2016). In addition, PFAS characterized by a lipophilic tail in a hydrophilic head (Figure 6.1) have been widely used as industrial surfactants and insecticides (EPA 2017; Benskin et al. 2012).

Table 6.1. Probability, *P*, that the leakage, *Q*, through a single composite liner will be exceeded (based on New York State landfills, Beck 2015)

Q (lphd)	*P* (%)	*Q* (lphd)	*P* (%)	*Q* (lphd)	*P* (%)
10	91	75	48	300	8
20	82	100	38	400	6
30	74	150	24	500	5
40	67	200	16	750	4
50	61	250	11	1000	4

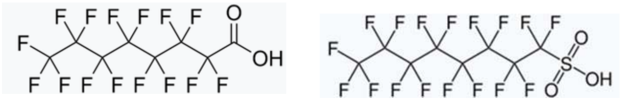

Figure 6.1 Two common PFAS with a tail comprised of 8 carbon atoms bonded to fluorine with different heads: (a) PerFluoroOctanoic Acid (PFOA), and (b) PerFluoroOctane Sulfonate (PFOS)

Studies by US Centre for Disease Control (CDC) suggests that 98% of Americans have PFAS in their blood serum, with PFOS being the most common form of PFAS identified in human blood (Benskin et al. 2012; EPA 2015; Lindh et al. 2012; Zeng et al. 2015; ATSDR 2015; CDC 2015). A more recent but less extensive study in Germany identified 37 PFAS with one or more in every human plasma sample tested (Göckener et al. 2020). Furthermore, studies indicate that PFAS are either known or suspected to (a) be carcinogenic, (b) affect human reproduction and development, (c) affect liver and kidney function, (d) affect immune system function, (e) elevate cholesterol levels, (f) cause thyroid hormone disruption etc. (ATSDR 2015, EPA 2016, OECD 2002; EPA 2017; Alexander et al. 2003; Alexander and Olsen 2007; Mandel and Johnson 1995; Thomford 2002; Eriksen et al. 2013; Frisbee et al. 2010; Nelson et al. 2010; Apelberg et al. 2007; Chen et al. 2015; Darrow et al. 2013; Maisonet et al. 2012; Washino et al. 2009).

Significant sources of PFAS include areas used for fire training purposes, military bases, airports, industrial areas, wastewater treatment facilities including sewage sludge and effluent water, and landfills and landfill leachate (EPA 2017; ITRC 2020; Bouazza 2021; Moody and Field 2000; Baduel et al. 2017; Cousins et al. 2016; Gallen et al. 2017; Hamid et al. 2018).

As a result of their ubiquitous nature, their persistence and their known or suspected health impacts, PFAS are contaminants of emerging concern. However, despite the relatively high concentrations in landfill leachate relative to allowable drinking water concentrations, there are no specific guidelines regarding suitable landfill barrier systems for the containment of PFAS.

6.2.1 *Modelling transport of PFAS through liners*

Using an approach developed by Rowe and Abdelrazek (2019), Rowe and Barakat (2021) published the first study of the potential implications of liner systems for PFAS. They focused their attention on PFOS in a landfill with an average waste thickness of 25 m and a barrier system with a leachate collection system, a geotextile protection layer, and a composite liner comprised of a 1.5 mm thick HDPE geomembrane on a 7 mm thick GCL on a 3.75 metres thick attenuation layer overlying a 3 m thick aquifer. The paper considered pure diffusion and advective transport of leachate through a hole in a wrinkle of length L_w.

To calculate the diffusive transport through the HDPE geomembrane with no advection, Rowe and Barakat (2021) adopted a permeation coefficient $P_g \sim 6 \times 10^{-16}$ m^2/s and a partitioning coefficient, S_{gf}~1 for PFOS based on data available, at that time, from ongoing studies at Queen's University. Continued testing has lowered the value to $P_g < 2\text{x}10^{-16}$ m^2/s and this will be periodically revised as more data becomes available. To put the numbers in context, in a diffusion test where benzene diffuses from a source chamber through a 1 mm thick HDPE geomembrane to receptor chamber, the benzene is detected within 10 days of the start of the test. A reasonably accurate estimate of the diffusion coefficient can be made based on about one month's data. At the same time, the test approaches equilibrium between source and receptor in a little over 2 months (Figure 6.2). With more than a year of testing of 0.26 mm thick HDPE film, PFOS in the receptor is barely detectable without any clear trend of an increase in the receptor concentrations or decrease in the source concentrations with time. One cannot obtain a definitive permeation coefficient until there is a clear trend and, at most, one can estimate an upper bound based on the detection limit and the length of time the test has been running. When data is maintained at or below the detection limit, the upper bound estimate of P_g becomes a function of the length of time the test has been running and the thickness of the specimen. Thus, the estimate of P_g decreases the longer the test runs until a clear trend of increasing concentration in the receptor and decreasing concentration in the source are observed. This difference in behaviour between benzene and PFOS is reflected in Table 6.2, which summarizes the diffusion coefficient, D_g, partitioning coefficient, S_{gf}, and permeation coefficient, P_g, for a number of contaminants of emerging concern discussed in this section as well as for benzene and chloride. The upper bound estimate of P_g, for PFOS is more than 5 orders of magnitude lower than that for benzene through HDPE.

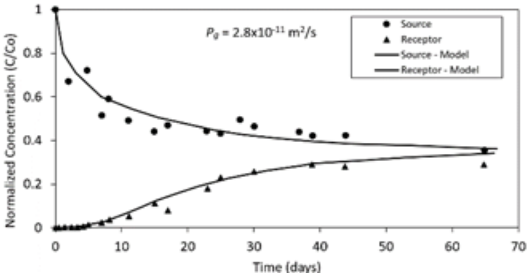

Figure 6.2 Variation in benzene concentration in the source and receptor compartments adjacent to a 1 mm thick HDPE geomembrane. Note that benzene is detected in the receptor within less than 10 days of the start of the experiment an equilibrium is approached after about 2 months.

To provide further context, a test examining the diffusion of chloride through 2 mm thick HDPE geomembrane has now been running continuously for 28 years and after this time chloride is still undetectable above the detection limit in the receptor. For contaminants like PFOS and chloride the partitioning coefficient $S_{gf} \leq 1$ and is very difficult to measure. Assuming an $S_{gf} \sim 1$ for both chloride and PFAS, the upper bound estimate of P_g after one year of testing a 0.26 mm thick film is very similar to, and marginally less than that of, chloride through a 2 mm thick geomembrane. This highlights the advantages of testing a very thin specimen when the diffusion coefficient is extremely low. Based on available data, it is estimated that $S_{gf} \sim 0.008$ for chloride and HDPE. Interpreting the same 28 years of data using this value of S_{gf}, $P_g < 7x10^{-18}$ m²/s. In any event, HDPE is an excellent diffusive barrier to both chloride and PFOS.

Table 6.2. Diffusion, partitioning and permeation coefficients for a number of contaminants through HDPE geomembranes.

Chemical	D_g (m²/s)	S_{gf} (-)	$P_g = D_g \times S_{gf}$ (m²/s)
Benzene	$2x10^{-13}$	140	$3x10^{-11}$
PCB	$1x10^{-14}$	100,000	$1x10^{-9}$
PDBE	$4x10^{-15}$	2,000,000	$8x10^{-9}$
BPA	$< 3x10^{-15}$	~1	$< 3x10^{-15}$
PFOS	$< 2x10^{-16}$	~1	$< 2x10^{-16}$
Chloride	$< 3x10^{-16}$	~1	$< 3x10^{-16}$
Chloride	$< 9x10^{-15}$	0.008	$< 7x10^{-18}$

Leakage was calculated assuming very good [VG] GCL k and GMB-GCL interface transmissivity, θ, representative of excellent CQA, and more typical parameters representative of average CQA. The concentration of PFOS in the leachate concentration was assumed to be a maximum reported in the literature (4,800 ng/L =4.8 μg/L = $4.8x10^{-6}$ g/L). The calculated leakage for the different conditions and the corresponding calculated peak impact in the aquifer assuming the service life of the barrier system exceeds 425 years (a shorter service life would indicate greater impact) are given in Table 6.3.

Table 6.3. Probability, P, that the leakage, Q, and peak concentration in the aquifer, c_p, will be exceeded for a single composite liner with a 3.75 m thick attenuation layer between the liner and a receptor aquifer (based on data from Rowe and Barakat 2021)

Holed wrinkles L_w (m/ha)	Note	Leakage Q (lphd)	Probability greater than Q	c_{peak} (ng/L)	Ok in? Juris-dictions
0	PD	0	99.9%	8	8
50	VG	9	90%	30	6
100	VG	18	88%	60	5
200	VG	35	76%	110	3
300	VG	53	67%	180	2
50	Typ.	71	57%	260	2
100	Typ.	140	30%	520	2
200	Typ.	280	10%	810	0
300	Typ.	430	6%	950	0

NOTES: PD = pure diffusion;
VG = very good: $\theta = 3x10^{-11}$ m²/s, $k_a = 2x10^{-11}$ m/s, $k_b = 2x10^{-10}$ m/s
Typ. = typical: $\theta = 3x10^{-9}$ m²/s, $k_a = 2x10^{-10}$ m/s, $k_b = 2x10^{-9}$ m/s

To provide a frame of reference for the calculated impacts, the allowable PFAS concentration in 4 of the most populous US states, Australia, Canada, and Europe, are summarized in Table 6.4. A comparison of the results shown for the peak impact in the aquifer c_p in Table 6.3 with the allowable levels in the 8 jurisdictions in Table 6.4 indicates that all the regulatory limits considered would be met with pure diffusion. However, based on leakage data, with a single composite primary liner and very little natural attenuation, there is a 99% probability that Michigan's guidelines would not be met.

Rowe and Barakat (2021) concluded that:

1. A 1.5 mm HDPE geomembrane was an excellent diffusion barrier to PFOS, and a single composite liner would be adequate for the jurisdictions considered if one could guarantee no holes. However, based on past experience, this is extremely unlikely. There is more than 99% probability that both Michigan and New York's proposed limits would be exceeded with a single composite liner of the form examined. However, it is noted that New York State requires a double composite liner, which very substantially increases the probability of their proposed limit being met.

Table 6.4. Allowable PFOS concentrations in jurisdictions (Based on Rowe and Barakat 2021)

Jurisdiction	Allowable PFOS conc. (ng/L)	Jurisdiction	Allowable PFOS conc. (ng/L)
Michigan	8	Europe	100
New York	10	Ontario	150
California	40	Texas	560
Australia	70	Canada	600

2. The suitability of a single composite liner for the other jurisdictions considered depended on the peak concentration of PFOS in the landfill leachate, the level of construction

quality assurance, and hence the number of holed wrinkles per hectare. For Australia, California, Texas, Ontario, and British Columbia, either a low peak leachate concentration and/or a very high level of construction quality assurance would be required to meet PFOS limits with a single composite liner. However, in Ontario, a double-lined barrier system would be required for landfills of the size considered in the example.

3. Analyses similar to those performed by Rowe and Barakat (2021) are recommended for all landfills with a single liner to ensure the barrier system's suitability for containing PFOS in a MSW landfill.
4. Given the persistence of PFAS and the relatively high concentrations relative to allowable levels in many jurisdictions, more consideration needs to be given to the geomembrane's service life in MSW landfills containing PFAS.

6.2.2 *Modifying GCL bentonite to retard PFAS migration*

Preliminary laboratory trials reported by Bouazza (2021) indicated that a standard needle-punched GCL with ~ 4 kg/m^2 NaB had $k_w = 2.8 \times 10^{-11}$ m/s when permeated by deionized (DI) water and $k = 4.4 \times 10^{-11}$ m/s when permeated by landfill leachate containing about 35 μg/L total PFAS (Figure 6.3).

Another GCL with activated carbon powder mixed with the bentonite (ACA GCL in Figure 6.3) had $k_w = 6.5 \times 10^{-11}$ m/s when permeated by DI water and $k = 9.0 \times 10^{-11}$ m/s when permeated with landfill leachate containing about 35 μg/L of PFAS. While the addition of the activated carbon increase k by 30% compared to k_w, it substantially reduced the PFAS concentrations in the effluent from the GCL (Bouazza, 2021). The latest results (after 30 pore volumes of flow, PVF; Figure 6.4) show that total PFAS dropped exponentially from an initial concentration of ≈ 35 μg/L to the limit of reporting (LOR) within 13 PVF (except for one measurement at 10.9 PVF). However, the sorptive capacity of the carbon black appears to have been reached by about 16 PVF and total PFAS had increased to 25.5 μg/L in the effluent by ≈ 30 PVF. These results highlight the need to conduct such trials for sufficiently long to attain more than 20 PVF.

The total PFAS measured in both the initial landfill leachate and effluent after passing through the activated carbon modified GCL was dominated by two short-chained PFAS analytes, PFBA and PFBS, which exceeded the adsorptive capacity of the reactive medium. PFBS concentrations initially decreased exponentially to LOR within 5.3 PVF but then increased exponentially in concentration from 21.6 PVF. PFBA concentrations decreased exponentially to LOR by 5.2 PVF but revealed a more sporadic albeit higher concentration from 16.5 PVF. Significantly for PFBA, the concentrations in the effluent from 16.5 PVF onward exceeded the initial PFBA concentrations in the landfill leachate, indicating that perhaps some degradation reactions had occurred or, more likely, that PFBA attenuated during initial penetration had broken through. PFHxA, PFPeA and PFHxA largely dropped to LOR (an exception being a single anomalous result for PFHxS after 5.2 PVF, then decreasing to its LOR up to 30 PVF). PFPeA evidenced breakthrough by 16.4 PVF and increased to over its initial values by 28 PVF, returning to around a third of its initial value by 30 PVF. Levels of PFOA, and PFOS, were below the LOR of 0.1 μg/L up to 30 PVF except for a single anomalous result for PFOS at 5.2 PVF, then also returning to LOR up to 30 PVF.

Concentrations of the three currently regulated PFAS (PFOS, PFOA and PFHxS) were reduced to LOR (Figure 6.5) with the ACA GCL, but only PFOS was reduced to LOR by a standard GCL. Given that these three PFAS largely remain at LOR after 30 PVF, the ACA GCL appears to provide a reasonable degree of resistance to their migration. Note, however, that due to the method of direct injection and single dilutions conducted at many commercial laboratories, the LOR does change with time, particularly for PFOS and PFOA. In addition, LOR also depends upon the instrumentation used. Nonetheless, these ongoing results highlight that a few shorter carbon-length PFAS commonly present in modern landfill leachate are highly mobile.

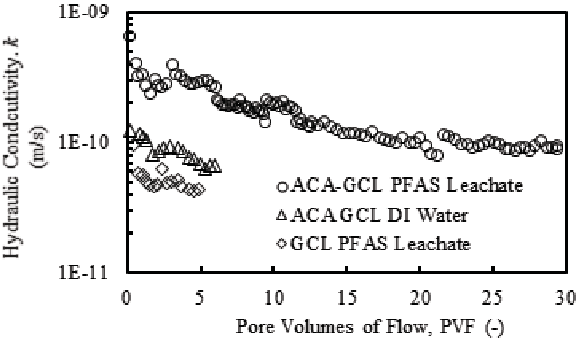

Figure 6.3 Hydraulic conductivity, *k*. As a function of pore volumes of flow of PFAS-containing landfill leachate (modified from Gates et al. 2020) and Bouazza 2021).

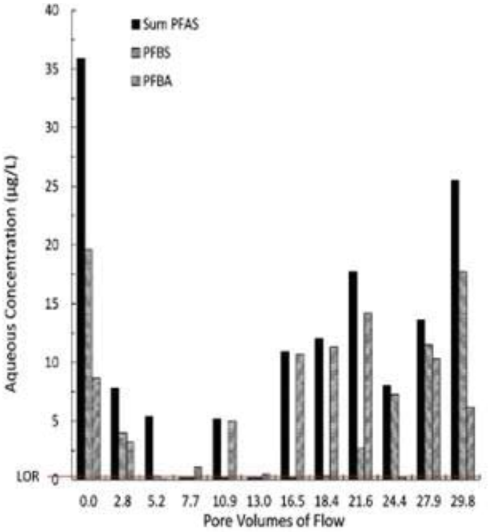

Figure 6.4 Landfill leachate PFAS concentrations in the effluent after permeation through a modified GCL containing powdered activated carbon as an additive. Initial PFAS concentrations are depicted at the "0" pore volume. The limit of reporting (LOR) is 100 ng/L (0.1 μg/L) (modified from Gates et al. 2020).

Furthermore, while these preliminary results, perhaps unsurprisingly, show that a GCL modified with activated carbon may only provide temporary respite against some shorter carbon-chain length PFAS depending on the level of exposure (e.g., volume, hydraulic head, and initial concentration) to the liquid, they do indicate that significant retention can occur, particularly for the regulated PFAS (PFOA, PFOS and PFHxS). Of concern is the relatively high temporal variability in the PFAS analyses. For example, PFOS was measured as high as 4000 ng/L at 5.2 pore volumes, more than 200-times its concentration in the original leachate. Hypothetically, this could result from analyte concentrate associated with its breakthrough when sorptive capacity within the modified GCL is attained. However, this is unlikely given the (i) number of PVF and estimated saturated pore volume of the specimen, (ii) return in measured values to LOR and (iii) variability in total PFAS analysis between 7.7 and 13 PVF. Instead, this is most likely associated with an as-yet-unidentified experimental error, particularly with the samples taken at 5.3 PVF. Further work on this and other systems is required to fully understand the efficacy by which GCL-based liner components can mitigate PFAS mobility.

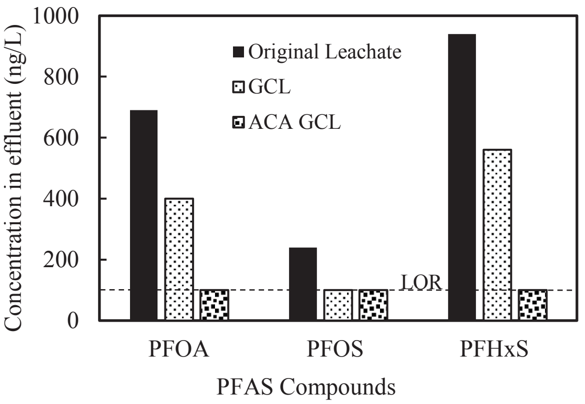

Figure 6.5. Residual concentrations of PFOS, PFOA and PFHxS after permeation of 2 pore volumes of flow in different GCLs. The limit of reporting (LOR) is 100 ng/L (0.1 μg/L) (modified from Bouazza, 2021).

6.3 Polybrominated diphenyl ether (PBDE)

Polybrominated diphenyl ethers (PBDE) are a family of organobromine compounds ($C_{12}H_{(10-x)}Br_xO$ (x = 1, 2, ..., 10) (Figure 6.6). Homolog groups (mono through deca) refer to the number of bromine atoms (represented by 'x' in the formula) replacing a hydrogen on the diphenyl structure. There are 209 PBDE congeners depending on the number and location of bromines. Extensively used as a flame retardant in textiles used in furniture and in electrical devices that can start fires, mixtures of PBDEs have been widely used and are typically released either as a result of manufacturing or from wear and degradation of products like carpets and sofas in which they have been used (U.S. EPA 2006). Consequently, PBDE is often found in household dust at concentration of more than 4,600 parts per billion (ppb) (UNEP 2004). Table 6.5 gives the composition of a typical commercial PBDE examined by Rowe et al. (2016c) and Saheli and Rowe (2016).

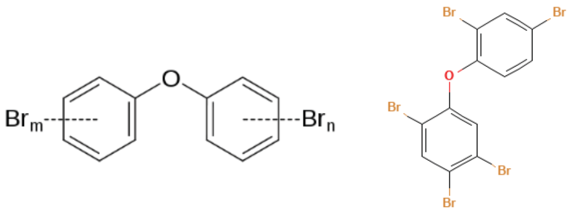

Figure 6.6 Left: General structure PolyBrominated Diphenyl Ether (PBDE) with 209 congeners based on 1 to 10 bromine atoms replacing a hydrogen on the ring structure. Right: one specific congener 2,2',4,4',5-Pentabromodiphenyl ether (Congener 99 in Table 6.5)

Table 6.5. Composition of commercial PBDE studied and analysed by Rowe et al. (2016c)

Congener	Percent composition	c_{omax} (ng/L)	D_g (m^2/s)	S_{gf}	Guideline (ng/L)	c_o/G.L
47	32.4	558	5.7×10^{-15}	0.7×10^6	24	23
85	2.4	47.1	3.7×10^{-15}	2.3×10^6	-	
99	43.9	1000	3.3×10^{-15}	4.9×10^6	3.90	256
100	8.9	210	2×10^{-15}	2.6×10^6	0.23	913
153	3.8	160	2.5×10^{-15}	7.5×10^6	120	1.3
154	3.3	119	1.5×10^{-15}	6×10^6	-	
All 6 congeners		2094	3.7×10^{-15}	1.8×10^6	-	

PBDEs are lipophilic and hydrophobic persistent organic pollutants. PBDEs bioaccumulate in fat tissues, blood, and breast milk and can be passed along the food chain. Humans ingest PBDEs through high-fat foods such as fatty fish (Szlinder-Richert et al. 2010), supermarket food (U.S. EPA 2006) and breast milk (U.S. EPA 2006), or by inhalation of PBDEs in household dust (UNEP 2004; Sjödin et al. 2008). The concentration of PBDEs in human blood and tissue has doubled every five years since production started in the 1970s (UNEP 2010). PBDEs are endocrine disrupters that disrupt the chemical signalling system in the human body and affect the development of the brain and reproductive systems (UNEP 2010).

Wastes containing PBDEs are commonly disposed in MSW landfills (e.g., household dust, old furniture, appliances, mobile phones etc.). PBDEs have been detected in landfill leachate (Osako et al. 2004; Danon-Schaffer et al. 2006; Haarstad and Borch 2008; Odusanya et al. 2009). Rowe et al. (2016c) conducted laboratory experiments for a commercial mixture of PBDEs (commercial name: DE-71). They reported congener-specific partitioning and diffusion coefficients and average partitioning and diffusion coefficients for an HDPE geomembrane (Table 6.5). The partitioning coefficients generally increased, and the diffusion coefficients generally decreased with the number of attached bromines. The partitioning coefficient for PBDEs in DE-71 were around 3-5 orders of magnitude higher than for BTEX or even about two orders of magnitude higher than for PCBs (Table 6.2). The diffusion coefficients for PBDE were around 2 orders of magnitude lower than for BTEX. However, multplying the very high partitioning coefficient, S_{gf}, by the low diffusion coefficient, D_g, to obtain the permeation coefficient, P_g where $P_g = S_{gf} \cdot D_g$ gave a permeation coefficient around 300-fold greater than benzene (Table 6.2). Analyses were performed to assess the potential implications for a single composite liner like that performed for PFOS. Diffusion parameters for the geomembrane were based on Rowe et al. (2016c). Table 6.6 summarizes the calculated impact in the aquifer of PBDE relative to allowable concentrations for four cases.

Table 6.6. Calculated impact in the aquifer of PBDE relative to allowable concentrations (Environment Canada 2013) for pure diffusion and advection with 5 holes/ha but only 1 hole in a wrinkle per ha (adapted from Rowe et al. 2016c)

Congener	Diffusion (No GMB) No wrinkle Peak/ Guideline	Diffusion (GMB) No wrinkle Peak/ Guideline	5 holes/ ha GMB/GCL 10 m wrinkle Peak/ Guideline	5 holes/ ha GMB/GCL 100 m wrinkle Peak/ Guideline
47	2.8	0.03	0.1	0.9
99	30	0.04	1.1	10
100	106	0.3	4	36
153	0.2	0.0002	0.01	0.05

The first case assumes no geomembrane but pure diffusion through the GCL and attenuation layer to the aquifer. The calculated impacts of the congeners 47, 99, and 100 ranged between about 3 and 106 times higher than the allowable concentration in drinking water based on Environment Canada (2013). The inclusion of a geomembrane substantially changes the situation and, due to the role of the geomembrane as a diffusive barrier, the impact in the aquifer is well below guideline limits for all congeners. The effectiveness of this geomembrane is primarily due to the high S_{gf} essentially locking up most of the PBDE within the geomembrane even though it contributes to the high permeation coefficient, P_g.

Considering 5 holes per hectare, as might be expected with good CQA, one of those holes coincides with a wrinkle. When the wrinkle with a hole was only 10 m long, the impact exceeded the guideline 4-fold for the congener 100 and just exceeded it for congener 99. Had the hole been in a 100 m long wrinkle, their impacts increased by about an order of magnitude relative to the

10 m wrinkle, and Cogener 47 was now approaching the regulatory limit. Like PFAS, it is found that a single composite liner is unlikely to be adequate for the long-term containment of PBDE unless there is also very good natural attenuation available at the site. This example highlights the need for more attention to potential PBDE release in landfill design and the evaluation and assessment of the site's suitability for expansion. Again, each site needs to be considered based on its size and the local hydrogeology to assess the likely impacts.

6.4 *Bisphenol A (BPA)*

Mass-produced for over 60 years, BisPhenol A (BPA; Figure 6.7) was, until recently, in the top 2% of chemicals produced worldwide (Nataraj and Aminabhavi 2010). More than 70 % of this large mass of BPA was used in polycarbonate production and more than 20% in epoxy resin production (Nataraj and Aminabhavi 2010; US EPA 2010).

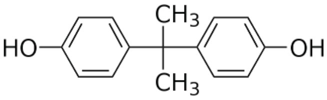

Figure 6.7. BisPhenol A (BPA): $(CH_3)_2C(C_6H_4OH)_2$

BPA has been extensively used in construction (roofing, internal safety shields for stadiums, and road signs), safety equipment (e.g., goggles, helmets, and safety shields for police), optical media (e.g., CDs and DVDs), electrical and electronic devices (e.g., cell phones, cameras and TVs), beverage bottles, infant feeding bottles, food containers and microwave ovenware, the interior lining of food and drink cans and metal lids on glass jars and bottles (Nataraj and Aminabhavi 2010; FAO/WHO 2010). Most of these items are eventually disposed in (MSW) landfills where the BPA can leach into landfill leachate (Yamamoto and Yasuhara 1999; Mansilha et al. 2013). Reported maximum BPA concentrations in MSW landfill leachate range from 12 μg/L to 17,200 μg/L (Yamamoto et al. 2001) with an average of 4,740 μg/L. The average value in leachate is almost 1000 fold higher than the 5 μg /L allowable in drinking water and almost 4000 times higher than the maximum concentration allowed to be released from a landfill into groundwater in Ontario.

BPA has emerged as a contaminant of concern because of its potential impact on human health and the environment. BPA mimics estrogen, raising concerns regarding the potential effects on the prostate gland in fetuses, infants, and children (NTP-CERHR 2008). Available evidence also suggests that BPA may have an effect on the brain including affecting the prenatal development of the brain and behavioural problems in children (NTP-CERHR 2008; FAO/WHO 2010; Erler and Novak 2010).

Saheli et al. (2016) studied the diffusion of BPA through a 0.5 mm-thick HDPE geomembrane. Over the 4.2 years that the diffusion tests were conducted continuously, BPA did not experience any measurable partitioning or decrease in the source concentration. Correspondingly, the concentration in the receptors showed no trend with time and remained essentially identical to that in the blank cell, indicating no measurable diffusion through the 0.5 mm geomembrane in over 4 years. An upper limit to P_g was obtained by assuming the receptor concentration was at the detection limit at 4.2 years, giving the value in Table 6.2. The inferred permeation and diffusion coefficient were obtained assuming S_{gf}~1. As in the case of PFOS and chloride, S_{gf} is not known with any certainty but is less than one. This, combined with the calculation method, means that the value of P_g in Table 6.2 for BPA is conservative, and HDPE is a highly effective diffusion barrier for BPA.

As with PFOS and PBDE, the effectiveness of a single composite liner, like that previously described and studied, was evaluated by modelling the impact on an underlying aquifer using the diffusion characteristics given in Table 6.2, and GCL properties given by Saheli and Rowe (2016). Once again, consideration was given to pure diffusion with no geomembrane, pure diffusion with a geomembrane, and diffusion and leakage for 5 holes/ha, where one of those holes aligned with a 10 m or 100 m long wrinkle.

Table 6.7 summarizes the results for the pure diffusion assuming no geomembrane and (i) a GCL and 3.75 m attenuation layer (denoted GCL/AL in Table 6.7), or (ii) a 0.75 m thick compacted clay liner underlain by a 3 m thick attenuation layer (denoted CCL/AL in Table 6.7). For these two cases the peak concentration in the aquifer was 11-fold above the allowable level with no significant difference between the cases with the GCL and CCL.

A geomembrane was then placed above the two clay liners and another pair of analyses were perfocmed assuming no holes in the geomebrane (pure diffusion). For these two cases the peak concentration in the aquifer was only 30% of the allowable level with no significant impact for either the GCL or CCL.

Assuming the geomembrane had 5 holes/ha with one in a wrinkle 10 m long, the impact was still acceptable with the GCL but almost twice the permissible concentration for the CCL. The difference in impact between the two different liner systems primarily arises from the much lower interface transmissivity that can be achieved between the geomembrane and GCL than can then be achieved between a geomembrane and CCL.

Assuming the length of the wrinkle with a hole was increased to 100 m, the impact on the aquifer significantly exceeded allowable levels by 5.7 fold and 10-fold for GCL and CCL, respectively (Table 6.7). Once again, demonstrating that minimal leakage can be tolerated through a single composite liner if it is the primary line of defence. For the impact to be acceptable with a single composite liner, it would be necessary to also have a very high level of hydrogeologic protection with a substantial attenuation capacity. Also, as in the other cases, to maintain an acceptable impact with no more than one hole in a wrinkle with $L_w \leq 10$ m, the service life of the geomembrane would have to exceed 270 years for the case considered.

Table 6.7. The calculated peak concentration of BPA in the aquifer normalized to water quality guideline ($c_{\text{peak}}/c_{\text{guideline}}$) [all number rounded to 2 significant digits] (adapted from Saheli and Rowe 2016)

Type of clay liner	Diffusion (No GMB) Peak/ Guideline	Diffusion (GMB) Peak/ Guideline	5 holes/ ha L_w= 10 m Peak/ Guideline	5 holes/ ha L_w= 100 m Peak/ Guideline
GCL/AL	11	0.3	0.7	5.7
CCL/AL	11	0.3	1.9	10

The studies outlined above all show that HDPE geomembranes are likely to be excellent diffusion barriers for the three contaminants of concern (PFOS, PBDE, and BPA) examined even though they are very different compounds covering a vast range of diffusion properties with P_g values ($2\text{x}10^{-16} \leq P_g \leq 8\text{x}10^{-9}$ m/s) spanning 7 orders of magnitude.

6.5 *A reality check: PolyChlorinated Biphenyls (PCBs)*

Polychlorinated Biphenyls (PCBs) are a group of 209 individual chlorinated hydrocarbons congeners. Each congener is unique, comprised of chlorine atoms substituted onto different positions of a biphenyl ring (Figure 6.8). Historically they would typically be used as a mixture of PCB congeners and given the commercial name Aroclor. For example, Aroclor 1242 is a mixture of over 100 PCB congeners containing 42% chlorine by mass. Similarly, Arclor 1254 was a mixture with 54% chlorine and Arcolor 1260 with 60% chlorine by mass. Arcolor mixtures (1242, 1254, 1260) were used in the large-scale manufacturing of electrical equipment. For example, all three were used in electrical transformers.

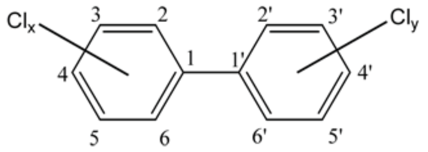

Figure 6.8 PolyChlorinated Biphenyls (PCBs): $C_{12}H_{10-x}Cl_x$

Non-volatile and hydrophobic, PCBs do not readily degrade and are persistent organic pollutants. PCBs have been reported to cause several adverse health effects and have been classed as probable human carcinogens (USEPA 2013a). Because they are harmful to human health, many countries restrict their incidence in drinking water to very low levels. For example, the United States EPA has set a maximum contaminant level of 0.5 µg/L in drinking water (USEPA 2014). The drinking water objective in Ontario, Canada, is 3.0 µg/L (MOE 2003), although the allowable landfill impact on clean groundwater is only 25% of the health-related drinking water objective (MOE 1998).

PCBs were recognized as hazardous, persistent pollutants in the environment and their industrial use was banned in Canada in 1977 (Environment Canada 2014) and in the United States in 1979 (USEPA 2013b). However, PCBs have a very long legacy. More than 40 years after they were banned, PCBs are still found in MSW landfill leachate at concentrations significantly exceeding both the United States' and Ontario's permitted impacts on groundwater from a landfill.

In the early 1980s elevated PCB levels in whole fish samples were identified in the Thames River in London (Ontario, Canada). Sampling identified PCB concentration up to 29,900 ppm in the sediments and soil in the Pottersburg Creek watershed New London. Between 1984 and 1987, the contaminated soils were excavated and placed in four engineered landfill cells (one per year) for "temporary" storage until destruction of PCBs was possible (Environment Canada 2013). All four cells had a composite liner (HDPE geomembrane over a CCL) as a final cover system. The bottom barrier system for Cells 1 and 2 comprised a leachate collection system, primary CCL, a sand/gravel leak detection zone, and secondary CCL. The bottom barrier system for Cells 3 and 4 comprised of a leachate collection system, HDPE geomembrane, sand protection layer, CCL, secondary leachate collection system, and secondary CCL (McWatters et al. 2020). The system was designed to operate with hydraulic containment, such as the only mechanism for outward PCB migration was diffusion. The diffusive properties of the HDPE and CCL liners were established. The partitioning coefficient, S_{gf}, for PCBs (and even more so for PBDE) was extremely high. This was manifested by a very rapid complete loss of PCB in a source compartment of a conventional diffusion test and unmeasurably small migration into the receptor as the PCB's preferentially partitioned to the HDPE geomembrane (Rowe et a. 2016). S_{gf} inferred from sorption tests was between 90,000 – 110,000, with an average of 100,000 (Table 6.2). The diffusion coefficient was obtained by microtoming the HDPE geomembrane and obtaining a PCB diffusion profile through the geomembrane, which gave a best of $D_g = 1\times10^{-14}$ m^2/s with a lower bound estimate of 5×10^{-15} m^2/s close to the bulk value inferred for PBDE (Table 6.2). Although S_{gf} is extremely high for PCB's (almost three orders of magnitude higher than for benzene), it was more than an order of magnitude lower than S_{gf} for PBDE (Table 6.2), and consequently, P_g for PCB's was almost an order of magnitude lower than for PBDE (Table 6.2; Rowe et al. (2016). The diffusive properties of the CCL are reported by McWatters et al. (2020).

In 2008, PCB Regulations required all PCB soils exceeding 50 mg/kg to be destroyed by incineration. Thus, in 2009 the PCB storage site was decommissioned with the excavation and transport of 107,000 tonnes (~35,600 m^3) of contaminated material for incineration. During decommissioning, the geotextile, geomembrane, and soil samples were taken from the cover and baseliner. In addition, soil cores were taken through the base layers to obtain the variation in PCB concentration with depth (McWatters et al. 2020).

Using the independently established parameters for the geomembrane and soil, the diffusion profiles for PCB's through the barrier system was predicted using the same computer model (POLLUTEv7; Rowe and Booker 1984a,b, 2004; Rowe et al. 2004) that was used to analyse the composite liner system for the contaminants of concern in the previous sub-sections. The model results were in very encouraging agreement with the observed PCB migration.

Based on the detailed investigation of the long-term (22-25 year) application of geosynthetics in a landfill barrier system designed to contain PCBs, McWatters et al. (2020) reached the following conclusions.

1. Over the 22-25 year operating period, the composite liner cover system limited percolation through the cover to an average of less than 12 lphd in an area with an approximate annual precipitation of 27,000 lphd (1 m/year of rain equivalent) and where a typical soil cover will typically permit 4100 to 5800 lphd percolation through the cover.
2. The base barrier successfully minimized PCB transport from the landfill to no more than a few centimetres in over 20 years.
3. PCBs remained bound to the geomembranes and GTXs on either side.
4. After more than two decades in service, no PCB concentrations were found in the groundwater.
5. Previously published laboratory HDPE geomembrane -PCB diffusion parameters combined with independently obtained clay liner parameters gave predictions in encouraging agreement with the observed PCB migration.
6. The storage facility could have continued operating, provided that leachate collection prevented outward advective transport. Cover integrity was maintained indefinitely (likely at least many centuries and possibly longer) without impacting groundwater under these low-temperature operating conditions. This finding cannot be generalized to MSW landfill barrier systems operating at substantially higher temperatures.

Rowe et al. (2016) used the same parameters used in the analysis of the field case described above to predict the long-term performance of a single composite liner with a GCL or CCL for the scenario as described in previous sections. Like the findings in the previous subsections, a single composite barrier system would provide adequate protection to the underlying groundwater provided the migration of contaminants was governed by diffusion. However, exceptional CQA would be required to limit the leakage to a very low acceptable level to maintain PCB concentrations below regulatory limits. Also, a very long service life would be required for the HDPE geomembrane.

Rowe et al. (2016) also concluded that the potential impact of contaminants with high S_{gf} values should not be based on a simplistic steady-state calculation using Fick's first law and the permeation coefficient (P_g) or using a computer program that does not explicitly model both partitioning and diffusion through geomembranes. Using P_g as the diffusion coefficient will give very misleading and incorrect results. For contaminants with high S_{gf}, consideration must be given to modelling Sgf and D_g as independent entities.

6.6 *Summary of current status and remaining questions*

Based on the preceding review of research related to the four synthetic or synthetic groupings of persistent organic pollutants of concern (PCBs, PBDEs, BPA, and PFAS), it was found that a typical 1.5 mm HDPE geomembrane was an excellent diffusion barrier to all the compounds examined. However, with typical construction quality assurance, there is high probability that the leakage of many of these contaminants through a single composite liner will eventually exceed allowable levels in the environment unless one or more of the following apply.

(a) there was an electrical leak location survey before and after the geomembrane was covered,
(b) there is a high-level of hydrogeologic protection and attenuation, or
(c) there is an extra level of engineering in the form of a secondary leachate collection/ leak detection system.

It may take decades before the problem is identified.

The impacts associated with the contaminants of emerging concern can be kept to an acceptable level for new facilities if they are designed and constructed to satisfy (a) and either (b) or (c) above.

Based on experience, the level of CQA required to achieve negligible leakage is extremely unlikely for existing landfills, and there is an 80-99% probability that allowable limits on groundwater would be exceeded for one or more of the four groupings of contaminants of concern if they were lined with a single composite liner of the form examined. Therefore, analyses similar to those performed by Rowe and Barakat (2021) are recommended for all landfills with a single liner to ensure the barrier system's suitability for containing PFOS (and likely other PFAS and contaminants of emerging oncer) in a MSW landfill.

Considering the persistence of the four groupings of compounds and the ratio of leachate concentrations relative to allowable levels in many jurisdictions, more consideration needs to be given to the service life of the geomembrane in particular the barrier system in general for MSW landfills containing PFAS, BPA, PCBs, and/or PBDE.

---

7 REGIONAL CONTEXT: OF AFRICA, ASIA, AND SOUTH AMERICA

There are 48 countries in Asia, most of which are developing countries, including China, India, Iran, Saudi Arabia etc. The Asia continent covers an area of around 44 million km^2, which accounts for 29.4% of the total land area of the world. The Asian continent, with a population of 4.5 billion, is the most densely populated area in the world. The economic development levels for the Asian countries vary widely, so do the regulations and technologies for waste management and contaminant containment. For example, Singapore and Japan have some of the most stringent environmental regulations worldwide, while some other Asian countries are still struggling with proper solid waste collection and disposal systems. The latest publication of the World Bank on waste management in 2018 concluded that significant investments are still needed for most of the Asian countries to establish integrated waste management systems to meet good international hygiene standards (Kaza et al. 2018). Other recent and notable articles related to waste management and containment in south-east Asia are authored by Jambeck et al. (2015) and Lebreton et al. (2017). Both articles consider the south-east Asian region as one of the “leakiest” regions for marine plastic waste.

Africa is the second largest continent with a population of 1.3 billion and along with Asia it is forecast to be the area of highest world population growth in coming decades. South America is the 4th largest continent and 5th on the world population list with 431 million people living there. Latin America is world renowned for mining activities including at extreme altitudes.

The growth of mineral production in the world results in the generation of large volumes of tailings from the ore beneficiation process and the consequent need for tailings storage facilities in the mining footprint. Robertson (2011) reports that the volume of tailings from mining activities has increased significantly, in excess of 10-fold every 30 years. As a result, more and more structures are needed in shorter periods of time. In 1900 the daily production of tailings was around 100 tons, which increased to 100,000 by 2000. Currently the tonnages are approximately 670,000 tons per day. It is estimated that by 2030 the volumes of waste will be of the order of 1,000,000 tons per day. Robertson (2011) also shows that the average height of tailings dams has doubled every 30 years.

The International Commission on Large Dams (ICOLD) carried out a study that concluded that the frequency and severity of failures were increasing globally, the majority of which would be preventable if diligence on the part of dam owners and operators was observed (ICOLD 2001). Chambers and Bowker (2017), analysing the risk of failures, considered that between 2016 and 2025, about 30 significant tragedies related to tailings dams should be expected.

Despite the context described above, as far as the authors are aware, regulations regarding the use of geosynthetics in Latin America are incipient or non-existent. For example, the Brazilian legislative system regarding dam safety promulgated its first law (Law No. 9,433) in January 1997, when the National Water Resources Council (CNRH) was created. Currently, the country has 34 national and state legislations, including laws, decrees, ordinances, normative deliberations, resolutions and provisional measures. Of this total, 15 laws were produced after the Fundão dam failure, Mariana, State of Minas Gerais, Brazil, in November of 2015. Law No. 12334, of September 20th, 2010, established the National Dam Safety Policy (PNSB), whereas law No. 14,066 of September 2020 is the most recent law dealing with dam safety policy.

In Africa, the development of water resources infrastructure reflects an increasing rate of consumption with time. Only in recent decades has an appreciation of water conservation with demand management and resource quality grown significantly. The process and practice followed in pursuit of authorization for waste management facilities have evolved significantly over the past three decades with changes in philosophy, technology and performance standards. The need for and process of change with time is reported along with some of the challenges to which the industry has been exposed and innovative solutions to overcome these challenges.

The intent of this section is to present the challenges faced in the planning, design, construction, and operation phases of contaminant barrier systems outside of North America and Europe. The range of experiences in municipal solid waste, mining and industrial waste and pollution control facilities reported on addresses changes in performance standards over time. It is not intended to be an all-embracing report on state-of-the-art technology and practice outside Europe and North America. Still, it is intended to give insight into the reasons for diverse practices and unique approaches. Reconciling water availability and increasing demand in the near future requires today’s decisions to provide sustainable mining practices in several regions.

7.1 *Overview of policy and legislation*

A brief overview of water resources development legislation and commensurate regulatory structures and objectives in the African region gives significant insight into the rate of change of development with time, with the associated generation of waste or pollution and significance attributed thereto.

Today South Africa is a relatively young developing country in which the industry matured following a foundation in both agricultural expansion and mining practices in the hinterland. A century ago the results of early mining raised very limited concerns with respect to pollution, and legislation was introduced in 1935 to assist with the management of water resources in the upper Vaal River catchment, which is one of the major rivers of the country and situated to the south of the gold mining reserves. Cities such as Johannesburg developed around these mining practices. For many years, pollution due to other sources such as municipal solid waste was not considered to be a serious threat to the water resources nor environment.

As recently as the 1970s a senior official within the regulatory system had stated publicly that landfill waste was not considered a source of pollution to be of concern. The practices for landfilling were thus unregulated and municipal solid waste was disposed of in unlined abandoned quarries, random valley fills, and in any other accessible positions including as fill material to reclaim wetlands.

It was during the 1980s that an academic institution established a research program to look into whether or not landfills were indeed a source of pollution. This program looked at two existing facilities, which had been operating for many decades. One facility known as Waterval was a site serving the early gold mining city of Johannesburg. The other waste facility was situated at the other end of the country, just outside the city of Cape Town and known as Coastal Park. The investigation into these waste bodies included aspects of conventional geotechnical engineering such as drilling auger holes through the waste body and profiling the holes with depth, keeping a record of moisture content, extent of waste degradation, type of waste, extent of ash, and layering, along with the presence of free liquid. This investigation concluded that landfill is indeed a source of pollution and that the main drivers of leachate development were related to drainage of surface and surrounding water; the moisture of the waste being deposited including whether co-disposal of liquids with solids was taking the place; and the climatic water balance at the site. The research process had also included monitoring of groundwater with distance from the waste facility and it was noted that in the case of Coastal Park landfill, a pollution plume was moving off site at about 4 m/annum.

7.1.1 *Development of initial waste management philosophy*

This 1980s research led to the belief or philosophy that it was only necessary to contain the most hazardous of waste material, whereas for small sites or low risk point sources of pollution the groundwater regime could employ the philosophy of attenuation for protection. During the early 1990s, the regulatory body responsible for water resource protection developed a suite of guidelines that became the accepted standard against which the permitting of landfills took place. These standards were based on the philosophy that mitigation of pollution impacts can be achieved by containment for the most severe pollution source and attenuation for the low significance pollution sources, with a range of standards between these two extremes as shown in Figure 7.1(a). The waste classification was thus addressed by toxicity and concentration, leading to the classification of waste as either hazardous or general. The size of a site was taken into consideration based on the rate of waste disposal, leading to a second parameter of large, medium, small, or communal facilities. Finally, to give effect to the research result which identified available water as a critical factor, it was accepted that a third factor would be water balance at the site, with the leachate producing facilities conceptualized as being those situated at positions where, for the wettest six months of a year, the rainfall would exceed evaporation as shown in Figure 7.1(b). Sites were thus classified with the third parameter as either water surplus or water deficit.

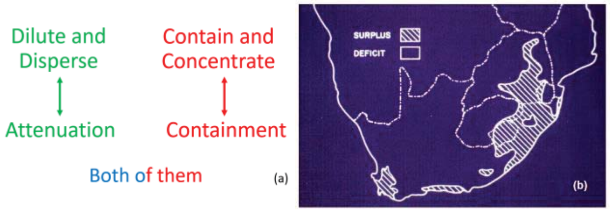

Figure 7.1 The 1990s' philosophy on pollution generation and range of mitigation (Ball 2002): (a) The extreme philosophies of dilution and dispersion relying on attenuation through a range of standards to containment; (b) The concept of water balance showing water surplus and water deficit areas based on precipitation and evaporation in South Africa

Classifying sites as hazardous or general, large medium or small, and water surplus or water deficit led designers to minimum requirements for containment barriers beneath such facilities. However, it is recognized that these prescriptive quasi containment barrier standards did not pursue containment to the extent that was reasonably achievable but allowed for some dilution and dispersion of pollutants. Thus, only hazardous waste facilities in recent years generally employed a double liner system of which at least the primary liner was a composite liner made up of both a geomembrane and a compacted clay liner. This compacted clay liner was made up of multiple layers with a total thickness of at least 600 mm. In all cases where double liners were specified as a minimum requirement, they were separated by a leak detection system. There was also a minimum requirement that, for all containment barrier systems incorporating a geomembrane, there should be a protection layer between geomembrane and the overlaying leachate collection system. For the general waste facilities, clay-only barriers were employed with thickness in proportion to size classification, and leachate collection systems were required only for those sites situated in a positive water balance area.

This range of documents gave waste facility owners guidance beyond design and construction and included operation and performance monitoring. In addition, the minimum requirements were used extensively when the country was going through significant change in legislation and a growing environmental awareness with recognition of the limits to natural resources. Thus, while these documents were employed for over a decade leading into significant law reform, the regulators and professional societies involved in waste management used the opportunity to ascertain the suitability of the philosophy and associated prescriptive standards for pollution control. As a result, these prescriptive standards were embraced at least in principle by neighbouring countries of Namibia, Botswana, Mozambique, Swaziland and Lesotho, and seen as guiding documents in many other parts of Africa. In addition, the guideline documents were used to motivate the development of standards in parts of Asia in the late 1990s. It is however recognized that although prescriptive in nature rather than performance based, they were seen to be one of the lowest standards of containment in the worldwide survey of regulatory standards (Koerner and Koerner 2007).

There were several lessons to be learnt from applying these requirements or standards in the local framework. It was recognized early on in their application that even in the driest of regions, falling well within the water deficit classification, leachate was indeed produced within the waste body and was as a result a source of pollution as seen in Figure 7.2(a). Similarly, it became quite apparent that the waste stream to landfill varied with time and position, and this had an influence on the performance of leachate collection systems in the water surplus areas. These leachate collection systems were found to block readily as seen in Figure 7.2(b), as they were not protected by filter systems defined within the standards and thus not employed by the owner or designer. So too was significant experience gained in the use of geomembranes as liner materials.

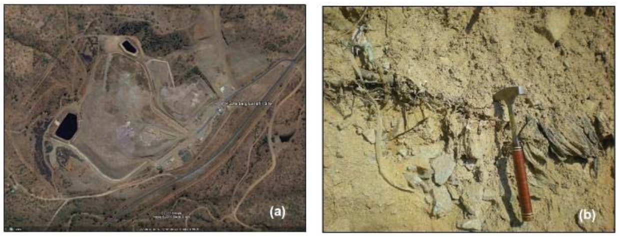

Figure 7.2. Experiences from applying the Minimum Requirements for waste disposal (DWAF 1998) philosophy: (a) Excessive leachate is generated even in a desert environment (Google Earth image of Kupferberg, Namibia (Alphabet Inc. 2019); (b) Aggregate leachate collection systems clog readily if not protected by a filter (Shamrock and Msiza 2015)

The use of geomembranes in South Africa had initially been for applications where water containment was required, often associated with inter basin transfers, or delivery of raw water over significant distance from its source and hence competent storage was required for this valuable asset.

7.1.2 *Development of a modern philosophy*

The new-found international relations with the world allowed South Africa to exchange technology with countries willing to do so, and the advent of the Internet facilitated an even greater rate of sharing of knowledge and experience.

The new legal framework in the Republic of South Africa (RSA) placed environmental protection and human rights high on the legislative agenda. The Constitution of RSA, 1992 and 1996, Bill of Human Rights demanded a rethink of waste management and pollution control measures. A hierarchy of waste management strategies emerged with a priority to address the rapidly deteriorating limited water resources as seen in Figure 7.3. It is widely known that with the long history of mining practices in certain parts of the country, that salts are a significant problem in the groundwater and river systems (Brink et al. 2009). The assimilative capacity of many watercourses and rivers was exceeded bringing about the de-oxygenation and anaerobic conditions with associated loss of biota. Many human lives and the health of communities or persons who made use of runoff river water supplies were placed at risk.

Figure 7.3. Visual evidence of waste and mining pollution in rivers: (a) The confluence of the Vaal and Klip Rivers (Google Earth Image of confluence the Vaal and Klip River); (b) The confluence of the Steelpoort and Klip River (photo courtesy RB Martin)

This attention to the significance of RSA's water resources was escalated largely by the World Commission on Dams South African Initiative, which recognized the scarcity of water in this and other regions of the world. Similarly, the dependence of poor persons on natural resources drew attention to the water quality of river systems which was further emphasized by acceptance of international treaties and the importance of biodiversity and wetlands in the remediation of water resources impacts.

Despite the privilege of a domestic geomembrane manufacturer, several lining installation contractors, and a local geotextile manufacturer with several suppliers, the investigations and performance assessment of geosynthetic products was undertaken by academic institutions to a large extent and to a lesser extent by the regulator itself. With the limited resources available for research, the use of international literature, access to material producers from around the world, and cooperative studies were pursued.

Developments in African countries, particularly South of the Sahara Desert, in which a waste disposal facility was required, tended to adopt the standard of the investor's host country if European or North American or alternatively followed the standard employed by South African legislation of the time.

7.1.3 *State of the art in the African Region*

Regulations employed in foreign countries were considered for their suitability to the South African landscape. In particular, Australia, Canada, Germany, and the USA, along with the supporting technology, were studied.

An analysis of international standards led the regulator to believe that South Africa had one of the lowest standards of containment for waste amongst those countries in the world that were regulating waste containment barriers systems at that time. A worldwide survey (Koerner and Koerner 2007) confirmed that the world standard for waste containment, irrespective of whether the waste was hazardous or general, was the employment of a composite (geomembrane plus compacted clay in intimate contact) liner within a barrier system. In contrast, South Africa was largely relying on clay-only liners for partial containment and, in many cases relying on rudimentary drainage layers and clay-only liners for controlling the rate at which groundwater pollution took place.

Although it was tempting to adopt a standard from another country with experience in modern containment standards for barriers systems, the South African situation of a large industrial and developed economy in a water-scarce environment had to be considered. In addition, the water availability per capita per annum needed consideration to reflect the acceptable assimilative capacity of our ecosystems within watercourses. The quantity of renewable water per person per annum varies widely across the planet. It was observed that regions with large quantities such as Canada, the North Americas, and Europe tended to have established legislation that relied extensively on the containment of contaminants achieved by composite liner systems. Although there is no known register of regulatory standards, it became apparent that numerous countries outside of North America and Europe did not have a standard for contaminant containment barriers (Msiza, 2020) despite less renewable water per person per annum being available. The predictions are that Chile, South Africa, and Australia will be among the world's first countries to have used between 80% and 100% of their available water resource by the year 2040, as shown in Figure 7.4, with other countries following not far behind in growing water scarcity.

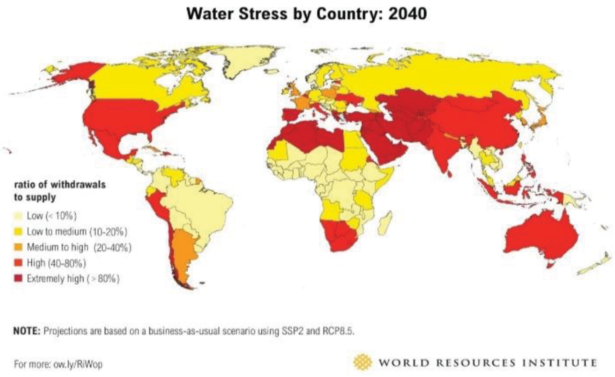

Figure 7.4. Water deficit regions for the world by 2040, as predicted by the World Resources Institute (2015)

While South Africa has a lean economy, it has an obligation to fulfil multiple responsibilities such as the alleviation of poverty; the provision of basic water of an acceptable quality to all its inhabitants; the right to a safe environment; and the protection of its environment for future generations. The prioritisation of needs and regulation required careful consideration to maintain a healthy economy. Furthermore, regulatory actions should be fair and just to participants within the social and economic framework. The opportunity to build more dams is limited, with water delivered becoming increasingly expensive, especially given the long-distance over which transfers are required. The development of new dams must be evaluated in terms of impact, economics, and alternative options. Water quality deterioration through pollution from agricultural, industrial, and mining activities and poor urban wastewater management, is arguably the most serious threat to the region's water resources. While treatment and reuse of water is one option in meeting growing demand, the prevention of pollution and water conservation by use of high-performance containment barrier systems was proposed as a more cost effective and broader benefit option.

It was thus decided to embark upon a consultative procedure from 2009 to 2013 with proposals to refine the historic minimum requirements leading to national norms and standards for the classification and containment of waste (following a revised waste assessment process) within the waste management hierarchy, which prioritised waste reduction and re-use only then followed with disposal to a facility designed for containment. This strategy would clearly lead to a change in waste stream and a change in resultant behaviour of the waste body. The intention was to move away from numerous small sites and move towards regionalisation of municipal solid waste facilities. An example of the change in waste stream was the regulator's introduction of paying for plastic bags, so readily used in society at that time. This change brought about a reduction in the plastics content of new municipal solid waste streams, which changed strength characteristics and resultant angle of repose of waste and hence the outer slopes.

Today's regulations for pollution control barrier systems in South Africa are based on a risk assessment of the pollutant informed by the concentration of toxic elements. Then for each waste risk type, a commensurate containment barrier standard is required (NEMWA Regulations 2013). All containment barrier standards require a composite liner and drainage system. A double composite liner separated by a leak detection drainage layer is required for the highest risk waste type disposed of at an engineered facility. Although the barrier system of drainage layers and composite liners is prescribed by material type and thickness, the regulations simultaneously require the performance of the design to be defined and thus also allow for the use of alternative materials provided the equivalent performance thereof can be demonstrated. This performance prediction is based on the design itself and the associated construction quality assurance plan (which includes quality control). It is to quantify service life for the barrier system and assess the total solute transport (seepage) anticipated post-construction of the barrier system. In addition, the authorities consider acceptability based on predicted performance for containing contaminants at a particular site and whether the predicted performance is acceptable to the receiving environment, be it the water resource, natural or physical resource, including air, and to society at present and for generations to come.

The principle of pollution containment is not unique to Southern Africa. For example, Ghana had established Landfill Guidelines in 2002, which followed on from the 1999 Environmental Sanitation Policy, which was revised in 2009 to broaden the application of the polluter pays principle (Government of Ghana 2002, 2009). These policy documents similarly pursue pollution containment.

The transition from the prescriptive standards based on the philosophy of pollution dilution and dispersion which relied on attenuation as mitigation, to the performance-based criteria, which rely on containment as mitigation and allowing extensive use of alternative geosynthetic materials as partial or full replacement of natural materials, has led to a multitude of challenges and some innovative solutions to meet contaminant containment objectives. While some challenges are common to Africa, Asia and South America, there are regional influences that bring about distinctive challenges, as discussed in the remainder of this section.

7.2 *Challenges in barrier system planning, design, construction, and operation: Africa*

7.2.1 *Changes in Philosophy, Legislation and Commensurate technology (influenced by attitude; knowledge, experience, and trust)*

A change in philosophy and commensurate legislation over time has been necessary for sustainable development of available water resources in a region where (a) they are finite although renewable annually and (b) there is a diminishing volume of renewable water per person per annum. This has led to improved standards of contaminant containment over time, with regulatory standards being influenced by research results that have demonstrated the advantages of geosynthetic materials when used in conjunction with or as partial or complete replacements of natural materials.

The regulations used in the Southern African region require a contaminant containment barrier system comprising drains and composite liners. The predicted performance of the design and construction quality assurance protocol forms the basis of the authorization. The regulation makes provision for the use of geomembranes and geosynthetic clay liners as full and partial replacement of soil liners, allowing for geotextiles as cushion layers to geomembranes and as filters, and allows for geodrains as a replacement for sand and aggregate drains, provided equivalent performance is shown. The challenge lies in demonstrating the equivalent performance of an alternative element in a barrier system where it is not just the primary function required to be equivalent. Still, the equivalence within the context of the barrier system must be demonstrated. For example, a GCL may be seen as equivalent to a CCL in respect of seepage by a particular permeant such as water. Still, the barrier system requires that the performance recognizes all attributes of the alternative material including the interface and internal shear strength, the performance under low and high confining stresses, and the performance over the service life (of operation plus post closure polluting period) for the specific chemical and physical exposure conditions.

Designers often fail to thoroughly investigate and evaluate the equivalence of the system, relying on product supplier's information on a particular element of geosynthetic materials, usually brand related without an appreciation of design complexity and uncertainty. It thus falls upon the regulator to have state of the art knowledge and experience to assess the appropriateness and correctness of a performance-based design, especially when influenced by material suppliers pursuing brand specification over performance requirements. Examples of non-performance-based specifications apart from brand name or product code include excessive descriptions or markings such as for the use of a GCL in a composite liner for a hazardous waste facility where the specification called for non-toxic ink markings to define the GCL overlap or in reinforcing grids defining the colour of the grid. Neither a marking ink nor the to be buried product colour will influence the systems performance but will influence the cost of the development.

The anti-competitive practice of brand specification without performance evaluation or specifications has led to substantial resistance to the use of geosynthetic materials in contaminant containment or pollution control barrier systems by facility owners to the extent that both the private and public sector have called for an abandonment of the geomembrane liner requirement. This resentment by developers of designers' behaviour has been led by the mining industry (Chamber of Mines 2016) and could have had significant detrimental impacts on society and the greater economy. This led to an assessment of the socio-economic impacts of competent containment systems which found that despite their site-specific cost, the benefit outweighed the impact. Furthermore, it has not been the geomembrane inclusion per se which has created the escalated unit costs of containment barrier systems, but (a) the cost of the drainage aggregate, which is the most expensive element, along with (b) anti-competitive geosynthetic material specifications that lead to alignment between some designers, contractors, and product suppliers. The latter has escalated costs unnecessarily and resulted in post construction substandard performance.

To overcome this, voluntary organisations such as the International Geosynthetics Society have pursued training exercises for the benefit of society and awareness of appropriate technology. Similarly, technical advisory notes on design and construction have been made available to the public to counter the misuse of otherwise sound geosynthetics materials. There are alleged instances where designers have specified unjustifiably thick leachate collection systems and larger aggregate size than the normal 53 mm to require a larger mass per unit area geotextile cushion layer only available from one supplier and restrict product supply to a subset of the available lining contractors. It is alleged that this behaviour has led to escalated costs of single composite liner barrier systems, for the benefit of the designer when contracted on a fee system related to a percentage of the capital cost. Similarly, there are alleged instances of a comfortable relationship having developed between designer having brand orientated specifications, the brand of supplier, and the lining contractor to whom the product supplier is aligned that has led to the installation of unacceptable geomembranes (which have suffered separation in plane and been supplied with factory faults including regular holes, despite having ISO 9000 certification (Figure 7.5).

The change in philosophy from relying on attenuation to the philosophy of containment relying on competent containment as mitigation of pollution is reflected in the modern regulations which require the use of geosynthetic materials and allow for still further geosynthetic substitution of natural materials is underpinned by the state-of-the-art technology and training provided by the International Geosynthetics Society, its regional Chapters and other voluntary organizations. The challenge posed by some designers alleged misuse of the standards and selective technology for unjustifiable financial gain through partial specifications or construction quality assurance plans is being resolved by exposing the practice in public forums and simultaneously sharing appropriate technology. The latter validates the benefit of competent barrier systems in the minds of developers and reduces the antagonism of parties opposed to geosynthetic materials used in regulations.

7.2.2 *Role Players and Responsibilities (relying on clear separation, avoiding disclaimers and alignment)*

The developer of a waste disposal facility (WDF) relies on the designer, usually, an engineer, to provide a specific solution meeting the developers needs and complying with regulatory norms and standards. The role of the developer's team and of the regulator is quite different in that the former is the proponent with a site-specific view whereas the latter has a broader responsibility to society.

The regulator is on occasion challenged on fairness and consistency of decision-making. However, there does is need to be a clear separation of roles and responsibilities between the designer and the regulator. This is emphasised particularly in forensic analysis following geotechnical structure failures such as of a tailings dam (Morgenstern et al. 2015). The reliance on observational methods and government inspections alone is inadequate to avoid many incidents because no amount of inspection will reveal the hidden flaws. Hence, further actions may be prescribed from time to time. Nevertheless, it is axiomatic that the regulator cannot regulate its own activities, and if the regulator were to usurp the role of the designer it would usurp its own role. Thus, reviews result in an assessment of acceptability, whereas the designer is responsible for the approval of reports and drawings.

Figure 7.5. (a) Separation in-plane for a geomembrane having 0.9 mm micro-spike height and (b) Geomembrane manufactured with discontinuities including ridges and holes installed despite the designer's specification requiring a 0.9 mm micro-spike height and minimum thickness of 1.5 mm.

Despite this separation of roles and responsibilities, it is not uncommon for a developer to seek guidance from the regulator or seek regulatory approval based on a report containing a disclaimer in which the designer absolves him or herself of all responsibility. In such cases, if the designer cannot trust its own work, the regulator certainly cannot trust the design report either and such an application should not receive authorization. The situation has also arisen in which once a developer has an authorization or a licence from the regulator, it is believed that such a licence and conditions are the fixed property of the developer and it is the responsibility of the regulator should there be an incident associated with the design or construction of the containment barrier system. However, in such situations reliance is made on the regions human rights entitlements and overarching law for which a judgement has been made as follows "licences are subject to administrative withdrawal and change. They are never absolute, often conditional, and frequently time-bound. They are never there for the taking, but instead are subject to specified pre-conditions. In time, a licence holder may cease to be suitable to hold the licence and they are also not freely transferable" (Froneman et al. 2015).

Other means by which such challenges are resolved include the mobilisation of public interest in the technology of containment barrier systems. This is partly achieved by addresses to public meetings during environmental impact assessment processes prior to a development taking place, and partly by addresses to the monitoring committees of public representatives which oversee developments where containment barriers are utilised. The results of social media commentary can be extremely beneficial to the developer and regulator in rectifying designer and contractor deviations from accepted practice. The recent growth in geosynthetic technology availability through webinars addressing aspects of design and construction technology has been particularly valuable in resolving disagreements between designers and the interested and affected parties (IandAPs) of a particular development ahead of construction, when these recorded webinars by international experts are made available to the IandAPs to substantiate engineering norms and rebut concerns about deficient designs and unsubstantiated claims.

7.2.3 *Designers reliance on material supplier's data sheets*

There are other unusual approaches outside the norm that affect the development consideration which takes a systems approach. Some designs specify performance based on product data sheets without validating the parameters relevance to a particular design, without ascertaining how the parameters change with time or temperature, and occasionally without ascertaining whether such materials are still available or whether technology has surpassed the specified test method, performance standard, material type or interaction with other materials.

An example of parameter change with time is the reported interface friction between a smooth geomembrane and particular soil such as flexible polypropylene geomembrane and Ottawa sand reported as 29.5° (Montell brochure 1997), let alone the change with other soil interfaces such as clays, or time related change to interface shear strengths due to polymer creep or effects of leachate irrespective of texturing. This lack of attention is especially true in respect of filter design for both granular and geotextile filter compatibility with adjacent soils and, in particular, fine grained cohesive soils as used in CCLs (Sherard and Dunnigan 1989).

Seldom is sufficient consideration given to the difference in performance between the office specimen and the material installed with respect to project specific specifications. The method of post-production storage also can influence geosynthetic performance prior to and during installation, especially for geotextiles (ICOLD Bulletin 55, 1986), and for GCL carrier components.

Observations on a particular day in a supplier's stockyard using an infrared thermometer revealed the following: black plastic sheet wrapping at 70 to 75°C; unwrapped geotextile rolls at 55 to 69°C with colour varying from pale grey to black and the darker the geotextile the higher the temperature; and even a red plastic sheet wrapping was cooler (than the geotextiles) at 57°C, as was the temperature of unwrapped black pipe surfaces which allowed ventilation through the stack (Legge, 2019).

This makes for interesting service life assessments when considering the rate of UV degradation, especially on polypropylene (PP) and polyester geotextiles in relation to cushion layer performance and thermal conductivity. Similar measurements on geomembranes in Limpopo Province, RSA at various sites have shown the upper exposed surface to be at 83 to 86°C at midday, and temperatures of 89 to 90°C measured in the Northern Cape when the ambient temperature was near 40°C. A limited drop in temperature of the order of 10°C was measured between the upper and lower surface of geotextiles deployed over geomembranes. However, when covered with 100 mm of soil, the temperature of the liner and the number of associated wrinkles reduced significantly. This data emphasizes the need to consider time-related activities and the consequences thereof, such as the diurnal expansion and contraction affecting the geomembrane/compacted clay liner interface performance, especially when textured geomembranes are employed, and the clay surface is effectively combed and soil particles displaced. It is similarly argued that designers should consider the time-temperature curve during operation and post-operation life, along with the pre-utilization period, to give a fair assessment of service life. The use of average temperatures at leachate outlet points does not necessarily reflect the containment liner temperature beneath the cell. Such temperatures do not reflect the effect of leachate mounding or energy dissipation and radiation for which models exist (Hao et al. 2017). The time-temperature service life curve for an HDPE geomembrane being hyperbolic will show that a short period at a high temperature can significantly reduce performance far more than the equivalent average temperature of exposure over the same period. Similar consideration of time of exposure to temperature and pH should be afforded to geotextiles when considering the acceptability of polymer (Mathur et al. 1994).

To avoid such shortcomings in the design, a regulators' checklist of performance parameter results is called for by the facility's developer. This checklist is aimed at assessing the relevance and diligence with which the designer interrogates facts and assumptions made and requires the predicted performance to be specified for the assessed service life and quantified total solute transport through the barrier system for the specific development. The developer and designer are both required to certify the check list as true and correct prior to submission to the authority. This management technique has led to an improved appreciation of the benefits and constraints of geosynthetic materials by owner's representatives other than the engineering profession and led to a reduction in the potential misrepresentation of predicted performance by designers and product suppliers.

Perhaps the most valuable innovation in resolving the application of inappropriate data sheet parameters is the statutory end of construction site inspection by the regulator in the presence of the facility owner and design engineer provided the regulator has adequate insight. The site inspection goes beyond comparing the construction completion report and its supporting evidence with the accepted design and specifications in that on site observations and physical measurements are made and samples collected for the regulator's independent assessment.

These activities take place under the scrutiny of the developer and design engineer with constant communication on reasons for the evaluation and implications of the assessment being made. The potential implication of the revised licence conditions on volume or type of waste that may be disposed or similar amendments to remedy designer's reliance on invalid data sheet parameter values have financial implications that are significant motivator for owner and designer to accept appropriate technology and a motivator for the regulator to be diligent in applying state of the art technology to avoid litigation and associated costs. This remedial behaviour has in recent years generated an eagerness for knowledge and application thereof in the design and construction of contaminant containment systems. The knock-on effect has been far reaching as designers revert to product suppliers on inappropriate data sheets and/or misleading guidance to the extent that product data sheets are amended to reflect specific product and date references as well as conditions under which parameters were derived such as at room temperature. The further consequences include the revision or updating of national standards to reflect current technology and in particular the move by designers to base designs on site specific evaluations including test results rather than reliance on data sheets and publications.

7.2.4 *Performance based Designs and alternative materials*

Barrier system designs are required to recognise the waste risk to inform the commensurate containment standard and reduce risk to the environment. Understanding the waste risk also requires an understanding of how the barrier system performance will be influenced by the waste material deposition, the way in which the waste mass itself will change with time as leaching or decay takes place if at all, and the consequences of such actions. Most mining waste streams are however relatively uniform and well-understood, which should lead to cost-effective containment by skilled and experienced designers. The use of relatively modern geosynthetic materials in barrier systems, relies on modern technology which was not available in formal educational structures until the last decade and even then, it is limited to postgraduate engineering studies. Many designers are thus faced with limited knowledge or experience and may be misled by guidance provided by materials manufacturers or product suppliers which is brand specific and not necessarily relevant to the system being designed.

There are distinct perceptions generated in the civil and mining industry which must be tested for relevance in each design. Some of these aspects are addressed below.

7.2.4.1 *Perceived performance of geotextile cushion layers above geomembranes to limit tensile strain.*

The regulations pertaining to pollution control barriers provide a schematic layout and suite of requirements to demonstrate the performance of a barrier system, which is to be taken into consideration when adjudicating the suitability of a barrier system design. Therefore, using geotextile cushion layers as an alternative to soil protection layers provided equivalent performance is demonstrated as acceptable. In practice, however, a perception has arisen that a geotextile having a mass of 1,000 g/m^2 provides equivalent protection to a 100 mm thick silty sand layer, which is not true for coarse grained and similar puncture-producing material under high compressive stress. This perception is further aggravated by product suppliers suggesting a hierarchy of needs in decision-making on geotextile selection should be driven by the type of polymer used in geotextile manufacture, be it polypropylene (PP) or polyester (PET).

The assessment of maximum allowable tensile strain in geomembranes has been addressed extensively in the literature, with early suggestions that strains as high as 6 to 8% in HDPE geomembranes could be acceptable (Peggs, 2005). The limit set by the German authority, Federal Institute for Materials Research and Testing (BAM) (BAM, 2015) of 3% is generally accepted as the appropriate upper limit, as advocated at the IGS specialty workshop on barrier systems held in Munich, Germany in 2017. It has been shown that the vertical load on aggregate causes tensile strains within the geomembrane, which can be measured by short-term laboratory tests using lead plates, aluminium plates or tin foil to record the deformation (Rowe et al. 2004; Hornsey, 2013) or by means of calculation. The method advocated by Tognon et al. (2000) is based on a combination of membrane and bending theory and has been shown to be most reliable (Rowe and Yu, 2019). Although the method advocated by Eldesouky and Brachman (2018) shows promise and is of significant value in that it acknowledges the increased strain effect due to aggregate rotation on slopes. Rowe and Yu (2019) show that the geomembrane peak tensile strain is related to particle size under particular loading conditions, with 16% strain for a 25 mm particle and 32% for a 50 mm particle above geomembrane without protection layer. They further emphasize the below geomembrane foundation layer influences by showing the 32% strain for a 50 mm aggregate above a GM plus CCL layer is reduced to 17% for a geomembrane/GCL composite liner, for all other variables being held constant. The influence of aggregate or stones within the soil layer beneath a geomembrane should thus not be underestimated. The study further confirmed that a sand layer under the loading conditions reduced the geomembrane strain to 0.2%, whereas for all geotextiles tested as cushion layers, the strain remained above the 3% limit, but for a particular geotextile of 2,200 g/m^{2,} the geomembrane strain is limited to 6%. However, the authors provide guidance on strain limitation by way of flattening slopes to reduce down drag, reducing above liner interface shear or increasing below liner interface shear or combinations thereof, and noting the effect of wrinkles on performance reduction.

There is a danger in extrapolating one study's results to all designs without recognizing the conditions under which the investigation was undertaken. Laboratory test results are influenced by the loading rate, as for interface shear, the duration of load applied and the temperature at which the test is undertaken.

Further to this, a geotextile protection layer performance will be influenced by its mass per unit area, the type of polymer(s) used in filament manufacture, the length and thickness of filaments, including the cross-sectional shape, the form of needling and needling density and the extent of in situ deformations before loading. To emphasize the difference in the performance of various geotextiles, the parameter of transmissivity or in-plane drainage is used to demonstrate the effect of normal load on transmissivity reduction for a range of geotextile variables. Figure 7.6 confirms that for the same mass per unit area, there is a significant difference in geotextile performance for materials made of continuous filament PET or staple fibre PP. Similarly, mass per unit area has a significant influence on performance for the same form of geotextile, and for the same resin, there is a significant difference between staple fibre and continuous filament performance. Geotextiles having multiple differences in various contributing elements can have significant differences in performance. Specifications should define the performance required and not be limited to a select group of geotextile parameters as this could be misleading.

The use of aggregate material in drains for tailings and similar monofill waste disposal facilities is usually limited in extent, but critical to performance of the barrier system and stability of the structure. It has been noticed that size of aggregate alone is not the only parameter influencing strain and geomembrane damage, but the aggregate shape has a marked influence due to both the type of point load and the workability during placement. Aggregate shape can be influenced by the type of crusher used in manufacture be it a jaw breaker or rotary crusher for the particular type of rock. However, the post crushing treatment by rolling with a smooth drum roller compactor can significantly reduce particle sharpness and improve roundness. Similarly, the method of placement of aggregate drainage layers is a significant contributor to construction damage leading to tears and folds rather than the commonly assumed holes and wrinkles, which if undetected would render assumed or assessed leakage rates misrepresentative. These incidents can, however, be reduced by defining the means of placement and spreading of aggregate to ensure aggregate is dumped before being distributed by a tracked vehicle rather than low pressure wheel vehicle (to avoid turning induced torsional tears) and post placement electric leak location surveys (Beck 2015; Rowe and Yu 2019). It is postulated that the fines or dust on aggregate that washes into the geotextile protection layer receiving face leads to a stiffening of the geotextile layer and improved performance as applied load increases over time; however, this is still to be quantified. Figure 7.7 shows typical damage induced during the spreading of protection layers or drainage aggregate, as well as the fines and dust component that may accumulate at the geotextile aggregate interface when unwashed aggregate is used in drainage applications.

The specification of drainage system aggregate by particle size limits alone can thus lead to poor performance of the barrier system due to highly angular material increasing tensile strain or poorer drainage performance as the material breaks down due to either mechanical damage or chemical weathering or combinations thereof. This unintended poor behaviour is noted in the metallurgical furnace waste disposal facilities where coarse slag is specified without assessing crushing strength nor appreciating the effects of wetting and drying on breaking down the slag used as drainage media.

To reduce the risk of substandard performance by drainage systems and their impacts on the liner component of the barrier, the design specifications should also include performance requirements related to the strength and durability of the drainage material. So too, should the CQA protocols include records of quality control tests on the aggregate. This, along with photographic records of the aggregate in-situ with a scale provided by either a tape measure or standard-sized items such as a golf ball, assists even inexperienced personnel in identifying outsized material as shown in Figure 7.8 taken from the primary drainage layer or leachate collection system of a hazardous waste facility by the regulator during a one-off inspection, despite full-time supervision by the design engineer and a CQA monitor.

It was the designer's "belief" that the larger size aggregate specified would be superior as a drainage layer (Jewaskiewitz 2019); however, the effect on geomembrane strain had not been quantified. The reliance on test results provided by the designer's preferred geotextile supplier relied on a test undertaken in a UK laboratory using up to 53 mm aggregate on the geotextile cushion layer and geomembrane as specified in the design, but on a stiff foam aimed at simulating the soil. This yielded a peak strain of 2.8% at 900 kPa load, whereas the evaluation, when repeated in an Australian laboratory using 53 mm nominal diameter aggregate from the site and the same geotextile and geomembrane as before but using a compacted soil also from the site, yielded a peak strain of 2.7% at a mere 675 kPa load. This shows that with nearly half the load, the strain did not halve for the more representative laboratory test, both of which were undertaken at ambient temperature and for which loading was applied over a 24-hour period – which does not replicate the field condition anticipated to be at 40°C and loaded over the years.

The above shows that the performance of geotextile cushion layers to limit total tensile strain in a geomembrane can be misled by reliance on use of sample aggregate not from the actual source to be used in the development or by laboratory tests which attempt to use a stiff foam as a replacement of the CCL. Such tests may be adequate for comparative indicators, but not for performance-based design. The promotion of such misrepresentation by product suppliers to influence designers increases distrust in advice from manufacturers, especially when the short-term tests do not take into consideration the effects of creep and elevated temperature to favour a particular brand of geotextile.

To overcome the advocation of inappropriate technology, which has been embraced by designers who have not recognized the complexity of the loading and exposure conditions and consequences thereof, design reviewers have promoted the use of a field test undertaken in the trial pad or early phase of construction of the containment barrier itself to confirm the designer's assumptions (e.g., Rowe et al. 1993). This evaluation follows the form of laboratory evaluations without long waiting times induced by sample recovery and transport to a suitable lab, laboratory sample preparation time and queuing time for access to laboratory equipment. This innovation has also allowed for field tests at more representative temperatures than a laboratory and may be expanded to incorporate longer loading periods to assess the effects of creep.

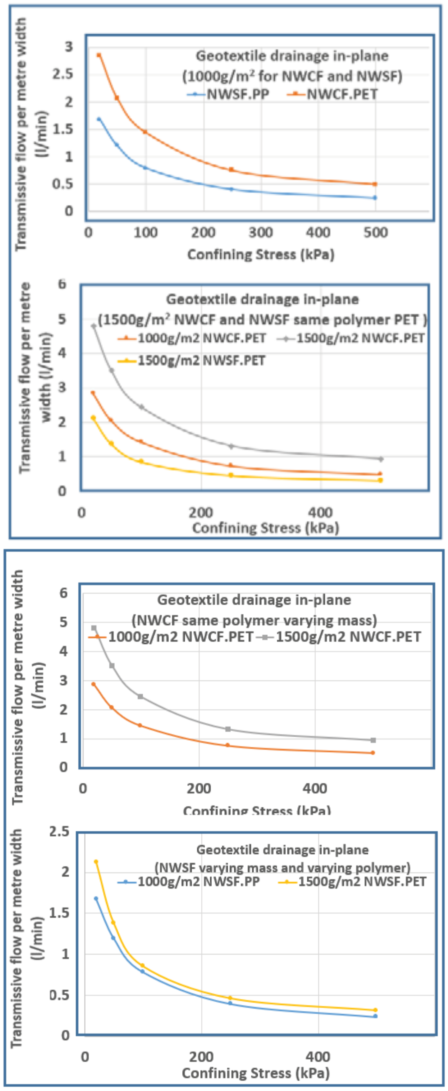

Figure 7.6. Transmissivity of various geotextiles under increasing load

7.2.4.2 *Perceived performance of geosynthetic clay liner (GCLs) layers as an alternative to compacted clay liners (CCLs).*

The potential benefit presented by GCLs as a partial or total replacement of CCLs has been advocated for two decades, and multiple investigations into the performance of GCLs have been published to address the concerns of designers who have had confidence in their knowledge and use of clay liners, mainly when related to origins in dam engineering. The performance of such composite liners has been evaluated and assessed for a range of conditions (Foose et al. 2001; Rowe 1998, 2005, 2011, 2012, 2020a). However, today there are some perceptions that a GCL offers only beneficial use without recognizing the limitations or a detailed investigation of the site-specific performance requirements. Recent developments in which GCLs are improved by adding polymers or bentonite modifiers to compete with sodium bentonite-based GCLs have had a further influence on perceptions (see §4).

It is noted that the inclusion of a blanket drain beneath the clay component of composite liner subjected to elevated temperatures, such as in heap leach pads and some mineral deposits, will probably lead to desiccation and reduced performance of mineral clay liners (Doll 1997), and similarly for

GCLs (Acikel et al. 2018; Lu et al. 2018) further compounded by the effect of salts and cations in the permeant.

Figure 7.7. Typical construction related problems: (a) Tear induced by material shearing (platinum tailings storage facility); (b) Rotational tear induced by wheel turning; (c) Dust penetration of a geotextile protection layer interface

Figure 7.8. Oversized aggregate recovered from the leachate collection system specified as 38 mm to 75 mm aggregate in a 300 mm thick layer above a geotextile cushion or protection layer aimed at limiting geomembrane strain.

It is commonly perceived that there is adequate moisture in the soil above or below a GCL, such as in capping and base liner applications, to ensure adequate hydration of the GCL for equivalent performance to a 600 mm thick CCL. However, this is not possible in composite liners above capillary breaks or drainage layers nor in double composite liner facilities (Legge et al. 2007) and may not be true for applications where the GCL is in direct contact with adjacent soils that have not been compacted with adequate moisture content or soils containing smectite. In such cases, the degree of GCL saturation may be even lower than the 30 to 70% typical of application in contact with non-cohesive soils (Rowe 2020a).

It may be presumed that the advective performance of a GCL is defined by the bentonite content and not the method of manufacture This may be true irrespective of particle size (granular or powdered) provided that the GCL is (1) fully hydrated, (2) under high confining stress, (3) the bentonite is from the same source, and (4) the products have the same bentonite mass per unit area. However, it is most unlikely to have these four parameters constant for different GCLs. Rowe (2020a) notes that the GCL structure can significantly influence the moisture content of the bentonite at the low confining stresses typical of the hydration phase, and thus finer may be better. Even this suggestion may not hold true for facilities in which containment is required soon after installation – because the initial wetting front advance through a GCL is higher for granular than powered bentonite. Thus, it may be preferable in some situations where the pollutant receiving face is on the opposite side of the GCL to the wetting face to make use of less finely ground bentonite.

Installation guidelines from GCL manufacturers usually recommend covering of a GCL within a timely manner to overcome panel shrinkage, the risk of which can be further reduced by specifying GCLs incorporating a scrim in their structure. The timely manner is ill defined and may be influenced by a range of factors including the moisture retention curves for the particular bentonite, local climatic conditions, and nature of materials adjacent to the GCL. While it is good practice to cover a GCL with a material that provides confining stress (and also usually reduces induced temperature and moisture loss as well) on the same day as placement, this may not always be practical in which case a more careful selection of GCL and alternative construction methodology may be required to limit loss in performance.

The influence of bentonite powder loss from a GCL on the performance of underlying thin drainage systems, especially if in the form of a geosynthetic drainage layer of net or cuspated sheet, can significantly affect drainage performance. The loss of gel from a modified GCL can have a similar detrimental influence on thin drainage systems, especially at the bottom of side-wall slopes where the bentonite or gel would accumulate within the thin geosynthetic drain and partially or wholly block the thin drain.

A further challenge arises fail to consider unintended consequence of all potential failure modes (see §5.6). For example, concerned with the potential of hydration of NaB from adjacent soil or groundwater containing cations or salts that would detrimentally affect NaB GCL performance, a designer may specify a GCL with a polyethylene coating in a composite base liner without recognise the implications of the polyethylene backing on structural stability. Consideration must also be given to the interface shear strength between polyethylene backing and adjacent soil or the influence on consolidated undrained conditions developing within the GCL bentonite layer between the polyethylene backing and overlying geomembrane should the bentonite be hydrated prior to the application of confining stress. A further consideration is the potential initial hydration of the bentonite by the leachate or pollutant itself at holes in the geomembrane increasing *k*. As discussed in §5, the designer must consider all these factors; unfortunately, they often fail to do so.

It is not unusual to expose bentonite samples from various GCL suppliers to a modified swell index test in which the fluid medium is replaced by leachate from site or a simulation thereof. The results of such tests have shown significant differences in the performance of various bentonite GCLs subject to the same leachate that could not be predicted from the manufacturer's product description. For example, in a recent case two GCLs each had initial properties given in the manufacturer's sheets indicating >80% montmorillonite, swell index SI > 24 mL/2g, and $k_w < 5\text{x}10^{-11}$ m/s. However, when permeated with sewage lagoon water at a low stress applicable to a sewage lagoon, the Wyoming bentonite in one GCL had k~$1\text{x}10^{-10}$ m/s (SI=12) while the bentonite in the second GCL, said to have been natural NaB from India, had k~ $2\text{x}10^{-8}$ m/s (SI=6). For the sewage lagoon with 2 m of head initially on the GCL, in 7 days this corresponded to a decrease in liquid level in the lagoon by 0.02 m and 1.8m, respectively. For a small community in remote area, this difference represents a difference between acceptable leakage and failure.

7.2.4.3 *Perceived performance of geosynthetic filters and drains as opposed to granular filters*

It is believed that a geotextile may be used as a replacement to filter sand in tailings and return water dam facilities or similar. This may be true provided the filtration and drainage system as a whole remains functional throughout the operational life and post-closure service life requirements, including incidents of earthquake loading or tremors and liquefaction. But, again, there are many caveats. Post-construction filter and drainage performance does not have the benefit of performance evaluation before use that geomembrane liner systems have by way of electric leak location surveys (Beck 2015). So too, is it important to recognize the extent of filter compatibility between waste material or tailings and the underlying material, particularly at holes or discontinuities in geomembrane-lined facilities. Chou et al. (2018) identify a critical stress condition where piping of tailings occurs through geomembrane defects where the underlying foundation or embankment soils do not meet conventional filter criteria, which could lead to underestimation of leakage and of pore pressures within an embankment.

The use of data sheets for designing geocomposite drains fails to recognize the effect of intrusion into synthetic drainage cores (Legge et al. 2014, 2015), which could lead to similar unacceptably high pore water pressure and reduced stability Factor of Safety. The loss of stability may be further aggravated in designs failing to take cognizance of the site-specific probability of seismic events for dams (Singh et al. 2010), and the effect of dynamic displacement on geosynthetic interface shear strengths which may be greater or lesser than static state values for various seismic events (Pavanello et al. 2018).

Empirical and theoretical design criteria are available for geotextile filter design. These may be augmented by short-term tests such as the gradient ratio, interface flow capacity, or fine fraction filtration tests. However, these tests do not reflect the medium to a long-term reduction in filter performance brought about by precipitate or biological clogging within the highly porous geotextile structure or porous granular drainage material. The chemical and biological clogging of geotextile-wrapped drains in gold tailings dams is well known.

The development of filter performance tests that recognize the influence of the fine fraction from the base soil on geotextile filter capacity has been a significant advancement in providing competent drainage components of contaminant containment barrier systems, in particular in mining applications where windblown or water-born fines may lead to a build-up of the fine fraction at the geotextile interface or within the geotextile structure in the early phase of operation, which leads to substandard performance. As a result, it has become good practice to either cover geotextile filters in drainage applications such as these with either a sacrificial geotextile which is removed immediately before waste placement or preferably to cover the geotextile with a compatible buffer layer of unsaturated tailings to avoid the risk posed by excessive fine mobile material. A further innovation in mining waste deposits of gold and coal is the specification of a P-trap on the outlet pipes, which are employed as a means of operating drains in an anaerobic condition to inhibit the rate of ferric oxide precipitate forming within the drains. It is recognized that micro-invertebrates develop and form a biological clogging risk under such stable habitat conditions. Thus, the P-trap is removed during the operational phase to induce a shock or sudden change in environmental conditions within the drain and reduce the volume of biological material as aerobic conditions develop before replacing the P-trap. This practice has also evolved in coal mining to reduce the risk of air intrusion into drainage layers and reduce the risk of spontaneous combustion.

The above reflects that performance-based designs which make use of geosynthetic materials as alternative elements to natural materials may be detrimentally affected if the barrier system is not considered as a whole by considering the performance of elements and their interaction with other components of the barrier as well as the change in loading conditions with time (see also §5). The assurance of predicted performance is improved by relatively simple, inexpensive, and short-term, site-specific nonstandard "test and measure" evaluations of components or the barrier system to confirm aspects of chemical compatibility, filter compatibility, and tensile strain limitation.

7.2.5 *Project specifications related to containment which may affect the stability*

Design reports have been submitted claiming safe structures based on a single interface shear test. Still other designs have been submitted in support of licence applications with a claim that stability will be addressed only after tender award or during construction. The failure to recognise the importance of interface shear limitations, and the effect of saturated conditions and strain compatibility poses an unfair risk and liability on the facility owner – the facility being either unsafe or having excessive conservatism.

In a particular facility in the coal mining industry, a low-risk waste stream was provided with a single geocomposite (LLDPE-S and GCL) liner with substantial overlying granular drainage layer. The authority's rejection of the design based on unproven stability resulted in confirmation of a Factor of Safety of 1.0 for the pollution control dams (PCDs) under construction. The challenge faced then was that the facility was under construction in advance of authorization or licensing. Hence, the regulator advised the applicant to profile the base of the intermediate walls in a saw-tooth cross-section so as to mobilize the base material shear strength. The consulting engineer embraced the concept and optimised the profile with increasing wave length between saw-teeth as the embankment wall height reduced above the composite liner. It is considered good practice to include drainage trenches and berms in liner systems so as to increase stability. Caution must however be taken in assessing the consequences of such drainage trenches on inducing excessive total tensile strain, particularly at positions where the drainage line changes direction which requires the intersection of three planes in the geomembrane and related geomembrane welding at these critical containment points of maximum pollutant or leachate flow concentration.

Recognition of interface shear limitations and managing the slip surface above the containment liner in designs incorporating geosynthetics is not adequate to ensure stability. The construction of composite (geomembrane plus CCL) liners in which the clay component compaction specification is 98% Standard Proctor maximum dry density (MDD) at minus 1% to plus 2% OMC can be compromised if construction takes place at excessive moisture contents. The pursuit of particular specifications requires justification.

The multiple failure of various HDPE geomembrane products at a particular water storage reservoir, emphasises the need to consider the nature of the material to be contained, especially the presence of oxidising agents before construction.

The same can be said for specifying drainage material and interface shear strength. The specification of an asperity height does not define interface shear for geomembranes. The texturing through micro-spikes or other features is dependent on more than just height, and is influenced by the density, stiffness and nature of the texturing in relation to the adjacent material. Table 7.1 provides a comparison of two series of interface shear results for a range of geomembranes having different micro-spike height and density of distribution. The nature of soil selected for the test series was a low permeability clay typically used in CCLs, and an ash as these are typically found in large facilities. It is critical that interface shear tests be conducted on the materials that will actually be used on a project to obtain the strength parameters and the concept of multi-layer shear box tests (Khilnani et al. 2017) to reflect not only interface but also internal stress-strain relationships of materials requires more consideration by designers. It is erroneous to assume a particular height of micro-spike will provide the highest interface shear or even adequate interface shear strength.

Table 7.1 Interface shear results for five geomembranes (having different micro-spike heights and distribution) with a compacted clay and ash, under different normal stresses (acknowledgement H Venter, NAKO LBE (Pty) Ltd for sponsoring the test series).

Test number	Textured geomembrane micro-spike height (mm)	Clay at interface MDD 1,509 kg/m^3 OMC 26.5%		Ash at interface MDD 1,130 kg/m^3 OMC 40.7%	
		c (kPa)	*φ(°)*	*c (kPa)*	*φ(°))*
1	0.40*	12.8	8.3	16.5	27.8
2	0.65	7.5	9.4	40.8	36.2
3	≥0.9	10.5	8.4	3.7	39.9
4	≥0.9	13.1	7.2	7.8	35.8
5	≥0.9	6.8	8.5	0	40.8
6	1.1	18	9.4	13.7	38

Shear tests were undertaken at normal stresses of 20, 200 and 400 kPa.
*Texturing is a random full surface treatment, not spaced micro-spikes.

The above results confirm the specification that micro-spikes height alone does not define maximum interface shear strength benefit. This has been recognized in the 2019 amendment of the Geosynthetics Research Institute (GRI) standard specification for geomembranes known as GRI GM13.

There is an increasing number of polymer enhanced bentonite GCLs (EB-GCLs) being marketed on the basis of improved hydraulic performance (§4). However, insufficient consideration has been given to the potential unintended consequences of polymer biodegradation, polymer leaching, and polymer elution. If polymer elution occurs, then open pores will remain within the bentonite and result in a substantially higher long-term the hydraulic conductivity of EB-GCLs (§4.6.3 and §5). Even if elution does not occur water soluble polymers will be leached and over time under field conditions and they may be biodegraded. Polymer elution also reduces interface shear strength (Chen et al. 2017). Furthermore, the effect of anions on increasing permeability of bentonite-polymer GCLs (Tian et al. 2017) has not been addressed in the cases referenced previously, nor has the effect on diffusion through such EB-GCLs been adequately considered (Sample-Lord et al. 2017). Until these issues are resolved, extreme caution is advised in the use of EB-GCLs and such use should only be considered after a careful failure modes and effects analysis (§5.6).

The challenges brought about by designs based on product specifications may be overcome by regulations and facility owners who demand performance-based designs that rely on evaluating the actual materials and their interaction. To enhance this performance-based approach, a check list requiring the results of a performance assessment or determination must be signed off by both the waste management facility owner and the designer responsible for the containment barrier needed to protect the environment and human life. This focus on accountability by sign-off significantly improves the quality of design confidence and predicted performance.

7.2.6 *Inadequacies and virtues of construction quality assurance (CQA) plans*

It is increasingly common to include material specifications in the CQA part of a design report. While these specifications on occasion contradict the specifications on the engineering drawings, there are occasions where particular specifications amend standards and test methods without technical substantiation. For example, the specification of particular ash content standard and/or high-pressure oxidation induction time (OIT) for a geomembrane does not necessarily add value to the design (Ewais et al. 2014). Still, it tends to increase costs by excluding material suppliers whose products comply with national or international standard specifications. Furthermore, no justifiable reason is provided for deviating from the rationale behind the GRI GM13 standard specification for geomembranes (Hsuan and Koerner, 2015) in almost all particular specifications of deviation. In addition, these limited specifications are indicators and do not inform the design with respect to polymer or resin performance in the specific containment application.

The differential scanning calorimeter (DSC) test provides invaluable insight into the resins and antioxidants/stabilizers used to formulate a black geomembrane (§2). For example, the temperature peak or spike at a transition such as at melt temperature is characteristic of a polymer (e.g., PE or PP etc.). By observing the DSC thermogram of energy absorption versus temperature for a particular polymer sample, one can identify with some certainty from the peak or multiple peaks the nature of the polymer that has been used (e.g., a blend of PE and PP). The area under the bell curve gives the comparative percentage of makeup of the specimen. The position of the peak reflecting the thermal transition temperature may give insight into the makeup of resin blends. However, the DSC will not identify the presence of inclusions such as polycarbonate nor polystyrene.

The interpretation of such DSC results requires careful consideration with respect to the particular application. It is known that some thin (less than 1 mm-thick) blended geomembranes have served as satisfactory lagoon liners for decades under exposed African conditions to hazardous substances including hydrocarbons. On the other hand, HDPE geomembrane liners have failed under similar exposure conditions when serving for potable water containment. Although in these applications the geomembrane is accessible for repair, they are included for an appreciation of the complexity in assessing liner suitability for particular applications. The type of geomembrane and its specific formulation is critical to its longevity (Koerner and Koerner 2017; Rowe 2020b; Rowe et al. 2020). It is recommended that the owner of a facility makes provision for geosynthetic performance evaluation at the discretion of themselves and/or reviewers, including the statutory review in particular, to enhance assurance in the materials being procured for projects. Such truly independent considerations may include analysis using DSC, gas or liquid chromatography mass spectrometry, infrared scanning or the EU 10/2011 test. Resin containing calcium carbonate has been marketed without consideration of its significant detrimental effects on service life. The value of thermogravimetry tests as used for determining carbon black but undertaken at even higher temperatures (approximately 900°C) should not be underestimated.

It is generally accepted that the higher the crystallinity (and associated transitional phase temperature), the more chemically resistant the geomembrane, however, this may also be coupled with lower stress crack resistance (§2 and Rowe et al. 2004). Significant variation has also been recorded in OIT test results, both prior to and post installation (Morsy and Rowe 2017). The importance of OIT testing is reasonably well recognized for geomembranes but received scant attention with respect to geonets and geotextiles. In recent evaluation the long-term performance of two physically very similar geonets, one product is Std-OIT$_o$~ 100 minutes the standard deviation of 7 minutes and data ranging from 80 – 110 min. This is at the minimum that would be expected for the geomembrane to be used conjunction with the geonet however it greatly exceeds that of the second geonet which had Std-OIT$_o$~70 minutes the standard deviation of 25 minutes and data ranging from 20 – 120 min.

It is thus recommended that the CQA report demonstrating compliance of the as-built facility with the accepted design should include not only the as-built drawings, but also the type of test, number of those tests undertaken; the maximum, minimum, mean values and standard deviation for the test method and an indication of where the tests were undertaken. This record should be for all materials – natural and geosynthetic (e.g., geomembranes, geonets, geotextiles), and include the aggregate leachate collection and detection systems where relevant. Similarly, an evaluation of geomembrane performance relative to standard or project specific specifications of OIT (standard and/or high pressure) should be sensitive to variation in results for the same material tested in a single machine or single laboratory or different laboratories. The results may be influenced by the machine, the operator or any contamination of the extremely small specimen (5 mg) by hydrocarbons or even finger oils. Reliance on ISO standards for manufacture is not adequate to define performance, as shown over the past five years during which ISO 9001 geomembranes have been supplied to RSA from European Manufacturers which upon installation have not met performance specifications, including visually obvious discontinuities.

Descriptions provided by an independent CQA monitor are inadequate and have been known to not reflect the offsite stored data. This aspect has brought the definition of independence into question. The value of electrical leak location survey cannot be understated.

It is with some disillusionment that design reports and drawings do not reflect instrumentation to the extent typical of other engineering structures. For example, the absence of site boundary definition, strain gauges, thermistors and flow gauges place the facility owner at risk in many situations. Similarly, the failure to address critical elements of barrier systems such as drainage pipes, drainage cores, sump liners, and filter materials to the same level of surety as geomembranes, clays, or GCLs introduces weaknesses in the design and performance of barrier systems.

To illuminate such shortcomings in CQA protocols critical to the performance of barrier systems, a standard CQA protocol has been developed for use by designers that address the above principles and procedures. This CQA document is made available by the CQA regulator for use by designers of public and private-owned barrier systems to enhance knowledge and skills development, although its use is not compulsory.

7.2.7 *Distinctive waste streams and particular barrier systems*

The conventional barrier system of a filter protected aggregate drainage layer for leachate collection and management, overlying a cushion layer of soil or geotextile to protect the composite containment liner of geomembrane in intimate contact with a compacted clay liner or GCL (or combinations thereof) does not always yield the optimum containment performance or cost-effective solution for the type of waste material to be contained due to chemical incompatibility or similar site-specific conditions.

7.2.7.1 *Brine and acid lagoons*

In the gold and coal mining industry, liquid waste streams with a high concentration of salts or strong acids are occasionally produced. Such liquid waste streams are generally considered difficult to contain due to the reaction between the liquid waste and clay or similar material.

It is noted that the brine discharge into the pollution control dam (PCD) or lagoon is not the concentrated condition representing the worst case rather, the end of the evaporation period represents the concentrated waste type to be contained for pollution prevention.

The historic lagoon containment standard of 1998 or modern post-2013 standard barrier system for such waste of double composite liners separated by a leak detection drainage layer could be made acceptable provided the performance of alternative barrier system recognizing hydraulic gradient across the alternative to the primary composite liner is demonstrated as having equivalent performance to that of a conventional system.

It is known that sodium bentonite GCLs react negatively to cation exchange (Elges 1985; Scalia and Benson 2011) and to salts (Petrov and Rowe 1997; Petrov et al. 1997a,b). Furthermore, the hydraulic gradient across thin geocomposite liners (2 mm thick geomembrane plus 6 mm thick GCL) or geomembrane only liners is orders of magnitude higher than across a composite (2 mm thick geomembrane plus 600 mm thick CCL). It is critical to address such gradient by mitigation thereof through ensuring at least direct/intimate contact and normal loading for composite liners, or by alternative means. Although direct contact between geomembrane and GCL or CCL is pursued by particular construction techniques and ballast layers to overcome wrinkling etc., the low interface transmissivity affecting barrier performance is achieved only when loading exceeds about 50 kPa.

Although it is normal practice to have a double composite liner separated by a LDS for hazardous liquid waste containment alternative designs of the same performance can be achieved without the use of a GCL or clay component to the primary composite liner when the nature of waste and loading requires so. This is achieved, typically for acids and concentrated brine liquid waste, by a triple geomembrane liner (Figure 7.9) pioneered in South Africa in the 1990s as a cost-effective alternative in the gold mining industry for strong acid containment, and later adopted for coal mine wastewater treatment works (reverse osmosis plants).

Although the upper two geomembranes separated by a drainage layer as shown in Figure 7.9 are accepted as serving equivalent performance to a primary composite liner, the underlying leak detection system (LDS) must still be above a bottom (tertiary) liner (often just a single geomembrane). The lowest (tertiary) liner often rests on a bed of sand or geotextile which renders its composite effect as null and void. This lower geomembrane/ geomembrane interface should be drained and preferably under gravity from the lowest point to a monitoring sump at which the performance of the overlying system is confirmed. It should be noted that a drainage layer is only effective when there is a low permeability layer beneath it.

In this design, the upper two geomembranes with separating drainage layer serve to reduce the hydraulic gradient across the tertiary liner to approximately unity irrespective of the depth of the brine.

There is often no ballast layer above the primary liner. Such ballast layer would normally protect the geomembrane from UV light and heat which accelerate degradation, as well as protect the liner from wind and/or mechanical damage. It is inconsistent to have a concrete access ramp into the lagoon for vehicles and then allow traffic of vehicles over the unprotected geomembrane liner.

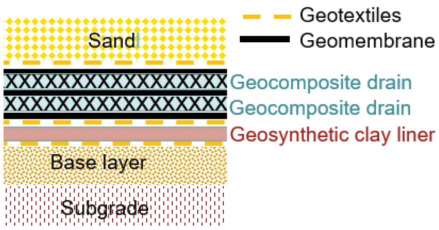

Figure 7.9 Triple geomembrane liner for brine evaporation barrier

The question of thermal conductivity across barrier systems has been studied by various investigators over the past decade. Early work in the Department Water and Sanitation, RSA laboratory in Pretoria West showed thermal gradients across double geocomposite liners to be about 2°C irrespective of the temperature, but note this primary liner had a moist GCL in contact with the overlying geomembrane. This research development was published at Landfill Interest Group (LIG) Durban 2005 and Sardinia 2007 (Legge et al. 2007).

When two liners are separated by an air void induced by a spacer of geonet, or cuspated drain, or geotextile, or similar material, the air void acts as a thermal barrier (see Singh and Bouazza 2013 for thermal conductivity of HDPE geomembranes, wet and dry GCLs, and wet and dry geotextiles.) As the primary geomembrane heats up due to say solar radiation in exposed conditions, so the enclosed air void reaches the same temperature and heats the drainage layer and secondary liner. The extent to which the drainage layer and in particular, in RSA the usually thinner, secondary geomembrane liner cools largely depends on the moisture content and conductivity of what lies beneath it. If it is moist/wet GCL or soil, then the heat in the secondary liner can be conducted away from the liner as quickly as it passes through that geomembrane without an increase in temperature of the materials above. The same can be said for designs with geotextiles beneath the secondary liner; however, the elevated temperature tends to drive off moisture from GCLs (Rowe 2020a). Obviously, the same drying applies to geotextiles well. If the air void remains trapped, such as in double glazed windows of northern Europe, then the temperature of the upper liner and barrier system rises even higher than the norm due to the lower thermal conductivity of underlying layers inhibiting heat escape (Take et al. 2014, 2015). The temperature difference of geomembranes at wrinkles is typically 10°C higher than areas adjacent to the wrinkle where the membrane is in direct contact with soil or hydrated GCL.

In the case of double geomembrane only liners, the primary liner could be cooled by overlying liquid, but more important is to avoid the air temperature in the spacer voids from rising excessively. By moving the air or ventilation, the separating structure or drainage spacer does not increase in temperature to the same extent. Even a 10°C drop in liner temperature will substantially increase the service life (Rowe 2005, 2012, 2020b). Alternatively, the liner could be covered with, say, cement stabilized soil layer if compatible with the waste stream, or a high-performance geomembrane specifically developed for such conditions could be used to partially mitigate this exposure impact. The nature and extent of cover layers in lieu of ballast bags would be influenced by the shape of the floor area and the nature of the sediment or precipitate to be removed.

7.2.7.2 *Wastes containing volatile organic compounds*

The performance of composite liners with respect to total solute transport is widely published (Foose et al. 2001). Similarly, it is widely known that the rate of diffusion of volatile organic compounds (VOCs) even though perfectly intact liner systems is influenced by temperature (Sangam and Rowe 2001; Rowe et al. 2004) and by the partition coefficients of the compounds being considered.

To mitigate this diffusive characteristic, designers may consider alternative materials (McWatters and Rowe 2010; McWatters et al. 2016a), alternative systems or combinations thereof to either contain the VOC stream to a greater extent or to remove the diffused VOCs from further diffusion potential and treatment (Legge et al. 2007). Interested persons are referred to methods of treatment of VOCs such as at Casey Station in Antarctica (McWatters et al. 2016b, 2019) and a petrochemical facility containing sludge (Meyer et al. 2014). In the latter case, the leak detection layer is subject to a negative pressure to draw moist air through the system to commensurately maintain hydration of the clay component to the primary composite liner and remove the VOCs that have diffused through that barrier. The exhaust fumes are passed through a treatment process incorporating carbon scrubbers to capture the VOCs for further treatment or disposal.

7.3 *Challenges in barrier system planning, design, construction and operation: Asia*

7.3.1 *Influence of MSW variants on stability, leachate collection and gas management*

This section will focus on challenges to managing the containment of municipal solid waste (MSW) in most of the Asian countries. Table 7.2 shows physical compositions of fresh MSWs collected from the Asian developing countries. In most developing countries like China, India and Indonesia, the food waste content is much higher than that in developed countries in Europe and North America. MSW with food waste making up over 40% can be classified as high-food-waste-content (HFWC) MSW, otherwise it is low-food-waste-content (LFWC) MSW. As shown in Table 7.2, the water content in the HFWC MSW is more than 50% (wet weight basis), greater than that in the LFWC MSW. When compared with the containment of LFWC MSWs in Europe and North America, the containment of HFWC MSWs has more technical challenges with respect to landfill stability, landfill gas collection, and control of leachate-related pollution (Chen et al. 2014). Any innovative solutions to the challenges posed by HFWC require an understanding of the degradation process of HFWC MSWs and the associated liquid-gas interaction at wet landfills.

Table 7.2. Physical components and initial water content of fresh MSWs in different countries (by wet basis, %)

Country	GDP per capita (US $)	Organic fractions				Inorganic fractions			Initial water content
		Food waste	Paper, cardboard	Textile, leather	Wood	Plastics	Metals	Others	
China	8643	57.91	10.55	2.72	1.69	11.85	0.76	14.52	52.44
India	1983	42.00	6.00	4.00	0.00	4.00	2.00	42.00	NA
Philippines	2976	41.60	19.50	0.00	0.00	13.80	4.80	20.30	NA
Indonesia	3876	74.00	10.00	2.00	0.00	8.00	2.00	4.00	NA
Sri Lanka	4085	76.40	10.60	0.00	0.00	5.70	1.30	6.00	NA
Nepal	834	80.00	7.00	0.00	0.00	2.50	0.50	10.00	NA
Thailand	6591	48.60	14.60	0.00	0.00	13.90	3.60	19.30	NA
Malaysia	9813	40.00	15.00	3.00	0.00	15.00	3.00	24.00	NA
Brazil	9895	42.90	19.70	4.50	5.20	18.70	1.50	7.500	50.00
U.K.	39735	25.00	31.00	5.00	0.00	8.00	23.00	32.00	32.00
U.S.	59501	13.60	35.50	4.60	3.40	13.20	6.90	22.80	18.00

7.3.2 *Degradation and stabilization of HFWC MSWs*

The behaviour of the HFWC MSWs was investigated by performing a large-scale bioreactor experiment (CELL1, 5m×5m ×7.5m, 91.3 tons of wastes) in Zhejiang University (Zhan et al. 2017a). Based on the experimental results and field observation, a degradation–consolidation model was developed to simulate the stabilisation process of HFWC MSWs at landfills (Chen et al. 2020). The model incorporated the biological degradation, skeleton deformation, two-phase flow, and solute transport. The experimental and simulation results showed that the stabilization process of HFWC-MSW landfills could be divided into three stages: rapid degradation, slow degradation, and post-stabilization, as shown in Figure 7.10. Rapid degradation occurs to the HFWC MSWs just after being disposed of at a landfill.

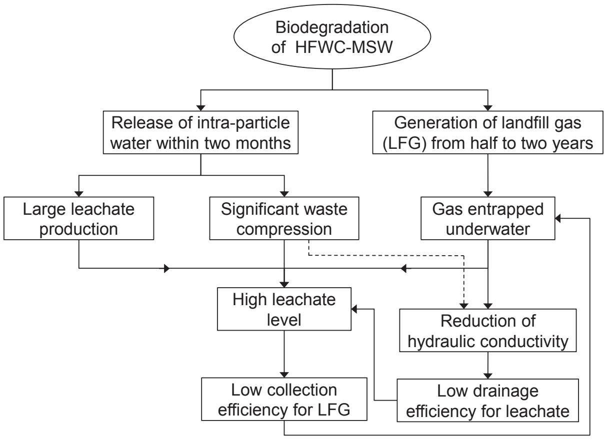

Figure 7.10. Stabilization stages of HFWC-MSW landfills (Chen et al. 2020)

This is because food waste contains a large proportion of rapidly degradable chemical components (e.g., fast cellulose, sugar, protein and lipids). The rapid degradation results in a release of intra-particle water embodied in the food waste, and a large quantity of leachate is produced. It is observed from the large-scale bioreactor experiment that 26.8 m^3 of leachate was collected from the 91.3 tons HFWC-MSW within the first two months after waste filling (Zhan et al. 2017a). The first two months of leachate production represented nearly 30 % of the total mass of the waste. The rapid degradation of food waste also resulted in a rapid generation of landfill gas (LFG). The time lag for LFG generation is only 0.5-1 year at the MSW landfills in China. The rapid degradation stage generally lasts about 2–3 years. Within that stage, 80% of the solid mass is hydrolyzed, 100% of the intra-particle water is released, 60% of the LFG is generated, and 80% of the compression is completed (Figure 7.11). During the subsequent slow degradation stage, which lasts about 20–30 years, over 90% of the solid mass is hydrolyzed, 90% of the compression is completed, and 80% of the LFG is generated.

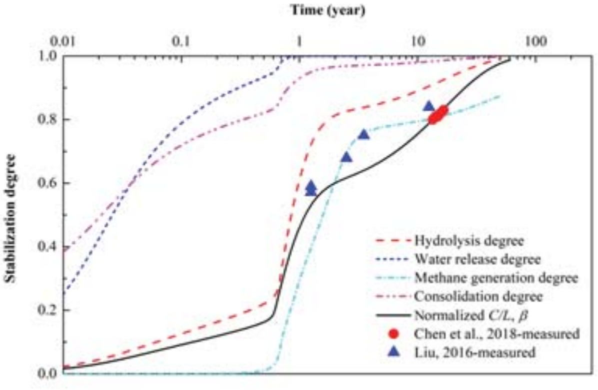

Figure 7.11. Liquid-gas interactions at HFWC-MSW landfills (Zhan et al. 2017b)

After that, the HFWC MSWs are almost stabilized. Due to the significant contribution of self-released leachate of HFWC MSWs during the rapid degradation stage, a modified leaching coefficient method was proposed to predict the leachate production rate at landfills (Chen et al. 2018):

$$Q = \frac{I_d}{1000} \times \left(C_{L1}A_1 + C_{L2}A_2 + C_{L3}A_3\right) + \frac{M_d \times (M_c - F_c)}{\rho_w} \qquad (7.1)$$

where Q is the daily leachate production (m^3/d), I_d is the daily average precipitation (mm/d), A_1 is the area of landfilling operation unit (m^2), A_2 is the area of intermediate cover unit (m^2), A_3 is the area of final cover unit (m^2), C_{L1} is the exudation coefficient of landfilling operation unit, C_{L2} is the exudation coefficient of intermediate cover unit, C_{L3} is the exudation coefficient of final cover unit, M_d is the daily landfilling of MSW (t/d), M_c is the initial water content of MSW (%), F_c is the field capacity of completely degraded MSW (%), and ρ_w is the density of water (t/m^3).

In addition, a two-stage LFG generation model was proposed for HFWC MSWs to capture the distinct behaviour of LFG generation during the rapid and slow degradation stages:

$$Q_n = \sum_{t=1}^{n-1} M_t \varphi (L_{\mathrm{R}0} k_{\mathrm{R}} e^{-k_{\mathrm{R}}(n-t)} + L_{\mathrm{S}0} k_{\mathrm{S}} e^{-k_{\mathrm{S}}(n-t)}) \qquad (7.2)$$

where Q_n is the LFG production for the n^{th} year of operation (m^3/year); n is the time since the start of operation of landfill (year); t is the time since MSW is filled (year); M_t is the filling amount of MSW in the nth year (t); φ is the conversion coefficient of degradable organic carbon (%); $L_{\mathrm{R}0}$ is the potential CH$_4$ generation capacity of rapidly degradable components, including food waste (m^3/t); $L_{\mathrm{S}0}$ is the potential CH$_4$ generation capacity of slowly degradable components, including paper, textile, wood, and so on (m^3/t); k_{R} is the CH$_4$ generation rate of rapidly degradable components (year^{-1}); and k_{S} is the CH$_4$ generation rate of slowly degradable components (year^{-1}). Calibration of LFG pumping test results from the landfills in China indicates that the value of k_{R} ranges from 1.1 to 1.4, and the value of k_{S} from 0.09 to 0.11.

To assess the degree of degradation of HFWC MSWs, the normalized ratio of cellulose to lignin ($\beta=1-R_{C/L}/R_0$) was proposed as the degradation degree index. T and the index is well correlated with static respiration index, fine fraction content, and leaching characteristic (Chen et al. 2018).

As shown in Figure 7.10, the value of β corresponding to the end of the rapid and slow degradation stages is 0.6 and 0.83, respectively. When the value of β is greater than 0.83, the landfilled MSW is basically stabilised. The food waste content and degradation degree would significantly influence the engineering properties of MSW. It is found that the primary compression ratio and bio-induced compression ratio of HFWC-MSW are both larger than those of low food waste content (LFWC) MSW (Xu et al. 2019, 2020), and the hydraulic conductivity and gas permeability of HFWC-MSW are both one order of magnitude smaller than LFWC-MSW, and the shear strength of MSW changes significantly with degradation degree (Gao et al. 2019).

7.3.3 *Liquid-gas interaction at wet landfills of MSWS and its counter measures*

The liquid-gas interactions are very complex at HFWC-MSW landfills, as shown in Figure 7.11. The great quantity of leachate production will cause a buildup of leachate or leachate mound at landfills with inadequate drainage conditions. Under such circumstances a large amount of LFG generated from the waste below the leachate level cannot be collected effectively (Zhan et al. 2015) but is accumulated in the waste piles below the phreatic line. It is observed from another large-scale bioreactor experiment (CELL2, 5m×4.2m×7.5m) performed in Zhejiang University that the gas accumulation zone was distributed randomly and the gas pressure in the zone increased and dissipated in cycles. The gas-breaking value was up to 10.5 kPa greater than the pore liquid pressure (Zhan et al. 2019). A similar phenomenon was observed at the Xingfeng landfill in China, where a maximum gas pressure of 80 kPa was measured at depths below 15–20 m (Ma et al. 2019). The gas accumulated underwater would further increase the leachate mound, and this contribution was estimated to be 21%–28% of the total leachate level (Zhan et al. 2017b). The combined effect of high leachate levels and high gas pressure was the critical cause of frequent landfill failure in Asian countries (Chen et al. 2017; Ma et al. 2019). Centrifuge model tests revealed that the ratio of critical leachate level and landfill height was 0.75-0.92 when the slope ratio was 1:1-1:3, and it increased with an increase in waste degradation (Chen et al. 2017). In addition, the gas accumulated underwater would result in a reduction of hydraulic conductivity, decreasing by one order with an increase in gas content from 13% to 21% (Zhan et al. 2017b). Under the condition of low hydraulic conductivity, the produced leachate is not easy to drain out of the waste pile, causing an inadequate drainage situation. The above complex liquid-gas interactions tend to develop into an adverse condition, resulting in great difficulty in managing wet landfills. Thus, effective measures should be taken to tune the interactions to solve the technical difficulty.

LFG collection for LFWC may be via either vertical or horizontal gas collection wells (Zheng et al. 2018, 2019a,b, 2020). However, for HFWC landfills, understanding the coupled leachate and gas flow in the waste body is needed for the scientific design of leachate drainage and LFG collection. Given that leachate and gas migration in a waste body is dominated by the preferential flow, a dual-porosity model for coupled leachate and gas flow has been established, in which the waste body is divided into fracture and matrix domains (Hu et al. 2020a). It has been verified by pumping test data that the dual-porosity model performed better than the single-porosity model. Pumping vertical wells is commonly used to lower the leachate level in wet landfills. However, the efficiency in the well pumping tends to decrease with a drawdown of leachate level, which can be explained by the gas volume of waste underwater increases with the drawdown of leachate level and therefore significantly reduces the hydraulic conductivity of waste (Rowe and Nadarajah 1996; Zhan et al. 2017b)—also clogging of the wells. The horizontal well is a potential alternative for the drawdown of leachate level at wet landfills. The trial construction and operation of horizontal wells at Tianziling and Xingfeng landfills in China showed that the leachate level could be lowered to near the elevation of horizontal wells (Hu et al. 2020b). Thus, a three-dimensional drainage system was proposed to control high leachate mounds in wet landfills (Figure 7.12). The drainage system involves a combination of layered horizontal trenches or wells and deep vertical extraction wells and serves in addition to the leachate collection system (LCS) at the base. Each layer of horizontal trenches or wells is set up to capture part of the leachate generated above the present layer and so as to relieve the leachate drainage pressure on the LCS. Vertical extraction wells are to collect LFG as well as to draw down the leachate level and so enhance the leachate drainage after the failure of the LCS. Thus, the leachate-gas interaction can be separated and the efficiency in draw down of leachate levels and collection of LFG can be enhanced. The configuration of a three-dimensional drainage system was successfully implemented at many landfills in China. For example, the drawdown of leachate level resulted in an increase of LFG collection rate from 2,000 to 10,169 m^3/h at the Xiaping landfill in Shenzhen of China (Figure 7.13; Zhan et al. 2015). With consideration of the rapid generation of LFG for HFWC, an enhanced temporary cover system was implemented at the Xiaping landfill. The cover system comprised: a 1 mm-thick HDPE geomembrane, a soil protection and gas diffusion layer, and gas collection pipes with a spacing of 20 m. Implementation of the enhanced temporary cover system resulted in a further increase of gas collection rate from 10,169 to 46,472 m^3/h at the Xiaping landfill. Half of the collected LFG was used to generate 38 MW of electricity per hour by using LFG power generators, and the other is used to recover automobile fuel.

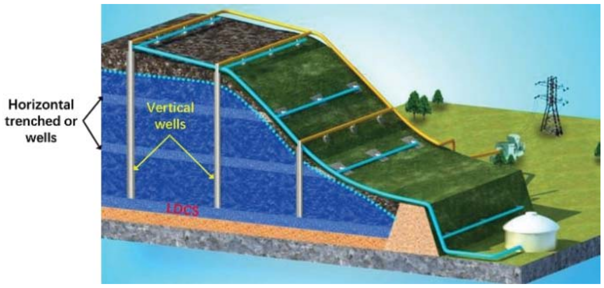

Figure 7.12. Configuration of three-dimensional drainage system at a wet landfill

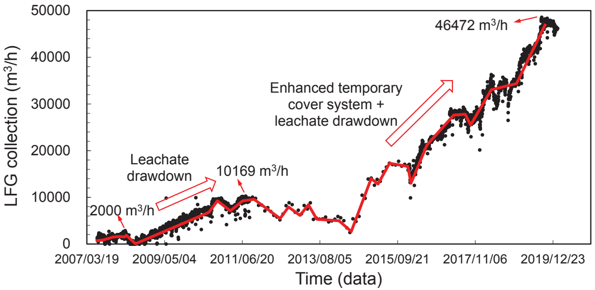

Figure 7.13. Total LFG collection rate measured at the Xiaping landfill

7.3.4 *Use of capillary barrier soil covers in the Asian monsoon regions*

Last century, the design of final covers in China followed the standards and procedures of developed countries, incorporating a geomembrane as an impervious barrier as specified in the current national standards. This century has seen the development of a new understanding of the degradation of HFWC MSW and identified the critical role of rapid hydrolysis leading to large leachate production and fast gas generation (Zhan et al. 2017a). After two or three years, the LFG generation rate decreases sharply to a low level. Additionally, much of China is subjected to monsoons and the consequent heavy rain coincides with the period of high temperature and vegetation growth. These factors have led to a revision in the design of final covers in China to accommodate the nature of HFWC MSW and the climate. With the successful application of soil covers incorporating the capillary barrier effect (capillary barrier soil covers, CBSCs) in arid and semi-arid areas of North America, many countries have explored the feasibility of CBSCs in response to their own climates. In recent years, research on the application of CBSCs in China has drawn much attention. Theoretical and experimental methods were used to assess the performance of two-layer CBSCs (see Figure 7.14a) in northwestern China in arid, semi-arid, and semi-humid climates (Jia et al. 2010; Zhan et al. 2016, 2017c; Long et al. 2018; Zhang et al. 2014, 2016). Zhan et al. (2016) constructed the first full-scale final cover test site (30 m × 20 m × 1.2 m, see Figure 7.15) at Jiangcungou landfill in Xi'an city, China, where the humidity index (i.e., the ratio of annual precipitation over potential evaporation) is higher than 0.5. The test site adopted a two-layer CBSC that used local loess as fine-grained layer material and gravel as coarse-grained layer material and was well-instrumented. Artificial rainfall events were implemented to the test site before and after the site was vegetated to measure the water storage capacity of the cover. Results demonstrated that the loess/gravel CBSC increased the available water storage by 41% compared with the monolithic loess cover due to the capillary barrier effect between the two layers (Zhan et al. 2017c). Vegetation had an insignificant influence on water storage capacity. Field tests were performed to investigate the on-site methane oxidation capacity of the cover. Results indicated that the maximum methane oxidation was 93.3 g $CH_4/m^2/d$, confirming effective methane mitigation and control for the HFWC-MSW that has completed the fast gas generation phase (Zhan et al. 2020a). 2-year monitoring of the hydrologic response of the test site indicated a good performance of the loess/gravel CBSC at limiting percolation. The accumulated percolation was around 8.0 mm/year, which was less than the recommendation of the USEPA alternative cover assessment program of 30 mm/year (Zhan et al. 2020b). The CBSC was also shown to be effective in reducing LFG emissions. This was in large part because notable water storage decreased the gas permeability in the loess near the fine-coarse interface by up to five orders of magnitude. The above observations facilitate the use of two-layer CBSCs at landfills in non-humid areas of China.

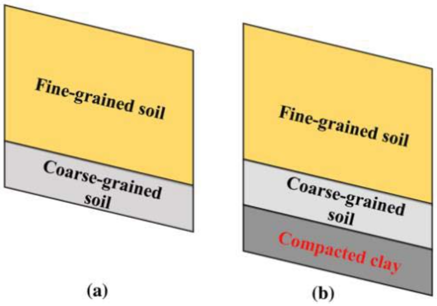

Figure 7.14. Conceptual diagrams of CBSCs: (a) two-layer CBSC; (b) newly proposed three-layer CBSC in China (Ng et al. 2016)

A new three-layer CBSC has been proposed for landfill closure in humid areas of China (Figure 7.14b). The cover system involves the addition of a fine-grained soil below a two-layer CBSC (Ng et al. 2015a, 2015b, 2015c 2016, 2019). The added layer has a lower water permeability at low suctions in rainy seasons. Thus, it can intercept the infiltrated water through the upper two layers and reduce the percolation when the upper two layers lose their effectiveness. The bottom layer can maintain a high volumetric water content in dry seasons attributed to the protection of the upper two layers as they have low water permeability at high suctions, indicating that the bottom layer can serve as a LFG emissions barrier. Results obtained from flame model tests and back-analysis indicated that the coarse-grained layer changed from being a capillary barrier in a conventional CBSC cover system to being a lateral diversion passage after the breakthrough of the upper two layers due to the presence of the bottom layer. The saturated hydraulic conductivity of the bottom fine-grained layer should be kept below 1×10^{-8} m/s to minimize percolation (Ng et al. 2015a).

By comparing the LFG emissions from three types of covers under dry weather conditions, including a single clay layer cover, a two-layer CBSC and a three-layer CBSC, it is found that the LFG emission rate through the three-layer CBSC was the lowest and this rate was lower than the criterion set by the Carbon Farming Initiative (Ng et al. 2015b). A full-scale test site (20 m × 12 m × 1.8 m) was constructed and instrumented at Xiaping landfill in Shenzhen city, China, which was located in a humid climatic region with a humidity index greater than 0.75, to validate the field performance of a three-layer CBSC using recycled construction waste. One section of the test site was planted with Bermuda grass while the other section was left bare. Results obtained from about 1.2-year monitoring showed that the accumulated percolation was about 27 mm and 20 mm for the bare and grass covered landfill cover respectively, both of which meet the recommended criterion of 30 mm/year (Ng et al. 2019). The LFG emissions data from the test site have not been reported in the literature yet, but the recorded high degree of saturation (higher than 80%) at the bottom layer suggests a good performance of the cover serving as a LFG gas emissions controller (Ng et al. 2015d).

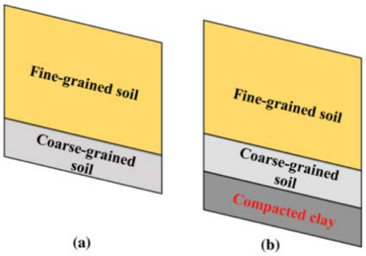

Figure 7.15. Conceptual diagrams of CCBEs: (a) two-layer CCBE; (b) newly proposed three-layer CCBE in China (Ng et al. 2016)

7.4 *Challenges in barrier system planning, design, construction, and operation: South America*

The primary waste problem in South America is mining waste. There is a diversity of geotechnical problems within a mining operation including stability of open pit and underground excavation, static and seismic stability of heap leach pads, drainage systems for tailings dams and ore stockpiles, reservoir waterproofing barriers for the disposal of fine tailings and waterproofing of tailings dam slopes, ore pile covers, reinforcement of associated infrastructure (roads, railways etc.) and dewatering and consolidation of fine tailings.

Geosynthetics use has been increasing in mining due to improved technical specifications, excellent manufacturing quality control and ease of installation. Their use has improved environmental protection by saving exploitation and usage of natural construction materials. Nevertheless, mining countries like Brazil, one of the largest ore producers of the world, Argentina, Chile, Peru, and others, still have no regulations with regard to the use of geosynthetics in mining, particularly as components of tailings dams and high piles of sterile rock and ore. Designs of facilities incorporating geosynthetic products have been based on the knowledge of the designers on classical geotechnical engineering, similar geosynthetics applications where the performance of such products is well established, and specifications provided by manufacturers. To obtain relevant geosynthetic design parameters, specific laboratory tests have been carried out in national and overseas laboratories.

The challenges of managing mine waste in South America are sufficiently large that §8 is devoted to their discussion.

7.5 *Synopsis of challenges and innovations to containment barriers outside North America and Europe*

7.5.1 *Regulations and Standards:*

The dearth of regulations, policies and national guidelines has led to the embracing of the South African regulations in much of the Sub-Saharan African region or shadowing of standards with which the designer is familiar where such obligatory standards are not regulated. This gives rise to large variations in design philosophy which is tempered by the sharing of appropriate technology through voluntary organizations, when making use of electronic media.

7.5.2 *Variations in contaminant significance*

The climatic conditions, population density and other factors influence the significance attributed to particular contaminants and associated containment technologies with particular aberrations being the food content of MSW in Asia, mine waste disposal at high altitude sites having steep and rugged founding conditions in Latin America, and the limited availability of renewable water resources per capita with associated constraints on assimilative capacity of the environment in the Southern Hemisphere in particular. These challenges have been addressed by adopting first-world technology and developing region-specific theory and practice for municipal, mining, and industrial contaminants. These aspects include addressing the higher-than-normal leachate and gas generation from MSW in humid parts of Asia, the development and implementation of regulations and standards modelled on North American and European practices with adaptations to accommodate domestic socio-economic and climatic conditions, and the pursuance of appropriate technology here and elsewhere through the support of regulators and voluntary organizations. The reduction and reuse of waste by recycling of polyester bottles to form continuous filament nonwoven geotextiles used as filters or cushion layers to geomembranes in waste facilities requiring protection from a relatively short polluting period due to the putrescible nature of the particular waste is a novel advance of containment barrier performance and economy, provided the performance of the geotextile for the type of load and adjacent materials are confirmed as limiting tensile strain in the geomembrane to a total of less than 3%.

7.5.3 *Containment barrier design and construction quality assurance*

The deviation from norms and standards in regulations or standard specifications occurs from time to time, even for materials having ISO 9000 certification; however, the development and implementation of domestic techniques to confirm the performance of materials and construction quality leads to rectification of deviations or omissions in many cases. Indicator tests have a limited value in assessing the consistency of a particular material. Hence, a suite of site-specific materials and techniques are used to assure the quality of the barrier system. Such techniques include pre and post construction confirmation of "swell index" of the bentonite in a GCL when exposed to site hydration media, groundwater or of leachate; the use of real time electronic data tracking of geomembrane seaming or welding parameters which are uploaded onto a cloud based system which can be viewed at any time; the in-situ confirmation of geomembrane strain limitation in a geomembrane by fitting the laboratory approach to a field test which allows for the influences of site aggregate shape and placement method, CCL and foundation conditions, and elevated temperature with longer loading periods to overcome in part the concerns of creep and material softening; and the evaluation of geotextile filter performance by test methods which recognise the influence of a build- up in fine fraction from base soil or waste (due to that being the fraction which controls permeability).

7.5.4 *Operational phase influence on barrier performance*

The operational phase influences of waste stoichiometry and biology can lead to chemical or biological clogging of filters and drains to barrier systems, and/or the development of elevated temperatures in gas and leachate adjacent to liner components with commensurate decrease in liner performance due to polymer degradation, diffusion rate increases and moisture loss of clay or geosynthetic elements which in turn reduces thermal conductivity and aggravates the rate of barrier performance degradation still further. The influence of chemical precipitate and biological clogging in drainage systems designed to operate under gravity and atmospheric pressure is partially mitigated by the incorporation of a "P-trap" on the outlet pipes of leachate collection systems in gold mines, which reduces air intrusion into drainage systems and hence reduces the rate of precipitate formation. Similarly, the removal of the outlet P-traps to suddenly change drains from anaerobic to aerobic conditions is employed to reduce the build-up in biological growth of bacteria which flourish in a habitat having fixed environmental conditions. The reduction in containment barrier performance and service life due to influences of elevated temperature on total solute transport is mitigated by the development of novel drainage systems adjacent to liners to facilitate the application of a negative pressure to draw fluid through the permeable drainage layer, which has allowed for options of introducing moisture for the hydration or rehydration of adjacent clay components, the removal of VOCs, and/or the removal of heat so as to extend service life and enhance performance. The efficiency of this unique system is influenced by multiple factors but notably the type of fluid drawn through the system and retention time within the cell.

8 MINING: A SOUTH AMERICAN PERSPECTIVE

Geomembranes used as liners for heap leach facilities (Figure 8.1) are probably the single biggest geosynthetics use in the mining industry in South America (Fourie et al. 2010). Fresh ore is transported directly from the pit, or crushed to a specific size, and stacked over the geomembrane before leaching with acidic or basic solutions. During the long leaching process, which could take many years, metals are dissolved and the leachate (pregnant solution) is transported by gravity to the HDPE drainage pipes above the geomembrane and conveyed to solution ponds. The pregnant solution is pumped from the ponds to the process plant for the recovery of metals such as gold, silver, copper, and nickel. Uranium is also a metal that is obtained by heap leaching but this has still not been exploited in South America. The biggest heap leach pad in the world is the ROM Sulfide Leach project of Escondida mine located in the Atacama Desert in Chile, where currently more than 1,000 ha of LLDPE geomembrane has been used to stack 5,000 Mt of ore (= average 5M t/ha =500 t/m^2 or >200 m^3/m^2) and additional expansion is planned.

HDPE geomembrane is usually used for the process and emergency ponds. These are essential facilities for a heap leaching project. Process ponds use double liner systems with a geonet or geocomposite between the two geomembranes for leak detection and recovery system. Emergency ponds are lined with a single liner.

Geomembrane liners are now also being used more frequently in tailings storage facilities (Figure 8.2) to protect the environment from polluting elements (tailings with acid drainage or metal leaching), as well as to comply with environmental and social commitments and to obtain operating permits.

Geomembranes are also used extensively in the potassium and lithium extraction industry from brine reservoirs in Chile, Argentina, and Bolivia, where a series of very large evaporation ponds, lined with HDPE or PVC geomembrane, contain salt-rich water and where evaporation occurs over months. When the lithium chloride in the evaporation ponds reaches an optimum concentration, the solution is pumped to a recovery plant. The Salar de Atacama in Chile is home to the largest PVC geomembrane installation globally, with more than 150 ha utilized in mining operations since 1996 (Berube et al. 2007).

In situations where mine waste rock has the potential for acid drainage or metal leaching, geosynthetics are used to minimize the generation of acid drainage and comply with environmental restrictions.

Geosynthetic clay liners (GCL) are used in mining as hydraulic barriers in composite liner systems for heap leach pads, tailings dams, waste rock dumps and ponds. In some cases, the GCL is used instead of compacted clayey soil.

Geotextiles are used extensively in the mining industry to construct drainage systems or solution collection systems. Since several cases of clogging of geotextiles have been observed over the years, the geotextile must be used with care, previously verifying its compatibility as a filter of the soils surrounding the drainage systems. When used in the collection system of a heap leach pad, in addition to verifying its filtering characteristics, consideration must be given to the potential for clogging due to chemical precipitates, especially when dealing with acid leaching. Geotextiles are also used as protection of the geomembrane to avoid puncturing.

Geonets, a synthetic drainage material manufactured of HDPE resin to transmit fluids (and gases), and geocomposite drains (typically a geonet with a geotextile on one or both sides to act as a separator/filter) are used as a leak detection layer in double-lined ponds. Also, in South America, geocomposites are used to protect geomembranes and GCLs from damage when installed on irregular/rocky slopes in heap leach pads.

HDPE pipes are used extensively for underdrain systems to collect underground water below heap leach pads, waste rock storage facilities, tailings storage facilities, solution ponds, and emergency ponds. Underdrain systems may also be used as a leak detection system below mining facilities.

Figure 8.1: Heap leach pad (gold) in South America

Figure 8.2: Tailings storage facility in South America

8.1 *Geosynthetics in difficult terrain*

The topography of much of South America (e.g., Argentina, Bolivia, Colombia, Ecuador, Peru, and parts of Mexico and Chile), is very unfavourable for the design and construction of mining facilities that involve the use of geosynthetics. Mining projects in the Andes region typically operate at altitudes of more than 3,000 meters above sea level with moderate to high precipitation and in an area of high seismicity. Usually, the only place available for constructing the mining facilities is a valley. The topography, the environment, and the scale of the projects invariably necessitate design criteria different to those used in flat areas or at lower altitudes (César et al. 2013). In areas of difficult terrain special consideration must be given to the optimization of earthworks, use of soil liner or GCL together with the geomembrane to form a composite liner or a secondary liner, geosynthetic installation, geosynthetic protection, etc.

8.2 *Selection of soil liner or GCL*

A decision as to whether to use low permeability clayey soil liner or GCL will involve consideration of the slope upon which the liner is to be placed. Generally speaking,

- Soil liner may be placed on slopes up to 2.5H:1V or even 2H:1V.
- Steeper slopes must be lined using a GCL.

Some projects in South America have been developed where there are no borrow sources suitable for a soil liner close to the project. Under these circumstances, a GCL may be used on slopes flatter than 2.5H:1V (e.g., as part of the barrier system for heap leach pad as shown in Figure 8.3).

8.3 *Some technical considerations for the use of GCL*

There are several technical considerations commonly associated with the use of a GCL:

- GCLs may be used on steep slopes subject to verification of heap leach pad stability.
- The effect of hydration of the GCL on shear strength must be based on project specific laboratory testing. During heap leach pad operation, the GCL is likely to be hydrated by solution leakage through the liner system or by underground water, making the shear strength even lower.
- In general, Renken et al. (2005) recommend the use of needle-punched GCLs with a nonwoven geotextile on top and a scrim-reinforced nonwoven geotextile on the bottom on slopes steeper than 3H:1V. The experience in several heap leach pad projects suggests that this recommendation is appropriate.
- Minimum overlap of the 25 cm in flat areas and 45 cm on slopes to reduce the risk of GCL separation by shrinkage as shown in Figure 8.4 (see also §5.5.2.2).

8.4 *Geosynthetics design and installation in difficult and steep slopes*

For heap leach pad facilities with very steep slopes, extra cuts are required to achieve the slope (usually less than 2.5H:1V or 2H:1V) so that it is possible to place and compact low permeability soil and facilitate liner installation. The slope will be lined with low permeability soil or GCL before a geomembrane is put in place, subject to a check that there is adequate stability.

Very steep rocky surfaces are often shaped by blasting, leaving irregular surfaces with sharp edges or cavities that could damage/puncture the GCL and geomembrane during operations (Figure 8.5). Figure 8.6 shows some techniques used on irregular slopes and final surfaces to protect the liner system.

8.5 *GCL design and installation*

Special attention is required in areas where the final slope after grading is steeper than 2H:1V (or 2.5H:1V in some places). A scrim reinforced nonwoven needle-punched GCL with the upper edge buried in an anchor trench and the roll deployed down the slope is commonly used. The slope and needle-punching should be such as to avoid significant bentonite migration under gravity. The GCL should only be installed in areas of the leach pad where overall stability is not compromised. These zones must be identified as part of the design process and verified during construction. Figure 8.7 shows the installation of geocomposite for protection (black) and GCL (white) on an almost vertical slope, with the installers hung on the slope with strict safety measures. It is essential that the installers are experienced and knowledgeable to ensure installation quality and safety.

8.6 *Geomembrane selection*

A soil liner, a GCL, or a zoned combination of both will be placed as a second containment layer on a prepared subgrade. The first and main containment will be the geomembrane liner, which will be installed over the soil liner or GCL.

Single side textured linear low density polyethylene (LLDPE) geomembranes are currently popular for use in heap leach pads (Parra et al. 2014). Typically, the textured side is placed in contact with the soil liner or GCL to improve the shear strength of this interface. High density polyethylene (HDPE) is still extensively used in single or double lined ponds. PVC has also been used in the past mainly in interlift liner applications in copper heap leach projects in Chile. Figure 8.8 shows a geosynthetic installation in difficult terrain in a valley heap leach pad located in the Andes.

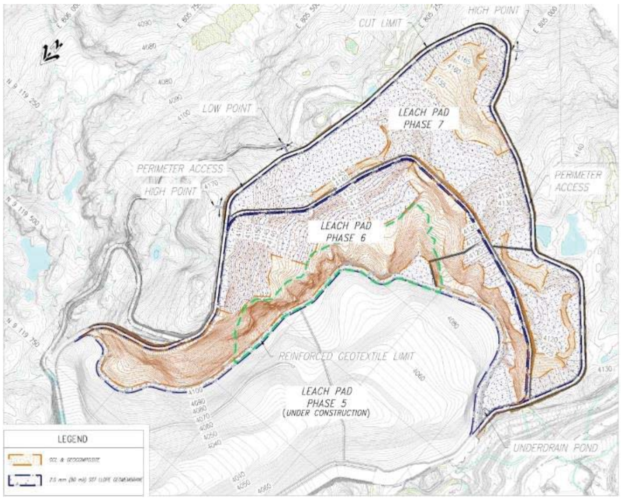

Figure 8.3: Optimized area for GCL utilization

Figure 8.4: Separation by shrinkage in two panels of GCL installed

Figure 8.5: Very steep rocky slope with irregular shape after blasting

Although the geomembrane thickness determination is typically based on puncture tests, César et al. (2013) presented a practical rule for thickness selection based on the design and construction experience of dozens of these kinds of facilities:

- 1.5 mm for heaps up to 100 m, or
- 2.0 mm for higher heaps.

If the heap leach pad is very high, then a geotextile protection is better and cheaper than a thicker geomembrane (2.5 mm); however, the final thickness to be used will depend on laboratory puncture testing. The focus here should be on minimizing short-term puncture and long-term stress cracking due to excessive tensile strains, which is not generally considered yet.

Figure 8.6: Typical protection with heavy geotextile (upper) and geocomposite (lower) for geosynthetics installation in difficult slopes

Figure 8.7: Installation of geocomposite for protection (black) and GCL (white) on an almost vertical slope

8.7 *Geomembrane integrity test (puncture test)*

The effect of the ore heap weight on the liner system on the integrity (e.g., punctures) is assessed by means of laboratory tests. The tests involve first placing the subgrade material (typically a soil subgrade or GCL) inside a square or cylindrical test device. A sample of the geomembrane proposed for the specific project is then placed over a subgrade material and covered with either an overdrain or ore. The entire system is gradually loaded to reach a pressure equivalent to the proposed height of the heap plus a factor of safety. The maximum load is held for 48 hours. The geomembrane sample is exhumed and subjectively inspected to assess whether it has experienced minor, moderate, or severe yielding or puncture. A vacuum box is used to physically confirm whether a hole has occurred. Figure 8.9 shows a puncture testing device and geomembrane samples after testing. This specimen shows evidence of pronounced yielding and holes. In South America, puncture testing has been carried out up to 4,400 kPa (about a 250 m heap).

Figure 8.8: Complex geomembrane and GCL liner installation on very difficult terrain

Figure 8.9: Puncture testing device and damaged geomembrane

8.8 *Geomembrane protection*

For very high heap leach pads, holes are possible even in a 2 mm LLDPE geomembrane. In this case, there are two options available to the design engineer to improve geomembrane behaviour:

- Increase the geomembrane thickness to 2.5 mm, or
- Use a geotextile to protect the geomembrane.

In both cases, the area to improve will be that in which damage (severe puncture or holes) is expected to occur. The first option is a little complicated to carry out because the installation must deal with two different geomembrane thicknesses. In addition, the second option is preferred because geotextile is easy to install and much cheaper than a thicker geomembrane. Tests have shown that placing a geotextile over the geomembrane liner reduces yielding and in this case, it is inferred (often incorrectly) that it's use achieves the design objective of adequate geomembrane protection. Based on this experience, Parra et al. (2014) recommend the following for preliminary design:

- Use at least 270 g/m^2 nonwoven geotextile or heavier if the heap is very high.
- Geomembrane protection must be provided in zones where the heap height exceeds 120 m or 130 m.

However, suitability of the proposed geotextile for these heights must be verified by testing.

Figure 8.10 shows an example of a 160 m height heap leach pad and the area in the pad base (blue hatching zone) where the 2 mm-thick LLDPE single-side-textured geomembrane was protected using a 270 g/m^2 nonwoven geotextile. Figure 8.11 shows the geotextile already placed and partially covered with the overliner and the ore of the heap.

The practice described above to limit punctures addresses the very short-term issue of puncture under static vertical load with the immediate objective of minimizing the loss of pregnant liquor to the environment. It presumes that a test with only vertical loading of the geomembrane and protection layer is indeed adequate for assessing the likelihood of punctures.

Control studies of the potential for puncture and strain in a geomembrane have shown that the potential for puncture is highly dependent on both the grain size distribution of the overliner material and the compressibility of the underliner (Rowe et al. 2013a; Brachman et al. 2014). Tests that do not adequately represent these two conditions will not provide a good indication of the likelihood of puncture. Also, with respect to the difference between high-quality LLDPE and HDPE, it has been found that for geomembranes of the same thickness there is a little difference in the puncturing (Rowe et al. 2013a) when tested under identical conditions. Consideration is only given to vertical load. However, holes can develop in the geomembrane at much lower vertical loads if the interface is also subject to shear (Abdelaal and Solanki 2021).

At present, the focus on geomembrane selection in South America is on minimizing puncture. While minimizing puncture is essential, it is not sufficient for providing long-term environmental protection. If the geomembrane is to provide environmental protection in the long-term, there must also be a limit on tensile strains that will result in stress cracking and potential environmental impact over time. This applies to both HDPE and LLDPE. Stress crack tests are generally not performed for LLDPE because either there is no yield strength or, if there is, the SCR_o is typically more than 30,000 hours and a single test can take more than 3½ years. However, this does not mean that stress cracking is not an issue. With ageing, once thermo-oxidative degradation commences the LLDPE stress crack resistance and tensile break strength decrease very rapidly and the LLDPE can become very brittle (Figure 8.12). While not a current priority, there is growing concern about environmental impacts of mining and the future failure of these geomembranes due to stress cracking and this is likely to become an issue as more people become aware of the potential consequences of the excessive strain developed in LLDPE liner in heap leach pads. Once the LLDPE becomes brittle, this excessive strain will cause extensive stress cracking and the liner will have reached its service life. As with HDPE, there can be a substantial difference in the performance of different LLDPE's in terms of service life.

8.9 *Bituminous geomembrane*

Bituminous geomembranes (BGM; Figure 8.13) have also been used as a liner in heap leach pads in South America (Lazaro and Breul 2014) but to a lesser extent. This geomembrane has some advantages over HDPE and LLDPE but has its own share of challenges and large-scale failures in mining applications (e.g., Addis 2016), particularly in terms of creep failure of seams and performance in hot and cold climates. The interested reader is referred to §3 for a fuller discussion of BGMs.

8.10 *Solution collection pipes*

Robust drainage systems to collect leach solutions are required to improve mineral recovery, reduce leaks through the liner system, improve slope stability, and reduce liquefaction potential. ROM or crushed ore heap leach pads are irrigated with solvent solution (dilute alkaline cyanide for precious metals and dilute sulfuric acid for base metals). This solution, along with any stormwater, snowmelt, and cumulative season surplus water is collected at the base of the leach pad through the solution collection system which typically consists of dual wall HDPE perforated pipes (smooth inner and corrugated exterior).

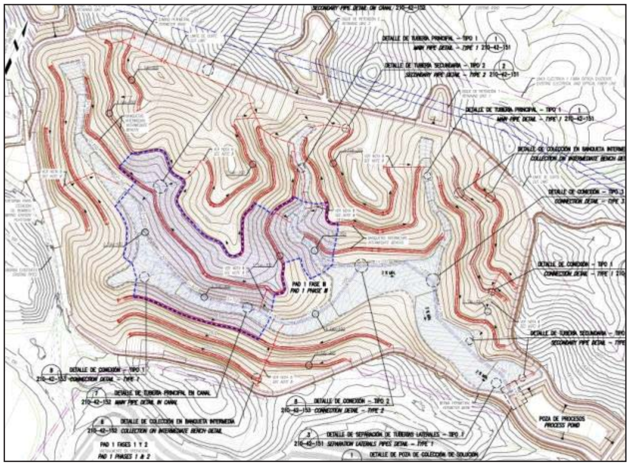

Figure 8.10: Very high heap leach pad and area where the geomembrane requires protection

Figure 8.11: Nonwoven geotextile placed for geomembrane protection

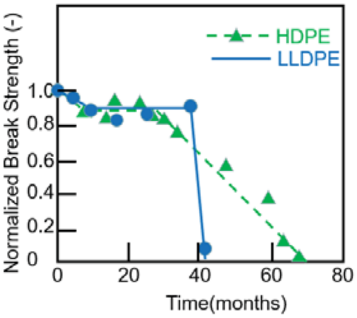

Figure 8.12: Variation in geomembrane normalized break strength with time after ageing in high pH heap leach solution at 85ºC (Abdelaal and Rowe 2022)

Figure 8.13: Construction equipment on bituminous geomembrane

The pipe diameter depends on the catchment area, irrigation rate, and the pipe slope. Bigger diameters are used for the main headers and primary collection pipes. Diameters up to 600 mm have been used in the industry, but in general the design of the primary collection system uses pipes up to 450 mm because bigger pipes will show more deflection, buckling, and potential for collapse. On the other hand, laterals or secondary (or tertiary) pipes are smaller. These are usually 100 mm, although in dynamic leach pads, 50 mm pipes are used.

Solution collection system design in difficult terrain is governed by the following considerations:

- Collection pipes are only used in areas where the slope is less than 4H:1V since collection will not be efficient on steeper slopes.
- It is generally good practice to use intermediate benches for evacuating solutions from subsequent phases directly into the process pond, or even to a process plant if possible.

Figure 8.14 shows a plan view of a solution collection system in very steep/difficult terrain with intermediate benches.

The behaviour of the collection pipes and their durability, when subjected to the loads of the heap, depends not only on the pipe stiffness but, more importantly, on the surrounding soil. Generally, the larger the pipe diameter the lower its stiffness. Thus, very large diameter pipes are generally not used because of the risk associated with large deflections, buckling, joint separation, and collapse that would decrease the pipe flow capacity and the efficiency of the collector system. The required flow capacity is achieved by increasing the number of pipes rather than their diameter. It is important to have adequate collection capacity to reduce the risk of an increase in the solution level inside the heap leach pad, which would generate a potential static instability, saturated ore liquefaction, and seismic instability; the last condition is not very common but is possible (Castillo et al. 2005).

8.11 *Pipes under high loads*

Underdrain HDPE pipes beneath heap leach pads, tailings impoundments and waste rock facilities are sometimes exposed to high loads because of the material weight above them (ore, tailings or waste rock), the thickness of which may exceed 180 - 200 m. Figure 8.15 shows a solution collection pipe from a heap leach pad facility that has undergone over 20 percent deflection but is still within the design deflection criteria for the collection and conveyance of leach solutions.

Current, design practice for secondary collection systems is to use 100 mm dual wall HDPE pipe based on test results (Smith 2004). Primary collection pipes are at least of 300 mm and commonly 450 mm diameter. These pipes are less stiff than the smaller secondary collection pipes. Usually, the HDPE pipes are placed directly on the geomembrane, however, when the pipes are used in heap leach pads with a thickness of 120 m or greater, the larger diameter primary collector pipes may be placed into trenches that will facilitate compaction of the drainage gravel around the pipe (Figure 8.16; Parra et al. 2014) to allow arching in the gravel when the pipe deforms, thereby minimizing load transfer into the pipe.

8.12 *Geomembrane overstressing*

Based on finite element models run and calibrated to both small- and large-scale laboratory tests, Leduc and Smith (2004) reported a significant reduction in the load (as compared to the overburden stress) immediately below the pipe. But the load increased to about 125% of overburden at a distance of one pipe diameter, and the zone of overstress extended to about 4 pipe diameters. These results mean that there are narrow strips of geomembrane on either side of each collection pipe that are receiving a higher stress than commonly considered. The authors note that the overstress will vary depending on the pipe stiffness, the type and the degree of compaction of the material surrounding it, and the height of the heap. This is confirmed by the numerical modelling performed by Castillo (2005) for the case shown in Figure 8.16, which indicated that for a single pipe the vertical stress on the liner close to the pipe increases in about 14% for 130 m heap and 13% for a 180 m heap.

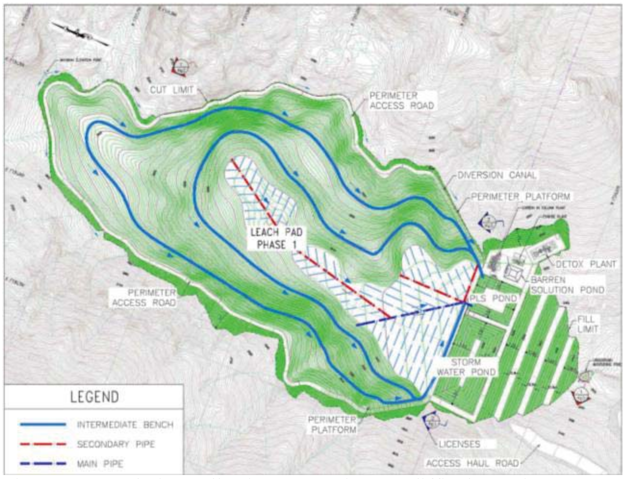

Figure 8.14: Solution collection system in very difficult terrain

Figure 8.15. Interior of a solution collection pipe below a heap leach pad

Based on the findings cited above, geomembrane protection inside the trench using a nonwoven geotextile is also needed, in a similar way to that suggested for areas in the heap where the loads are very large. In Figure 8.16 the geotextile used for geomembrane protection is shown as well as the secondary pipes connecting to the primary pipe. Figure 8.17 shows the pipe installation in trenches with geotextile for geomembrane protection. As noted earlier, large strains can be anticipated in the geomembrane at these loads with a 250 g/m^2 geotextile as a protection layer (Rowe et al. 2013; Brachman et al. 2014) and can be expected to significantly influence the service life of the geomembrane, particularly if there is any shear or generation of heat from exothermic reactions or during heap leaching, and/or the leach solution has a high pH or contains any surfactant.

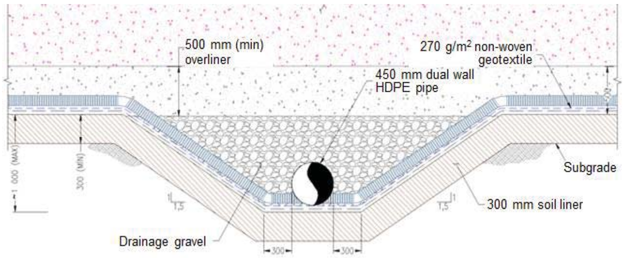

Figure 8.16. Primary collection pipe placed into trench for pipe protection

Figure 8.17. Primary collector pipe installation with geotextile for geomembrane protection

8.13 *Raincoats*

Raincoat terminology is used in the mining heap leach industry in reference to a temporary exposed geomembrane cover that minimizes rain stormwater infiltration into the stacked ore and diverts cover surface storm runoff to a dedicated pond or natural drainage (Breitenbach and Smith 2007).

Some gold and silver mining operations, which use heap leaching technology, located in rainy regions use raincoats on the top of the ore heap to reduce the amount of rainwater that enters the heap. The raincoats are used in inactive areas of the ore heap still under irrigation. Various experiences of heap leach pads on an industrial scale indicate that the entrance of rainwater into the system causes solution dilution, making metal recovery less efficient. It also produces surplus contaminated water that requires recirculation or treatment before it can be discharged into the environment, causing significant additional costs. Figure 8.18 shows a heap leach pad in Peru using raincoat system.

In addition, raincoats can be used in dry regions, where water is scarce, to avoid evaporation, thus reducing the water demand.

Figure 8.18. Gold heap leach pad in Peru covered almost entirely with raincoats.

8.14 *Fazenda Brasileiro Mine and Jacobina Yamana Gold Mine, Brazil*

Two field experiments to investigate the performance of HDPE and PVC geomembranes were conducted at gold tailings dams. Santos (2014) conducted one study at four gold tailings dams built between 2006 to 2010 at Fazenda Brasileiro Mining (FBM). The second experiment was conducted by Sampaio (2015) at Jacobina dam located in the state of Bahia, Brazil, to verify the performance of the 1.5 mm thick textured HDPE geomembrane installed in the dam reservoir and of the nonwoven geotextile used as a filter of the drainage system. These studies evaluated the physical properties of HDPE and polyvinyl chloride PVC geomembranes intended as barriers for the slopes and foundations of the tailings dams. The system operation basically consists of pumping tailings from the processing plant to Lake II. The underflow is disposed as a pile in Lake II and the overflow is released to Lake III, which also receives the supernatant of Lake II. **Error! Reference source not found.**19 shows a view of Lake II.

Figure 8.19. A view of Lake II (FBM) - PVC geomembrane 0.8 mm thick (Santos 2014).

Error! Reference source not found.20 shows a view of Jacobina, Yamana Gold Mining (JYGM) dam. The tailings from the gold ore processing have damaging environmental contaminants such as arsenic and cyanide, and they should be stored appropriately.

Figure 8.20. Gold tailings dams – Jacobina Dam (JYGM) – 1st step (Sampaio, 2015).

Santos (2014 and 2016) evaluated the physical properties of HDPE and PVC geomembranes with thicknesses of 1.5 and 0.8 mm, respectively, that were installed for four years, from 2006 to 2010, by Fazenda Brasileiro Mining (FBM). Tests were carried out on four types of samples: virgin samples (GMV), samples aged in the laboratory (GMD), samples aged in a weathering chamber (GMC) and samples exhumed from the dams (GMEX) after 18 months. The JYGM geomembrane samples were tested in an ageing chamber under the same field conditions (immersed in cyanide fluid from the dam, temperature of 40°C and subjected to ultraviolet radiation) for a period of 6 years (Gardoni and Morais 2019). This method made it possible to compare the durability of aged/exhumed samples to that of virgin samples and to assess the geomembrane's degree of ageing and durability.

Exhumed geomembrane samples were extracted from the tailings lake and security dikes which were part of the dam structure. Exhumed sample details are given in Table 8.1 and sampling at one location is shown in Figure 8.2

All samples were subjected to tensile tests, thermo-gravimetric analysis, Oxidative Induction Time (OIT) tests, Scanning Electron Microscopy (MEV), and Atomic Force Microscopy (AFM). Figure 8.22 shows some MEV results. The following mechanical properties were evaluated as a possible way to measure degradation: tensile strength, deformation, and stiffness. The results showed that geomembranes have differentiated behaviour over time: PVC geomembranes become more rigid whereas HDPE exhibited a more stable behaviour, despite having a tendency for increased rigidity. However, both geomembranes were considered to have exhibited satisfactory properties for the project, even under severe exposure conditions

Table 8.1. Locations of samples exhumation (Santos, 2014).

Sample Data					
Identification Dam/Dike	Sample ID	Type	Installation Date	Sample Thickness (mm)	Exposure Conditions
Security Dike	GMEX-A1	HDPE	2010	1.50	Exposed to weather and contact with cyanide fluid
Security Dike	GMEX-A2	HDPE	2010	1.50	Exposed to weather
Jacobina dam (1)	GMEX-A3	HDPE	-	1.50	Exposed to weather and contact with cyanide fluid
Lake III	GMEX-B	PVC	2009	0.80	Exposed to weather
Lake III	GMEX-C	PVC	2010	0.80	Exposed to weather
Lake II	GMEX-D	PVC	2006	0.80	Exposed to weather

Note: (1) Only this sample was exhumed from Jacobina mining (JYGM); the others were exhumed from Fazenda Brasileiro Mining (FBM).

Figure 8.21. Exhumation of HDPE samples – FBM Security dike (Santos, 2016).

The results obtained by MEV showed good mechanical resistance for HDPE geomembranes. However, PVC geomembranes showed a much greater loss of strength than HDPE. The PVC geomembrane installed in 2006 showed a structure with a totally cracked surface with deep cracks indicating a compromise of its waterproof barrier property.

8.15 *Maracás Menchen Mine*

The Maracás Menchen Mine property totals 17,690 hectares and is located in the eastern region of Bahia State, Brazil. The Nº 4 (BNM-04) non-magnetic tailings deposit basin of vanadium ore was built in three stages, with an estimated final storage capacity of 1,047,532 m^3 of non-magnetic tailings. Vanadium is an essential ore used for the processing of steel for aerospace, oil and gas industries, and for the production of surgical materials. The Maracás Menchen Mine has one of the highest-grade vanadium resources in the world (1.34%) and is one of the lowest cost primary producers of vanadium in the world (Botelho 2019). Figure 8.23 shows a view of Maracas' dam.

The barrier system on the bottom and slopes of this basin comprised four layers of geosynthetics (from top to bottom), namely: a 1.5 mm HDPE geomembrane, a 5.5 mm thick polyethylene geonet leak detection layer, a second 1.5 mm HDPE, and 400 g/m^2 nonwoven polyester geotextile on a compacted soil layer to protect the geomembrane (Figure 8.24).

8.16 *Behaviour of geotextile filters*

8.16.1 *Performance of geotextile filters under severe conditions*

Geotextile filters have been extensively used in mining, commonly under severe conditions where mechanical damages, in addition to clogging potential, may compromise the filter performance. Figure 8.25 (Beirigo 2005; Palmeira et al. 2010) shows examples of geotextile filter applications in the Germano and Fosfertil tailings dams, in Brazil.

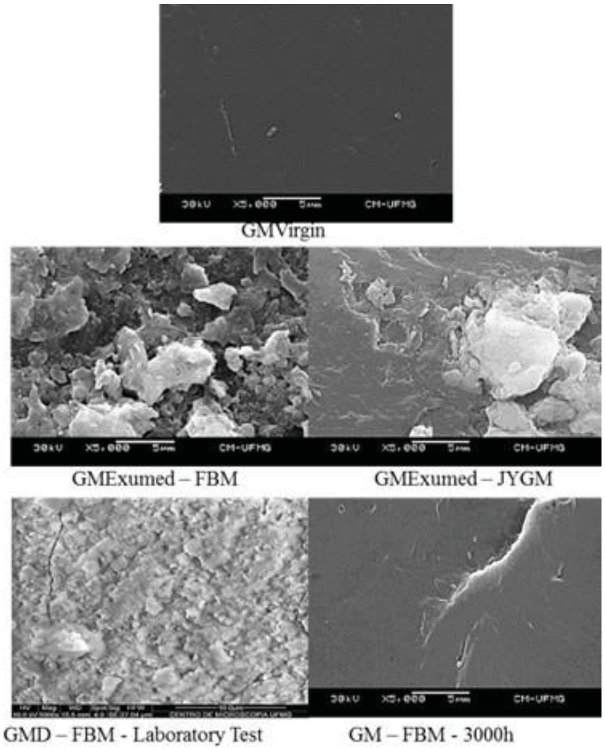

Figure 8.22. Scanning electron microscopy results (Gardoni and Morais, 2019).

Figure 8.23. A view of vanadium Maracás dam.

Results of tailings-geotextile compatibility tests are reported by Palmeira et al. (2010) using samples of tailings collected in the Germano and Fosfertil dams (Figure 8.25). The main properties of the tailings tested are shown in Table 8.2. Tailings FA was collected in the Fosfertil dam, whereas tailings SA and SL were collected in the Cava do Germano dam and in the drying bays of the Germano dam, respectively. The properties of the geotextiles tested are listed in Table 8.3. The performance of 3 nonwoven, needle-punched geotextiles, manufactured from polyester was investigated, with masses per unit area varying between 200 and 627 g/m^2 and filtration opening sizes varying between 0.06 and 0.23 mm. A gradient ratio apparatus capable of performing tests with vertical stresses of up to 2000 kPa was used.

Figure 8.26 shows the results of gradient ratio tests (as per ASTM D5101) versus normal stress on the soil sample obtained with the systems tailings FA-G1 and FA-G3 for a system gradient (i_{system}, total hydraulic gradient along the system height) equal to 1. The results show low values of gradient ratio (GR), rather constant with normal stress, indicating piping mechanisms. This behaviour may be attributed to the potential internal instability of the tailings. The same behaviour can be noted in the test with geotextile G3, which has a smaller filtration opening size. However, the holes left by the needle-punching process were clearly visible in that geotextile, which may have influenced the results. Under field conditions it is likely that these needle holes will have their sizes reduced due to distortion of the geotextile during deposition of the tailings and increasing vertical stress. The tailings-geotextile systems investigated remained stable throughout the durations of the tests.

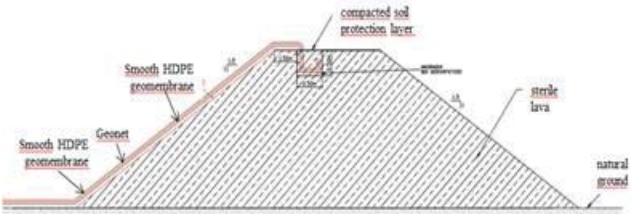

(a) Cross section of the dam

(b) Double barriers construction

Figure 8.24. Double layer barrier for upstream waterproofing at Maracas' dam.

The variations of GR with normal stress obtained in tests with tailings SA and geotextiles G1, G2 and G3 are shown in Figure 8.27 (for i_{system} =1). In this case, the GR values were very close to unity and rather constant or slightly increasing with normal stress. The same pattern of variation was observed for the system SL-G1, as shown in Figure 8.28.

Table 8.2. Properties of the tailings tested.

Property$^{(1)}$	FA	SA	SL
D_{15} (mm)$^{(1)}$	0.066	0.033	0.007
D_{50} (mm)	0.128	0.065	0.041
D_{85} (mm)	0.251	0.105	0.099
C_u	3.7	2.6	9.2
C_c	0.9	1.0	0.8
% < 0.074mm	29	66	72
ρ_s (g/cm^3)	3.46	2.97	3.12
w_L (%)	NP$^{(2)}$	NP	14
w_P (%)	NP	NP	7
PI (%)	NP	NP	7
e_{max}	1.13	0.93	0.91
e_{min}	0.67	0.46	0.50

Notes: (1) D_n – particle diameter for which *n*% of the remaining particles have smaller diameters, C_u = coefficient of uniformity, C_c = coefficient of curvature, w_L = liquid limit, w_P = plastic limit, PI = plasticity index, e_{max} = maximum void ratio, e_{min} = minimum void ratio, $^{(2)}$NP = non plastic.

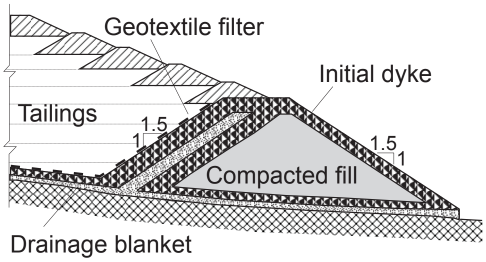

(a) Drainage system-Germano tailings dam.

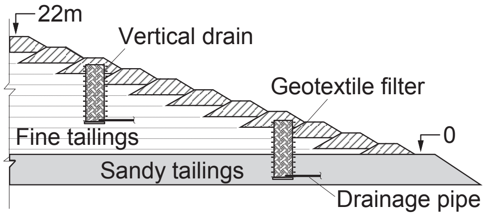

(b) Drying bays of the Germano tailings dam.

(c) Drying bays – Germano tailings dam.

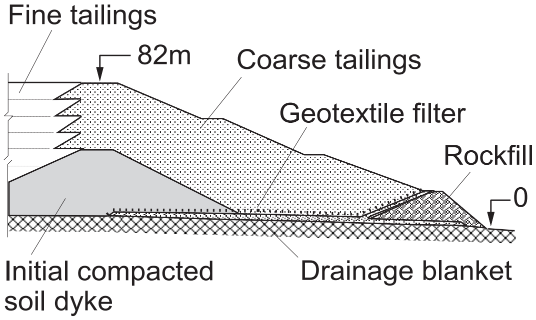

(d) Drainage system -Fosfertil tailings dam.

Figure 8.25. Geotextile filters in Germano and Fosfertil tailings dams (modified from Palmeira et al. 2010).

Table 8.3. Properties of the geotextiles.

Property	G1	G2	G3
M_A (g/m^2)	200	400	627
t_{GT} (mm)	2.3	3.7	4.5
n	0.93	0.92	0.90
FOS (mm)	0.13-0.23	0.09-0.16	0.06-0.13
k_n (m/s)	0.004	0.004	0.004
ψ (s^{-1})	1.9	1.1	0.9
d_f (mm)	0.027	0.027	0.027

Notes: M_A = mass per unit area; n = porosity; t_{GT} = geotextile thickness under 2kPa normal stress; FOS = Filtration Opening Size (hydrodynamic sieving); k_n = normal permeability; ψ = permittivity; d_f = diameter of the fibres.

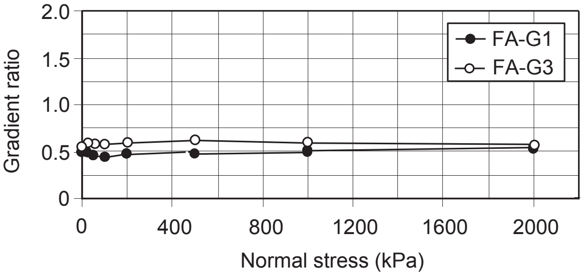

Figure 8.26. GR vs. normal stress for tests with tailings FA.

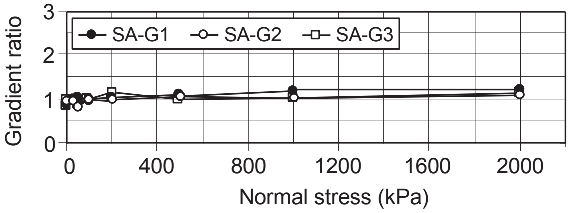

Figure 8.27. GR vs. normal stress for tests with tailings SA.

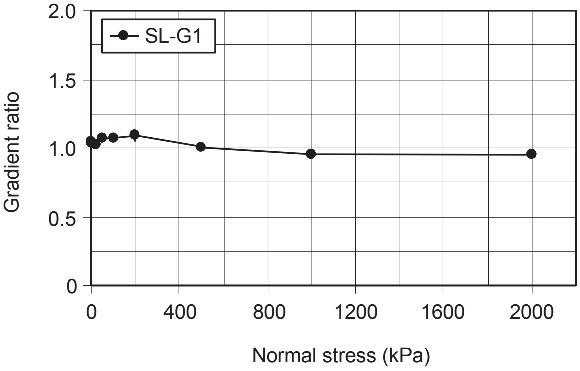

Figure 8.28. GR vs. normal stress for tests with tailings SL.

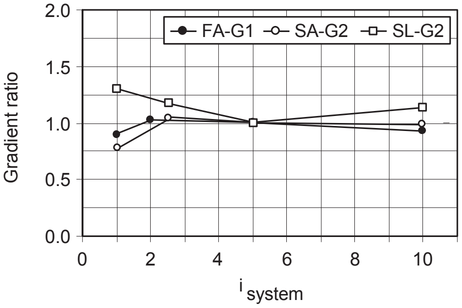

Figure 8.29. Variation of GR with system hydraulic gradient.

Satisfactory performance was also observed for the systems FA-G1, SA-G2 and SL-G2 in terms of values of GR for system hydraulic gradient varying between 1 and 10 in tests without confinement (no vertical stress on the sample top), as depicted in Figure 8.29. The measured values of GR were close to 1 even for large hydraulic gradients. The same pattern of behaviour can be seen in Figure 8.30, which shows the variation of GR with vertical stress for a system hydraulic gradient of 10. The values of GR for the 3 systems tested remained rather constant or decreased with increasing vertical stress, reaching a value slightly smaller than 1 for the largest vertical stress applied in the tests.

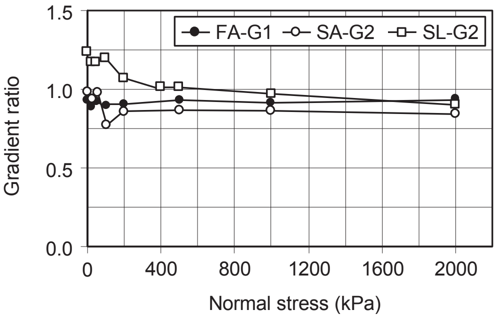

Figure 8.30. Variation of GR with vertical stress for $i_{system} = 10$.

Samples of the geotextile filter were exhumed from the Germano tailings dam. Some images from microscopy are presented in Figure 8.31, where different levels of impregnation of the filter voids by tailing particles can be identified. Figure 8.31(a) shows an image of a specimen with open voids and very few particles inside the textile matrix. Figure 8.31(b) shows that the tailings deposition process or the liquid flow could cause intrusion of large particles into the geotextile voids. Significant impregnation of the filter by tailings particles can be observed in Figure 8.31(c).

The amount of impregnation of the pores of a geotextile filter can be quantified by the impregnation level (λ), defined as the ratio between the mass of particles in the geotextile voids per unit area and the mass of geotextile fibers per unit area (Palmeira et al. 1996). The entrapment of particles in the geotextile voids can have a marked effect on some of its properties, such as permeability coefficient, compressibility, and filtration opening size (Palmeira et al. 1996; Palmeira and Gardoni 2000; Palmeira and Trejos Galvis 2017). Figure 8.32 and Table 8.4 show values of λ obtained in 9 specimens from a sample of a geotextile filter with 431 g/m^2 mass per unit area which was exhumed from vertical drains (Figure 8.25b) of the Germano tailings dam (Palmeira et al. 2010).

Figure 8.32 also presents the values of λ obtained at the end of gradient ratio tests carried out in the laboratory. Some values of λ in the field (λ ranging from 2.0 to 10) were significantly greater than those obtained in the laboratory, indicating the influence of the tailings disposal. Table 8.4 also presents the fraction of geotextile open voids (FOV), which can be obtained as a function of the values of density of geotextile fibers, density of the particles entrapped in the geotextile, λ, and geotextile porosity (n). Values of FOV are presented for different values of n. Under virgin and unconfined conditions, the porosity of the geotextile was 0.92 and this corresponded to FOV values ranging from 62.1 to 92.4%. However, if the geotextile was compressed to the extent of reaching a value of n equal to 0.6, the results of FOV obtained suggest that the exhumed sample of geotextile filter would be completely clogged by the entrapped particles in some locations, which is consistent with the image in Figure 8.31(c). The variability of values of λ and FOV in the geotextile layer is certainly a consequence of the heterogeneity of the tailings mass and segregation process during tailings deposition. Hence, these results suggest the worst conditions expected for the geotextile filter should be simulated in laboratory performance tests.

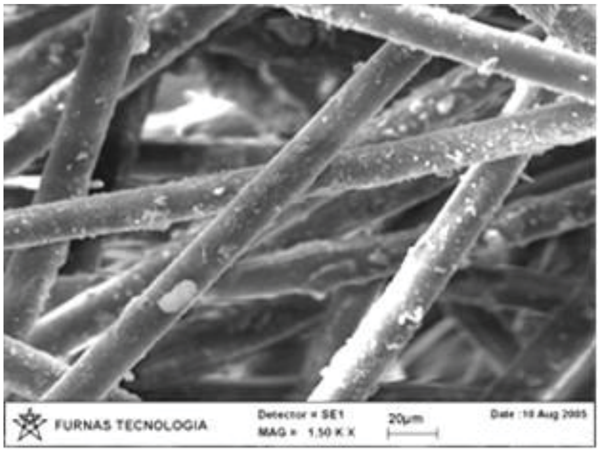

(a) Low impregnation level.

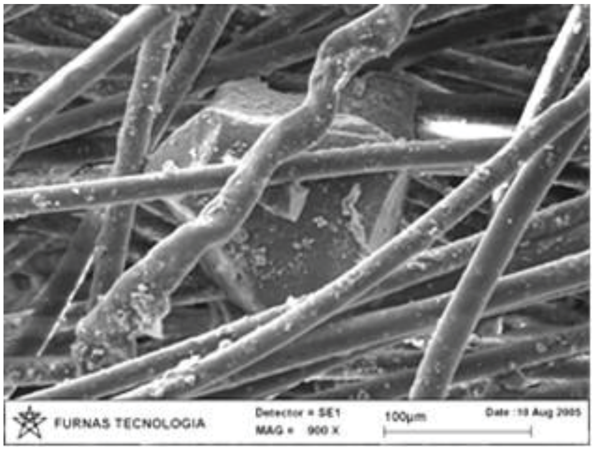

(b) Large tailings particle in the geotextile void.

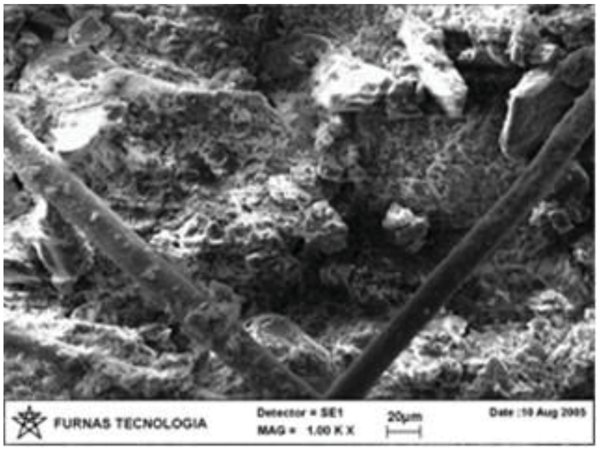

(c) High impregnation level.

Figure 8.31. Different levels of geotextile filter impregnation by tailings particles (Beirigo 2005).

8.16.2 *Geosynthetics for the reduction of ore moisture content*

Serra de Carajás mine (Figure 8.33), which belongs to the Vale Mining Company, produces one of the best iron ores in the world, but it has one undesirable characteristic: high moisture content. This characteristic is significantly aggravated by the wet sieving process utilized to obtain the adequate grain size distribution of the final product.

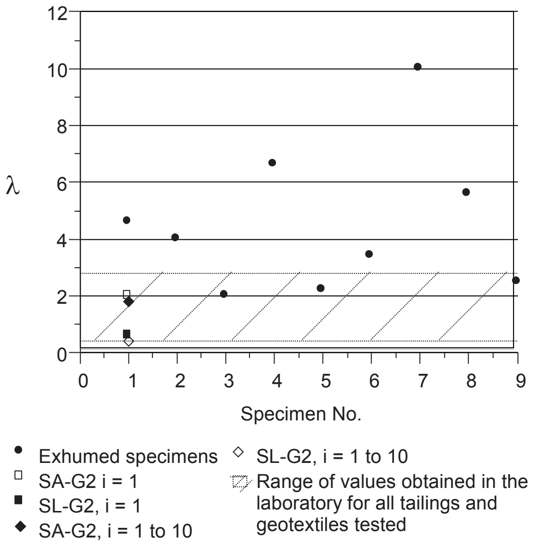

Figure 8.32. Impregnation level in specimens of an exhumed geotextile filter layer (Palmeira et al. 2010).

Table 8.4. Impregnation levels in geotextile specimens exhumed from Germano tailings dam (modified from Palmeira et al. 2010).

Specimen No.	λ	FOV (%)		
		n = 0.92	n = 0.75	n = 0.6
S1	4.6	82.6	33.2	0
S2	4.0	84.8	41.9	0
S3	2.0	92.4	70.9	41.9
S4	6.6	75.0	4.1	0
S5	2.2	91.7	68.0	36.1
S6	3.4	87.1	50.6	1.2
S7	10.0	62.1	0	0
S8	5.6	78.8	18.6	0
S9	2.5	90.5	63.7	27.4
Average	4.5	82.8	39.0	11.8
Standard deviation	2.4	9.7	26.9	17.8

In the mine, the sinter feed typically leaves the sieving process with a moisture content of 12% and it is transported on a conveyor belt to the storage yard, where it is deposited on piles that may reach 20 m in height (Figure 8.34) to be exposed to drying for 2 to 3 days. The ore water content may cause the instability of the piles in the storage yard. The ore transportation by Vale's railway allows some drainage of the water from the ore pores through drainage outlets in the wagons. However, piped ore fines contaminate the railway ballast and the subgrade and therefore decrease the balast's life. At the port located in São Luis, MA, Brazil, the iron ore is stocked in the storage yards and its moisture content can increase because of the constant rains in northern Brazil. After shipping, the presence of free water complicates the removal of the bottom part of the iron ore from the ship cargo compartments (note the presence of significant free water can lead to dangerous liquefaction during the shipping of ores). This fact results in a high cost of transportation and unloading at the destination. Final moisture contents ranging from 10 to 12% imply the transport of a large volume of water with the iron ore, given 35 million tons per year of ore and water transported.

The use of geosynthetics to enhance the drainage of fluids from the iron ore (piles and wagons) produced by Carajás mine was investigated. Based on this study, a prototype drainage system was designed consisting of a nonwoven geotextile and a geonet installed on the side walls and bottom of the freight train wagons that transported the iron ore to the São Luis port. The drainage system conducts the water drained from the ore to a reservoir installed at the wagon bottom, and then the water collected is appropriately discarded at the port. Numerical analyses were performed to evaluate the efficacy of the geosynthetic drainage system at the base of ore piles and in the train wagons (Figure 8.35). For the wagon transport, the numerical analyses examined moisture movement and collection over a period of 12 hours, which was the approximate time for transporting iron ore from the Carajás mine (Pará state) to the Port of São Luis (Maranhão state). For the iron ore piles, a typical pile cross-section with a height of 20 m and a base width of 56 m was considered. The results showed that after 12 hours the geocomposite for drainage would be able to decrease the ore water content to 6% (Figure 8.35, Gardoni et al. 2010 and Moreira 2011), with favourable implications for shipping costs.

Figure 8.33 General view of Carajás mine.

Figure 8.34. View of ore piles showing the excess of moisture.

Additional studies were carried out in the laboratory using the Gradient Ratio test. Ferreira (2009) investigated the use of geosynthetics for the reduction of moisture content of sinter feed and pellet feed materials from Carajás mine. The objective was to assess the efficiency of drainage layers to be used at the base of the piles and in the train wagons that transported the ore departing from the mine, as mentioned above. Gradient ratio tests on unconfined and confined ore-geosynthetics (geotextiles and geocomposites for drainage) systems were carried out as part of the research programme. The same equipment used by Palmeira et al. (2010) was employed, with some adaptations to accommodate the geocomposites specimens at the base of the cell. Tests with the application of vacuum at the base of the system were also performed to assess the increase in drainage efficiency.

Table 8.5 presents the main properties of the ore materials tested, which consisted of a pellet feed (code PF) and a sinter feed (code SF). The pellet feed has a value of D_{85} (diameter for which 85% of the remaining particles are smaller than that value) of .095 mm, whereas the sinter feed has a D_{85} value of 1.70 mm, with dry density of each material equal to 22.6 kN/m^3 and 24.1 kN/m^3, respectively. The ore specimens in the GR tests were prepared with a relative density of 50%.

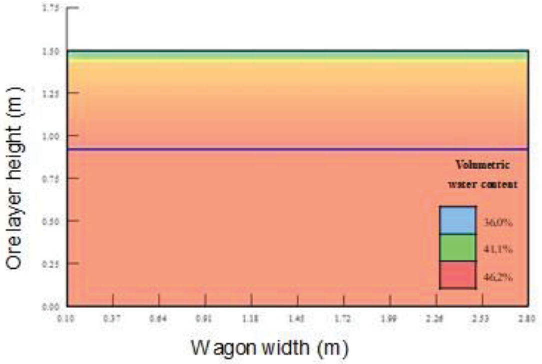

(a) Without geosynthetic drainage system in the wagon.

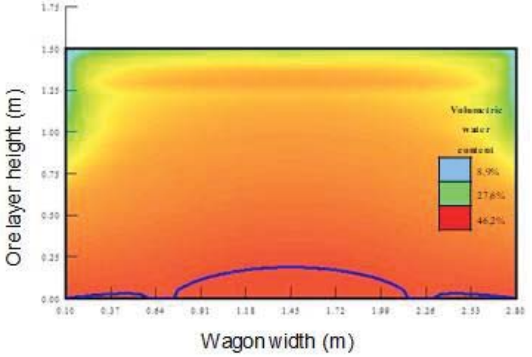

(b) With geosynthetic drainage system in the wagon.

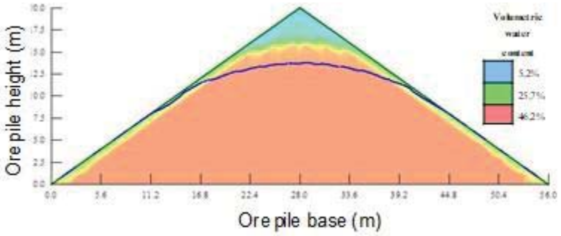

(c) Ore pile moisture content diagram without basal drainage.

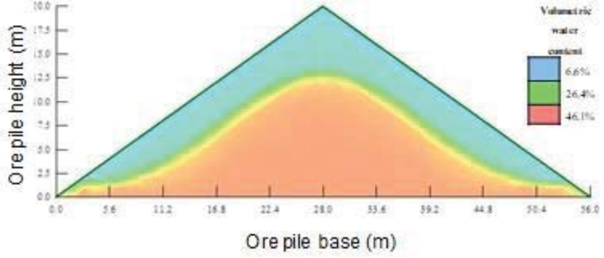

(d) Ore pile moisture content diagram with basal drainage.

Figure 8.35. Results of numerical analysis – Ore water content in the wagons and in piles (Moreira 2010).

The properties of the geosynthetics tested are listed in Table 8.6. Geosynthetics GT1 and GT2 are polyester nonwoven, needle-punched, geotextiles with masses per unit area of 400 g/m^2 and 600 g/m^2, and filtration opening sizes in the ranges 0.13-0.23 mm and 0.11-0.19 mm, respectively, according to the manufacturer's catalogues. Geosynthetics GC1 and GC2 are geocomposites for drainage consisting of a geomat between nonwoven, needle-punched, geotextile layers in the case of GC1 and of a geonet also between layers of nonwoven, needle-punched, geotextile in the case of GC2.

Table 8.5. Properties of the ore materials.

Property	PF	SF
D_{85} (mm)	0.095	1.70
D_{50} (mm)	0.048	0.18
D_{10} (mm)	0.0081	0.007
C_u	6.8	44.3
% finer than 0.074 mm	80	30
G (g/cm^3)	4.94	4.95
e_{max}	1.40	1.17
e_{min}	0.89	0.85
γ_d (kN/m^3)	22.6	24.1
k (m/s)	8.4 x 10^{-7}	3.0 x 10^{-5}

Notes: (1) PF = pellet feed, SF = sinter feed; (2) D_n – particle diameter for which *n*% of the remaining particles have smaller diameters, C_u = coefficient of uniformity, G = particle density, e_{max} = maximum void ratio, e_{min} = minimum void ratio, γ_d = dry unit weight, k = permeability coefficient.

Table 8.6. Properties of the geosynthetics tested.

Property	GT1	GT2	GC1	GC2
M_A (g/m^2)$^{(1)}$	400	600	950	900
t_G (mm)	1.6	2.2	7.8	11.7
k_n (m/s)	0.0035	0.0035	0.0011	0.003
ψ (s^{-1})	2.0	1.5	NA	3.0
θ (m^2/s)	NA$^{(2)}$	NA	0.4	NA
FOS (mm)	0.13-0.23	0.11-0.19	0.145	0.16
q (l/s/m)	NA	NA	NA	0.41

Notes: (1) M_A = mass per unit area, t_G = thickness, k_n = permeability coefficient normal to the plane (ASTM D4491), ψ = permittivity (ASTM 4491), θ = transmissivity (ASTM D 4716), FOS = Filtration Opening Size (AFNOR G 38017), q = discharge capacity (for a hydraulic gradient of 1 and under a vertical stress of 100 kPa); (2) NA = not available or not applicable.

Figure 8.36 shows results of gradient ratio tests on unconfined sinter feed-geosynthetic systems in terms of GR versus system hydraulic gradient (i_{system}). Very low GR values were obtained for the geotextiles tested. The value of GR was below 0.4 for GT1 during the entire duration of the test, whereas for GT2 GR values of approximately 0.5 were measured for i_{system} greater than 2. Significantly low values of GR were also observed for geocomposite GC1. These results indicate severe piping of fines from the ore through the geotextile filters. A different behaviour was observed for geocomposite GC2, for which large values of GR (between 2.5 and 3) were observed up to a i_{system} of 2 and values of GR close to 1 for greater gradients. This behaviour may be a consequence of an initial blinding mechanism of the geotextile filter of GC2 for lower values of i_{system}. With the increase of the hydraulic gradient, the fine particles accumulated on the geotextile filter must have been washed out through the geotextile, yielding to values of GR close to 1.

After a value of system hydraulic gradient of 4 was reached in unconfined GR tests with sinter feed, the vertical stress on the system was increased up to a value of 2000 kPa. The variation of GR with vertical stress in tests with sinter feed and an i_{system} equal to 4 is depicted in Figure 8.37. It can be noted that the values of GR remained quite constant for tests with GT1 and GC1, whereas it increased for GT2 and GC2. Despite the initial severe piping observed in some tests, the systems remained stable until the end of the tests. Large entrapped ore particles were also found in the voids of the geotextile filter at the end of the tests (Figure 8.38), consistent with what was also observed in geotextile samples exhumed from tailings dams, as reported by Gardoni and Palmeira (2002), Beirigo (2005) and Palmeira et al. (2005 and 2010).

The drainage capability of the draining geosynthetics for the reduction of ore moisture content was also investigated using the gradient ratio test. In these tests, the ore was placed in the testing cell and the system was subjected to water flow as in the GR tests under vertical stress of 2000 kPa. After the stabilization of the flow rate, the water flow was halted, and the system was allowed to drain through the base (with and without vacuum application).

The moisture content at different elevations of the specimen was measured after water stopped exiting the system. Despite the difference in scales, this test may be useful to evaluate the use of draining geosynthetics to reduce the moisture content of ore piles in the mining footprint. Tests without and with the application of vacuum at the drainage layer were carried out to investigate to what extent the application of vacuum would increase the dewatering efficiency. Under gravity conditions, the water flows towards the drainage layer until the capillary forces in the ore pores halts its movement. Thus, vacuum in the drainage layer should increase its dewatering action. Figures 8.39 and 8.40 show results of variation of ore moisture content along the ore specimen height in tests with geocomposites GC1 and GC2 and sinter feed, with and without the application of vacuum. Under gravity conditions only (no vacuum) the reduction in moisture content regarding its initial value under saturated conditions varied between 18% and 37% for the system with CG1 and between 21% and 45% for the system with GC2, depending on the elevation (Figures 8.39 and 8.40) considered. Greater reductions in moisture content along the specimen were caused by the vacuum and ranged from 53% to 67% for GC1 and 53% to 62% for GC2. If the moisture content reduction without vacuum is taken as the reference, the application of vacuum caused reductions between 44% and 48% in the test with GC1 and between 31% and 40% in the test with GC2. Despite the encouraging results, it is acknowledged that the application of vacuum to the drainage layer under field conditions may not be simple or economically feasible. The cost-effectiveness of such solution must be analysed on a case-by-case basis.

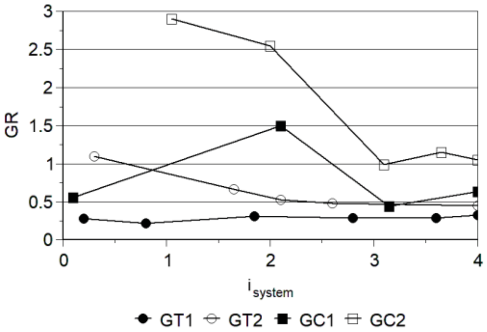

Figure 8.36. GR versus i_{system} in tests on unconfined sinter feed-geosynthetics systems.

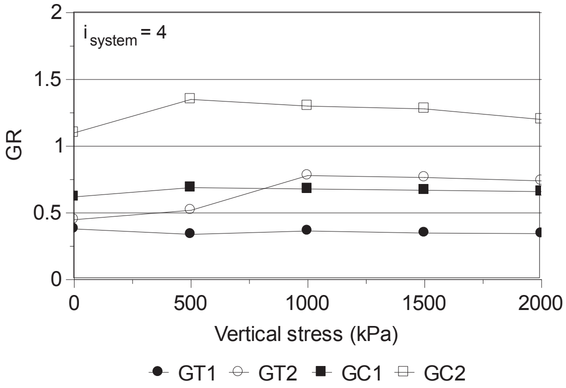

Figure 8.37. GR versus vertical stress for $i_{system} = 4$.

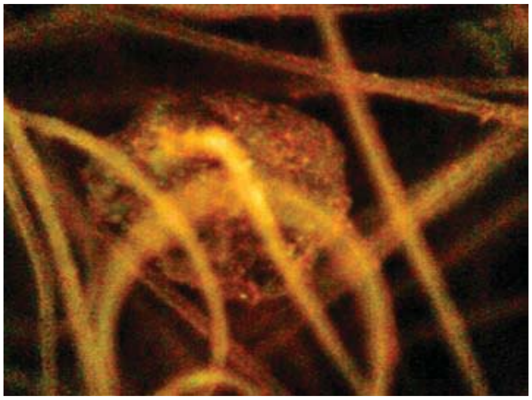

Figure 8.38. Large ore particle in the geotextile filter void – 600 X magnification (Ferreira 2009).

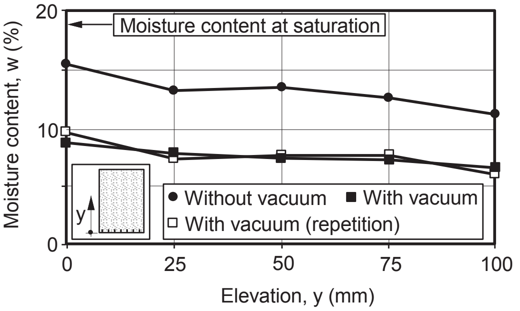

Figure 8.39. Moisture content profile – Geocomposite GC1/sínter feed.

Figure 8.41 shows the results of tests with vacuum on the system consisting of pellet feed and geotextile G1. Less efficiency can be noted in the case of the fine-grained pellet feed material. Nevertheless, if the moisture content at saturation is taken as a reference, the application of vacuum caused a reduction in moisture content between 22% and 33%, depending on the elevation considered. The lower efficiency in this case may be a consequence of the characteristics of the ore material tested and lower drainage capability of the geotextile in comparison to those of the geocomposites, particularly under a vertical stress of 2000 kPa.

8.17 *Performance of geotextile tubes (geotubes)*

Silva (2017) conducted a study to evaluate the use of woven geotextile tubes to dewater, confine and stack gold ore tailings. A stacked geotextile tube structure was built in the Fazenda Brasileiro tailings dam, Bahia, Brazil, owned by Yamana Gold mining company. Figure 8.42 shows a view of the tailings dam. The investigation started by submitting the gold ore tailings to geotechnical tests. The specific gravity of the tailings particle (G) obtained was equal to 2.85 and the particles size distribution showed that 75% of the tailings consisted of fine particles. The woven geotextile used had a tensile strength of 100 kN/m, mass per unit area of 554 g/m^2, and a thickness of 1.8 mm. Dewatering efficiency was evaluated by means of jar-tests, geotextile cone tests and geotextile dewatering tests (GDT). From the dewatering tests results, it was defined that the flocculant Magnafloc LT27 should be added to the tailings to avoid excessive losses of fine particles. Once the flocculant dosage was defined, the experimental geotextile tubes were assembled in the mining footprint (Figures 8.43 and 8.44).

The tests were conducted inside the mining area, on the top of a tailings pile since there were no scheduled works to take place in that area in the coming years. Thus, the geotextile tubes were installed and expected to be monitored for at least two years. The dimensions of the test area were 7 m x 9 m and a drainage layer was placed on a geomembrane liner installed at the base of the stack to collect the fluid during the dewatering process. The test setup was designed for a three-level structure, being 9 geotextile tubes units in the first level, 4 in the second level, and 1 in the third level of stacking. Every geotextile tube unit was 2.0 m wide, 6.0 m long and was designed to have a maximum height of 1.0 m during the filling process. Figure 8.43 and Figure 8.44 show the geotextile tube experimental setup (dimensions in meters).

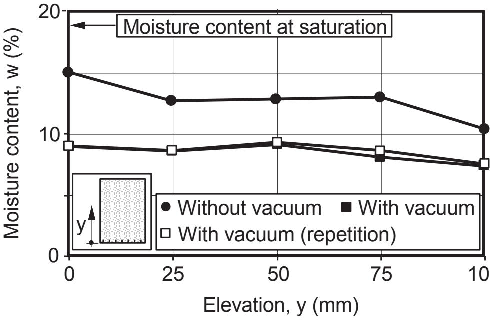

Figure 8.40. Moisture content profile – Geocomposite GC2/sinter feed.

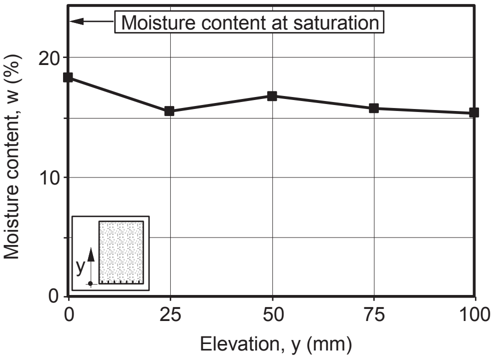

Figure 8.41 Moisture content profile – Geotextile G1/pellet feed.

The solids concentration of the tailings confined in the geotextile tubes was evaluated by taking samples close to the tube inlet port. After the last filling stage, samples were taken after 24h, 48h, 72h, 7 days, 21 days, and 28 days. Figure 8.45 shows the variation of solids concentration with time. The greatest increase in solids content occurred in the first 24 hours when the solids concentration increased from 53% to 75%. These values correspond to a water content reduction from 100% to 25% in a day. After the first 24 hours, the desiccation rate decreased and the increase in solids content was approximately 10% after 13 days. Each geotextile tube unit was able to dewater and confine an amount of 5.4 m^3 of tailings.

Figure 8.42. A view of Fazenda Brasileiro tailings dam (Moraes, 2020)

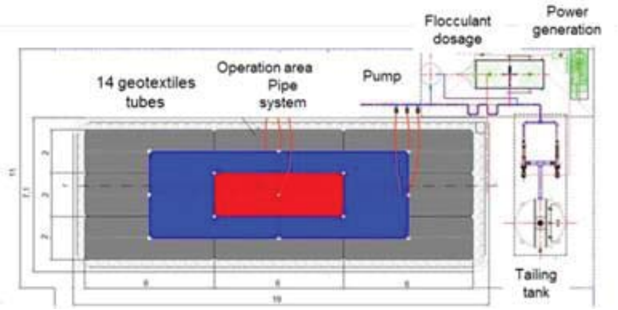

Figure 8.43. Geotextile tube experimental setup (Moraes et al. 2020).

Figure 8.44. Geotextile tubes stacking – Transversal direction

A numerical analysis of the geotextile tubes was carried out using the computer code Abaqus version 6.14. A parametric analysis was performed to verify the influence of the filling pressure and the woven geotextile's tensile stiffness, as well as which elements of the finite element program used would be most representative of the behaviour of the geotextile tube under field conditions. In addition, this analysis provided insights on how suitable the computer code is for such simulations. Predictions from analytical methods were also obtained. The analytical methods proposed by Plaut and Suherman (1998) and Guo (2014) were employed in the research, and the results were calculated using a numerical algorithm developed by Silva (2019). The results predicted by the analytical methods were consistent with the ones found in the literature, as well as with the results obtained in the field study. The numerical modelling was also able to represent the behaviour of the geotextile tube during its filling. Figure 8.46 shows some images of the field experiment and of the numerical modelling.

It was also found in the research that the correct choice of the finite element to be used in the numerical analysis is a determining factor for the simulation of the stress–strain behaviour of the geotextile tube. The filling pressure has a direct influence both on the shape of the tube cross section and on the stresses generated during the filling process. Despite the limitations of the analysis, the analytical method and the numerical modelling were able to represent the geotextile tube behaviour during filling.

After filling and stacking the geotextile tubes, the structure remained in the field for 24 months prior to the exhumation of samples to be examined in the laboratory test program (Moraes, 2020). Figure 8.47 shows the geotextile tubes after two years. Figure 8.48 presents the extraction of disturbed and undisturbed samples of consolidated tailings, as well as samples of the geotextile tube.

After 24 months of sludge consolidation inside the tubes, initially containing 50% solids, it was found that the apparent dry density was 1.8 t/m^3. This value corresponds to a final percentage of solids of 83%. According to Bittar (2017), the apparent dry density of tailings from gold ore in the field reaches values around 1.2 to 1.4 t/m^3. Therefore, the result obtained by the consolidation of fine tailings in geotextile tubes proved the exceptional efficiency of the process for disposal of fine mining tailings and its feasibility as safe mining structures.

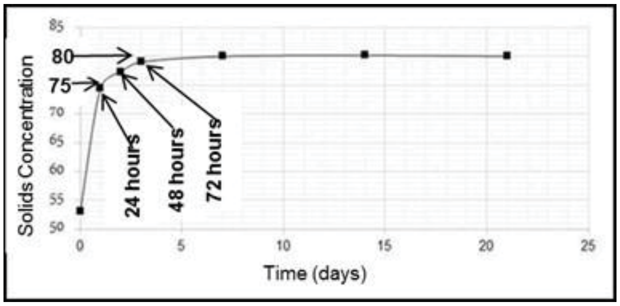

Figure 8.45. Tailings solids concentration versus time in the geotextile tubes (Silva, 2017).

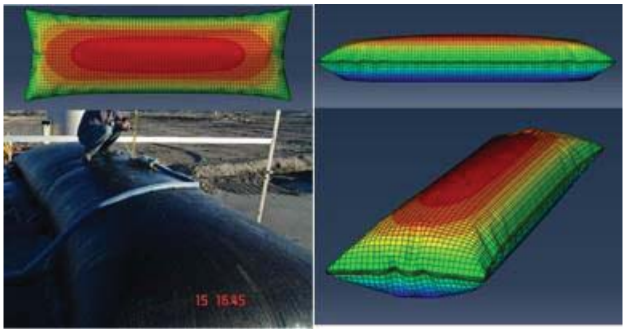

Figure 8.46. Images of the experiment in the field and of the numerical modelling.

Figure 8.47 Bird-eye view of the drained stacking of geotextile tubes that remained in the field for 24 months.

8.18 *Soil reinforcement in mining*

Soil reinforcement using geosynthetics has been employed in mining plants and infrastructures (roads and railways) associated with ore production and transportation. Figure 8.49 shows the use of geosynthetic reinforcement in a retaining structure. Becker (2006) investigated the behaviour of a 5 m high and 1700 m long geogrid reinforced wall to increase the height of an existing dyke constructed to contain bauxite residues at a mining plant owned by Alcoa Aluminum, in Poços de Caldas, MG, Brazil (Figure 8.50). The wall was constructed with a silty-clay soil and geogrids with tensile strengths of 35 and 55 kN/m and tensile stiffness values of 700 and 1100 kN/m. Instrumented sections showed that the structure behaved very well.

Fernandes et al. (2008) studied the use of mining residues as an alternative subballast material for the Victoria-Minas railway, which is subjected to intense traffic of freight trains transporting ore from mines owned by Vale Mining Company. Figure 8.51(a) shows a cross section of the instrumented experimental sections, which were subjected to the same traffic of trains as the railway. Figure 8.51(b) shows four instrumented sections, where section S1 is the reference section, constructed with the traditional subballast material. Sections S2 and S3 were constructed with the alternative subballast reinforced with geogrid at the base (section S2) and at the top (Section S3) of the layer. Section S6 was constructed with the alternative subballast material, but without reinforcement, for comparison purposes.

Figure 8.48. Extraction of samples from the geotextile tubes (Morais 20 20).

Figure 8.49. Geosynthetic reinforced wall for a crusher.

The alternative subballast material consisted of a mixture of 50% of a local soil (silty sand), 25% of mining residues (sandy silt) and 25% of the conventional subballast material. The alternative subballast was considerably finer (D_{85} = 0.9 mm, D_{50} = 0.076 mm, D_{10} = 0.0012 mm) than the conventional ballast (D_{85} = 23.0 mm, D_{50} = 5.1 mm, D_{10} = 0.008 mm).

The reinforcement used was a polyester geogrid, with 30 x 30 mm apertures, tensile strength of 65 kN/m, and tensile stiffness at 5% strain of 520 kN/m. Figure 8.51(c) shows one of the experimental sections during a Benkelman beam test. Figure 8.52 presents results of Benkelman beam tests from which it can be seen that the geogrid reinforced sections behaved in a similar way to the reference section, constructed with the conventional subballast material. As expected, the poorest performance was obtained in the section with the alternative subballast without reinforcement. The presence of the reinforcement layer also reduced the horizontal strains in the subballast (Figure 8.53). An additional benefit brought by the reinforcement was less breakage of the ballast grains, as shown in Figure 8.54. Thus, geosynthetic reinforcement may allow the use of an alternative and cheaper subballast material built with mining residues, providing a better and more environmentally friendly usage of mining residues.

8.19 *Current*

Geosynthetics are versatile and cost-effective materials that can serve many functions in a mine footprint. However, due to the characteristics of the mining activity, appropriate selection and specification of geosynthetic products is of utmost importance.

1.5 or 2 mm-thick LLDPE and HDPE have found extensive use in heap leach pads and more recently in tailings storage facilities. In both cases it is important to design to minimize holes/punctures in the geomembrane in the short-term. Geotextile protection layers may be needed in large heap leach pads to achieve that objective.

Geomembranes may also be used as “Raincoat” covers over heap leach pads in rainy regions to minimize dilution of leach solutions and reduce water treatment cost. In addition, raincoats may be used in dry regions to minimize evaporation and reduce the demand for water.

(a) General view of the bauxite residues reservoir.

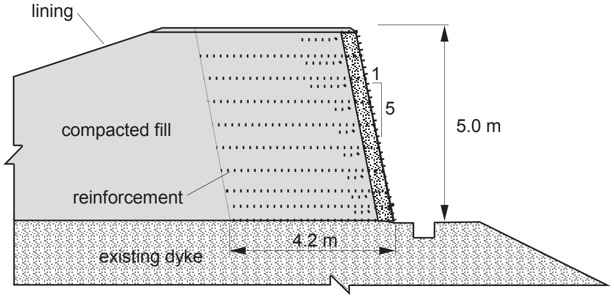

(b) Cross-section of the reinforced structure.

(c) Load test on one of the instrumented sections.

Figure 8.50. Geogrid reinforced wall to increase the storage capacity of a mining reservoir (Becker 2006).

Geotextile filters may be used in critical and severe conditions. Performance tests are required under conditions as close as possible to those expected in the field to assess their suitability for a given application. Comprehensive filter criteria (including retention, permeability, anti-clogging, and endurance/durability criteria) should be used, and due care exercised in geotextile filter installation.

A significant increase in the use of geotextile tubes to dewater mining tailings is foreseen in the coming years. Investigations on this type of geotextile application have shown that geotextile tubes can provide significant reductions in moisture content in addition to a safer accumulation of tailings in the mine footprint.

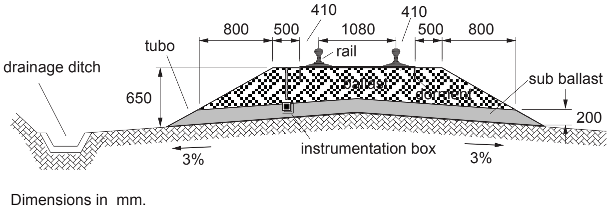

(a) Cross-section of the experimental sections.

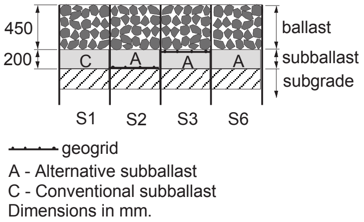

(b) Characteristics of the experimental sections.

(c) Benkelman beam tests in one of the sections.

Figure 8.51. Use of alternative subballast material from mining residues in a railway (Fernandes et al. 2008).

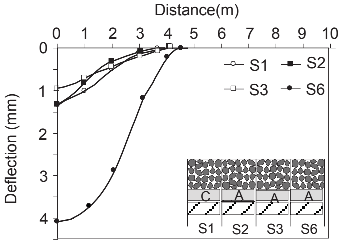

Figure 8.52. Results of Benkelman beam tests on the experimental sections (modified from Fernandes et al. 2008).

Geosynthetic reinforcement can improve the performance of soil structures such as walls and unpaved roads in the mining footprint, as well as infrastructures associated with the mining business. Geosynthetics can also be used as reinforcement in future tailings dams and for the increase of height and storage capacity of existing dams.

It has been common in Brazil to find thin geomembranes being used as barriers for waterproofing of contaminated tailings dams (gold, vanadium etc.). Thicknesses equal to or smaller than 1.5 mm for HDPE geomembranes and even less than 1.0 mm for PVC geomembranes have been found. These are very thin membranes, and such thicknesses are unacceptable in many countries. Therefore, there is an urgent need to improve the specification of the type and thickness of polymeric barriers in mining. Specific standards on the use of geosynthetics in mining activities should be developed.

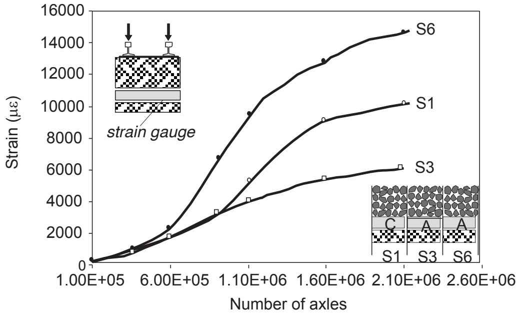

Figure 8.53. Horizontal strains in the subballast layer.

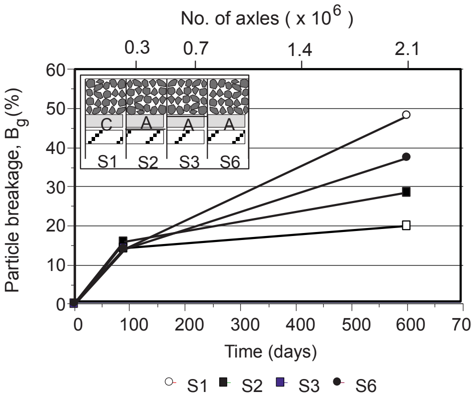

Figure 8.54. Breakage of ballast grains.

Some regions in Brazil are subjected to strong winds. To avoid air pollution by contaminated dust, mining companies have used nonwoven geotextiles as covers for high ore piles and fine tailings. However, this solution has not been efficient, since the nonwoven blanket is very light, it is commonly displaced or removed by the wind. Thus, new geosynthetic products and installation procedures should be investigated and developed for a better performance of geosynthetic covers for ore and tailings piles.

Regarding geosynthetic installation, qualified personnel and high-quality installation and construction control are required. The lack of knowledge on the properties and characteristics of different geosynthetic products may lead to problems such as those caused by the lack of subgrade preparation and high temperatures. GCLs and geomembranes on irregular surfaces and steep slopes must be protected from puncture using geocomposites, geotextiles, or other systems. In addition, a suitable criterion must be used to select suitable needle-punched GCLs for use on slopes greater than 3H:1V.

Mining activity is characterized by the existence of high loads and the presence of chemically and mechanically aggressive materials and liquids. In addition, the consequences of failures can be extremely serious in terms of loss of human life and environmental damage. In this context, researchers and the geosynthetics industry must continue to study and develop products capable of meeting the growing challenges imposed by mining activities and by increasingly restrictive environmental legislation.

PART B: REMEDIAL ENVIRONMENTAL GEOTECHNICS

9 VAPOUR BARRIERS FOR CONSTRUCTION OVER BROWNFIELD SITES

Brownfield sites are defined here as locations that had been deserted because of historical contamination prior to remediation. Despite remediation, many of these sites have persistent low levels of residual contamination. Re-development of these sites can allow substantial and beneficial use of these prime locations. Engineered polymeric vapour barriers are used in the construction of buildings over remediated contaminated sites (brownfield sites, landfills) to minimize moisture, radon, and volatile organic compound (VOC) migration into the building. Vapour barriers have a specified minimum thickness of 0.15 mm (NYSDOH 2006) although the US EPA recommends a higher 0.75 mm minimum thickness to minimize puncture risk (EPA 2008).

In many countries, there are limits on the maximum concentrations of residual contaminants in remediated sites. Benzene, toluene, ethylbenzene, and xylenes are often used as indicator chemicals because they are some of the most common and volatile. The National Institute for Occupational Safety and Health (NIOSH) recommended exposure limits (REL; e.g., in a building) are: benzene 3.2 mg/m^3; toluene 375 mg/m^3; ethylbenzene 435 mg/m^3; xylenes 435 mg/m^3 (CDC 2015a,b,c,d,e,f,). An effective barrier for VOC intrusion must prevent the peak indoor air quality of a building from exceeding the guidelines and minimize the intrusion.

The mechanisms of migration of VOCs into a building are advection and diffusion. Advection is driven by differential pressures between inside and out and will occur through holes in the vapour barrier or geomembrane. Diffusion is driven by a difference in concentration and will be governed by the diffusion, partitioning, and permeation coefficients of the particular VOC, and thickness and polymer used for the vapour barrier or geomembrane. Many researchers have examined VOC diffusion through polyethylene (PE) based materials (Aminabhavi and Naik 1998a,b,c, 1999a,b,c,d,e,f; Sangam and Rowe 2001, 2005; Edil 2003; Joo et al. 2004, 2005; McWatters and Rowe 2007, 2009, 2014, 2015; Park et al 2012; Touze-Foltz et al. 2013; Eun et al. 2014). Jones and Rowe (2016) examined the diffusion of BTEX for a range of common vapour barriers. McWatters and Rowe (2010, 2018) examined the diffusion of BTEX through a coextruded LLDPE/EVOH/LLDPE vapour barrier while DiBattista and Rowe (2020) examined PCE and TCE diffusion through a coextruded LLDPE/EVOH/LLDPE vapour barrier.

Under steady-state conditions for the mass flux, f, (the mass of contaminant per unit area per unit time) passing through the geomembrane or vapour barrier of thickness, H, is given by Fick's first law:

$$f = \Delta c \cdot P_g / H \tag{9.1}$$

where Δc is the difference in concentration between the two sides of the membrane and P_g is the permeation coefficient. The relative resistance of the different products to permeation by VOC's is expressed in terms of the permittivity ratio, P_g/H. For example, the permittivity of 11 different vapour barriers or geomembranes are expressed relative to the permittivity of a 1.5 mm thick HDPE geomembrane in Table 9.1.

The vapour barrier shown at the top of Table 9.1 allows a benzene flux 15-fold greater than through HDPE while the coextruded LLDPE/EVOH/LLDPE geomembrane would only allow 1/5 of the benzene that would permeate through HDPE. Thus, there is a 75-fold difference between the best and the worst diffusion barrier given in Table 9.1

Table 9.1 Permittivity $[P_g/H]$ of 11 commercially available vapour barriers/geomembranes relative to that of a 1.5 mm thick HDPE geomembrane

Benzene diffusion at 22°C Material	Thickness H (mm)	$[P_g/H]$ / $[P_g/H]_{HDPE}$
Perminator Vapour Barrier	0.37	15
Viper Vapour Barrier	0.28	14
Husky Yellow Guard Vapour Barrier	0.36	12
Stegowrap Vapour Barrier	0.35	9.3
PVC	1.02	8
XR5 8130 (coated polyester)	0.84	3.7
Petrogard VI (coated polyester)	0.81	3.6
LLDPE	0.79	2.9
CSPE (Hypalon)	1.14	2.2
LLDPE	1.5	1.5
HDPE	1.5	1
LLDPE/EVOH/LLDPE	0.53	0.2

Techniques are now readily available that allow the use of both the partitioning and diffusion coefficient in modelling the impact of a particular brownfield site (e.g., McWatters et al. 2019). A 1.5 mm thick HDPE/EVOH/HDPE has been effectively used in biopiles to remediate hydrocarbon contaminated soil which was then reused together with a LLDPE/EVOH/LLDPE vapour barrier and the McWatters et al. (2019) method of analysis to allow safe reuse of this remediated material below tightly sealed buildings constructed at Casey Station in Antarctica.

10 VERTICAL BARRIERS – CUT-OFF WALLS

10.1 *Cut-off wall construction*

Vertical barriers (cut-off walls) can be formed by many techniques including:

a) excavation under a self-hardening cement-bentonite slurry using a backhoe, clam-shell or cutter-miller to create a cement-bentonite cut-off wall (the choice is of excavation technology will be mainly dependent on the depth of the excavation and the materials to be excavated for example, a toe-in to rock can require use of a cutter miller).
b) as above with insertion of a geomembrane prior to the set of the cement-bentonite slurry.
c) excavation under a bentonite slurry followed by backfilling with a soil-bentonite mix to create a soil-bentonite cut-off wall.
d) excavation under a bentonite slurry followed by backfilling with a soil-cement-bentonite mix to create a soil-cement-bentonite cut-off wall.
e) trench cutting with a trench cutter/trench saw with simultaneous injection of a cement-bentonite slurry to produce an in-situ soil-cement-bentonite wall.
f) deep soil mixing using a vertically mounted mix head fitted with cutters rotated about horizontal axes with simultaneous injection of a cement-bentonite slurry to create a deep soil mixed (DSM) .
g) deep soil mixing using single or multiple augers rotated about vertical axe(s) with simultaneous injection of a cement-bentonite slurry. This approach is more often used for area treatment rather than wall formation.
h) jet grouting.
i) vertical barriers formed by concrete diaphragm walls or secant piles.
j) any of the above barrier systems coupled with treatment cells to produce funnel and gate systems.

These are all mature technologies. Cement-bentonite and soil-bentonite cut-off walls were widely used for containment of contamination in the last century but currently, they tend to be used for contaminated land management only when other remediation technologies do not allow destruction of the contaminants to regulatory acceptable levels, where the contaminants cannot be removed due to the presence of buildings, infrastructure, etc., or as an interim control measure. Containment may, in effect, create a landfill which requires long-term management and regulatory supervision.

Cut-off walls are currently, and have been for decades, very widely used for hydraulic structures, for example, on the major programme of post Hurricane Katrina upgrading of dams and levees in the USA.

The review presented below will focus processes (a) to (d) above though the discussion on cement-bentonite systems is relevant to all cut-offs using these materials. In the review key issues will be presented but in the interest of brevity, they will not be discussed in detail, rather readers are referred to significant references. For example, discussion, analysis and review of the application of vertical barriers for pollution containment is given in Dominijiani et al. (2021); Evans et al. (2021); Manassero (1994, 1997); Manassero et al. (1995, 1996, 2000); Manassero and Viola (1992). For an overview of cement-bentonite systems see Jefferis (2012) and for grouts and slurries more generally see Jefferis (2014).

10.2 *Early cut-off walls*

The concept of excavation under a bentonite slurry to form a continuous structural wall was advanced by Professor Christian Veder in 1938 (Xanthakos 1997) though the use of fluids to carry cut soil and support excavations for water and oil well drilling is much older.

The first field trials of a soil-bentonite slurry trench cut-off wall began in September 1945 under the supervision of Major General M.C. Tyler, United States Army (Retired) 'as the originator of the basic idea' (Kramer 1946). A cut-off 20 ft deep was formed to protect levees on the Mississippi river from erosion and sand boils.

Cement-bentonite walls formed by what is now known as the vibrated beam method were used for the construction of watertight banks on the Upper Danube and Moselle in the late 1950s (Maillard and Serota, 1963).

Ryan et al. (2022) gives a history of cut-off walls, mainly soil-bentonite and from a broadly US perspective. Jefferis (1997) gives a review of UK practice. Evans and Dawson (1999) consider the differences between US and UK practice.

There is a very substantial body of research on cut-off walls. For cement-bentonite walls, the work of Caron (for example, Caron 1973) provides some of the earliest comprehensive studies. The doctoral thesis of Guner (1978) on slurry mixing, the fluid properties, and the stress-strain behaviour blastfurnace slag-cement-bentonite slurries at different slag proportions by weight of total cementitious material is a seminal study (see also Jefferis 1981). Card (1981) provides data on the hydraulic conductivity of these systems (see also Jefferis 1997 but note §11 below regarding the continuing availability of ground granulated blastfurnace slag, ggbs). Other major works on cut-off walls include those by Evans, Fratalocchi and Manassero and their co-workers as cited in the references.

10.3 *Specifications for vertical barriers*

The first cut-off walls were principally for the control of seepage through and below hydraulic structures such as dams, dykes and levees and this continues to be a major application. For such barriers, a typical requirement was a hydraulic conductivity of $<1x10^{-8}$ m/s with a minimum specified wall thickness typically of 600 to 750 mm, though the actual thickness was often controlled by the width of the tool required for the trench excavation. The use of cut-off walls for contamination migration control ushered in tighter hydraulic conductivity specifications, typically requiring $<1\mathrm{x}10^{-9}$ m/s. Yet lower hydraulic conductivity requirements were regarded as unnecessary as below $1\mathrm{x}10^{-9}$ m/s diffusion could dominate and there might be little net benefit (Manassero and Shackelford 1994).

Hydraulic conductivities at and below $1\mathrm{x}10^{-9}$ m/s are now routine and the specification of $<1\mathrm{x}10^{-8}$ m/s for hydraulic structures can be reduced to $<1\mathrm{x}10^{-9}$ m/s. In principle, this should improve the durability of a cut-off, especially for cement-bentonite systems as permeating water (even of benign chemical content), over extended periods, can leach the cementitious phases, for example, removing calcium from the principal cementitious components, the calcium silicate hydrates.

Further information on specifications can be found in Jessberger et al. (1991); Schluchter et al. (1991, 1993); Millet et al. (1992); Jefferis et al. (1999).

10.4 *Hydraulic conductivity of cut-off wall materials*

As discussed above a typical specification requirement for a cut-off wall may be a hydraulic conductivity $<1\mathrm{x}10^{-9}$ m/s. This should be readily achievable with soil-bentonites and also for cement-bentonite materials at economic total cementitious contents provided the cementitious material has a high slag proportion. This hydraulic conductivity may not be achieved at 28 days but is usually achieved by 90 days. Fratalocchi et al. (1996), Fratalocchi and Pasqualini (2007) and Jefferis (2012) show that a plot of log hydraulic conductivity – log time gives a straight line until at least 1 year. This provides an excellent indicator of hydraulic conductivity development which is useful in the design phase of a cut-off to avoid long delays before test results are available, to avoid tests of long duration, to select the optimum mix formulation taking into account long term performance and to investigate hydraulic conductivity trends when undertaking groundwater compatibility testing. Jefferis (2012) finds that this log-log plot tends to very slightly over-predict hydraulic conductivity reduction with time (i.e., it gives very slightly low values).

Hydraulic conductivity reduction cannot continue without limit. It appears to be the result of both continuing hydration of the cementitious phases (Fratalocchi and Pasqualini 2007) and also reaction with species such as dissolved inorganic carbon (e.g., bicarbonate ion) if present in the permeating water or from air, if this is used to pressurise the water in a triaxial permeameter cell without an intermediate gas-proof membrane (carbon dioxide coming from the air).

In relation to the hydration of the cement phases, it should be recognized that clays are not stable in the high pH of cementitious systems and will react. Jefferis (2008) found that bentonite could not be identified by x-ray diffraction in samples of slag-cement-bentonite systems. Evans et al. (2020) provide a detailed analysis of the topic. As the bentonite reacts, it should be expected that modest increases in the bentonite content of a cement-bentonite mix will increase its strength. This sometimes comes as a surprise to those unfamiliar with the underlying reaction processes. It also should be noted that the bentonite particles may act as nucleation sites for the deposition of hydrates as the cement reacts with water. If the bentonite is not pre-hydrated or is poorly hydrated so that it is not well dispersed to colloidal dimensions the resulting mix will be of higher (poorer) hydraulic conductivity.

Tallard (1984a,b, 1992, 1995, 1997a,b, 1997a,b) developed a self-hardening slurry based on ggbs and attapulgite. This material (Trade name Impermix) can achieve hydraulic conductivities as low as 10^{-12} m/s. It is a fascinating material as attapulgite has a lath-like particle shape and not the plate-like structure of bentonite (which has, on occasion, been wrongly assumed to provide low hydraulic conductivity in slag-cement-bentonite mixes). The exceedingly low hydraulic conductivity of Impermix demonstrates that although the particle size of the reacting materials, at the time of reaction, can exert a strong influence, it is the pore-structure of the final product and not the mineral structure of the raw materials that dominates the hydraulic conductivity of the final product. It can be expected that the attapulgite reacts with and is removed from the mix just as bentonite is from slag-cement-bentonite mixes.

10.5 Strength and stiffness of the cut-off wall materials

There appear to be no generally established criteria for setting the required minimum or maximum strengths of a cut-off wall material (though there can be for specialized applications such as for cement-bentonite walls used as shear walls for downstream stability of hydraulic structures in the event of liquefaction).

Specifications can be more focused on ensuring that a coherent low hydraulic conductivity material is achieved than a requirement for a particular strength and as strength is traditionally used as an index to assess the quality of engineered materials, minimum unconfined compressive strengths are frequently required (e.g., 100 kPa at 28 days, Jefferis et al. 1999).

On occasion, it has been suggested that the stiffness of the cut-off material should match to that of the adjacent ground but this leads to problems in that (a) it is difficult to design cement-bentonite mixes to achieve particular stress-strain behaviour, and (b) the strength and stiffness of cement-bentonite mixes will increase with time. At what age are stiffnesses to be matched? A year might seem appropriate in terms of property development but can sign-off of the work be delayed so long and what if the match is not then achieved? Also, under what drainage conditions should stiffness be assessed?

10.6 *Strain at failure*

Some specifications, for example, those typically in the UK used to require the set material to have a hydraulic conductivity $<1\mathrm{x}10^{-9}$ m/s coupled with a strain at failure of greater than 5% under low or zero effective confining stress. However, low hydraulic conductivity requires either a high Portland cement content or a high slag proportion both of which lead to higher strength. Strain at failure under low confining stress to strength ratios tends to be low and indeed poorly predictable under all conditions. The 5% strain a failure criterion was debated in the consultations held when developing the UK National Specification for pollution migration control (Jefferis et al. 1999). After careful consideration, it was not included in the final version of the specification on the basis that a cement-bentonite material with such properties did not exist under undrained conditions and/or at low confining stress to strength ratios (and indeed it still does not exist) or if it did/does exist it cannot be reliably produced over the full extent of a major wall (Jefferis et al. 1999). From this time, for certainty of hydraulic conductivity for cement-bentonite systems, slag proportions of 70 to 80% of total cementitious material are regularly adopted (previously the slag proportion was lower to give some reduction in hydraulic conductivity without substantial increase in strength).

Evans et al. (2021) give detailed advice for soil-bentonite materials.

10.7 *Quality control / quality assurance vertical barriers*

For all vertical barrier systems quality assurance of raw materials is fundamental. This will require certificates from suppliers and, if appropriate, control tests on materials as they arrive on site.

Accurate batching of the solids into the fluids is also essential. For bentonite slurries, this is often done by checking density using the industry-popular mud balance. However, the mud balance has a resolution of only about 15 kg/m^3 (Jefferis and Lam 2018) which is insufficient as a bentonite slurry is likely to be batched at a bentonite concentration of perhaps 30 to 60 kg/m^3. If the bentonite concentration in a bentonite slurry is to be checked it should be by moisture content determination with allowance for the moisture in the bentonite powder as delivered which may be 10% or more. Poor bentonite hydration prior to Portland cement addition may result in excessive bleed of the fresh slurry and high k of the set material.

Similarly for cement-bentonite slurries, it is important that the total cementitious content is controlled preferably by moisture content determination.

If slag is being used it is essential that the individual masses of slag and cement are accurately batched as the slag/total cementitious ratio will have substantial impact on the properties of the final product. Note that addition of more than the design quantity of Portland cement will reduce the slag/cement ratio and so may impair the properties of the set material. Just as small additions of Portland cement to ‘accelerate hardening’ will fail – high slag mixes have greater strengths than low slag mixes at all times (see, for example, Guner 1978). These are messages that can be difficult to get accepted.

For soil-cement-bentonite mixes, the cement-bentonite mix must be batched as discussed above with soil batched to appropriate accuracy and considering its moisture content.

Quality control/assurance testing of the final mix for both cement-bentonite and soil-bentonite is usually by taking samples of the fluid/mix as delivered to the excavation and at various depths within it. Tests on-site will include tests for the fluid properties. Samples also will be taken for off-site laboratory testing. These should be stored in sealed tubes under appropriate temperature conditions and protected from shock, vibration etc. (taking particular care during transport of samples from site to the test laboratory). For fuller advice see the Notes for Guidance in Jefferis 1999.

10.7.1 *Soil-bentonite walls*

By way of example of the considerable level of testing necessary for quality control of wall construction, Ruffing and Evans (2022) suggest the following schedule of tests (Tables 10.1, 10.2 and 10.3) for soil-bentonite walls.

Filtrate loss testing and sand content are specified for fresh bentonite slurry but not for in-trench slurry. Filtrate loss testing of the in-trench slurry and sand content (fresh or in-trench) can be performed, but the results should not be compared to acceptance criteria (Ruffing et al. 2022) but rather, if measured, they should be collected for information and used as needed to influence decisions in the context of the other results.

The field testing for fines content is used to provide a preliminary indication of the anticipated hydraulic conductivity. If the fines content of the base soil used to prepare the backfill mixtures is below 15%, additional dry bentonite powder or native fines may need to be added to the SB mix depending upon the target hydraulic conductivity of the backfill. Pre-construction bench scale studies are used, along with the recognition of the differences between field and laboratory mixing, to assess the expected hydraulic conductivity for the site-specific base soils including their fines content.

The moisture content of the base soils does not significantly impact the final properties of the SB backfill. The base soils are prepared with bentonite-water slurry to meet the required slump. For base soils with low moisture content, more slurry may be necessary to achieve the desired slump and workability. For base soils with high moisture content, less slurry may be necessary to achieve the desired slump and workability. Since on most projects, the bentonite in the final SB backfill comes from the bentonite in the slurry, as the quantity of slurry added increases, the bentonite content of the mixture also increases. Generally, these minor adjustments have no measurable effect on the performance of the backfill. As always, the expected variability of the slurry addition rate should be assessed in the pre-construction bench scale study.

Table 10.1 Tests on fresh bentonite slurry and trench slurry at a frequency of 2 per shift

Subject	Standard	Type of Test	Target Value
Fresh Bentonite Slurry	API 13B-1	Viscosity	>36 s
		Filtrate Loss	<25
		Density	>1.02 g/cm^3
		pH	6 to 10
Trench Slurry		Viscosity	>36 s
		Density	>1.02 g/cm^3
		pH	6 to 10

Table 10.2 Commonly specified targets for soil-bentonite backfill at frequency of 2 per shift:

Subject	Standard	Type of Test	Target Value
SB Backfill	ASTM C-143	Slump	100 mm ± 25
	API 13B-1	Density	>1.6 g/cm^3
	ASTM D-1140	Fines Content	>15%

Table 10.3 Laboratory tests on soil-bentonite backfill at a frequency of 1 per shift

Subject	Standard	Type of Test	Target Value
SB Backfill	ASTM D-5084	Hydraulic conductivity	<1x10^{-9} m/s
	ASTM D-1140	Fines Content	>15%

The backfill is essentially 100% saturated and therefore the measured density of the backfill depends at least partially on how the material is packed into the mud balance used for density measurements. The placement of the SB includes enough effort to ensure there are no air bubbles.

Hydraulic conductivity testing is done on grab samples sent for off-site hydraulic conductivity testing. The grab samples are collected from the backfill, prior to placement into the trench. Hydraulic conductivity testing should be performed at a minimum frequency of 1 per shift, 1 sample per 30 linear metres along the wall, or 1 sample per 500 cubic metres of backfill placed, whichever results in the highest number of samples. An example QC table for offsite soil-bentonite backfill testing is shown below with common specified targets.

As discussed below, the hydraulic conductivity of soil-bentonite materials will be affected by the confining pressure used in triaxial tests.

10.7.2 *Cement-bentonite walls*

For cement-bentonite walls, test schedules similar to those shown in Tables 10.1 to 10.3 will be necessary with tests on both the bentonite slurry and the cement-bentonite slurry (additionally bleed tests will be required for the latter). Samples must be taken for laboratory testing of set properties (hydraulic conductivity, density, strength). Typical procedures and sampling regimes are set out in Jefferis et al. (1999).

Test regimes such as those set out above will be followed in many countries. For example, Fratalocchi (2022, pers. comm.) confirms that quality control of properties of cement-bentonite cut-off walls in Italy is by sampling from the trench though for major projects a test panel can be built where piezometric instruments can be installed whilst the slurry is still fluid for periodic hydraulic conductivity tests once the mix has sufficiently hardened.

Piezocone testing has been successfully applied (Manassero 1994) at least to check the order of magnitude of the hydraulic conductivity and the wall continuity (defect checking).

10.7.3 *Soil-cement-bentonite walls*

Although not regularly used for cement-bentonite or soil-bentonite walls, coring followed by in-situ hydraulic conductivity testing is regularly used for soil-cement-bentonite walls in the USA. For these tests, the wall is cored with core recovery for separate viewing and testing, if required. The borehole is then subjected to cleaning to remove smeared material from the walls, tele-viewer inspection and in-situ falling or rising head tests (though note there are concerns about the analysis of falling head tests conducted in the higher levels of a wall if above the adjacent groundwater level at the time of the test). Coring of the wall requires that the cut-off mix has achieved a sufficient strength and this can become an important consideration when specifying the strength of the material but see also the discussion on inducing cracks in the wall at §10.9.

10.7.4 *Test boxes*

On occasion, perhaps too rarely, the hydraulic conductivity of walls has been investigated by forming a box-out in the wall. For this, a parallel wall is created and connected to the main wall by closing sections perpendicular to the main wall. A 'box' was created during the first application of the TRD trench cutter for soil-mix cut-off wall construction (Gularte et al. 2007). In a much earlier test on a cement-bentonite barrier in the UK in the 1980s, a 2 x 10 m box was created. A well was sunk in the centre and fitted with a submersible pump. After the initial drawdown of water in the well, the flow ceased. The soil was relatively coarse and it was suggested that the slurry in the surrounding trenches had penetrated into the soil in the box and effectively grouted it up. A second, a 6 x 6 m box, was formed but again there was effectively zero flow. A hole was then excavated at the centre of the box and used as a well. The wall was demonstrated to have a hydraulic conductivity of the order of 10^{-9} m/s. Key lessons from these test are that the box needs to be of appropriate dimensions and pumping continued for sufficient time to achieve steady state so that water movement in the unsaturated soil above the pumped level has stabilized. Hydraulic conductivity may be more readily assessed by monitoring the water levels in the box and in the surrounding ground whilst the box is subject to continuous water inflow at an appropriately low rate. The test duration necessary to prove a hydraulic conductivity of 10^{-9} m/s. is to be likely of the order of months. A further complication is that the groundwater regimes on either side of the cut-off wall (and hence the box) may be distinct.

10.7.5 *Depth of a cut-off wall*

The depth termination criterion for a cut-off wall will be specified by the designer but achievement of the required depth must be confirmed in the field throughout the works. This requires continuous and preferably independent observation and confirmatory measurements, for example, with a weighted tape at defined intervals along the wall. This will be particularly important if the depth criterion is a specified penetration into an aquiclude layer rather than an overall depth – there can be local deep pockets of high hydraulic conductivity soils. On site checking of depth is fundamental to the formation of effective cut-off walls (as is confirmation that the design overlap is achieved for walls formed in panels). As for liners you get what you inspect, not what you expect.

10.8 *Durability of cut-off walls*

Durability of cut-off walls has been a concern from their first use (see for example, Caron 1972). However, they are very few, if any, reports of failure in service. Indeed, it would be useful and instructive to have documentation on any in-service failures.

As a general principle, it should be noted that very long-term leaching by water can be expected to lead to a change in the properties of cement-bentonite slurries, typically a reduction in hydraulic conductivity but accompanied by a reduction in strength and if subject to confining stress, a reduction in overall volume (Jefferis 2012). For his tests, Jefferis used samples of higher than usual hydraulic conductivity to be able to achieve substantial volumes of water permeated – over 300 times the volume of the sample (consideration of pore volumes, though often used, is not appropriate when considering leaching and/or reaction processes). It should be noted that the hydraulic conductivity tests took several years. Had a material been used with a hydraulic conductivity typical of current cut-off walls the tests would have required many decades.

For contaminated land, there is considerable potential for interactions between the contained chemicals and any barrier material. Much research has been done on the effects of chemicals on cut-off materials. Fratalocchi and her co-workers have carried out detailed investigations of the effects of aggressive chemicals on cement-bentonite materials (Fratalocchi et al. 2005, 2006, 2013, 2016, 2021; Fratalocchi and Pasqualini 2007; Brianzoni et al. 2013). Jefferis (1996, 2001) found that hydraulic conductivity is a dynamic property of cement-bentonite materials (the cement-bentonite material can react with chemicals in an earlier permeant so as to change its hydraulic conductivity to later permeants). Tedd et al. (1997) and Joshi et al. (2010) report investigations on two trial containments installed through chemically aggressive gas works waste. One had a slag-cement-bentonite cut-off and the other had the same cut-off material plus and HDPE membrane. The containment with an HDPE membrane performed significantly better over time in this very aggressive, sulfate-rich ground.

The inclusion of a substantial proportion of pulverized fuel ash (pfa) in cement-bentonite mixes can improve their resistance to acid and sulfate (Jefferis and Fernandez 2000). However, it should not be assumed that the use of high proportion of blastfurnace slag will improve sulfate resistance as it does in concrete (Card, 1981).

For soil-bentonite cut-offs, see, for example, Ruffing et al. 2018.

Jefferis (1992, 2003, 2008 and 2012) demonstrated that understanding the effects of contaminants moving through cut-off materials require consideration of reaction fronts which can be addressed via retardation factors which are necessarily concentration dependent (the concentration of each of the reactive species in the contaminant and their interactions),

Cut-off walls may provide not only a hydraulic barrier but also retard contaminants migration through the wall (Evans et al. 1997 is perhaps the first paper on this for soil-bentonite walls).

For research on migration parameters for different contaminant species through cement-bentonite materials, see for example, Fratalocchi et al. (2005, 2006, 2013, 2016 and 2021).

10.9 *Volume change of cement-bentonite materials*

As discussed in Jefferis (2012) and Evans and Jefferis (2014) post-cement-bentonite materials can undergo shrinkage post-placement in the trench as a result of bleed and filtration from the fluid material and for the setting and set material, cooling from in trench temperature to that of the adjacent ground, continued hydration of the cementitious material and drying for material above the adjacent groundwater level.

Shrinkage is unlikely to be of any significance for walls constructed in panels and not exposed to significant drying (slight movements, which can self-heal, may be accommodated at the regular inter-panel joints) However, for soil-cement bentonite walls constructed in long reaches coring the wall for in-situ hydraulic conductivity testing has led to the initiation of cracks across the wall – it could be confirmed that these cracks were not present prior to the coring as the recovered cores were not themselves cracked, Evans and Jefferis (2014).

10.10 *Repair of vertical barriers*

Whilst durability of any structure will be a concern, a useful aspect of vertical barriers is that they are repairable provided that the surface trace of the barrier remains available – though as for all barrier systems in-service, identifying zones of leakage is the greater challenge. In practice reports of failure of slurry trench cut-offs for hydraulic structures in service if they exist are extremely rare.

Conversely, vertical barriers formed by the slurry trench technique are regularly used for the installation, repair or deepening of low permeability cores in dams, levees and hydraulic structures generally. Little (1975) gives examples of slurry trenches backfilled with plastic concrete for repairs to the cores of four embankment dams. Currently, cut-off walls are being used for the upgrading of dams and levees in the USA.

10.11 *Composite vertical barriers*

Just as for liners, composite vertical barriers have been developed. Jefferis and Fernandez (2000) discuss the inclusion of an HDPE geomembrane in a cement-bentonite wall to contain acid sulfate waters. The HDPE panels were joined together with hydrophilic rubber seals in the joints (it was confirmed, by on-site testing, that these swelled in the strongly alkaline environment of the cement-bentonite slurry). The acid sulphate soils were underlain by uncontaminated low hydraulic conductivity clay. A key cost issue was the depth of toe-in of the membrane into this clay. A penetration of 1.5 m was adopted and this was confirmed as necessary by advection diffusion, reaction modelling with data from laboratory tests extending over many months whilst cut-off construction itself was underway.

Barr et al. (2015) give an example of the application of a composite vertical barrier for embankment dams and Zhan (see §10.16) an example of a composite wall in China employing a GCL as the membrane.

10.12 *Research on cut-off walls relating to their use in China*

Cut-off walls for contamination containment are currently much used in China. Professor Zhan from Zhejiang University and his colleague have provided the following overview of the situation in China.

Cut-off walls are commonly constructed for containment of contaminated sites. Typically, a trench, filled with slurry to maintain the trench stability, is excavated in the ground, and then backfill is placed into the trench displacing the slurry to form a cut-off wall. The hydraulic conductivity of the backfill is required to be low, typically less than 1×10^{-9} m/s below this diffusion may become significant in contaminant transport mechanism. Many laboratory tests have been performed to measure the hydraulic conductivity of soil-bentonite (SB) backfills (Evans 1994; Yeo et al. 2005) and for cement-bentonite (CB) (Jefferis 2003, 2008 and 2012; Opdyke and Evans 2005; Joshi et al. 2010) and to study the factors influencing the hydraulic conductivity.

The recent advances in the research and practice of cut-off walls include stability analyses for slurry trenches in layered soils, determination of stresses in soil-bentonite walls and backfill consolidation, breakthrough time-based design of cut-off walls and the use of composite cut-off walls with an HDPE geomembrane or a geosynthetic clay liner (GCL). A brief review of the above advances follows below.

10.13 Stability analysis of slurry trenches in layered soils

The stability of a slurry trench during excavation and prior to backfilling is a major concern with the slurry providing a lateral supporting force to the trench walls. In practice, variably distributed surcharges from landfill berms, adjacent solid waste, excavation machines and nearby buildings may induce large deformation in the surrounding soils and even trench collapses during excavation (and of course the converse, if an SB wall is constructed too close to a structure, consolidation of the trench backfill over time may cause damage to the structure). Several cases of collapse were observed for the trenches excavated in soft clay in coastal areas of China. Commonly force equilibrium methods considering a two-dimensional wedge with an assumed planar failure surface under plane strain conditions are used to analyse trench stability. While soil stratification is often observed in natural environments due to geological sedimentation and weathering, stability analysis of slurry trenches considering such stratification has not been widely reported. A horizontal slice method (Li et al. 2013) and a Rankine Theory-based approach (Li et al. 2018) for stability analysis of slurry trenches with stratification has been developed.

10.14 Stress in soil-bentonite walls and backfill consolidation

The in-situ stress state of soil-bentonite backfills has a considerable effect on the hydraulic barrier performance of cut-off walls. The effective stress state in these walls is much lower than that predicted by a geostatic approach as first demonstrated by Evans et al. (1985) and further investigated in the field and by back-analysis (Evans et al. 2021). If the confining stress used in the laboratory tests is based on the vertical geostatic stress distribution the hydraulic conductivity of soil-bentonite backfill may be significantly underestimated, leading to a non-conservative design (Filz et al. 2003).

A model considering both the arching mechanism (Evans et al. 1995) and lateral squeezing effect (Filz 1996, Filz et al. 2004) was proposed by Li et al. (2015) to predict the steady-state effective stresses in the backfill of soil-bentonite slurry trench cut-off walls. The arching effect is considered via force equilibrium, and the lateral squeezing effect of inward displacement of the trench sidewalls is considered by assuming the cut-off wall is surrounded by soil which is represented by a Winkler idealization, as shown in Figure 10.1 This model successfully simulated the stress distribution in a soil-bentonite cut-off wall at Mayfield, New South Wales, Australia, offering a significant improvement in the prediction of stress in walls. Another model considering the interaction between backfill and surrounding soil by assuming a sliding wedge under limit equilibrium conditions based on Coulomb's theory was proposed by Ke et al. (2018).

After placement in a trench, the soil-bentonite backfill consolidates under the vertical load from the weight of the backfill above and the horizontal force from adjacent soils. Full-scale tests have been performed in the past 5 years to monitor the changes of earth pressures and pore water pressures in backfills with time to understand consolidation behaviour of soil-bentonite cut-off walls (Evans et al. 2017; Barlow et al. 2018; Tong et al. 2020). The wall constructed at Bucknell University was about 194 m long, 0.9 m wide and had an average depth of 7 m, while two walls constructed by Zhejiang University, were both 0.6 m wide, 15 m long, 10 m deep (W1) and 10 m long, 6 m deep (W2). The earth pressures, pore water pressures in the wall and the lateral deformations of adjacent soils have been monitored. The monitoring data show that the effective stress states of the backfills were nearly isotropic and low (<20 kPa) and that the primary consolidation required 3~8 months. The Zhejiang University test also revealed that the interfacial friction on the trench sidewall played an important role in reducing the total stress and causing a translational soil movement (Tong et al. 2020).

10.15 *Breakthrough time-based design of cut-off walls*

In the design of a cut-off wall, the time for the contaminant to break through the wall should be not less than the designed service life. Transient contaminant transport through slurry walls is typically regarded as a one-dimensional advective-dispersive process. The analytical solutions available to calculate the contaminant transport in cut-off walls contain non-elementary functions or require the solution of Eigen equations. The evaluation of these analytical solutions is nontrivial and generally requires the use of a computer. Accordingly, the wall thickness corresponding to a designed service life has to be searched in a trial-and-error manner. This often leads to the determination of the wall thickness by practical experience and practicality of construction instead of contaminant transport analysis. A simplified method for determining the wall thickness of slurry walls is proposed by Chen et al. (2018) via an assumption of decoupled advection-dispersion in the analysis of contaminant migration (Figure 10.2). If the wall thickness is given, the breakthrough time of the cut-off wall can be estimated by this method. The relative error for column Peclet numbers P_L over the range 0.01 to 1000 is not greater than 4% when the breakthrough criterion of c^*/c_0 is less than 0.1. This covers common practical situations for cut-off wall design.

When diffusion is dominant in contaminant transport through a cut-off wall, the breakthrough time is significantly extended by increasing the retardation factor of the backfill materials. Wang et al. (2016) found that the loess amendment of an SB backfill increased its adsorption capacity with respect to heavy metals. The Pb(II) adsorption capacity for the SB backfill containing 20% loess by mass was found to be 2 times greater than that of the unamended SB backfill. With this finding, the breakthrough time for Pb(II) through the loess amended SB wall was evaluated to be about twice that for the unamended SB wall when the hydraulic gradient was less than 3. The retardation effect of the loess amendment was verified by a centrifuge modelling test performed in Zhejiang University. The centrifuge modelling test demonstrated that the Pb(II) transport distance in loess amended SB wall corresponding to a duration of 50 years in the prototype was 44.3% shorter than that in the unamended SB wall (Zhan et al. 2020). The research finding shone a light on the use of loess which is widely deposited across the world as an adsorptive amendment in the barrier materials for the containment of heavy metal contaminated sites.

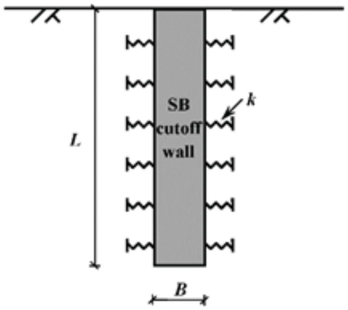

Figure 10.1. Schematic of the model to estimate the stresses in soil-bentonite cut-off walls (not to scale) (Modified from Li et al. 2015).

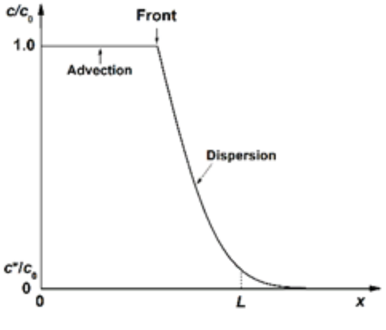

Figure 10.2 Configuration of contaminant concentration profile in slurry wall at breakthrough time for the proposed method (Modified from Chen et al. 2018)

10.16 *Applications of cut-off walls in China*

For the control of subsurface contamination, containment by cut-off walls is almost the first choice in China due to its low cost. They can prevent further spread of contamination and provide time for remediation processes. Cut-off walls are sometimes used as a long-term solution for contaminated lands with careful design and high-quality construction in China. Currently, the plastic concrete cut-off wall is the most popular wall type as much practical experience is available from hydraulic engineering. Soil-bentonite cut-off walls (using sodium activated Ca-bentonite) are becoming accepted by more and more designers due to their cost-effective features. Cement-bentonite (CB) cut-off walls are rarely used as the backfill has relatively high hydraulic conductivity unless high cement contents are used (or at least 65% of the total cementitious material is ground granulated blastfurnace slag, Card 1981; Jefferis 1997. The use of slag is now standard practice for CB walls in many parts of the world but it is not economically available at all locations). Furthermore, the experience with backfill composition, especially with respect to additives, is relatively slight in China.

Some technical guidelines for cut-off walls are now available in China and are being improved by the increasing number of practical applications.

Composite cut-off walls consisting of an HDPE geomembrane have been applied to about 20 containment and remediation projects of polluted sites in the past 10 years in China. Both the steel frame method and the mechanical roller method are used to install the geomembrane in the slurry supported trench. The maximum geomembrane insertion depth to date, 40 m was reached on a site in Changsha city (Figure 10.3).

Figure 10.3 HDPE GM cut-off wall (40-m depth) in Changsha, China.

Installation of a GCL in a slurry trench was first implemented in China in 2017 in Tianjing (Figure 10.4). The maximum depth of installation reached 15 m. An overlap of 50 cm was made at the joint of the adjacent GCL panels. After the GCL was installed, the trench was backfilled with cement-bentonite materials. The GCL/CB cut-off wall was designed to contain a simple dump of municipal solid wastes. The potential for leakage at the GCL panel joints and its countermeasures are under investigation in the laboratory of Zhejiang University (readers may be interested to note that the overlap approach was adopted for the first ever composite geomembrane cut-off wall in the late 1970s. This employed an HDPE geomembrane in conjunction with an attapulgite-cement-Dead Sea Water self-hardening slurry, Brice and Woodward 1984).

Figure 10.4 GCL/CB cut-off wall implemented in China.

11 RECYCLED MATERIALS

The construction industry is a major mover and user of materials and so offers very many opportunities for energy use reduction and for the re-use of materials especially as it generates so much potentially re-usable material. Indeed, today there is almost an implied duty on all involved in the construction matrix to achieve minimum materials and energy use – trajectory net zero carbon and to maximise the re-use, re-purposing and recycling of materials. In this respect one may note that many of the key decisions with regard to the re-use of materials are made at high level – the project scoping stages of works. There is a real need for advice at the muddy-boots level for the engineers and other on-site operatives.

In the coming years, we can expect major changes in the materials we use. Some will cease to be available or be the subject of major price rises due to limited production and/or demand from new users. Thus, for example, we can expect pulverised fuel ash (pfa) derived from coal burning to cease to be available although if existing ash dumps can be mined to produce useful material availability may continue for some years.

Ground granulated blastfurnace slag (ggbs) has been used for very many years as a replacement for Portland cement in concrete. For example, in the UK sulphate resisting Portland type cement is scarcely available as ggbs-Portland cement blends at appropriately high ggbs levels can provide resistance to sulphate attack. Ggbs is a by-product of the reduction of iron ore to iron in a blast furnace. However, the iron and steel industry can be expected to move away from the use of carbon as the reducing agent (in the process the carbon is oxidised to carbon dioxide). Thus, ggbs may well be phased out (Tallard 2021, pers. comm.).

Currently ggbs is rated as having a lower carbon footprint than Portland cement as its carbon burden is shared with the primary product of the blastfurnace, iron. Ggbs is a major constituent of some low carbon cements – a growing market competing for ggbs supplies.

Slag-cement-bentonite cut-off walls mixes may contain perhaps 65 to 80% slag (by weight of total cementitious components). A phasing out of slag or major price rises due to competition for limited/dwindling supplies will require new cut-off wall mix formulations or, more radically, re-thinking how to create low hydraulic conductivity vertical barriers in the ground.

The extensive geoenvironmental literature on recycling materials is often focused on the sustainability benefits and on research to demonstrate that environmental impacts such as heavy metal concentrations in aqueous leachates are acceptable. In contrast, much less has been published about the long-term behaviour of recycled and secondary materials. Are they chemically and mechanically stable? Do they have the potential for shrinkage, expansion or to damage structures formed from them or built upon them? Will they emit toxic, explosive or asphyxiant gases? Are the vendors able to provide guarantees regarding suitability for engineering use or will they choose to limit their liability to the value of the materials supplied? Who will bear the risks relating to possible in-service failure? The owner may specify recycled materials and secondary but expect the engineer to bear the risks and the financial consequences of failure.

Furthermore, the environmental significance of more mundane chemical parameters such as pH tends to receive insufficient attention and there is too often inadequate precautionary advice.

Jefferis (2019) explored some problems that could flow from the use of recycled crushed concrete with the aim of providing a baseline from which to explore some of the problems that can arise from the re-use of construction materials more generally. The paper focused on the pH of waters which have been in contact with crushed concrete and more briefly on sulfate attack on crushed concrete.

pH is important as regulatory authorities may place limits on the pH of water discharged from a site. A typical range of permissible pHs being 6 to 9. It may be noted with regard to the lower limit that water in equilibrium with atmospheric carbon dioxide will have a pH of about 5.6 without any contribution from sulphur and nitrogen oxides that can be significant in areas affected by industrialization. For the higher pH limit, the sodium and potassium oxides and free lime in crushed concrete can result in it having a pH at or over 12.6. Even if/when these species have been leached the pH of leachate in equilibrium with crushed concrete will be over 9 as a result of dissolution calcium hydroxide from the calcium silicate hydrates which make the principal contribution to the structural strength of concrete. Whilst the pH of leachate from crushed concrete can be expected to reduce as leaching progresses it is likely to remain >9 and thus above typical regulatory limits for very substantial times.

If the crushed concrete is used as a structural fill it is important to recognize that the rate of attack by any aggressive chemicals including leaching by water will be much higher than for intact structural concrete because of its much higher surface area to volume ratio and because it will have sustained some internal cracking in the crushing process. It is also unlikely that any information will be available on the original mix design including its water/cement ratio – indeed much crushed concrete will have been derived from crushing concretes with a variety of mix designs. For all these reasons guidance on the effects of chemicals on structural concrete (for example, sulphates) should not be assumed to apply to crushed concrete.

11.1 *Some other risks associated with recycled materials*

Risks from other materials offered for re-use in construction include not only high pH leachates but also deleterious expansion and emission of gases. These materials include secondary materials, such as: steel slag, old blast furnace slag and incinerator bottom ash aggregate (IBAA) derived from the incineration of municipal solid waste. Problems associated with the ferrous slags are discussed in BRE IP/05 (Dunster et al. 2005).

Calcium containing leachates from crushed concrete will precipitate calcium carbonate on contact with air or with waters containing inorganic carbon species. There is therefore a risk of blockage of drainage systems etc.

As crushed concrete will come from the demolition of buildings and other structures, there is a risk that it may contain unwanted and potentially undesirable materials, such as asbestos from asbestos insulation, asbestos cement sheeting and pipes. Asbestos fibres may be released by the crushing processes. The potential for harmful materials should be included in risk assessments for all recycled materials; risks must be identified and appropriately managed to protect all those involved from the production process, through storage, transport, re-use, future demolition and re-re-use and all associated laboratory testing.

11.2 *Residues from incineration of municipal solid waste*

Incineration can be used to reduce the mass and volume of municipal solid waste (MSW) and to recover energy. Crudely perhaps two thirds of the mass of the waste will become stack gases. The remaining one third will be mainly incinerator bottom ash (IBA) though there will be a modest amount of flue dust which may have to go to hazardous waste landfill. It will be desirable to re-use the incinerator bottom ash. After suitable and sufficient processing the ash may be used as incinerator bottom ash aggregate (IBAA). The composition of this ash will depend on the composition of the MSW and can be expected to vary across and between countries and indeed to change over time.

Expansive reactions can occur in IBAA, notably reaction of metallic aluminium in the IBAA with water in the alkaline environment of the ash, and then further reactions of the aluminium reaction products (Eden 2017). Ideally, metals such as iron and aluminium should be removed from the MSW prior to incineration. However, they may remain. If an alkali such as sodium hydroxide or sodium carbonate is added to a sample of an aluminium containing IBA then some fizzing and hydrogen release can be expected. As many ashes are alkaline there can be some production of hydrogen without alkali addition. There have been claims/litigations in respect of hydrogen release.

12 WASTE MINIMISATION

As is set out in this paper it is clear that there is a great deal of current research on landfill engineering and in particular landfill lining systems. However, looking to the future we must work towards minimising landfills and seek every opportunity to maintain materials within the cycle of utility. Waste minimisation is now a well-established concept through considerable opportunities remain in respect of its actual implementation in construction and more generally in society.

We should also expect landfill mining technology to advance, returning the landfilled (stored) materials to the cycle of utility and the land ideally to multifunctional use. Currently, landfill mining tends to be driven by land value. Thus, landfill mining is is limited to landfills in areas where there are currently significant opportunities for development and particularly hard developments such as residential units.

Landfill mining will generate significant amounts of material for re-use, including metals, building rubble, crushed concrete etc. which will need to be re-purposed. There also may be incinerator bottom ash and flue dust from the incineration of the mixed organic debris for energy recovery. These materials and other recycled and secondary materials will be offered and indeed perhaps imposed on the geotechnical community. They may come with acceptable environmental credentials (leach rates etc.) but with minimal information on their in-service geotechnical behaviour. For example, are they mechanical stable? Will they swell, shrink etc. in the medium and long-term? Similar problems may arise from their use as have become apparent with crushed concrete and incinerator bottom ash aggregate as discussed above. The potential for such problems should act as a caution to those who choose or are required by specifications to use them. It is hoped it will also stimulate the geoenvironmental community to undertake research and performance assessments. It is trite to say that long-term testing takes a long time. It should be put in train now.

12.1 *Mixing of materials*

The fundamental aim of re-using materials is to keep them in the cycle of utility. The first uses or re-uses should not compromise future re-uses. Use and re-use of construction materials therefore should be undertaken recognising that within a generation or two a structure may be demolished and that, at that time, its materials must be fit for return to the cycle of utility.

A use or re-use that ultimately dooms a material to landfill rather than further use has bought time but potentially at the cost of very expensive landfills in later generations. Such action will be particularly unfortunate if the mass and volume of the material have been increased by blending it with other materials (virgin or recycled) so that the combined material later fails criteria for re-use or worse still, as has happened, results in the combined material being designated as not-inert and requiring expensive landfill, indeed possibly toxic waste landfill – a mixture of crushed concrete and soil will have high pH from the cement possibly making the combined materials toxic waste as it is no longer simply crushed concrete for which regulatory exemptions may be available. Similar problems can occur during use or re-use, if materials react with chemicals in adjacent materials (e.g., natural and anthropogenic chemicals in soils) and so become unfit for further re-use. The problems associated with multiple re-uses invites consideration of an entropy based approach to recycled materials

13 OVERARCHING ISSUES

The paragraphs below set out a few examples of overarching issues – issues that will affect all of us but on which geoenvironmental engineers should have particular insights.

13.1 *Interconnection and Interdependence*

We live in an interconnected world with ever increasing interdependencies not only at the personal level but also in relation to key areas such as infrastructure and energy supply. The drive to sustainability and more recently net zero carbon is likely to increase interdependency unless this is recognised and managed. As a very simple example consider the move towards electric vehicles. These must be re-charged and will stop if a failure of supply persists beyond their charge time. A localised storm which knocks out part of a distribution system will knock out all that depends solely on it: homes, industry, infrastructure, telecommunications and now electric vehicles. Depots providing fuel for vehicles running on liquid fuels or gas (lpg) provide a distributed system (provided there is power to dispense the fuel). The net effect is a loss of system redundancy. Very localised battery stations would be/will be required to provide the same level of redundancy. Geoenvironmental engineers must add interdependence to the key touchstones of sustainability, net zero and resilience.

Interdependence means that the economic cost of events such as floods, storms, earthquakes, volcanic eruptions are many times greater than the costs of the physical damage caused by the event (see papers from the Oxford Environmental Change Institute, for example, Adshead et al. 2021).

The production of batteries and the magnets for electric motors is of course not without impacts from the mining and processing necessary to produce the essential metals.

13.2 *Covid 19 and future pandemics*

We must expect future construction to be influenced by the revised thinking induced by the Covid pandemic and improving preparedness for and resilience to future pandemics. For example, it may reverse the current trend for population movements into cities from more rural areas.

The trend towards home-based working also may have major impacts on the type and distribution of homes, offices, and other commercial premises. Indeed, we could be at the beginning of a major re-visioning of the built environment and associated transport and service infrastructures.

Many questions hover in our thoughts: How long will any re-visioning endure? Will we return to pre-Covid 19 thinking? What will happen/should happen in regions where the state of development is too limited for pandemics to be the issue of the greatest concern?

13.3 *Climate change*

Climate change is a matter of immediate concern and engineers are able to drive change not only with regard to reduction in emissions of greenhouse gases but also the design of new works and the adaptation of the old for climate resilience. Here resilience includes impacts of sea level rise, more violent storms and sea states, more intense rainfall, drought, and more extreme climates. Net zero has become the by-word but of course this must include minimisation of all greenhouse gas emissions –

noting that methane is a powerful greenhouse gas and that herbivores such as cows are significant producers. It is not simply a matter of changing our approach to hard construction but also to agricultural and personal practices.

Climate change is currently associated with more extreme weather, periods of intense rain, high winds, and sustained periods of drought. Massive geotechnical works will be required to build resilience and there may be wholesale movements of populations from environments which become unsustainable – managed retreat – always provided that it is managed.

Whilst climate change deniers may still seek to debate whether anthropogenic carbon dioxide emissions are the cause of climate change there can be no doubt that carbon dioxide levels in the atmosphere have increased substantially over the last two centuries (from 350 to the current 412 ppm). Amongst so many other impacts, this will lead a reduction in the pH of oceans.

13.3 *Energy production*

In terms of carbon dioxide production, the fossil raw materials for energy generation in order of decreasing carbon dioxide production are coal (worst), oil and then gas (least emission). However, we can and should expect all fossil use for energy production to be phased out with green(er) energy derived from hydro, wind, solar and nuclear. The need to store wind and solar energy is prompting interest in the construction of pump storage schemes including the use of old mines. Countries, like Canada, the development of vast resources for Hydro production once uneconomic now becomes economic. Liner systems are playing an increasingly important role in these developments. However, many of these developments will take considerable time before they are built and oil and gas may remain as chemical feedstocks until replaced by the green alternatives. These undertakings will displace land that otherwise could be used for forestry or food production. Major changes can be expected from the drive to reduce meat consumption which will not only increase the efficiency of food production (calories per unit area of land) but also reduce methane emissions from those flatulent domesticated animals.

13.4 *Mobile energy*

Alongside the move to green energy production there will be a change in the energy carrier for vehicles, construction plant etc. Electric cars soon may be the norm as governments set regulations for the phase-out of petrol/diesel cars. Battery operation also is being found practical for quasi-static construction plant such as piling rigs. For heavy vehicles and plant hydrogen currently appears the favoured energy carrier.

13.5 *Biocementation*

Across the world there is a substantial corpus of research in progress on the use of biological techniques for ground modification. A significant part of this work is on calcite precipitation. In comparison, rather little work seems to be addressing the precipitation of other minerals. Work also continues on the effects of vegetation including plant roots.

The amount of work in progress is so extensive that it is not possible to provide a concise overview. There will be papers on bio-manipulation in the conference and readers are directed to them. However, it is perhaps appropriate to raise a number of issues.

How is biocementation/biomodification to be applied? All those familiar with geotechnical grouting will be aware of the problems associated with achieving sufficiently complete ground treatment even with grouts that seal the soil so that treatment can be at reducing centres working against already partly sealed ground. With low viscosity systems which do not seal, loss of grout via preferential pathways or simple gravity driven flow of dense solutions becomes a real problem. Is the bio-grout where you think it is? Furthermore, grouting at the necessary close centres is expensive. It is not sufficient to research biomodification materials alone. Delivery and treatment-verification systems also require research.

What is the durability of the bio-grout in service? If there is potential for groundwater flow/the ground is permeable there will be leaching. Indeed for grouted barriers leaching of grout components (e.g., calcium from Portland cement grouts) should be recognised as one of the major mechanisms of barrier degradation. Many aquifers and all rainwaters are under-saturated with respect to calcite. Will bio-precipitated calcite remain in-situ? How can design life be estimated?

Conversely, if leaching is not significant, will growth of larger crystals with depletion of finer crystals (a natural process to reduce the overall surface energy) affect the mechanical performance of the bio-grout? Can this and other aspects of Ostwald ripening be an issue?

No doubt these and many other issues will be addressed in the conference.

---

14 ENVIRONMENTAL GEOTECHNICS:

The discipline of Environmental Geotechnics has evolved since its beginnings in the late 1970s to early 1980s through the adoption and adaptation of geotechnical engineering knowledge to produce practical solutions for problematic environmental situations (Sarsby 2019). The design of low-permeability pollutant barriers, such as waste containment liners and cut-off walls, may be mentioned as an example of the application of geotechnical engineering expertise, which was mainly gained from the design of earth dams and embankments and then refined for environmental purposes (Mitchell et al. 1965; Mitchell 1991; Daniel 1993; Rowe et al. 1993; Rowe et al. 2004; Shackelford 2014; Rowe 2018). When facing these new challenges, geotechnical engineers understood that knowledge of traditional soil mechanics was a necessary, but not sufficient condition to obtain satisfactory results, and started to broaden their formal education to include chemistry, geochemistry, and groundwater hydrology (Goodall and Quigley 1977; Quigley et al. 1983, 1988; Quigley and Rowe 1986; Shackelford 2005). The performance of a containment barrier is in fact not only related to its mechanical and hydraulic features, but also to its ability to limit the mass transport of a pollutant to the groundwater. The need to integrate hydrogeology and civil engineering became apparent (Rowe 1988, 1992). This was followed by a need to integrate polymer engineering in civil engineering and the increase in knowledge needed to effectively apply geosynthetics to waste containment applications (Rowe 1998, 2018, 2020).

Nowadays, Environmental Geotechnics issues include, among others, waste containment, waste mechanics, the stability of landfill liners and covers, the stability of tailing dams and heap leach pads, the surface containment of lagoons and ponds, soil remediation, contaminated and damaged land reclamation, biologic processes for soil improvement, underground energy exploitation, carbon dioxide sequestration, and nuclear waste disposal. As a result, the professional identity of an expert in the field of Environmental Geotechnics is characterized not only by a traditional background in soil mechanics and geotechnical engineering, in addition to structural mechanics and hydraulics, but also by a robust basic training in mathematics, and in physical, chemical and biological sciences, which enables them to handle the manifold and complex phenomena that occur in environmental applications. The distinctive traits of the discipline are the propensity to face new problems through an open-minded approach and the ability to interact with other disciplines, including social and economic sciences and law. The pressing need to find practical solutions for the wide range of problems that involve the environment has favoured the tendency to explore new fields of knowledge and expand the boundaries of the discipline, in contrast to the mainstream tendency to develop a hyper-specialization focused on particular subjects.

A possible answer to the question "where are we going?" is that our discipline will continue along the path of searching for practical solutions for the emerging, and frequently unexpected, environmental problems that we will have to face in the future, relying on an approach which combines geotechnical engineering expertise with a multidisciplinary cultural background. Even though we cannot foresee what the future will bring, we may envisage how we will take on the future challenges, as the practice in our discipline has built a forma mentis to deal with problems posed by human progress and the future evolution of nature (e.g., climate change). In comparison to other disciplines in the field of geotechnical engineering, Environmental Geotechnics is not characterized by a specialistic list of topics, but by a context (i.e., the ground), a goal (i.e., to find practical solutions for environmental problems) and a method (i.e., broadening knowledge through a multidisciplinary approach).

We should not be surprised in the future to find individuals who have a professional identity in the discipline of Environmental Geotechnics who are engaged in modelling the coupled mechanical, chemical and thermal behaviour of geo-structures interacting with the environment (e.g., through emissions) with the aim of developing a sustainability and resilience assessment to select the best design option among the available technical and technological alternatives. A systematic analysis of the expected evolution of Environmental Geotechnics may be attempted based on the current perception of our discipline. It can be postulated that three fundamental interactions will take place in the future in the field of Environmental Geotechnics (Figure 14.1):

- an interaction with technical/technological development,
- an interaction with the society, and
- an interaction with new environmental issues.

The previous sections of this state-of-the-art paper have focused on the description of the most advanced technical and technological solutions that are available for the containment of contaminants. The future application of these solutions will increase the efficiency of containment and clean up systems and will determine a relevant environmental benefit. This benefit, in turn, will stimulate new scientific research to further improve the outcome of the implemented projects.

Technological developments will significantly enhance the potentiality of the monitoring systems that are used to assess and control the performance of operational geo-structures, so that the inherent risk to a site can be reduced. Among the emerging technologies that may change the way geotechnical monitoring is conducted in the future, Soga et al. (2019) mentioned satellite Imaging, distributed fibre optic sensing, LiDAR (Laser Imaging Detection and Ranging) and computer vision techniques. Monitoring is expected to play a fundamental role in the environmental field, due to the increased acceptance of Monitored Natural Attenuation (MNA) and Monitored Natural Recovery (MNR) as tools for the remediation of contaminated sites (Yong and Mulligan 2019). Monitoring typically involves collecting soil (or sediment) and water samples to analyse them for the presence of contaminants. Laboratory research includes microcosm studies on the evaluation of the degradation and transformation of the target organic chemical contaminants, and partitioning tests for both inorganic and organic chemical contaminants, such as tests for the determination of adsorption isotherms, leaching column tests, and desorption tests. Field monitoring related to the modelling of transport and the fate of contaminants, to validate theoretical assumptions, and to verify the reduction in time of contaminant concentrations.

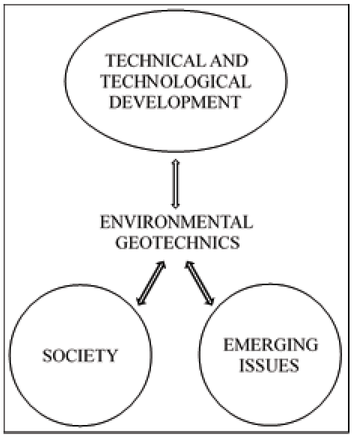

Figure 14.1. Fundamental interactions of the discipline of Environmental Geotechnics.

Technical and technological advances should make the collection and management of large sets of data possible, including chemical and biological information, which is necessary to support modelling activities.

The development of Environmental Geotechnics is driven by the evolution of social needs, such as the minimisation of materials and energy consumption, the preservation of natural resources, the minimisation of waste generation, and the maximisation of future reuse options for polluted sites. As a result, a fundamental role is played by the interaction with society, which takes place through the development of new regulations and design guidelines. From this point of view, we can already perceive a move toward a holistic approach, which evaluates environmental, economic, and social benefits of any project as well as the potential impacts and unintended consequences. Design choices should be based not only on the best technical and technological options that are available, but also on a sustainability assessment (e.g., through a life cycle analysis) for the quantification of the direct costs (e.g., construction cost), indirect costs (e.g., social cost of greenhouse gas emissions), and benefits (e.g., employment opportunities). In this way, the key indicators of the environmental, economic and social impacts across the entire project life cycle can be identified and quantified to make decisions that are fully sustainable (Reddy et al. 2019). Moreover, with the global climate change and the consequent extreme events that are occurring, a necessary feature of projects is their ability to be resilient and maintainable/repairable (i.e., capable of responding to a perturbation or disturbance by resisting damage and recovering/being recovered quickly). Resilience with respect to extreme events, such as earthquakes, storms, floods, permafrost melting, and desertification, is dependent on the mechanical resistance of geo-structures, which must be able to protect the environment from the consequences of catastrophic failures. While the paradigm of sustainability drives the design toward a rational risk-based approach, which considers the natural attenuation mechanisms that contribute to preserving or restoring the environment, the paradigm of resilience highlights the relevance of the mechanical behaviour of geo-structures in protecting the environment against extreme events.

Although the future will inevitably be characterized by a certain degree of unpredictability, we can expect that future generations of engineers will have to face emerging issues related to the impact of human activity on the environment. These emerging issues may be unexpected, but future engineers must be ready to face them by adapting their knowledge and by finding suitable solutions. A terrible example of an emerging issue is that of the COVID-19 epidemic. Soon, the need to face the impact of this epidemic on the environment will represent an extraordinary challenge, and this challenge will also involve our discipline and will require engineers to study and learn from reactions to the many previous pandemics that that plagued the World, see for example, Karlen (1995) and Kilbourne (2008).

Two specific topics are analysed in the following sub-sections: the evolution towards performance-based design in place of the prescriptive-based design and the possible contribution of Environmental Geotechnics to facing the emerging issue of the COVID-19 pandemic and future pandemics. The aim of the first topic is to give an example of the interaction between the discipline of Environmental Geotechnics and society. Similarly, the second topic is an example of the interaction with an emerging issue.

14.1 *Performance-based design of landfill lining systems*

The design of pollutant barriers, such as waste containment liners, is aimed at minimising both leachate exfiltration and contaminant transport from the waste to the groundwater system (Rowe et al. 2004, Shackelford 2014). The release of contaminants that are contained in landfill leachate can be reduced to environmentally acceptable levels by a barrier system that includes a leachate collection system and a liner system. The leachate collection system typically involves a series of perforated pipes in a granular drainage layer that are aimed at minimizing the leachate ponded head. Modern liners may be constituted by compacted clay liners (CCLs) and geosynthetic components, such as geomembranes (GMBs) and geosynthetic clay liners (GCLs). GMBs can be coupled with CCLs and/or GCLs to form composite liners that provide an optimal groundwater protection performance. Moreover, the aquifer located beneath a landfill is typically not only separated from the waste by these artificial layers, but also by a natural foundation or attenuation layer (AL), which plays an important role in limiting contaminant migration (Rowe and Brachman 2004).

Rowe (2009) stated that in order to minimize the environmental impacts of a landfill, a systems engineering approach to the design should be adopted. This approach involves decomposing the entire system into subsystems consisting of simpler identifiable components. The performance of the individual components, as well as the interactions between the different components of the system, must be assessed before the response of the entire system can be quantified to obtain its overall engineering performance.

A performance-based design of a lining system implies a profound change with respect to the traditional prescriptive-based design, which is still nowadays the most widespread in worldwide regulations. Though note that performance based requirements are typical for vertical barrier systems. For example, hydraulic conductivity and thickness will be specified but not the materials to be used (Jefferis et al. 1999). The benefits of a performance-based design include (Estrin and Rowe 1995):

- allowing engineers to bring state-of-the-art knowledge to a project, which in turn is expected to encourage both theoretical and practical research investigations and the application of innovative technology in the field.
- putting emphasis on pre-approval design examination rather than on post-construction monitoring.
- stimulating a more in-depth scrutiny by regulators and concerned members of the public regarding the adequacy of the proposed design prior to approval.
- performing an analysis of the interaction of the proposed engineering system with the particular hydrogeologic conditions in which the landfill would be located.

Performance-based design allows an assessment of the:

- contaminating lifespan of a landfill in the context of the local hydrogeology and how construction of the facility will affect the hydrogeologic conditions,
- service life of the components of the system and how interactions between system components will change with time and ageing,
- potential implications of climate change on the performance of the facility,
- potential failure modes and effects,
- potential unintended consequences,
- nature and likely effectiveness of monitoring, both in the short and long-term,
- when impacts are likely to be detected by the different components of the monitoring system and establishing trigger levels for various types of pre-emptive or remedial action was taken, and
- the need for perpetual (i.e., multigenerational) care and maintenance.

A common performance criterion is that a liner must ensure that the concentrations of pollutants in the groundwater remain less than prescribed threshold levels at a specified compliance point, which is commonly represented by a monitoring well located in the underlying aquifer and downstream from the landfill. In fact, the pollutant concentration can be related to a corresponding risk to human health and the environment through a toxicological model that considers the pollutant properties and the exposure paths (Dominijanni and Manassero 2021). The pollutant concentration in the groundwater is obtained from a transport analysis, which considers the migration process from the waste contained in the landfill to the compliance point.

The approach to follow is similar to the procedure used for the risk assessment of contaminated sites that was first developed in the US in the late 1980s (US EPA 1989) and subsequently standardised by the ASTM (ASTM 1995; 2000). This procedure is structured in three tiers (Sethi and Di Molfetta 2019):

- the first tier essentially involves comparing the site contamination with screening concentration values.
- the second tier involves a simplified contaminant transport analysis based on analytical, semi-analytical, or simple numerical solutions, in which part of the input data are derived from on-site investigations, while missing information is obtained from validated and up-to-date databases or from the literature.
- the third tier represents a more detailed appraisal of risk, based on sophisticated models that are solved through advanced numerical methods. These models require enough site-specific chemical, physical and biological data to carry out a full experimental system characterization.

Although the first tier is not amenable to a risk assessment for the design of a landfill lining system, the second and third tiers can be applied profitably to evaluate the impact of pollutants, released from waste, on groundwater quality.

The application of such a risk assessment to the performance-based design of landfill lining systems can therefore be carried out based on a conceptual model that identifies the leachate produced by the waste with the source of contamination and a monitoring piezometer (which may be real or virtual), placed downstream of the landfill, with the point of compliance, as shown in Figure 14.2.

The limit value that the pollutant concentration in the groundwater can assume, in correspondence to the point of compliance, without producing an unacceptable risk for human health or the ecosystem may be determined based on a toxicological model (Redfearn and Roberts 2004; Sethi and Di Molfetta 2019). As a result, the verification of the effectiveness of the lining system and the attenuation layer in containing the waste contamination is obtained through a contaminant transport analysis, which provides the theoretical value of the contaminant concentration at the point of compliance. A value of the calculated concentration that is lower than the limit value given by the toxicological model is indicative of a satisfactory design, as the related risk is acceptable.

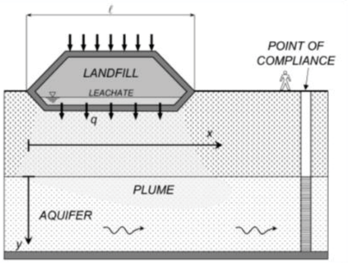

Figure 14.2. Reference scheme for the application of the risk assessment procedure to the performance-based design of a landfill lining system. The pollutant released by the waste migrates vertically through the engineered barrier system and the natural attenuation layer to the underlying aquifer, where pollutant transport then becomes horizontal.

Manassero et al. (2000), Rowe and Booker (2000), Guyonnet et al. (2001), Foose (2010) and Dominijanni and Manassero (2021) derived analytical and numerical solutions for the contaminant transport from landfills under the restrictive assumptions of steady-state conditions and a constant source concentration in the waste leachate. These conditions exclude the possibility of modelling time-varying properties and time-dependent phenomena and typically result in conservative predictions of the groundwater contaminant concentration (Shackelford 1990; Rabideau and Khandelwal 1998; Rowe et al. 2004). As a result, such solutions should be considered suitable for a conservative estimate of the risk, in a similar way to a tier 2 analysis for a polluted site. The solutions developed by Dominijanni and Manassero (2021) allow the contaminant concentration distribution to be evaluated in the horizontal direction within the aquifer beneath the landfill. In such a way, the progressive increment of the contaminant concentration that occurs along the direction of the groundwater flow can be appreciated. The analyses contemplate both the case of thin aquifers (i.e., aquifers whose thickness is no more than a few metres) and the case of thick confined aquifers, in which the vertical distribution of the contaminant concentration needs to be considered. An analytical solution for the calculation of the leakage rate through a composite liner, which consists of a geomembrane overlying a geosynthetic clay liner, is presented in Guarena et al. (2020) for the case of a hole located in correspondence to a wrinkle in the geomembrane. This solution, which can be implemented in a contaminant migration analysis, considers the influence of bentonite swelling on the determination of the hydraulic transmissivity at the interface between the geomembrane and the underlying geosynthetic clay liner, and the chemico-osmotic component of the water flow that is generated by the gradient in the solute concentration. Dominijanni et al. (2021) have extended the available solutions to scenarios that involve unconfined flow conditions in thick aquifers. These solutions offer the possibility of conducting an analysis that involves a limited number of parameters and allows the influence of the liner properties (e.g., hydraulic conductivity, thickness, defects) and the field conditions (e.g., aquifer thickness, groundwater velocity) on the final result to be appreciated under conservative assumptions (steady-state conditions and constant source concentration).

Semi-analytical solutions implemented in popular software products, such as POLLUTE (Rowe and Booker 1985a; Rowe et al. 2004; Rowe and Booker 2005) and MIGRATE (Rowe and Booker, 1985b), are available to evaluate the groundwater contaminant concentration below a landfill, taking into account the time-evolution of the source concentration in the landfill leachate, as well as time-dependent phenomena, such as adsorption, ion exchange and bio-degradation. These solutions can be compared to a tier 3 analysis for a polluted site, which can be conducted when a more reliable evaluation of the contaminant concentration in the groundwater is considered necessary.

The variation of dominant transport mechanisms that takes place between the vertical movement across the landfill lining system and the underlying attenuation layer and the predominantly horizontal movement that occurs within the aquifer represents a difficulty in conducting a contaminant migration analysis. The vertical transport, which can develop under unsaturated conditions, is in fact characterized by a low velocity and is therefore mainly controlled by molecular diffusion (Shackelford 2014). On the contrary, horizontal groundwater movement is typically characterized by a velocity that is some orders of magnitude higher, and the related contaminant transport is dominated by advection. The numerical methods that are suitable for vertical transport may be unsuitable for solving the horizontal transport in the aquifer, and this may implicate a loss of accuracy in the calculation within one of the two components of contaminant transport. Semi-analytical methods (Row and Booker loc. cit.) provide one solution to this problem. Another possible solution to this problem is to resort to the Domain Decomposition Method (Bellomo and Preziosi 1995; Tang et al. 2020). In this method, the domain of the considered mathematical problem is partitioned into sub-domains, which can be analysed separately by introducing additional interface conditions at the boundaries between them. One of the main advantages of the method is the possibility of running a parallel calculation for the different sub-domains. In the scenario of contaminant migration from a landfill, the domain can be divided into a first sub-domain that includes the landfill lining system and the underlying attenuation layer, and a second sub-domain for the aquifer. The interface between the two sub-domains is represented by the top surface of the aquifer, in correspondence to which the continuity of the hydraulic head, the volumetric flux, the contaminant concentration, and the contaminant mass flux must be imposed. By using such a strategy, it is possible to optimize the choice of the numerical method, as each sub-domain can be solved separately, while an iterative procedure is implemented to check that the interface conditions are satisfied. For instance, a value of the hydraulic head and the contaminant concentrations, at the top of the aquifer, can be assumed at the beginning of the iterative procedure. The vertical volumetric flux and the vertical contaminant flux exiting from the attenuation layer are calculated since these values. By using these fluxes to impose the boundary conditions at the top of the aquifer sub-domain, a distribution of the hydraulic head and contaminant concentration is found for the groundwater, so that a new estimate of the hydraulic head and the contaminant concentration at the top of the aquifer can be derived. The iterative procedure is stopped when the values of the hydraulic head and the contaminant concentration at the top of the aquifer do not change appreciably between two consecutive calculation steps.

Another interesting development of the contaminant migration analysis is its application in the frame of a probabilistic approach in which the boundary conditions and the model parameters have a random nature. In fact, a significant difficulty in the analysis arises from the uncertainty that is encountered in the evaluation of the representative values that need to be assigned to various parameters, such as the leachate contaminant concentration, the hydraulic conductivity of the mineral layers and the number, size and location of the geomembrane defects. In a deterministic approach, the designer must trust in his own judgement to make the most opportune choice of the values that have to be assigned to the parameters but cannot, however, know the combined effect of the variance of the various parameters on the final result of the analysis. The adoption of a probabilistic approach instead allows the random nature of the involved parameters to be considered explicitly. In such a way, the final results may be related not only to the most representative values of the involved parameters but also to their variance (e.g., Rowe and Fraser 1995). Probabilistic analysis is implemented in the well-established contaminant migration models CONSIM and LANDSIM models developed by Golder Associates for the UK Environment Agency (http://www.consim.co.uk and http://www.landsim.co.uk).

A performance-based design is an ideal tool for the evaluation of the project choices based on a sustainability approach, as it allows the most advanced technologies to be used. Moreover, the site vulnerability and the natural attenuation mechanisms can be introduced into the analysis, thereby avoiding recourse to oversized lining systems, with relevant economic and environmental savings.

The resilience of a project can only be guaranteed through the coupling of a contaminant migration analysis with a mechanical stability analysis. Mechanical stresses and strains can influence the barrier performances of the components of a lining system. Rowe and Yu (2018), for instance, reviewed the strains that can develop in a geomembrane from gravel above and below it and from down-drag due to the weight of the waste and from subsequent degradation and consolidation of the waste. These strains play a critical role in the long-term performance of a geomembrane. Stability analyses should consider the effects of seismic actions, extreme rainfall events and large variations of the groundwater levels. A key feature for a good design is represented by the attention paid to the consequences of mechanical failures on the barrier performance of a lining system.

All the above will be subject to the time and financial constraints imposed by the owner. Deciding what is essential and what merely desirable in a design analysis may be challenging; at what point does one refuse to proceed? Furthermore, when adopting/being required to adopt advances in technology, designers and contractors must first establish who will carry the liability for failure should a new advance in technology not meet expectations. An analysis of some problems relating to the use of recycled and secondary materials is set out in Jefferis (2019). Unexpected problems can, and often do, lead to litigation.

14.2 *Emerging issues in Environmental Geotechnics: the COVID-19 pandemic*

The world-wide spread of the Severe Acute Respiratory Syndrome Coronavirus 2 (SARS-CoV-2), a highly infectious and pathogenic strain of the newly emerged coronaviruses SARS-CoV-1 and MERS-CoV, has become a major public health concern in many countries, and has led governments to close national borders, limit the movement of citizens on national territories, implement quarantine measures and shut down workplaces, retail activities, schools and universities. In addition to the fatalities caused by the related disease (COVID-19), other adverse consequences are currently being faced by countries affected by the pandemic, such as financial instability and decline in the social order, thus evidencing that effective solutions to global-scale threats, like the global climate change looming over the near future, can only be provided through international cooperation, which implies the real-time transmission of scientific information and research outcomes across borders (Tang et al. 2021).

Although the mechanisms by which the pathogenic agent is transmitted to human beings and animals, infects the living hosts and replicates within their cell tissues are primarily investigated by microbiologists, epidemiologists and public health experts, new questions have emerged during the emergency, whose answers can only be provided through a highly cross-disciplinary approach (Paleologos et al. 2021; Tang et al. 2021; Vaverková et al. 2021). For instance, the way viruses interact with and migrate through the soil environment is largely unknown, as well as how they can affect the physico-chemical properties of soils (e.g., hydraulic conductivity and sorptive capacity) through their own activities. Any assessment of the sanitary risk related to the migration of viruses in the subsoil requires the development of accurate, reproducible, and cost-effective techniques to identify and quantify the presence of pathogens and their infectiousness in particulate media, so that these techniques become familiar to most geoenvironmental researchers and engineers. Because of the ability of enveloped viruses to retain infectivity for days to months in aqueous environments, and because of the observed persistence of SARS-CoV-2 in unfiltered water with a high content of organic compounds and suspended solids, major concerns have arisen concerning the discharge of waste waters from hospitals and health care facilities into the municipal sewerage systems, due to the likelihood of a significant viral load during the pandemic besides the need for in situ disinfection before discharging, the geosynthetics industry may provide novel lining products (e.g., geomembranes and geosynthetic clay liners) to prevent virus leakage from buried pipelines and containers, which are used to temporarily store pathogen-laden waste water. Furthermore, the massive usage of disinfectants in medical centres, households and public spaces represents in itself an additional risk factor, as the percentage of both liquid and solid waste that contains traces of sodium hypochlorite or similar substances is expected to increase during the pandemic, and in turn causes the formation of a number of water disinfection by-products, such as the four primary trihalomethanes, which pose potential genotoxic and carcinogenic health risks.

Given the above challenges introduced by the outbreak of the pandemic, the Environmental Geotechnics community is called upon to contribute to mitigating the negative consequences of the current emergency. As such, the COVID-19 pandemic represents an opportunity for the development of our discipline, to build upon the unique expertise of geoenvironmental researchers and engineers in solving environmentally related geotechnical engineering problems, and upon the wealth of knowledge that comes from microbiology, medicine and other related disciplines. With the aim of further illustrating how Environmental Geotechnics can play a prominent role in safeguarding public health during the pandemic emergency, the remaining part of this section is devoted to analysing a single issue in detail, namely the disposal of pathogen-laden municipal solid wastes in sanitary landfills and the expected performance of mineral bottom liners in preventing the migration of the infectious pathogen to the surrounding geoenvironment.

14.2.1 *The disposal of SARS-CoV-2 contaminated solid waste*

SARS-CoV-2 contaminated waste streams that do not undergo a suitable treatment, aimed at reducing the viral load, such as incineration, sterilization by means of autoclave or high-temperature disinfection, pose severe threats to their safe disposal, both in the short-term for the employees who are involved in the management of solid waste and, hence, are exposed to the contaminated bioaerosol (Carducci et al. 2013), and in the long-term for the preservation of the quality of the groundwater, which may represent an effective vehicle for the transmission of the virus in the environment and, as the main source of drinking water, to humans. Because of its potentially high viral load, healthcare, and medical waste (H&MW) represents the contaminated waste stream of greatest concern, also considering that the number of existing medical incineration/disinfection facilities and regular waste-to-energy plants may not be sufficient to cope with the exceptionally large volume of H&MW generated during the pandemic, so that relying on sanitary landfills becomes the only viable alternative. Similarly, waste streams that are generated from domestic and workplace garbage may also contain a non-negligible concentration of the virus, due to the spread of the pandemic, and their management therefore requires the adoption of analogous precautions.

Modern engineered landfills are provided with bottom lining systems, whose purpose is to facilitate the removal of the leachate, which accumulates in the drainage layer placed above the lining system, and to prevent migration of pollutants and pathogenic microorganisms into the surrounding subsoil. Bottom lining systems comprise a geomembrane overlying a low-permeability mineral layer which, in turn, consists of a compacted clay liner (CCL) or a geosynthetic clay liner (GCL). The assessment of the risk for human health that results from the migration of the virus requires the transport of the pathogen through the engineered barriers and the underlying aquifer to be modelled, and the virus concentration in the groundwater to be predicted at a specified compliance point, which is usually downstream of the landfill (Dominijanni and Manassero 2021; Guarena et al. 2020).

As an alternative approach, the “P-trap” has been used to manipulate redox conditions in drainage lines of mine storage heaps, so that temporary storage with the ability to alternate redox conditions (aerobic/anaerobic) may help to kill bacterial hosts for some viruses. Creation of anaerobic conditions by temporary storage in geomembrane bags has been used to kill the cholera bacteria in the sewage from refugee camps.

14.2.2 *Virus adsorption, inactivation, and transport through landfill composite liners*

The migration of a virus through the geomembrane liner of a composite liner is governed by the same mechanisms as those of inorganic chemicals, as the relatively wide dimensions of viruses cause an extremely slow diffusion, if any at all, through the polymer-based barrier and a preferential transport pathway through geomembrane defects (Shackelford 2014). Viruses may undergo inactivation even before interacting with a clay barrier, as specific viral components that are required for infection, such as the nucleic acid core and the outer protein capsid on which the host-recognition sites are located, are naturally subjected to degradation. Moreover, the leachate itself may pose a harsh environment for the survival of viruses, as the mechanisms of viral inactivation are accelerated upon an increase in temperature and a deviation from neutral pH conditions. In fact, the microbially mediated consumption of organic matter determines the release of energy in the form of heat and the generation of volatile organic acids, which are responsible for the relatively low pH during the early degradation stages of solid waste (Chen et al. 2019). On the basis of the results of an experimental study aimed at measuring the survival of the H6N2 avian influenza virus, Graiver et al. (2009) calculated persistence times within methanogenic landfill leachate ranging from approximately 30 days to more than 600 days and observed that the decay in the concentration of the infectious virus could be modelled as a first-order reaction, (i.e., the decline is exponential with time.

When the mass balance equation between the liquid and solid phases must be established, the ability of viruses to be reversibly adsorbed by the clay particles should be considered. Such attachment and detachment phenomena are governed by electrostatic forces, as the protein capsid of viruses carries a net electrical charge, due to the ionization of carboxyl, amino and other functional groups (Harvey and Ryan 2004). The net electrical charge of the virus depends to a great extent on the pH of the pore solution, and is therefore characterized by an isoelectric point (pI; i.e., the pH value at which the net electrical charge is null). The number of deprotonated carboxyl groups above the pI exceeds the number of protonated amino groups, and the sign of the virus surface charge is negative, whereas the opposite situation is encountered below the pI. On the basis of the typical values that are assumed for pI, which usually fall within the 3.5 to 7 range (Michen and Graule 2010; Scheller et al. 2020), viruses are negatively charged under neutral conditions. This result has been confirmed for SARS-CoV-2 as a relatively high value of pI, equal to about 6.2, has been measured, as reported by Calligari et al. (2020). Because clay particles are also characterized by a negative charge under neutral conditions, the system remains stable and unfavourable to pathogen adsorption, unless an increase in electrolyte concentration (Sadeghi et al. 2011) and/or the electrochemical valence of the cationic species that are dissolved in the pore solution (Sadeghi et al. 2013) cause a compression of the diffuse double layers and a reduction in the electrostatic repulsive forces, thereby enabling the pathogen and mineral surface to approach each other as a result of the overwhelming van der Walls forces (Syngouna and Chrysikopoulos, 2010; Theng, 2012).

The adsorption process described above should not be regarded as a complete immobilization of the virus, since a perturbation in the chemical boundary conditions of the clay barrier can cause a fast detachment of the adsorbed pathogen, e.g., because of dilution of the permeating solution. Such a likelihood of pathogen release from the soil particles poses the issue of its survival time when attached to geologic media (i.e., whether its inactivation rate is decreased or increased with respect to the free-solution conditions). According to Harvey and Ryan (2004), inactivation is slowed down by its attachment to porous media with a high content of clay minerals, whereas an acceleration occurs when the virus is adsorbed on coarse-grained soils with a high content of iron and aluminium oxides, which are characterized by an alkaline isoelectric point. In the former case, both the adsorbate and adsorbent carry a net negative electrical charge and, thus, the interaction forces are relatively weak: in such a case, the pleomorphic structure of betacoronaviruses allows a relevant deformation of the protein capsid to take place, so that it can adapt to the clay particle surface, and at the same time provides high mechanical stability that preserves the integrity and infectiousness of the virus for a longer period of time than in free-solution conditions (Block et al. 2016). In the latter case, the net electrical charges that are carried by the adsorbate and adsorbent have opposite signs under near-neutral conditions, so that the virus and mineral surface are held by strong electrostatic attractive forces, which in turn lead to the disruption of the virus structure and its inactivation. However, an inversion in the sign of the net electrical charge of the virus can take place upon minor pH perturbations on the acidic side, which might be encountered in landfills during the anaerobic digestion of organic matter. Under such conditions, as the intersurface potential energy becomes negative (attractive), an enhanced virus uptake and an increased inactivation rate are expected to occur when in contact with clay minerals (McLaren and Peterson 1965). These favourable conditions for virus adsorption and degradation on the clay particle surface are further enhanced when GCLs are used in place of CCLs in composite liners, since montmorillonite is able to maintain an approximately stable negative net electrical charge at low pH values and is characterized by a higher cation exchange capacity (CEC ≈ 100 meq/100g) and specific surface area (S ≈ 750 m^2/g) than, for instance, kaolinite (CEC ≈ 5 meq/100g; S ≈ 15 m^2/g) (Lipson and Stotzky 1983; Theng 2012). Finally, the design of CCLs could be optimized to improve their containment performances against SARS-CoV-2 through the addition of sandy soils with a high isoelectric point, such as magnetite sands, which might result in a larger virus adsorption and inactivation capacity (Moore et al. 1981).

The development of a theoretical model that can simulate the movement of viruses through clay-based barriers should account for the typical dimensions of the considered pathogen. Indeed, in the case of SARS-CoV-2, the diameter of the virus is approximately equal to 120 nm and, as such, is of the same order of magnitude as the width of the conductive pores (i.e., the void space wherein the transport of solvent and solutes takes place) of the GCL bentonite layer, which usually ranges from a few tenths to several hundreds of nanometres (Manassero 2020). Furthermore, several experimental studies have shown that the transport of inorganic electrolytes through montmorillonite-rich clay soils is partially restricted, due to the repulsive electrical forces that arise between the anionic species and the negatively charged clay particles (Musso et al. 2017; Dominijanni et al. 2018). Thus, GCLs are expected to behave as semipermeable membranes, with respect to negatively charged viruses, because of two different concurrent mechanisms, namely *steric hindrance*, whereby the narrower bentonite pores are not accessible to the large-sized pathogen, and *electrical hindrance*, whereby the wider bentonite pores can also impose a certain degree of restriction on the migration of the pathogen because of the overlapping of the diffuse-ion swarms.

14.3 *Pre-emptive consideration of performance and possible consequences*

Current environmental geotechnics is focused on design, construction, and operation to ensure safety and environmental protection in the context of the known knowns. This is necessary, but not sufficient. Occasionally, consideration is given to the known unknowns. No consideration is given to the unknown unknowns because they are unknown at the time a facility is designed and approved. Unfortunately, in most jurisdictions once a landfill has been approved despite it then being developed over many years (often decades), there is no reconsideration of the design when new knowledge (e.g.., better insight into what were previously known unknowns or the revelation of previously unknown unknowns) affects the likely performance of what has been approved. There is generally no systematic periodic re-evaluation of the approved facility. However, the first 20 years of the 21st century have shown that this approach is unsatisfactory (e.g., see Sections 5 and 6 of this paper). There is a need for a systematic approach to managing over time the known unknowns and the unknown unknowns when the facility was approved. Perhaps the branch of civil engineering that comes closest to meeting this objective the engineering of large dams where monitoring and maintenance are embedded in dam systems engineering.

A large dam may have a conceptual design life of 100 years but is unlikely to be decommissioned, if it is playing an essential role in flood control and/or generation of green electricity. Regulators commonly expect periodic dam safety reviews that implicitly recognize that dams require continuing care and maintenance and during their service life may have to deal with known unknowns and unknown unknowns at the time they were constructed. One of the known unknowns when most dams were designed may have been the service life of engineered components, (e.g., spillway gates, spillway, the concrete dam wall, an embankment dam subject to predicted but at the time otherwise unknown settlement). An unknown unknown at the time most existing dams were constructed was the extent to which human use of fossil fuels over the last century would impact the global climate resulting, for example, in more frequent extreme weather events. However, a practice of conducting periodic reviews of large dams allows a periodic evaluation or re-evaluation of potential failure modes and effects including but not limited to the possible:

(a) consequences due to components of the system approaching the end of their service life, and
(b) changes to environmental conditions such as climate change.

This allows initiation of pre-emptive repair, or replacement, or whatever other action is required to maintain minimal danger to human life, property, and the environment. The service life may have been a known unknown at the time of construction but will become evident from monitoring over time. The rapid impact of the human use of fossil fuels on changing climate and hence the impact of climate change on the maximum probable flood was an unknown unknown at the time many dams were designed and built but it can be addressed by appropriate upgrades, changes to operating rules, and or infrastructure. Appropriate changes made today can accommodate the currently predictable maximum probable flood but may need to be revised in future periodic reviews if, for example, climate change is locally more significant than was anticipated.

The contaminating lifespan of even large MSW landfills, hazardous waste landfills, low-level radioactive waste, and many tailings storage facilities and heap leach facilities could have been estimated using the known contaminants of concern last century (a known known based on the contaminants of known concern). However, it was not practical to estimate a service life of the geosynthetics used in these facilities in the last century. It is now possible to make service life predictions and develop a design that, based on what we know today, will have a service life greater than the contaminating lifespan. However, in the brief 40-year history of environmental geotechnics it has been shown that what we might have considered a reasonable contaminating lifespan for the contaminants of concern in the last century is no longer reasonable for the contaminants of emerging concern discussed in §6.

Many landfills produce annual monitoring reports documenting leachate collection, certain aspects of leachate chemistry, groundwater monitoring data from discrete generally widely spaced monitoring wells around the facility, and if there is a leak detection/secondary leachate collection/groundwater control layer monitoring data from that layer. These reports generally do not consider the big picture questions or what factors are likely to affect performance over the next decade. Also, except for the data from a leak detection/ secondary leachate collection/groundwater control layer, the data collected generally provides very little insight as to the actual performance of the facility. At best they may detect an unexpected leakage but even this is doubtful for a single lined landfill monitored by discrete widely distant monitoring wells. This is particularly likely for closed landfills, tailings storage, and mine waste rock disposal facilities. Thus, environmental geotechnics needs to face the challenge of finding better approaches to the monitoring and periodic review of the performance of these large potential sources of contamination with a very long contaminating lifespan.

---

15 CONCLUDING COMMENTS

In the coming decades, geoenvironmental engineers can expect to have to design, construct, manage, and live with some of the most radical changes in every aspect of life including energy and raw materials production, waste minimisation, water shortages, infrastructure resilience, transport systems, land use, and more frequent flooding and failures due to climate change and systems interdependence and interconnectedness.

One of the many consequences of climate change will be the need for geoenvironmental and geotechnical engineers to follow the lead of dam engineers in performing a potential failure modes and effects analysis for all significant geotechnical and geoenvironmental engineering projects. In the third decade of the 21st century it is no longer sufficient to ensure an adequate factor of safety for slopes and bearing capacity. While this is still necessary, we also need to consider the potential unintended consequences of the proposed facility, including environmental impacts, and identify all knowable/evolving unknowns relevant to proposed undertaking. The next step must be to develop appropriate mitigative strategies for all identified failure modes and address the known unknowns either directly or by monitoring and contingency plans. Given that there will always be unknown and unknowns, once constructed, the project should be periodically reviewed to identify any deviations from the intended behaviour and identification of new issues that were previously unknown. This should be followed by the implementation of appropriate action to address those changes.

It is recognised that all this will require funding streams to be available throughout a project's life and beyond, until it is decommissioned. The cost of this post-closure monitoring and ongoing maintenance and repairs must be included in the initial business case. It is also recognized that geoenvironmental engineers must be appropriately trained to meet the coming challenges.

This paper has touched on current advances and challenges on all continents and highlighted the new issues and materials that have emerged in the first two decades of the century. A summary of key observations and findings is provided below.

1. Geosynthetics play a major role in many geoenvironmental projects. Because they are easy to use, there is a great tendency to select the cheapest material and have it laid down by unskilled labour. There is a prevalent lack of understanding of appropriate design and construction evident in many applications. Geosynthetics need more attention in undergraduate education by integration, where appropriate, into existing courses and in professional development of graduated engineers.
2. There are many different resins, antioxidants/stabilizers, and carbon blacks that can be used in polyethylene and polypropylene geosynthetics. The time to nominal failure and service life of these geosynthetics will be highly dependent on compatibility of their constituents with its chemical, thermal, and UV exposure as well as tensile stresses. This can only be assessed by performance-based testing. Index tests are useful for confirming that the material delivered to site is consistent with specified properties (i.e., for quality control and CQA), but they do not provide design parameters.
3. HDPE, LLDPE, or PVC geomembranes are extensively used in fluid containment applications. All three materials will ultimately become brittle and fail to maintain their function as a hydraulic barrier when they crack. One important element in the life of polyethylene is the loss of the efficacy of antioxidants whereas for PVC it is the leaching of plasticizers. This needs to be better understood and considered in design.
4. When designing with HDPE geomembranes, the most important design parameter is the stress crack resistance. However, initial values that are measured, SCR_o, are generally not representative of the true material stress crack resistance since it is influenced by residual stresses developed during manufacture. With time, these stresses will relax and the stress crack resistance will decrease to a representative value SCR_m. Available data indicate that SCR_m has an average value of about 37% of the initial value with most values falling between 27% and 47% of the initial off-roll value. The actual value can only be estimated based on testing that will take at least 3 months.
5. Depending on the constituents other than the base resin, PVC may uptake moisture which results in significant change in its properties with time. Again, this can only be assessed by testing over a period.
6. New resins and products are coming onto the market and the popularity of multi-layered geomembranes is increasing. Multi-layered geomembranes have notable advantages but the potential impact of those layers on long-term performance requires much more consideration than received to date.
7. Bituminous geomembranes have proven to be very effective in canals and in the retention of potable water. There is a growing use of them as liners in mining applications and covers. Care is needed to evaluate their suitability for any given project. Problems have been observed at both high and low temperatures and with seams.
8. The hydraulic conductivity, *k*, of a GCL after several years in a field application is highly dependent on the nature of the bentonite, the subgrade pore water and permeant chemistry, applied stress, and temperature. *k* can also be substantially affected by cation-exchange associated with hydration followed by wet-dry and freeze-thaw cycles.
9. A useful way of screening GCLs with bentonites from different sources and selecting the most appropriate candidates for a given project is to perform a modified swell index test replacing the usual distilled water by either the actual or simulated fluid to be contained by the GCL. The bentonite(s) with the largest swell index in this modified test are the most likely to be a suitable for the testing indicated below. This modified swell index test can be part of a specification and can be more useful in CQA than the standard test.
10. Most designers pay little attention to the geotextiles, the type of bentonite, the amount of needle-punching (especially bundle size), or the mass of bentonite in a GCL in the selection of an appropriate GCL. This is because they have no effect on the GCL hydraulic conductivity when the GCL is fully hydrated and permeated with distilled water at 35 kPa and it is this hydraulic conductivity that is placed on the manufacturer's GCL product sheets. However, this test bears no similarity to most real field situations and the corresponding hydraulic conductivity given on the manufacturer's GCL product sheets is <u>not</u> a design parameter.

    The in-field hydraulic conductivity is highly dependent (by up to 4 to 5 orders of magnitude) on the aforementioned parameters. Therefore, the design hydraulic conductivity for a GCL must be established by performing appropriate tests on the candidate GCL(s) hydrated with actual or simulated subgrade pore fluid or, if that is unknown, 10 mmol $CaCl_2$ solution, and permeated with either the actual or simulated fluid to be contained. The test should be conducted at representative stress levels. Thus, if the GCL is to be used in a composite liner, a test will be required at both a very low stress (3 to 5 kPa) to simulate conditions below a geomembrane wrinkle and at the anticipated normal stress where the geomembrane is in direct contact with the GCL. If wet-dry or freeze-thaw cycles are anticipated, then appropriate tests should be conducted on specimens with the expected cation-exchange to assess the effect of wet dry or freeze-thaw cycling on hydraulic conductivity and geomembrane-clay liner interface transmissivity.
11. The short-term hydraulic performance of GCLs permeated by aggressive solutions (e.g., very high or low pH, or high concentrations of cations, organic solutions) can be substantially improved by adding polymers to the bentonite to create an EB-GCL. However, insufficient consideration has been given to the potential consequences of polymer biodegradation, polymer leaching, and polymer elution. If polymer elution occurs, then open pores will remain within the bentonite and result in a substantially higher long-term hydraulic conductivity of EB-GCLs. Even if elution does not occur, water soluble polymers will be leached over time under field conditions, and they may be biodegraded. Polymer elution also reduces interface shear strength. Until these issues are resolved, extreme caution is advised in the use of EB-GCLs, and such use should only be considered after a careful failure modes and effects analysis and implementation of a plan for monitoring longer-term field performance.
12. Applying a polypropylene or polyethylene coating or laminate to a traditional sodium bentonite GCL can also substantially improve the short-term hydraulic performance of the GCL. Very little is known about the long-term performance of these coatings.
13. Combining a geomembrane and GCL (or CCL) to form a composite liner introduces an important parameter: the

GMB-GCL or GMB-CCL interface transmissivity, which defines the ability of fluid to spread laterally at the interface contact between the two materials.

14. The design objective for a barrier system should be to ensure optimal performance of the entire system, not the components in isolation. More generally, the potential interaction between the soils or other materials above or below a component in a liner system must be considered in any design.
15. Unfortunately, it is not uncommon for a designer to specify an appropriate GCL considering all the factors above and then, during construction, the contractor substitutes an alternative GCL to the one that was specified. The alternative is usually proposed because it is cheaper (i.e., it has less mass per unit area of geotextile, and/or GCL coating, and/or bentonite mass per unit area and/or an inferior bentonite) and has the same hydraulic conductivity based on the manufacturer's product information sheet. This can lead to failure because the cheaper product is not equivalent in terms of field performance and the actual mobilized k in the field can be orders of magnitude higher than was given on the manufacturer's specification sheet, with the failure often occurring a few years after construction and initial operations for ponds/lagoons, 5 to 10 years for a cover system, and several to decades for landfill bottom liners. Most of the liability for any such failure will likely land with whomever approved the substitution of the alternative material for the originally specified material.

    A similar situation arises for geomembranes to be used in either severe conditions (e.g., aggressive chemical contact or elevated temperatures) or requiring a long service life.

    No substitution of a material that does not fully meet the specifications should be permitted without the express written approval of the designer of record.
16. Care is needed in handling and storing geosynthetics prior to installation. Left exposed to the sun, material rolls can heat up to 60°C in Canada and 75°C in South Africa. A few months exposure at these temperatures can substantially reduce the time to nominal failure and ultimately the service life of the material, particularly geotextiles and geonets that are generally not as well stabilized as geomembranes.
17. On projects where the barrier system plays a critical role, the risks of problems during construction can be minimized by the construction of trial sections during the early phase of construction. This will allow identification of unsuitable materials and construction methods, making all parties familiar with the issues that are going to require careful attention during the full-scale construction. The work should be undertaken under supervision of the CQA consultant. Once the test section has been constructed, it should then be exhumed and carefully inspected. Lessons learned need to be documented and implemented in the construction of the facility. In barrier system construction: '*you get what you inspect, not what you expect*'. The CQA should be conducted by an appropriately qualified expert independent of the contractor who should have a budget and enough staff to visually monitor all stages of the construction with backup staff to allow time to do the paperwork.
18. Based on available data from monitoring leakage through a primary composite liner in 122 double-lined landfill cells, with good quality assurance but no leak location survey, the most likely leakage is 70 litres per hectare per day (lphd) with a 66% probability that the leakage will lie between 40 and 100 lphd and a 95% probability that the leakage will exceed 5 lphd but be less than 430 lphd.
19. Most landfill regulations were developed to contain the contaminants of concern in the last century. Many new contaminants of concern have arisen this century. Examples include PBDEs, BPA, and PFAS. An intact 1.5 mm HDPE geomembrane is an excellent barrier to all these compounds. However, with typical construction quality assurance, there is high probability that the leakage of many of these contaminants through a single composite liner will exceed allowable levels in the environment unless one or more of the following apply.
    (a) there was an appropriate electrical leak location survey before and after the geomembrane was covered,
    (b) there is a high-level of hydrogeologic protection and attenuation, or
    (c) there is an extra level of engineering in the form of a secondary leachate collection/ leak detection and liner system.
20. The impacts associated with the contaminants of emerging concern can be kept to an acceptable level for new facilities that satisfy (a) and either (b) or (c) in §15.19 above.
21. The design life of ponds and lagoons may be a few decades. The design life of a liner for a dam is commonly about a century. The contaminating lifespan of a waste disposal facility depends on its size (predominantly the thickness of waste) and the nature of the waste. It typically ranges from about 100 to 300 years for municipal solid waste to over 500 years for low-level radioactive waste, to millennia for some mine waste and long-lived low-level radioactive waste. Thus, the service life of the barrier system components is a critical consideration since the system requires a service life greater than the contaminating lifespan or design life as appropriate.
22. Geosynthetics are versatile and cost-effective materials that can serve many functions at a mine-site. However, due to the characteristics of the mining activity, appropriate selection, and specification of geosynthetic products is of utmost importance. 1.5 mm- or 2 mm-thick LLDPE and HDPE have found extensive use as liners for heap leach pads and more recently for liners and/or covers in tailings storage facilities. In both cases, it is important to design to minimize holes/punctures in the geomembrane in the short-term. Since many of these facilities will require containment for many decades, if not centuries, it is as important to select the right materials for the given exposure conditions and design to minimize tensile strains in the geomembrane.
23. Geotextile used as filters in landfills, dams and mining applications need to be designed with careful consideration of the potential for particulate, chemical or biologically induced clogging

    A significant increase in the use of geotextile tubes to dewater mining tailings is foreseen in the coming years.
24. Subject to appropriate consideration of the issues raised in this paper including the effects of exposure conditions and the selection of compatible materials, the service life of a composite liner will be equal to the shorter of the service life of the geomembrane or the GCL. Thus, with appropriate design (including the selection of materials) and construction, a 1.5 mm- or 2 mm-thick HDPE underlain by a GCL can provide very long service life and is suitable for use in dams, ponds, or lagoons, or in covers for closure of landfills or mine waste facilities, or as a bottom liner for landfills or mine waste facilities. Depending on the exposure conditions, the likely achievable service life may range from decades to millennia.
25. Slurry trenching and allied techniques to form vertical cut-off walls are mature technologies with long and successful track records.
26. The current generation of these cut-off walls is based on cementitious systems and their properties such as strength and hydraulic conductivity are well established. If a project requires material properties such as special stress-strain behaviour or unusual chemical resistance beyond current experience, then it may be wise to look to other

systems.Developing and proving new systems can take years and certainly will not be possible within a typical contract tender period.

27. New systems will evolve because of innovation but also may be driven by changes in material availability (pulverised fuel ash and ground granulated blastfurnace slag) and the drive to reduce carbon emissions (low carbon cements).
28. The use of sorbents within cut-off walls can delay contaminant breakthrough. However, unless the sorbed species are degraded within the barrier they are merely stored and can be expected to be eluted in due time. Sorption is a competitive process and in most cases a concentration dependent process. Contaminants may be desorbed much earlier than predicted from studies using just a single contaminant or if the chemistry of the leachate changes.
29. Over time, substantial quantities of contaminants can build within a sorbent system. If contaminants are to be retained within a barrier, then provision must be made for their management if/when the barrier is decommissioned. Jefferis (2013) gives an example of arsenic accumulation in iron slime in the ballast of an underground railway track. Significant quantities of arsenic accumulated despite the probably very low concentrations the permeating water.
30. The extensive geoenvironmental literature on recycling materials is often focused on the sustainability benefits. While recycling is a notable objective, we need to be vigilant in avoiding unintended consequences. Consideration must not only be given to the benefits but to the many questions that arise. For example, in the proposed application for a recycled material is it chemically and mechanically stable? Does it have the potential for shrinkage, expansion or damage to structures formed from them or built upon them? Will it emit toxic, explosive or asphyxiant gases? Who will bear the risks relating to possible in-service failure?
31. As use of fossil is phased out there will be a need to store wind and solar energy that is prompting interest in the construction of pump storage schemes including the use of old mines. It also makes the of new hydro-electric schemes more economic. Liner systems will likely play an increasingly important role in these developments.
32. Environmental geotechnics needs to face the challenge of finding better approaches to the monitoring and periodic review of the performance of large potential sources of contamination (e.g., large landfills, tailings storage facilities) with a very long contaminating lifespan.

16 ACKNOWLEDGEMENTS

The drafts of different sections of this paper were prepared by groups of authors and edited by R.K. Rowe and S. Jefferis. The authors of the initial drafts of the discrete sections are as follows:

§1: R. Kerry Rowe and Stephan Jefferis
§2: John Scheirs, Fady B. Abdelaal, and R. Kerry Rowe
§3: Fady B. Abdelaal
§4: Charles D. Shackelford, Joseph Scalia IV, Gemmina Di Emidio, Mario Manassero, Craig H. Benson, and Takeshi Katsumi
§5: R. Kerry Rowe
§6: R. Kerry Rowe and Malek Bouazza
§7: Kelvin Legge, Ennio Palmeira, and Tony Zhan
§8: Ennio M. Palmeira, Maria G. Gardoni and Denys Parra
§9: R. Kerry Rowe
§10: Tony Zhan, Stephan Jefferis, Evelina Fratalocchi, and Jeffrey C. Evans
§11: Stephan Jefferis
§12: Stephan Jefferis
§13: Stephan Jefferis
§14: Andrea Dominijanni and R .Kerry Rowe
§15: R. Kerry Rowe and Stephan Jefferis

As far as possible, the lead authors have endeavoured to revise, and integrate the various contributions to provide a consistent narrative. Opinions presented within the paper are those the lead authors and not necessarily shared by all those who contributed to the paper.

The authors are grateful for the careful reviews of portions of this paper conducted by Anna Norris of Colorado State University and Nicolò Guarena of the Politecnico di Torino, and for the contributions from Michela De Camillis and Khizar Khan at Ghent University.

The proof-reading skills of Drs. F. Abdelaal, A. Bouazza, A. V. DiBattista, Dominijanni, K. Legge, E. Palmeira, J. Scheirs, C. Shackelford, and Queen's University PhD students: Ahmad Al Shafie, Antara Arif, Farah Barakat, Mathew Clinton, Yunhui Fan, YuYan Li, Samuel Makinde, Juliana Reinert, Rodrigo e Silva, Jose e Silva, Michael Somuah, and Mohsen Zafari are greatly appreciated.

The assistance of Dr. Natalie Touze with the French abstract is also very greatly appreciated.

17 APPENDIX: NOTATION

AL	Attenuation layer	MFI (MFR)	Melt Flow Index (also known as Melt Flow Rate)
BFE	Blown Film Extrusion	MSB	Multiswellable bentonite
BPA	BisPhenolA	MSW	Municipal solid waste
BPC	Bentonite polymer composite	MWD	Molecular Weight Distribution
BTEX	Benzene, Toluene, Ethylbenzene, Xylenes	N	Total porosity of the bentonite
CaB	Calcium bentonite	NaB	Sodium bentonite
CBSC	Capillary Barrier Soil Cover	$N_{l,AV}$,	Average number of layers or lamellae per tactoid
c_i	Molar concentration of ionic species *i*	NMR	Nuclear magnetic resonance
CCL	Compacted Clay Liner	OIT	Oxidative Induction Time (often used for Std-OIT)
COC	Cyclic organic carbonate compounds	P	Probability leakage will exceed the specific Q
c_p	Peak concentration in the aquifer for the PFOS leakage case examined	PBDE	PolyBrominated Diphenyl Ether
DTP	Diene terpolymer (additive to increase SCR)	PC	Propylene carbonate
D^*_ω	Osmotic effective diffusion coefficient	PCB	PolyChlorinated Biphenyls
E	Void ratio of the bentonite = $n/(1 – n)$	PERT	Polyethylene for Raised Temperature
EB	Enhanced bentonite	PFAS	Per- and PolyFluoroAlkyl Substances
EB-GCL	Enhanced Bentonite GCL	PFOA	PerFluoroOctanoic Acid
FBE	Flat Bed (also known as slot die or flat die) extrusion	PFOS	PerFluoroOctane Sulfonate
FRR	Flow Rate Ratio (ratio of MFI at two loads; typically 21.6 and 2.16 kg)	P_g	Permeation coefficient through a geomembrane ($P_g = D_g \times S_{gf}$)
FTIR	Fourier-transform infrared	POP	Persistent Organic Pollutant
GC	Glycerol carbonate	Ppb	Parts per billion
GCD	GeoComposite Drain	PVF	Pore volumes of flow
GCL	Geosynthetic clay liner	Q	Leakage through a hole in a wrinkle (lphd)
GMB	Geomembrane	QUELTS	Queen's University Environmental Liner Test Site
GTX	Geotextile	RSA	Republic of South Africa
HAS (HALS)	Hindered Amine Stabilizers (also known as Hindered Amine Light Stabilizers)	SAP	Ssodium polyacrylate
HC	HYPER clay	SCR	Stress Crack Resistance
HDPE	High Density Polyethylene	SCR_o	Initial Stress Crack Resistance
HFWC	High-Food-Waste-Content	SCR_m	Representative Stress Crack Resistance
HP-OIT	OIT test performed at 150ºC as per ASTM D5885 to detect retained stabilizer content.	SEM	Scanning electron microscopy
I	Ionic strength = $½\sum c_i z_i^2$ summed over all ionic species	S_{gf}	Partitioning coefficient
K	Hydraulic conductivity	Std-OIT	OIT test performed at 200ºC as per ASTM D3895 to detect retained antioxidants.
k_w	Hydraulic conductivity with respect to water	NCTL	Single Point-Notched Constant Load Test
LCS	Leachate Collection System	UK	United Kingdom
LDS	Leak detection system	USA	Unied States of America
LFG	LandFill Gas	UV	Ultra-violet radiation
LFWC	Low-Food-Waste-Content	XRD	X-ray diffraction
LLDPE	Linear Low Density Polyethylene	θ	GMB-GCL interface transmissivity (m^2/s)
lphd	Litres Per Hectare per Day	τ_m	Dimensionless matrix tortuosity factor
L_w	Length of a wrinkle with a hole per hectare for the PFOS leakage case examined	ω_i	Membrane efficiency coefficient
MDL	Method Detection Limit	z_i	Charge of ionic species *i*
MDPE	Medium Density Polyethylene	*§*	Section of this paper

18 REFERENCES

Abdelaal, F.B., and Solanki, R., 2021. Shear strength of the geomembrane–subgrade interface in heap leaching applications. Environmental Geotechnics, 40:1-17.

Abdelaal, F.B., Rowe, R.K., and Brachman, R. 2014. Brittle rupture of an aged HDPE geomembrane at local gravel indentations under simulated field conditions. Geosynthetics International 21(1), 1-23.

Abdelaal, F. Rowe, R.K., Hsuan, Y., and Awad, R. 2015. Effect of high temperatures on the physical and mechanical properties of HDPE geomembranes in air. Geosynthetics International 22(3), 207-224.

AbdelRazek, A., and Rowe, R.K. 2019. Performance of GCLs in high salinity impoundment applications. Geosynthetics International 26(6), 611-628.

Acikel, A., Bouazza, A., Gates, W., Singh, R., and Rowe, R.K. 2020. A novel transient gravimetric monitoring technique implemented to GCL osmotic suction control. Geotextiles and Geomembranes 48(6),755-767.

Acikel, A., Bouazza, A., Singh, R. M., Gates, W. P. and Rowe, R.K. 2022. Challenges of the filter paper suction measurements of geosynthetic clay liners: method, time, capillarity, and hysteresis. Geotechnical Testing Journal (in press).

Acikel, A., Gates, W. , Singh, R., Bouazza, A., Fredlund, D., and Rowe, R.K. 2018b. Time-dependent unsaturated behaviour of geosynthetic clay liners. Canadian Geotechnical Journal 55(12), 1824-1836.

Acikel, A., Gates, W., Singh, R., Bouazza, A., and Rowe, R.K. 2018a. Insufficient initial hydration of GCLs from some subgrades: factors and causes. Geotextiles and Geomembranes 46, 770-781.

Acikel, A. , Rowe, R.K., and McWatters, R. 2021. Unsaturated behaviour and cation self-diffusion of geosynthetic clay liners in Antarctica. Geosynthetics International 28(4), 350-367.

Acikel, A., Singh, R., Bouazza, A., Gates, W., and Rowe, R.K. 2015. Applicability and accuracy of the initially dry and initially wet contact filter paper tests for matric suction measurement of geosynthetic clay liners. Géotechnique 65, 780-787.

Addis, P., Andruchow, B., and Wislesky, I. 2016. Bituminous geomembrane failure at a co-disposal tailings storage facility. Proc. Tailings and Mine Waste, Banff, AB, Canada, 9 p.

Adshead, D., Román García, O., Thacker, S. and Hall, J.W. 2021. Infrastructure strategies for achieving the global development agenda in small islands. Earth's Future, 9(2).

Ali, M., Bouazza, A. Singh, R., Gates W., and Rowe, R.K. 2016. Thermal conductivity of geosynthetic clay liners. Canadian Geotechnical Journal 53(9), 1510-1521.

Alphabet Inc. 2019. Google Earth image, https://bitly.com/

Al-Tarawneh, K., Buzzi, O., Krabbenhøft, K., Lyamin, A., Sloan, S. 2009. An indirect approach for correlation of permeability and diffusion coefficients. Defect and Diffusion Forum 283-286, 504-514.

Anderson, R., Rayhani, M., and Rowe, R.K. 2012. Laboratory investigation of GCL hydration from clayey sand subsoil. Geotextiles and Geomembranes 31, 31-38.

Ashe, L. Rowe, R.K., Brachman, R.W.I. and Take, W.A. 2014. Laboratory simulation of bentonite erosion by downslope flow of a GCL, ASCE Journal of Geotechnical and Geoenvironmental Engineering, 140 (8): 04014044-1 to 04014044-9 DOI: 10.1061/(ASCE)GT.1943-5606.000114

Ashe, L. Rowe, R.K., Brachman, R., and Take, W.A. 2015. Laboratory study of downslope erosion for ten different GCLs. Journal of Geotechnical and Geoenvironmental Engineering 141(1), 04014079.

Ashmawy, A., El-Hajji, D., Sotelo, N., and Muhammad, N. 2002. Hydraulic performance of untreated and polymer-treated bentonite in inorganic landfill leachates. Clays and Clay Minerals 50(5), 546-552.

ASTM D3895. Standard test method for oxidative induction time of polyolefinsby differential scanning calorimetry, ASTM International, West Conshohocken, Pennsylvania, USA.

ASTM D4318 2017. Standard test method for liquid limit, plastic limit, and plasticity index of soils, ASTM International, West Conshohoken, Pennsylvania, USA.

ASTM D4703. Standard practice for compression molding thermoplastic materials into test specimens, plaques, or sheets, ASTM International, West Conshohoken, Pennsylvania, USA.

ASTM D4839 2017. Standard test method for total carbon and organic carbon in water by ultraviolet, or persulfate oxidation, or both, and infrared detection, ASTM International, West Conshohoken, Pennsylvania, USA.

ASTM D5101 2017. Standard test method for measuring the filtration compatibility of soil-geotextile systems clogging potential, ASTM International, West Conshohoken, Pennsylvania, USA.

ASTM D5397. Standard test method for evaluation of stress crack resistance of polyolefin geomembranes using notched constant tensile load test, ASTM International, West Conshohoken, Pennsylvania, USA.

ASTM D5514. Standard test method for large-scale hydrostatic puncture testing of geosynthetics, ASTM International, West Conshohoken, Pennsylvania, USA.

ASTM D5885. Standard test method for oxidative induction time of polyolefin geosynthetics by high pressure differential scanning calorimetry, ASTM International, West Conshohoken, Pennsylvania, USA.

ASTM D5890 2019. Standard test method for swell index of clay mineral component of geosynthetic clay liners, ASTM International, West Conshohoken, Pennsylvania, USA.

ASTM D6693. Standard test method for determining tensile properties of non-reinforced polyethylene and nonreinforced flexible polypropylene geomembranes, ASTM International, West Conshohoken, Pennsylvania, USA.

ASTM D6766 2020. Standard test method for evaluation of hydraulic properties of geosynthetic clay liners permeated with potentially incompatible aqueous solutions, ASTM International, West Conshohoken, Pennsylvania, USA.

ASTM D8117. Standard test method for oxidative induction time of polyolefin geosynthetics by differential sanning calorimetry, ASTM International, West Conshohoken, Pennsylvania, USA.

ASTM E1739 . Standard guide for risk-based corrective action applied at petroleum release sites, ASTM International, West Conshohoken, Pennsylvania, USA.

ASTM 2000. E2081 – 00. Standard guide for risk-based corrective action, Technical report, West Conshohocken, PA.

Athanassopoulos, C., Benson, C., Donovan, M., and Chen, J. 2015. Hydraulic conductivity of a polymer-modified GCL permeated with high pH solutions. Geosynthetics 2015, IFAI, Roseville, Minnesota, USA, 181-186.

Azad, F., El-Zein, A., Rowe, R.K., and Airey, D. 2012. Modelling of thermally induced desiccation of geosynthetic clay liners in double composite liner systems. Geotextiles and Geomembranes 34, 28-28.

Azad, F., Rowe, R.K., El-Zein, A., and Airey, D. 2011. Laboratory investigation of thermally induced desiccation of GCLs in double composite liner systems.Geotextiles and Geomembranes 29(6),534-543

Bahram, M., Mohseni, N., and Moghtader, M. 2016. An introduction to hydrogels and some recent applications. Emerging Concepts in Analysis and Applications of Hydrogels, Majee, Ed., IntechOpen. DOI: 10.5772/64301.

Ball, J. 2002. Milestones towards minimum requirements. Proc. International Waste Congress IWMSA, August, Durban, South Africa.

BAM 2015. Guidelines for the certification of protection layers for geomembranes in landfill sealing systems, Issued by Division 4.3, Contaminant Transfer and Environmental Technologies, Germany.

Bannour, H., Barral, C., and Touze-Foltz, N. 2013. Flow rate in composite liners including GCLs and bituminous geomembranes. 3rd International Conference on Geotechnical Engineering (ICGE'13), Feb. 21-23, Hammamet, Tunisia, 21-23.

Barr, K.M.H., Berry, C.W. and Parker P.J. 2015. The use of a composite HDPE membrane/ bentonite-cement slurry trench cut-off at Broadwood Loch, Cumbernauld, In The prospect for reservoirs in the 21st Century, Tedd, P. (ed), ICE Publishing.

Barlow L, Malusis, M. 2018. Assessment of backfill hydraulic conductivity in an instrumented soil- bentonite cut-off wall. Faculty Conf. Papers and Presentations. 46.

Barroso, M., Touze-Foltz, N., and Saisi, F. 2006. Validation of the use of filter paper suction measurements for the determination of GCL water retention curves. Proc., 8th International Conference on Geosynthetics, Millpress, Rotterdam, The Netherlands, 171-174.

Beck, A. 2015. Available technologies to approach zero leaks. Geosynthetics 2015, Feb. 15-18, 2015, Portland, Oregon, IFAI, Roseville, Minnesota, USA.

Beddoe, R., Take, W., and Rowe, R.K. 2010. Development of suction measurement techniques to quantify the water retention behaviour of GCLs. Geosynthetics International 17(5), 301-312.

Beddoe, R., Take, W., and Rowe, R.K. 2011. Water retention behaviour of geosynthetic clay liners. Journal of Geotechnical and Geoenvironmental Engineering 137(11), 1028-1038.

Beirigo, E. 2005. Filter behaviour of geotextiles in tailings dams, MSc. thesis, Graduate Programme of Geotechnics, University of Brasilia, Brasilia, Brazil (in Portuguese).

Bellomo, N., and Preziosi, L. 1995. Modelling Mathematical Methods and Scientific Computation, CRC Press, USA.

Benson, C., Chen, J., and Edil, T. 2014. Engineering properties of geosynthetic clay liners permeated with coal combustion product leachates, Report No. 3002003770, Electric Power Research Institute (EPRI), Palo Alto, California, USA.

Benson, C., Jo, H., and Musso, T. 2015. Hydraulic conductivity of organoclay and organoclay-sand mixtures to fuels and organic liquids. Journal of Geotechnical and Geoenvironmental Engineering 141(2), 04014094.

Benson, C., Kucukkirca, I., and Scalia, J. 2010a. Properties of geosynthetics exhumed from a final cover at a solid waste landfill. Geotextiles and Geomembranes 28(6), 536-546.

Benson, C., and Meer, S. 2009. Relative abundance of monovalent and divalent cations and the impact of desiccation on geosynthetic clay liners. Journal of Geotechnical and Geoenvironmental Engineering 135(3), 349-358.

Benson, C., Oren, A., and Gates, W. 2010b. Hydraulic conductivity of two geosynthetic clay liners permeated with a hyperalkaline solution. Geotextiles and Geomembranes 28(2), 206-218.

Berube, D., Diebe, P., Rollin, A., and Stark, T. 2007. Massive mining evapouration ponds. Geosynthetics, IFAI, Roseville, Minnesota, USA, 27-33.

Block, K.A., Katz, A., Alimova, A., Trusiak, A., Morales, J., Wei, H., Bucher, D., and Gottlieb, P. 2016. Montmorillonite-mediated aggregation induces deformation of influenza virus particles. Applied Clay Science 124-125, 211-218.

Blond, E. and Breul, B. 2014. Behaviour of bituminous geomembranes under elevated-compression stress. Proc. Geosynthetics Mining Solutions, Vancouver, British Columbia, Canada, 325-337.

Bohnhoff, G. 2012. Membrane behaviour, diffusion, and compatibility of a polymerized bentonite for containment barrier applications, Ph.D. dissertation, Colorado State University, Fort Collins, Colorado, USA.

Bohnhoff, G., and Shackelford, C. 2013. Improving membrane performance via bentonite polymer nanocomposite. Applied Clay Science 86, 83-98.

Bohnhoff, G., and Shackelford, C. 2014. Hydraulic conductivity of chemically modified bentonites for containment barriers. Proc., 7th International Conference on Environmental Geotechnics, A. Bouazza, S. Yuen, and B. Brown, Eds., Engineers Australia, Melbourne, Australia, 440-447 (ISBN 978-1-922107-23-7).

Bohnhoff, G., and Shackelford, C. 2015. Salt diffusion through a bentonite-polymer composite. Clays and Clay Minerals 3, 145-162.

Bohnhoff, G., Shackelford, C., Malusis, M., Scalia, J., Benson, C., Edil, T., Di Emiddio, G., Katsumi, T., and Mazzieri, F. 2013. Novel bentonites for containment barrier applications. Proc., 18th International Conference on Soil Mechanics and Geotechnical Engineering-Challenges and Innovations in Geotechnics, P. Delage, J. Desrues, R. Frank, A. Puech, F. Schlosser, Eds., Presses des Ponts, Paris, Vol. 4, 2997-3000.

Bohnhoff, G., Shackelford, C., and Sample-Lord, K. 2014. Calcium resistant membrane behaviour of a polymerized bentonite. Journal of Geotechnical and Geoenvironmental Engineering 140(3), 04013029.

Bokobza, L. 2018. Spectroscopic techniques for the characterization of polymer nanocomposites: a review. Polymers 10, 7.

Bostwick, L., Rowe, R.K., Take, W.A., and Brachman, R. 2010. Anisotropy and directional shrinkage of geosynthetic clay liners. Geosynthetics International 17(3),157-170.

Botelho, C. 2019. Behaviour of waterproof barriers and leak detection for risk management in vanadium mining tailings dam, Ph.D. dissertation, Federal University of Bahia, Bahia, Brazil (in Portuguese).

Bouazza, A. 2002. Geosynthetic clay liners. Geotextiles and Geomembranes 20(1), 3-17.

Bouazza, A. 2021. Interaction between PFASs and geosynthetic liners: current status and the way forward. Geosynthetics International, 28(2), 214-223.

Bouazza, A., Ali, M., Gates W., and Rowe, R.K. 2017a. New insight on geosynthetic clay liner hydration: the key role of subsoils mineralogy. Geosynthetics International 24(2),139-150.

Bouazza, A., and Bowders, J., 2010. Geosynthetic clay liners for waste containment facilities, CRC Press Balkema, Leiden, The Netherlands.

Bouazza, A., and Gates, W. 2014. Overview of performance compatibility issues of GCLs with respect to leachates of extreme chemistry. Geosynthetics International 21(2), 151-167.

Bouazza, A., Jefferis, S., and Vangpaisal, T. 2007. Investigation of the effects and degree of calcium exchange on the Atterberg limits and swelling of geosynthetic clay liners when subjected to wet–dry cycles. Geotextiles and Geomembranes 25(3), 170-185.

Bouazza, A., Rouf, M., Singh, R., Rowe, R., and Gates W. 2017b. Gas diffusion and permeability for geosynthetic clay liners with powder and granular bentonites. Geosynthetics International 24(6), 604-614.

Bouazza, A., Singh, R., Rowe, R., and Gassner. F. 2014. Heat and moisture migration in a geomembrane-GCL composite liner subjected to high temperatures and low vertical stresses. Geotextiles and Geomembranes 42(5), 555-563.

Bouazza, A., Vangpaisal, T., and Jefferis, S. 2006. Effect of wet-dry cycles and cation exchange on gas permeability of geosynthetic clay liners. Journal of Geotechnical and Geoenvironmental Engineering 132(8), 1011-1018.

Brachman, R., and Gudina, S. 2008. Geomembrane strains and wrinkle deformations in a GM/GCL composite liner. Geotextiles and Geomembranes 26(6), 488-497.

Brachman, R., Rentz, A., Rowe, R.K., and Take W.A. 2015. Classification and quantification of downslope erosion from a GCL when covered only by a black geomembrane. Canadian Geotechnical Journal 52(4), 395-412.

Brachman, R.W.I., Rowe, R.K. and Irfan 2014. Short-Term Local Tensile Strains in HDPE Heap Leach Geomembranes from Coarse Overliner Materials. ASCE J. of Geotech. and Geoenvir. Engineering, 140(5): 04014011-1 to 04014011-8.

Brachman, R.W.I, Joshi, P., and Rowe, R.K. 2016. “Hydraulic performance of overlapped geosynthetic clay liner seams requiring field-applied supplemental bentonite” ASCE Journal of Geotechnical and Geoenvironmental Engineering, 142 (12): 4016067-1 to 11.

Brachman, R., Rowe, R.K., and Take, W.A. 2018. Reductions in GCL overlap beneath an exposed geomembrane. Journal of Geotechnical and Geoenvironmental Engineering 144(12), 04018094.

Bradshaw, S., Benson, C., and Scalia, J. 2013. Hydration and cation exchange during subgrade hydration and effect on hydraulic conductivity of geosynthetic clay liners. Journal of Geotechnical and Geoenvironmental Engineering 139(4), 526-538.

Breen, C. 1999. The characterization and use of polycation-exchanged bentonites. Applied Clay Science 15, 187-219.

Breitenbach, A., and Smith, M. 2007. Geomembrane raincoat liners in the mining heap leach industry. Geosynthetics, IFAI, Roseville, Minnesota, USA, 32-39.

Breul, B., Reinson, J., Eldridge, T., Stenson G., and Harmon, A. 2006. Bituminous geomembrane in extremely cold conditions. Proc., 8ICG, September 18-22, Yokohama, Japan, Millpress, Rotterdam, Netherlands, 395-398.

Brice, G.J. and Woodward, J.C. 1984. Arab Potash Solar Evaporation System: Design and development of a novel membrane cut-off wall. Procedure. Instn, Civil Engrs, Part 1, 1984, 76., Feb., 185-205.

Brink, D., Shamrock, J., Nortje, R., Johns, J., and Msiza, J. 2009. Some pitfalls in the design of lining and capping systems for landfills. Landfill Interest Group Conference, Western Cape, South Africa.

Brianzoni, V., Fratalocchi, E., Pasqualini, E. 2013. Long-term performance of cement-bentonite cut-offs in saline and acidic solutions. Proc. 18th ICSMGE: Challenges and Innovations in Geotechnics, Vol. 4, 3001–3004.

Brinkmann, F.J.J. 1981. Lekkerkerk, Studies in Environmental Science, Elsevier, Volume 17, 1049-1051.

Buchholz, F., and Graham, A. 1998. Modern superabsorbent polymer technology, Wiley-VCH, New York.

Building Research Establishment (BRE) 2005. Special Digest 1 Concrete in aggressive ground, 3rd edn, Watford.

Building Research Establishment (BRE). 2011. DG 522. Hardcore for supporting ground floors of buildings: Part 1. Selecting and specifying materials, Watford.

Calligari, P., Bobone, S., Ricci, G., and Bocedi, A. 2020. Molecular investigation of SARS-CoV-2 proteins and their interactions with antiviral drugs. Viruses 12(4), 13 pp.

Card, G.B. 1981. Properties and performance of bentonite-cement slurries for use as hydraulic cut-offs, University of London PhD thesis, 334.

Carducci, A., Federigi, I., and Verani, M. 2013. Virus occupational exposure in solid waste processing facilities. Annals of Occupational Hygiene 57(9), 1115-1127.

Carman, P. 1956. Flow of gases through porous media, Butterworths, London.

Carnero-Guzman, G., Bouazza, A., Gates, W., Rowe, R.K. and McWatters, R. 2021. Hydration/dehydration behaviour of geosynthetic clay liners in the Antarctic environment. Geotextiles and Geomembranes,49(1),196-209.

Caron, C. 1972. Pérennité des systems argile-ciment ou bentonite-ciment dans divers types d'application. Construction Tome 27, No. 10, Paris 291-296.

Caron, C. 1973. Un nouveau style du perforation: la boue autodurcissable. Annales de l'Institut Technique du Batiment st des Travaux Publiques, Tome 26, No. 311 Paris, 1-40.

Castillo, J. 2005. Pipe deflection numerical analysis. Personal communication.

Castillo, J., Hallman, D., Byrne, P., and Parra, D. 2005. Dynamic analysis of heap leach pad under high phreatic levels. Proc., XXVII Convención Minera, Instituto de Ingenieros de Minas del Perú, Arequipa, Peru.

César, C., Mendoza, J., and Parra, D. 2013. Heap leach pad design in very aggressive terrains. Proc., Heap Leach Solutions 2013, pp. 291-303, Vancouver, Canada.

Chai, J., and Prongmanee, N. 2020. Barrier properties of a geosynthetic clay liner using polymerized sodium bentonite. Geotextiles and Geomembranes 48, 392-399.

Chambers, D., and Bowker, L. 2017. In the dark shadow of the supercycle tilings failure risk and public liability reach all time highs. Journal of Environments 4, p. 76.

Chappel, M., Brachman, R., Take, W.A., and Rowe, R.K. 2012a. Large-scale quantification of wrinkles in a smooth, black, HDPE geomembrane. Journal of Geotechnical and Geoenvironmental Engineering 138(6), 671-679.

Chappel, M., Rowe, R.K., Brachman, R., and Take, W.A. 2012b. A comparison of geomembrane wrinkles for nine field cases. Geosynthetics International 19(6), 453-469.

Chen, J, Benson, C., Likos, W., and Edil, T. 2017. Interface shear strength of a bentonite-polymer geosynthetic clay liner and a textured geomembrane. Proc. GeoFrontiers, ASCE, Reston, Virginia, USA, 219–226.

Chen, J., Benson, C., Edil, T., and Likos, W. 2018. Hydraulic conductivity of geosynthetic clay liners with sodium bentonite to coal combustion product leachates. Journal of Geotechnical and Geoenvironmental Engineering 144(3), 0401800.

Chen, Y., Li, J., Yang, C., Zhu, B., and Zhan, L. 2017. Centrifuge modeling of municipal solid waste landfill failures induced by rising water levels. Canadian Geotechnical Journal 54(12), 1739-1751.

Chen, Y., Liu, X., Xu, W., et al. 2019. Analysis on stabilization characteristics and exploitability of landfilled municipal solid waste: Case of a typical landfill in China. SCIENCE CHINA Technological Science 49, 199–211, (in Chinese).

Chen, J., Salihoglu, H., Benson, C., Likos, W., and Edil, T. 2019. Hydraulic conductivity of bentonite-polymer composite geosynthetic clay liners permeated with coal combustion product leachates. Journal of Geotechnical and Geoenvironmental Engineering 145(9), 04019038.

Chen Y., Xu, W., Ling, D., Zhan, L., and Gao, W. 2020. A degradation–consolidation model for the stabilization behaviour of landfilled municipal solid waste. Computers and Geotechnics 118, 103341.

Chen Y., Zhan, L., and Gao, W. 2018. Waste mechanics and sustainable landfilling technology: comparison between HFWC and LFWC MSWs. Proc., 8th International Congress on Environmental Geotechnics, Vol.1, 3-37.

Chen G-N, Cleall PJ, Li Y-C, Yu Z-X, Ke H, Chen Y-M. 2018. Decoupled advection-dispersion method for determining wall thickness of slurry trench cut-off walls. International Journal of Geomechanics-ASCE, 18(5):06018007.

Chou, Y., Rowe, R.K., and Brachman, W. 2018. Erosion of silty sand tailings through a geomembrane defect under filter incompatible conditions. Canadian Geotechnical Journal 55(11), 1564-1575.

Chou, Y-C, Brachman, R.W.I and Rowe, R.K 2021. "Leakage through a hole in a geomembrane beneath a fine-grained tailings", Canadian Geotechnical Journal, DOI: 10.1139/cgj-2020-0289

Christian, W., Zainab, B., Tian, K., and Abichou, T. 2020. Effect of specimen preparation on the swell index of bentonite-polymer GCLs. Geotextiles and Geomembranes (in press).

Clinton, M., and Rowe, R.K. 2017. Physical performance of a bituminous geomembrane for use as a basal liner in heap leach pads. Proc., 70th Can. Geotech. Conference, Ottawa, Canada.

Cnudde, V., and Boone, M. 2013. High-resolution x-ray computed tomography in geosciences: a review of the current technology and applications. Earth-Science Reviews 123(8), 1-17.

Daniel, D.E. 1993. Introduction. In: Daniel, D.E. (Ed.), Geotechnical practice for waste disposal, Chapman and Hall, United Kingdom, 33-65.

Daniel, D., Bowders, J., and Gilbert, R. 1997. Laboratory hydraulic conductivity testing of GCLs in flexible-wall permeameters. Testing and Acceptance Criteria for Geosynthetic Clay Liners, L. Well, Ed., ASTM STP 1308, 208-226.

De Camillis, M. 2017. Experimental and numerical study of wet and dry cycles on an innovative polymer treated clay for geosynthetic clay liners, PhD dissertation, Ghent University, Ghent, Belgium.

De Camillis, M., Di Emidio, G., Bezuijen, A., and Verastegui-Flores, R. 2016. Hydraulic conductivity and swelling of a polymer modified bentonite subjected to wet-dry cycles in seawater. Geotextiles and Geomembranes 44, 739-747.

De Camillis, M., Di Emidio, G., Bezuijen, A., Verastegui Flores, D., Van Stappen, J., and Cnudde, V. 2017. Effect of wet-dry cycles on polymer treated bentonite in seawater: Swelling ability, hydraulic conductivity and crack analysis. Applied Clay Science 142, 52-59.

De Camillis, M., Di Emidio, Verastegui-Flores, D., and G., Bezuijen, A. 2014. Polymer treated clays subject to wet-dry cycling with seawater. Proc., 7th International Conference on Environmental Geotechnics, A. Bouazza, S. Yuen, and B. Brown, Eds., Engineers Australia, Melbourne, Australia, 1002-1008 (ISBN 978-1-922107-23-7).

Department of Water Affairs and Forestry (DWAF) 1998. Minimum Requirements for Waste Disposal by Landfill 2nd Edition, Waste Management Series, ISBN 0620-22993-4.

Di Emidio, G. 2010. Hydraulic and chemico-osmotic performance of polymer treated clays, Ph.D. dissertation, University of Ghent, Ghent, Belgium.

Di Emidio, G., Mazzieri, F., Verastegui-Flores, R., Van Impe, W., and Bezuijen, A. 2015. Polymer-treated bentonite clay for chemical-resistant geosynthetic clay liners. Geosynthetics International 22(1), 125-137.

Di Emidio, G., Meeusen, J., Snoeck, D., and Verástegui Flores, R. 2019. Enhanced sustainable soils: a review. Proc., 8th International Congress on Environmental Geotechnics, L. Zhan, Y. Chen, and A. Bouazza, Eds., Springer Nature Singapore Pte Ltd., Vol. 3, 515-522.

Di Emidio, G., Van Impe, W., and Verástegui Flores, R. 2011. Advances in geosynthetic clay liners: polymer enhanced clays. Geo-Frontiers 2011, ASCE, Reston, Virginia, USA.

Di Emidio, G., Veratsegui-Flores, R., Bezuijen, A. 2013. Beneficial impact of polymer treatment on the swelling and long-term hydraulic efficiency of Ca-bentonites compared to the standard sodium activation method. Geosynthetics 2013, IFAI, Roseville, Minnesota, USA, 588-594.

Di Emidio, G., Verastegui-Flores, R., Mazzieri, F., and Dominijanni, A. 2017. Modified clays for barriers: a review. Innovative Infrastructure Solutions 2, 47.

Doll, P. 1997. Desiccation of mineral liners below landfills with heat generation. Journal of Geotechnical and Geoenvironmental Engineering 123(11), 1001-1009.

Dominijanni, A., and Manassero, M. 2021. Steady-state analysis of pollutant transport to assess landfill liner performance. Environmental Geotechnics 8(7), 480-494.

Dominijanni, A., Manassero, M., and Puma, S. 2013. Coupled chemical-hydraulic-mechanical behaviour of bentonites. Géotechnique 63(3), 191-205.

Dominijanni, A., Guarena, N., and Manassero, M. 2018. Laboratory assessment of semi-permeable properties of a natural sodium bentonite. Canadian Geotechnical Journal 55(11), 1611-1631.

Dominijanni, A., Guarena, N., and Manassero, M. 2021. Risk assessment procedure for the performance-based design of landfill lining systems and cut-off walls, Proc. 3rd International Symposium on Coupled Phenomena in Environmental Geotechnics (CPEG), 20-21

October 2021, Kyoto, Japan. Japanese Geotechnical Society Special Publication 9(5), 199-204.

Dunster, A.M., Longworth, T.I., Nixon, P.J., Lane, S.J. and Collins, R.J. 2005. BRE Information Paper IP/05. Development of sites containing expansive ferrous slags, Watford

Eden, M. 2017. Mechanisms of expansion in incinerator bottom aggregate (IBAA) used as aggregate in concrete and as fill in engineering applications. Proceedings of the 16th Euroseminar on Microscopy Applied to Building Materials, Les Diablerets, Switzerland.

Ejezie, J.O., Jefferis, S.A., Lam, C., Sedighi, M. and Syed, M.A. 2020. Permeation Behaviour of PHPA Polymer Fluids in Sand. Geotechnique,

El-Dana, A., and Breul, B. 2010. Coletanche life expectancy. Axter Coletanche.

Eldesouky, H., and Brachman, R. 2018. Calculating local geomembrane strains from a single gravel particle with thin plate theory. Geotextiles and Geomembranes 46(1), 101-110.

Elges, H. 1985. Problem soils in South Africa – state of the art dispersive soils. The Civil Engineer in South Africa, July 1985.

El-Sebaii, A., Aboul-Enein, S., Ramadan, M., and Khallaf, A. 2011. Thermal performance of an active single basin solar still (ASBS) coupled to shallow solar pond (SSP). Desalination 280 (1), 183-190.

EPA 2001. Geosynthetic clay liners used in municipal waste landfills, EPA530-F-97-002 (Revised Issue), US Environmental Protection Agency, Washington, D.C. (http://www.epa.gov/garbage/landfill/geosyn.pdf).

Esford, F., and Janssens, G. 2014. Laboratory test results on a bituminous liner exposed to a weak acidic solution. Proc., Geosynthetics Mining Solutions, Vancouver, Canada. 10 pp.

Estrin, D., and Rowe, R.K. 1995. Landfill design and the regulatory system. Proc. 5th International Landfill Symposium, Sardinia, Italy, Vol. 3, 15-26.

Evans, J. C. 1994. Hydraulic conductivity of vertical cut-off walls. Hydraulic Conductivity and Waste Containment Transport in Soil, ASTM, Philadelphia, 79-94.

Evans, J. C., Costa, M. J., and Cooley, B. 1995. The state-of-stress in soil-bentonite slurry trench cut-off walls. Geoenvironment 2000: Characterization, Containment, Remediation, and Performance in Environmental Geotechnics, ASCE, Geotechnical Specialty Publication, New York, NY, 1173-1191.

Evans, J.C. and Dawson, A.R., 1999, December. Slurry walls for control of contaminant migration: A comparison of UK and US practices. In Geo-Engineering for Underground Facilities (pp. 105-120). ASCE.

Evans, J.C., Fang, H.Y. and Kugelman, I.J., 1985. November. Containment of hazardous materials with soil-bentonite slurry walls. In Proceedings of the 6th National Conf. on the Management of Uncontrolled Hazardous Waste Sites, 249-252.

Evans, J.C. and Jefferis, S.A. 2014. Volume change characteristics of cut-off wall materials, Proc. 7th Int. Congress on Environmental Geotechnics, Melbourne.

Evans, J.C., Larrahondo, J.M. and Yeboah, N. 2020. 2020. Fate of bentonite in slag-cement-bentonite slurry trench cut-off walls. Proceedings of the Institution of Civil Engineers -Environmental Geotechnics, 2020. (ahead of print).

Evans J. C., Ororbia M., Gutelius J., Ruffing D., Barlow L., Malusis M. 2017. Soil-bentonite slurry trench cut-off wall lateral deformations, consolidation, stress transfer and hydraulic conductivity, Proceedings of the 2nd Symposium on Coupled Phenomena in Environmental Geotechnics (CPEG2), Leeds, UK 2.

Evans, J.C., Prince, M.J. and Adams, T.L. 1997. Metals attenuation in minerally-enhanced slurry walls. No. CONF-970208--PROC.

Evans, J.C., Ruffing, D. and Elton, D. 2021 Fundamentals of Ground Improvement Engineering. CRC Press, London, p430.

Ewais, A., Rowe, R.K., Brachman, R., and Arnepalli, D. 2014a. Service-life of a high-density polyethylene geomembrane under simulated landfill conditions at 85oC. Journal of Geotechnical and Geoenvironmental Engineering 140(11), 04014060.

Ewais, A., Rowe, R.K., and Scheirs, J. 2014b. Degradation of 2.4 mm HDPE geomembrane with high residual HP-OIT. 10th International Conference on Geosynthetics, Berlin, Germany.

Fan, J-Y and Rowe, R.K. 2021. "Seepage through a Circular Geomembrane Hole when covered by Fine-Grained Tailings under Filter Incompatible Conditions" Canadian Geotechnical Journal, (in press). http://dx.doi.org/10.1139/cgj-2020-0788

Fan, J-Y and Rowe, R.K. 2022. "Piping of silty sand tailings through a circular geomembrane hole". Geotextiles and Geomembranes (in press).

Fan, J-Y, Rowe, R.K., and Brachman, R.W.I. 2022. "Compressibility and Permeability of Sand-Silt Tailings Mixtures", Canadian Geotechnical Journal, https://doi.org/10.1139/cgj-2021-0356

Fan, R., Reddy, K., Yang, Y., and Du, Y. 2020. Index properties, hydraulic conductivity and contaminant-compatibility of CMC-treated sodium activated calcium bentonite. International Journal of Environment Research and Public Health 17, Article 1863.

Fannin, R., Palmeira, E., Atitep Srikongsri, and Gardoni, M. 2008. Interpretation of the gradient ratio test for geotextile filtration design. Proc., 1st Pan American Geosynthetics Conference and Exhibition, Cancun, Mexico, 1, 95-105.

Fehervari, A., Gates, W., Bouazza, A., and Shackelford, C. 2019. Assessment of bentonite compatibility with salinity using centrifugation-based water retention. Geotechnical Testing Journal 42(2), 275-295.

Fehervari, A., Gates, W., Patti, A., Turney, T., Bouazza, A., and Rowe, R.K. 2016a. Potential hydraulic barrier performance of cyclic organic carbonate modified bentonite complexes against hyper-salinity. Geotextiles and Geomembranes 44, 748-760.

Fehervari, A., Gates, W., Turney, T., Patti, A., and Bouazza, A. 2016b. Cyclic organic carbonate modification of sodium bentonite for enhanced containment of hyper saline leachates. Applied Clay Science 134, 2-12.

Fernandes, G., Palmeira, E., and Gomes, R., 2008. Performance of geosynthetic-reinforced alternative sub-ballast material in a railway track. Geosynthetics International 15(5), 311-321.

Ferreira, J. 2009. Studies on drainage and moisture content reduction of the iron ore of Carajás mine with the use of geosynthetics, MSc. dissertation, Graduate Programme of Geotechnics, University of Brasília, Brasília, DF, Brazil (in Portuguese).

Filz, G. M. 1996. Consolidation stresses in soil-bentonite backfilled trenches. The 2nd International Congress on Environmental Geotechnics, Balkema, Rotterdam, 497-502.

Filz, G.M., Adams, T. and Davidson, R.R. 2004. Stability of long trenches in sand supported by bentonite-water slurry. Journal of geotechnical and geoenvironmental engineering, 130(9), 915-921.

Filz, G.M., Evans, J.C. and Britton, J.P. 2003. Soil-bentonite hydraulic conductivity: measurement and variability. In Proceedings of the 12th Pan American Conf. on Soil Mechanics and Geotechnical Engineering, Cambridge, Mass. 22-26.

Fleming, I.R., Rowe, R.K. and Cullimore, D.R. 1999. Field observations of clogging in a landfill leachate collection system. Canadian Geotechnical Journal, 36(4):685-707.

Flynn, B., and Carter, G. 1998. Waterproofing material and method of fabrication thereof, US Patent Number: 6,537,676 B1, March.

Folwell, J., Gassner, F., and Phillips, G., 2021. Accelerated ageing testing of geomembranes for tailings liquor, https://www.ausimm.com/globalassets/conferences-and-events/mine-waste-and-tailings/abstract-82-accelerated-ageing-testing-of-geomembranes-for-tailings-liquor.pdf

Foose, G.J. 2010. A steady-state approach for evaluating the impact of solute transport through composite liners on groundwater quality. Waste Management 30(8–9), 1577-1586.

Foose, G., Benson, C., and Edil, T. 2001. Analytical equations for predicting concentration and mass flux from composite liners. Geosynthetics International 8(6), 551-575.

Fourie, A., Bouazza, A., Lupo, J., and Abrão, P. 2010. Improving the performance of mining infrastructure through the judicious use of geosynthetics. Proc., 9th International Conference on Geosynthetics, Guarujá, Brazil, 193-219.

Fowler, J., Larkins, K., and Duke, M. 2005. Dredging aerobis digested biosolids into geotextile tubes for dewatering, New Orleans East Municipal Sewage Treatment Plant, New Orleans, LA. Proc., 25th Technical Conference of the Western Dredging Association, New Orleans, USA, Report No. 507, 247.

Fratalocchi, E., 1996. Hydraulic behaviour of cement-bentonite mixtures. Ph.D. Thesis, Politecnico di Torino, Turin, Italy (in Italian).

Fratalocchi, E., Brianzoni, V., Di Sante, M., Mazzieri, F., Pasqualini, E., 2013. Migration of aggressive solutions through CB walls. Proc. 1st CPEG, Coupled Phenomena in Environmental Geotechnics, Turin (Italy), Taylor and Francis Group, London, p. 243-252.

Fratalocchi, E., Brianzoni, V., Mazzieri, F., Pasqualini, E., 2016. Durability of Cement-Bentonite Cut-Off Walls in Sulphate Solutions.

ASCE GSP 275, Geo-Chicago 2016. 695-704. DOI: 10.1061/9780784480168.068.

Fratalocchi E., Domizi J. and Felici M., 2021. Migration parameters and interaction of saline solutions through cement-bentonite cutoffs. Proc. 3rd CPEG, Kyoto, Japan.

Fratalocchi, E., Domizi, J., Mazzieri, F., 2019. Hydraulic Conductivity and Sorption Capacity of Special Barrier Materials in Inorganic Solutions. Proc. 8th Int. Congress on Environmental Geotechnics, Hangzhou (China), Vol. 2, p. 461-469.

Fratalocchi E., Manassero M., Pasqualini, E, Roccato M. and Spanna C. 1996. Predicting hydraulic conductivity of cement-bentonite slurries. In: Environmental Geotechnics. p. 503-508, A.A. Balkema, Rotterdam, ISBN: 9054108487, Osaka (Japan), November, 5-8, 1996.

Fratalocchi, E., Pasqualini, E., 2007. Vertical barriers for site containment. Proc. XXI CGT, Turin Geotechnical Conf., Torino, Italy.

Fratalocchi, E., Pasqualini, E., Balboni, P., 2006. Performance of a cement-bentonite cut-off wall in an acidic sulphate environment. 5th ICEG (Osaka, Japan) Vol.1, 133–139.

Fratalocchi, E., Pasqualini, E., Balboni, P., Mozzi, R., 2005. Durability assessment of a confinement cut-off wall for a phosphogypsum landfill. Proc. 16th ICSMGE: Geotechnology in Harmony with the Global Environment, Vol. 4, 2257–2260.

Froneman, J., Moseneke, D., and Madlanga, J. 2015. Shoprite Checkers (Pty) Limited v Member of the Executive Council for Economic Development, Environmental Affairs and Tourism, Eastern Cape and Others (CCT 216/14) [2015] ZACC 23; 2015 (6) SA 125 (CC, 2015 (9) BCLR 1052 (CC) (30 June 2015).

Gao, W., Chen, Y., Zhan L., et al. 2015. Engineering properties for high kitchen waste content municipal solid waste. Journal of Rock Mechanics and Geotechnical Engineering 06, 646-658.

Gardoni, M., and Morais, F. 2019. Evaluation of the resistance of geomembranes aged in laboratory and exhumed from gold mining tailings dams. Proc., 8th Brazilian Conference of Geosynthetics and 9th Brazilian Conference of Environmental Geotechnics (Regeo-Geossintéticos'2019), São Carlos, SP, Brazil (in Portuguese).

Gardoni, M., and Palmeira, E. 2002. Microstructure and pore characteristics of synthetic filters under confinement. Geotechnique 52(6), 405-418.

Gardoni M., Villar L., Ferreira J., and Monteiro M. 2010a. The behaviour of geosynthetics in drainage systems in Carajás mine. Proc., 6th International Congress on Environmental Geotechnics, New Delhi, India.

Gardoni, M., Villar, L., Ferreira, J., and Monteiro, M. 2010b. Laboratory study on the performance of geosynthetics drainage systems in contact with ore from Carajás mining. Proc., 9th International Conference on Geosynthetics, Guarujá, Brazil

Gassner, F. 2009. Field observation of GCL shrinkage at a site in Melbourne Australia. Geotextiles and Geomembranes 27(5), 406-408.

Gates, W.P., MacLeod, A., Fehervari, A., Bouazza, A., Gibbs, D., Hackney, R., Callahan, D.L. and Watts, M., 2020. Interactions of Per-and Polyfluoralkyl Substances (PFAS) with Landfill Liners. Advances in Environmental and Engineering Research, 1(4), 40. https://doi.org/10.21926/aeer.200400

Gates, W., Shaheen, U., Turney, T., and Patti, A. 2016. Cyclic carbonate-sodium smectite intercalates. Applied Clay Science 124-125, 94-101.

Geng, W., Likos, W., and Benson, C. 2016. Viscosity of polymer-modified bentonite as a hydraulic performance index. Geo-Chicago 2016, GSP 271, ASCE, Reston, Virginia, USA, 498-507.

Ghavam-Nasiri, A., El-Zein, A., Airey, D., Rowe, R.K. 2017. Hydration and desiccation of geosynthetic clay liners in composite lining systems under brine pond conditions: a laboratory investigation. Proceedings of the 2nd Symposium on Coupled Phenomena in Environmental Geotechnics (CPEG2), Leeds University, Leeds, UK.

Ghavam-Nasiri, A., El-Zein, A., Airey, D., Rowe, R., and Bouazza, A. 2019. Numerical simulation of geosynthetic clay liners desiccation under high thermal gradients and low overburden stress. International Journal of Geomechanics 19(7), 04019069

Ghavam-Nasiri, A., El-Zein, A., Airey, D., Rowe, R.,K. and Bouazza, A. 2020. Experimental investigation of desiccation of geosynthetic clay liners under brine pond conditions. Geosynthetics International 27(6), 593-605.

Ghazizadeh, S., Bareither, C., Scalia, J., and Shackelford, C. 2018. Synthetic mining solutions for laboratory testing of geosynthetic clay liners. Journal of Geotechnical and Geoenvironmental Engineering 144(10), 06018011.

Gilson-Beck, A. 2019. Controlling leakage through installed geomembranes using electrical leak location. Geotextiles and Geomembranes 47(5), 697-710.

Giroud, J., and Bonaparte, R. 1989a. Leakage through liners constructed with geomembranes - Part I: Geomembrane liners. Geotextiles and Geomembranes 8, 27-67.

Giroud, J., and Bonaparte, R. 1989b. Leakage through liners constructed with geomembranes - Part II: Composite liners. Geotextiles and Geomembranes 8, 71-111.

Giroud, J., and Fluet Jr., J. 1986. Quality assurance of geosynthetic lining systems. Geotextiles and Geomembranes 3(4), 249-287

Giroud, J., and Morel, N. 1992. Analysis of geomembrane wrinkles. Geotextiles and Geomembranes 11(3), 255 276 (Erratum: 12(4), 378).

Giroud, J., Tisseau, B., Soderman, K. and Beech, J. 1995. Analysis of strain concentration next to geomembrane seams. Geosynthetics International 2 (6), 1049–1097.

Gleason, M., Daniel, D., and Eykholt, G. 1997. Calcium and sodium bentonite for hydraulic containment applications. Journal of Geotechnical and Geoenvironmental Engineering 123(5), 438-445.

Goodall, D.C. and Quigley, R.M. 1977. Pollutant migration from two sanitary landfill sites near Sarnia, Ontario. Canadian Geotechnical Journal, 14(2), 223-236.

Government of Ghana Guidelines 2002. Government of Ghana Ministry of Local Government and Rural Development Environmental Protection Agency Landfill Guidelines.

Government of Ghana Guidelines 2009. Government of Ghana Ministry of Local Government and Rural Development Environmental Sanitation Policy.

Graiver, D.A., Topliff, C.L., Kelling, C.L., and Bartelt-Hunt, S.L. 2009. Survival of the avian influenza virus (H6N2) after land disposal. Environmental Science and Technology 43(11), 4063-4067.

Guarena, N., Dominijanni, A., and Manassero, M. 2020. From the design of bottom landfill liner systems to the impact assessment of contaminants on underlying aquifers. Innovative Infrastructure Solutions 5(1).\

Guner, A. 1978. The properties and behaviour of bentonite/cement slurries. University of London PhD thesis, 279.

Gularte, F., Barneich, J., Burton, J., Fordham, E., Watt, D., Johnson, T., and Weeks, J. 2007. First use of TRD construction technique for soil mix cut-off wall construction in the United States. In Designing our Underground Space 1-12.

Guo, W., Chu, J., Yan, S., and Nie, W. 2014. Analytical solutions for geosynthetic tube resting on rigid foundation. Geomechanics and Engineering 6(1), 65-77.

Gustitus, S., and Benson, C. 2020. Assessing polymer elution and hydraulic conductivity of bentonite-polymer composite geosynthetic clay liners permeated with aggressive solutions, Proc., GeoAmericas 2020, 4th Pan American Conference on Geosynthetics, Rio de Janeiro, Brazil.

Gustitus, S., and Benson, C. 2021. Flow-swell index as an indicator of chemical compatibility of bentonite-polymer composite geosynthetic clay liners. Proc., Geosynthetics 2021, IFAI, Roseville, Minnesota, USA.

Gustitus, S., Nguyen, D., Chen, J., and Benson, C. 2020. Quantifying polymer loading in bentonite-polymer composites using loss on ignition and total carbon analyses. Geotechnical Testing Journal 44(5), 1448-1466.

Guyonnet, D., Perrochet, P., Côme, B., Seguin, J.-J., and Parriaux, A. 2001. On the hydro-dispersive equivalence between multi-layered mineral barriers. Journal of Contaminant Hydrology 51(3-4), 215-231.

Haase, H., and Schanz, T. 2016. Compressibility and saturated hydraulic permeability of clay-polymer composites – experimental and theoretical analysis. Applied Clay Science 130, 62-75.

Hanson, J., Risken, J., and Yesiller, N. 2013. Moisture-suction relationships for geosynthetic clay liners. Proc., 18th International Conference on Soil Mechanics and Geotechnical Engineering-Challenges and Innovations in Geotechnics, P. Delage, J. Desrues, R. Frank, A. Puech, F. Schlosser, Eds., Presses des Ponts, Paris, 3025-3028

Hao, Z., Sun, M., Ducoste, J. and Barlaz, M. 2017.A model to describe heat generation and accumulation at municipal solid waste landfills. Proc. GeoFrontiers, ASCE, Reston, Virginia, USA, 281–288.

Harvey, R.H., and Ryan, J.N. 2004. Use of PRD1 bacteriophage in groundwater viral transport, inactivation, and attachment studies. FEMS Microbiology Ecology 49(1), 3-16.

Haug, M., and Boldt-Leppin. B. 1994. Influence of polymers on the hydraulic conductivity of marginal quality bentonite-sand mixtures. Hydraulic Conductivity and Waste Contaminant Transport in Soil, Daniel, D. and Trautwein, S., Eds., ASTM STP 1142, ASTM, West Conshohoken, Pennsylvania, USA, 407-421.

Heller, H., and Keren, R. 2002. Anionic polyacrylamide polymers effect on rheological behaviour of sodium-montmorillonite suspensions. Soil Science Society of America Journal 66(1), 19-25.

Hoai, T., and Mukunoki, T. 2020. Combined effects of ammonium permeation and dry-wet cycles on the hydraulic conductivity and internal properties of geosynthetic clay liners. Geotextiles and Geomembranes 48, 912-927.

Hofford, S. 2015. Survey of fatigue resistance quantification of asphalt mixture. International Journal of Advanced and Applied Sciences 2(1) 2015, 42-49

Hoor, A., and Rowe, R.K. 2013. Potential for desiccation of geosynthetic clay liners used in barrier systems. Journal of Geotechnical and Geoenvironmental Engineering 139(10), 1648-1664.

Hornsey, W. 2013. Performance of cushion geotextiles for liner protection applications. GeoAfrica 2013, 18-20 November, Accra, Ghana.

Hsuan, G., and Koerner, R. 2015. Rationale and background for the GRI GM13 specification for HDPE geomembranes. GSI white paper no. 32, Geosynthetic Institute, Folsom, Pennsylvania, USA.

Hu, J., Ke, H., Lan, J., Chen, Y., Meng, M. 2020a. A dual-porosity model for coupled leachate and gas flow to vertical wells in municipal solid waste landfills. Geotechnique 70(5), 406-420.

Hu, J., Ke, H., Zhan L., Chen, Z., Lan, J., Powrie, W., Chen, Y. 2020b. Installation and performance of horizontal wells for dewatering at municipal solid waste landfills in China. Waste Management 103, 159-168.

ICOLD 1986. Geotextiles as filters and transitions in fill dams, Bulletin 55, Paris, France.

ICOLD 2001. Tailings dams: risk of dangerous occurrences, lessons learnt from practical experiences, Bulletin 121, Paris, France, 144 p.

Jambeck, J., Geyer, R., Wilcox, C., Siegler, T., Perryman, M., Andrady, A., Narayan, R., and Law, K. 2015. Plastic waste inputs from land into the ocean. Science 347(6223), 768-771.

James, A., Fullerton, D., and Drake, R. 1997. Field performance of GCL under ion exchange conditions. Journal of Geotechnical Engineering 123(10), 897-901.

Jefferis, S.A., 1981. June. Bentonite-cement slurries for hydraulic cut-offs. In Proceedings, Tenth Int. Conf. on Soil Mechanics and Foundation Engineering, Stockholm, Sweden, Vol. 1, 435-440.

Jefferis, S.A. 1992. Contaminant - grout interaction, ASCE Specialty Conf., Grouting, Soil Improvement and Geosynthetics, New Orleans, February.

Jefferis, S.A. 1996. Contaminant - barrier interaction: Friend or foe?, Mineralogical Society Conf., Chemical containment of wastes in the Geosphere.

Jefferis, S.A. 1997. The origins of the slurry trench cut-off and a review of cement-bentonite cut-off walls in the UK. Proc. Intl Containment Technology Conf., St Petersburg, Florida. 9-12 February.

Jefferis, S.A. 2001. Permeability a dynamic property of barrier materials, Int. Containment and remediation technology Conf. and Exhibition, Orlando, Florida, June.

Jefferis, S.A. 2003. Long-term performance of grouts and the effects of grout by-products, ASCE Specialty Conf., Grouting and Ground Improvement, New Orleans, February.

Jefferis, S.A. 2008. Reactive transport in cut-off walls and implications for wall durability, GeoCongress 2008. Annual Conf. of the Geo-Institute of the American Society of Civil Engineers, New Orleans.

Jefferis, S.A. 2012. Cement-bentonite slurry systems, Proc. Fourth International Conference on Grouting and Deep Mixing, Deep Foundations Institute and Geo-Institute of the American Society of Civil Engineers, pp 1-24, New Orleans.

Jefferis, S.A. 2013. Some unexpected effects of natural and anthropogenic chemicals on construction, Geotechnique, March.

Jefferis, S.A. 2014. Grouts and slurries, in: The Construction Materials Reference Book, second edition, Doran, D.K. and Cather, R., Editors, Routledge.

Jefferis, S.A. 2019. Recycled crushed concrete: engineering and environmental issues. Proc. XVII European Conf on Soil Mechanics and Geotechnical Engineering. Reykjavik.

Jefferis. S.A., Doe, G. and Tedd, P., assisted by a steering group 1999. UK National Specification for cut-off walls for pollution migration control, Institution of Civil Engineers.

Jefferis, S.A. and Fernandez, A. 2000. Spanish dyke failure leads to developments in cut-off wall design, Int. Conf. on Geotechnical and Geological Engineering, Melbourne, Australia, November.

Jefferis, S.A. and Lam, C. 2018. Using density to determine the solids content of construction slurries, Proceedings of the 19th Int. Conf. on Soil Mechanics and Geotechnical Engineering, Seoul, 1695-1698.

Jefferis, S.A. 2019a. Recycled crushed concrete: engineering and environmental issues. Proc. XVII European Conf on Soil Mechanics and Geotechnical Engineering. Reykjavik.

Jefferis, S.A. 2019b. Low Permeability Vertical Barriers: The State of the Art and the Research Needs for the Future: Towards a Sustainable Geoenvironment. Proceedings of the 8th Int. Congress on Environmental Geotechnics Volume 1 212-214. 10.1007/978-981-13-2221-1_16.

Jessberger H. L., Soyez B., Manassero, M., Street A. 1991. Progress of the work of the European technical committee no.8 of ISSMFE. Milano: C.I.P.A. s.r.l., S. Margherita di Pula (CA), October, 13-15, 1993.

Jesseberger H.L., Soyez B., Manassero M., Street A. 1995. Engineering waste disposal (geotechnics of landfill design and remedial works), Key-note lecture. In: Waste disposal by landfill, Green '93. 21-33, A.A. Balkema, Rotterdam, ISBN: 9789054103561, Bolton (UK), 28 June - 1 July 1993.

Jewaskiewitz, S., 2019. Envitech Solutions (Pty) Ltd letter to the Department Environment Affairs, Forestry and Fisheries, ES560-2016-L005, 2 October.

Jia, G., Zhan, T., Chen, Y., and Fredlund, D. 2010. Influence of rainfall pattern on the infiltration into landfill earthen final cover. Advances in Environmental Geotechnics, Springer, Berlin, Heidelberg, 641-645.

Jo, H., Benson, C., and Edil, T. 2006. Rate-limited cation exchange in thin bentonitic barrier layers. Canadian Geotechnical Journal 43, 370-391.

Jo, H., Katsumi, T., Benson, C., and Edil, T. 2001. Hydraulic conductivity and swelling of nonprehydated GCLs permeated with single-species salt solutions. Journal of Geoetchnical and Geoenvrionmental Engineering 127(7), 557-567.

Joshi K, Kechavarzi C, Sutherland K, Ng M Y A, Soga K, Tedd P. 2010. Laboratory and in situ tests for long-term hydraulic conductivity of a cement-bentonite cut-off wall, Journal of Geotechnical and Geoenvironmental Engineering, 136(4):562-572.

Joshi, P., Brachman, R.W.I and Rowe, R.K. 2017 Hydraulic performance of GCL seams without field-applied supplemental bentonite below a geomembrane wrinkle, ASCE Journal of Geotechnical and Geoenvironmental Engineering, 143(9): 04017086-1 to 10, doi/10.1061/(ASCE)GT.1943-5606.0001756

Joshi, P., Rowe, R.K. and Brachman, R.W.I 2018. Hydraulic performance of GCL seams with factory-applied powered bentonite below a geomembrane wrinkle. Environmental Geotechnics, 5(5): 263-270http://dx.doi.org/10.1680/ jenge. 16 .00027

Joshi, P., Rowe, R.K. and Brachman, R.W.I 2017. “Physical and hydraulic response of geomembrane wrinkles underlying saturated fine tailings", Geosynthetics International, 24(1):82-94,http://dx.doi.org/10.1680/jgein.16.00017

Jury, W., Gardner, W., and Gardner, W. 1991. Soil physics, 5th edition, John Wiley and Sons, Inc., New York.

Kang, J., and Shackelford, C. 2011. Consolidation enhanced membrane behaviour of a geosynthetic clay liner. Geotextiles and Geomembranes 29(6), 544-556.

Karlen, A. 1995. Plague's progress, a social history of man and disease. Victor Gollancz, London.

Katsumi, T., and Fukagawa, R. 2005. Factors affecting the chemical compatibility and barrier performance of GCLs. Proc., 16th International Conference on Soil Mechanics and Geotechnical Engineering, Osaka, Japan, Sept. 12-16, 2005, Millpress, Rotterdam, The Netherlands, Vol. 4, 2285-2288.

Katsumi, T., Ishimori, H., Onikata, M., and Fukagawa, R. 2008. Long-term barrier performance of modified materials against sodium and calcium permeant solutions. Geotextiles and Geomembranes 26, 14-30.

Kaza, S., Yao, L., Bhada-Tata, P., and Van Woerden, F. 2018. What a waste 2.0: a global snapshot of solid waste management to 2050. The World Bank.

Ke H, Tong X, Li Y-C, Chen Y-M, Wen Y-D. 2018. Force-equilibrium based model for predicting stresses in soil-bentonite cut-off walls. Journal of Geotechnical and Geoenvironmental Engineering ASCE, 144(2):04017112.

Khan, M., Di Emidio, G., and Bezuijen, A. 2021. Matric suction of untreated clay and polymerised HYPER clay geosynthetic barriers. Journal of Environmental Geotechnics, Special Issue: Polymers in Geoenvironmental Engineering, under review.

Khilnani, K, Stark, T., and Bahadori, T. 2017. Comparison of single and multi-layer interface strengths for geosynthetic/geosynthetic and soil/geosynthetic interfaces. Proc., GeoFrontiers, ASCE, Reston, Virginia, USA, 42–51.

Kilbourne, E.D. 2008. Plagues and pandemics: past, present and future. In Global catastrophic risk Bostrom, N and Cirkovik, M.M. Eds Global catastrophic risk, pp 287-307, Oxford University Press.

Koerner, R. 2005. Designing with geosynthetics, 5th edition, Pearson-Prentice Hall, Englewood Cliffs, New Jersey, USA

Koerner, R. 2017. Utilizing PVDs to provide shear strength to saturated fine-grained foundation soils, GRI report no. 46, Geosynthetic Institute, Folsom, Pennsylvania, USA

Koerner, R., and Daniel, D. 1995. A suggested methodology for assessing the technical equivalency of GCLs to CCLs. Geosynthetic Clay Liners, R. Koerner, E. Gartung, and H. Zanzinger, Eds., Balkema, Rotterdam, 73-98.

Koerner, R., and Koerner, J. 2007. GRI's Second Worldwide Survey of Solid Waste Landfill Liner and Cover Systems, GRI report no. 34, Geosynthetic Institute, Folsom, Pennsylvania, USA

Koerner, G., and Koerner, R. 2017. The durability of exposed geomembrane covers. Proc., GeoFrontiers, ASCE, Reston, Virginia, USA, 139-145.

Kolstad, D., Benson, C., Edil, T., and Jo, H. 2004. Hydraulic conductivity of a dense prehydrated GCL permeated with aggressive inorganic solutions. Geosynthetics International 11(3), 233-241.

Kozeny, J. 1927. Uber kapillare leitung des wassers im boden. Sitzungsber Akad. Wiss. 136(2a), 271-306.

Kramer, H. 1946. Deep cutoff trench of puddled clay for earth dam and levee protection, Engineering News Record, 136(26), 76-80.

Lage, S., Lindner, P., Sinha, P., Kiriy, A., Stamm, M., and Huber, K., 2009. Formation of Ca2+ induced intermediate necklace structures of polyacrylate chains. Macromolecules 42, 4288- 4299.

Laird, D. 2006. Influence of layer charge on swelling of smectites. Applied Clay Science 34(1-4), 74-87.

Lam, C. and Jefferis, S. A. 2021. Effect of sorption on the active concentration of polymer support fluids, Géotechnique Letters 11, 1–6, https//doi.org/10.1680/jgele.20.00062.

Lazaro, J. and Breul, B. 2014. Bituminous geomembrane in heap leach pads. Proc., Heap Leach Solutions 2014, Info mine, Lima, Peru, 291-303.

Lebreton, L., Van Der Zwet, J., Damsteeg, J., Slat, B., Andrady, A., Kaza, S., Yao, L., Bhada-Tata, P., and Van Woerden, F. 2018. What a waste 2.0: a global snapshot of solid waste management to 2050. The World Bank.

Lebreton, L., Van Der Zwet, J., Damsteeg, J., Slat, B., Andrady, A., and Reisser, J. 2017. River plastic emissions to the world's oceans. Nature Communications 8, 15611.

Leduc, M., and Smith, M. 2004. Solution collection pipes and overstressing of geomembrane liners. The Mining Record, 22-24.

Lee, J., and Shackelford, C. 2005. Impact of bentonite quality on hydraulic conductivity of geosynthetic clay liners. Journal of Geotechnical and Geoenvironmental Engineering 131(1), 64-77.

Lee, J., Shackelford, C., Benson, C., Jo, H., and Edil, T. 2005. Correlating index properties and hydraulic conductivity of geosynthetic clay liners. Journal of Geotechnical and Geoenvironmental Engineering 131(11), 1319-1329.

Lee, S., Oren, A., Benson, C., and Dovantzis, K. 2012. Organoclays as variably permeable reactive barrier (VPRB) media to manage NAPLs in ground water. Journal of Geotechnical and Geoenvironmental Engineering 138(2), 115-127.

Legge, K. 2019, An economy and ecosystem symbiosis: barrier systems for water conservation and pollution control. International Paste Conference, Cape Town, South Africa.

Legge, K., Fricker, C., and Mnisi, K. 2015. Pollution prevention awareness for municipal managers in South Africa. SAICE Civil Engineering Magazine 23(9).

Legge, K., Fricker, C., Mnisi, K., Nemusibi, K., and Seake, B. 2014. Service life considerations of pollution control barrier systems. SAICE Civil Engineering Magazine 22(7).

Legge, K., Legg, P., and Meyer, P. 2007. Coupled solution to heat induced degradation of containment barriers. Proc., 11th International Waste Management and Landfill Symposium, 1-5 October, Sardinia, Italy.

Li, X., and Zhang, L. 2009. Characterization of dual-structure pore-size distribution of soil. Canadian Geotechnical Journal 46(2), 129-141.

Li, T., and Rowe, R.K. 2020. GCL Self-healing: fully penetrating hole/slit hydrated with RO water and 10 mM CaCl2 solution. Geosynthetics International 27(1),34-47

Li, T., and Rowe, R.K. 2022. Self-healing of laboratory eroded defects in a GCL on silty sand. Geosynthetics International (in press).

Li Y-C, Pan Q, Cleall PJ, Chen Y-M, Ke H. 2013. Stability analysis of slurry trenches in similar layered soils. Journal of Geotechnical and Geoenvironmental Engineering ASCE, 139(12):2104-2109.

Li Y-C, Cleall PJ, Wen YD, Chen YM, Pan Q. 2015. Stresses in soil-bentonite slurry trench cut-off walls. Geotechnique, 65(10: 843-850.

Li Y-C, Wei L, Cleall P J, Lan J-W. 2018. Rankine theory based approach for stability analysis of slurry trenches. International Journal of Geomechanics ASCE, 18(11):06018029.

Li, Q., Chen, J., Benson, C., and Peng, D. 2021. Hydraulic conductivity of bentonite-polymer composite geosynthetic clay liners permeated with bauxite liquor. Geotextiles and Geomembranes in press.

Lieske, W., Christ. F., Baille, W., Di Emidio, G., and Wichtmann, T. 2020. Suction and crack propagation in GCLs subjected to drying and wetting in CaCl2-solutions. Geotextiles and Geomembranes 48(6), 973-982.

Likos, W., and Lu, N. 2006. Pore-scale analysis of bulk volume change from crystalline interlayer swelling in Na+- and Ca2+-smectite. Clays and Clay Minerals 54(4), 516-529.

Likos, W., and Wayllace, A. 2010. Porosity evolution of free and confined bentonites during interlayer hydration. Clays and Clay Minerals 58(3), 399-414.

Lima, M., Azevedo, M., Zornberg, J., and Palmeira, E. 2018. Capillary barriers incorporating nonwoven geotextiles. Environmental Geotechnics 5(3), 168-175.

Lin, L., and Benson, C. 2000. Effect of wet-dry cycling on swelling and hydraulic conductivity of GCLs. Journal of Geotechnical and Geoenvironmental Engineering 126(1), 40-49.

Lipson, S.M., and Stotzky, G. 1983. Adsorption of reovirus to clay minerals: effects of cation-exchange capacity, cation saturation, and surface area. Applied and Environmental Microbiology 46(3), 673-682.

Little, A.L. 1975 in situ diaphragm walls for embankment dams. Proc. Conf. on Diaphragm walls and anchorages, Institution of Civil Engineers, London. Manassero, M. 1994. Hydraulic conductivity assessment of slurry wall using piezocone test. Journal of Geotechnical Engineering, vol. 120(10), 1725-1746, ISSN: 0733-9410.

Liu, Y., Bouazza, A., Gates, W., and Rowe, R.K. 2015. Hydraulic performance of geosynthetic clay liners to sulfuric acid solutions. Geotextiles and Geomembranes 43, 14-23.

Long, X. , Huang, Y., Chi, H., Li, Y., Ahmad, N., and Yao, H. 2018. Nitrous oxide flux, ammonia oxidizer and denitrifier abundance and activity across three different landfill cover soils in Ningbo, China. Journal of Cleaner Production 170, 288-297.

Lu, Y., Abuel-Naga, H., Leong, E., Bouazza, A., and Lock, P. 2018. Effect of water salinity on the water retention curve of geosynthetic clay liners. Geotextiles and Geomembranes 46, 707–714.

Lupo, J., and Morrison, K. 2005. Innovative geosynthetic liner design approaches and construction in the mining industry. Proc., Geo-Frontiers Congress 2005, GSP 140, Reston, Virginia, USA, 1-16.

Lupo, J. and Morrison, K. 2007. Geosynthetic design and construction approaches in the mining industry. Geotextiles and Geomembranes 25(2), 96-108

Ma, P., Ke, H., Lan, J., Chen, Y., and He, H. 2019. Field measurement of pore pressures and liquid-gas distribution using drilling and ERT in a high food waste content landfill in Guangzhou, China. Engineering Geology 250, 21-33.

Malusis, M., and Daniyarov, A. 2016. Membrane efficiency and diffusive tortuosity of a dense prehydrated geosynthetic clay liner. Geotextiles and Geomembranes 44, 719-730.

Malusis, M., Dominijanni, A., Scalia, J., Guarena, N., Sample-Lord, K., Bohnhoff, G., Shackelford, C., and Manassero, M. 2021. Assessing the influence of chemico-osmosis on solute transport in bentonite membranes based on combined phenomenological and physical modeling. 3rd International Symposium on Coupled Phenomena in Environmental Geotechnics, October 20-22, Kyoto, Japan.

Malusis, M., Kang, J., and Shackelford, C. 2013. Influence of membrane behaviour on solute diffusion through GCLs. Coupled Phenomena in Environmental Geotechnics, M. Manassero, A. Dominijanni, S. Foti, and G. Musso, Eds., July 1-3, 2013, Torino, Italy, CRC Press/Balkema, Taylor and Francis Group, London, 267-274.

Malusis, M., Kang, J., and Shackelford, C. 2015. Restricted salt diffusion in a geosynthetic clay liner. Environmental Geotechnics 2(2), 68-77.

Malusis, M., and Shackelford, C. 2002a. Chemico-osmotic efficiency of a geosynthetic clay liner. Journal of Geotechnical and Geoenvironmental Engineering 128(2), 97-106.

Malusis, M., and Shackelford, C. 2002b. Coupling effects during steady-state solute diffusion through a semipermeable clay membrane. Environmental Science and Technology 36(6), 1312-1319.

Malusis, M., Shackelford, C., and Olsen, H. 2001. A laboratory apparatus to measure chemico-osmotic efficiency coefficients for clay soils. Geotechnical Testing Journal 24(3), 229-242.

Manassero, M. 2020. Second ISSMGE R. Kerry Rowe Lecture: on the intrinsic, state, and fabric parameters of active clays for contaminant control. Canadian Geotechnical Journal 57(3), 311-336.

Manassero, M., Benson, C.H., and Bouazza, A. 2000. Solid waste containment systems. Proc. GeoEng2000, Technomic, Lancaster, PA, 1, 520-642.

Manassero, M., and Dominijanni, A. 2003. Modelling the osmosis effect on solute migration through porous media. Géotechnique 53(5), 481-492.

Manassero, M., Dominijanni, and A., and Guarena, N. 2018. Modelling hydro-chemo-mechanical behaviour of active clays through the fabric boundary surface. Proc. China-Europe Conference on Geotechnical Engineering, W. Wu and H. Yu, Eds., Springer International Publishing, Springer Nature Switzerland AG, Vol. 2, 1618-1626.

Mathur, A., Netravali, N., and O'Rourke, T. 1994. Chemical ageing effects on the physio-mechanical properties of polyester and polypropylene geotextiles. Geotextiles and Geomembranes 13(9), 591-626.

Mazzieri, F., and Di Emidio, G. 2015. Hydraulic conductivity of a dense prehydrated geosynthetic clay liner. Geosynthetics International 22(1), 138-148.

Mazzieri, F., Di Emidio, G., and Pasqualini, E. 2016. Effect of wet-and-dry ageing in seawater on the swelling properties and hydraulic conductivity of two amended bentonites. Applied Clay Science 142(6), 40-51.

Mazzieri, F., Di Emidio, G., and Van Impe, P. 2010. Diffusion of calcium chloride in a modified bentonite: Impact on osmotic efficiency and hydraulic conductivity. Clays and Clay Minerals 58(3), 351-363.

Mazzieri, F., and Pasqualini, E. 2008. Effect of dry/wet cycles and cation exchange on the permeability of a dense prehydrated GCL. Proc., Eurogeo4, Fourth International Conference on Geosynthetic, N. Dixon, Ed., Edinburgh CD-ROM, paper 125.

McLaren, A.D., and Peterson, G.H. 1965. Physical chemistry and biological chemistry of clay mineral-organic nitrogen complexes. Soil Nitrogen - Monograph 10, American Society of Agronomy, Wisconsin, 259-284.

McRory, J., and Ashmawy, A. 2005. Polymer treatment of bentonite clay for contaminant resistant barriers. Geo-Fronteirs 2005, E. Rathje, Ed., GSP 142 Waste Containment and Remediation, ASCE, Reston, Virginia, USA.

McWatters, R. and Rowe, R.K. 2010. Diffusive transport of VOCs through LLDPE and two Co-Extruded Geomembranes. Journal of Geotechnical and Geoenvironmental Engineering, 136(9): 1107-1177.

McWatters, R.S., Rowe, R.K., Wilkins, D., Spedding, T., Jones, D., Wise, L., Mets, J., Terry, D., Hince, G., Gates, W.P., Di Battista, V., Shoaib, M., Bouazza, A. and Snape, I. 2016b. Geosynthetics in Antarctica: Performance of a composite barrier system to contain hydrocarbon-contaminated soil after 3 years in the field. Geotextiles and Geomembranes, 44(5):673-685. http://dx.doi.org/10.1016/j.geotexmem.2016.06.001

McWatters, R.S., Rutter, A. and Rowe, R.K. 2016a. Geomembrane Applications for Controlling Diffusive Migration of Petroleum Hydrocarbons in Cold Region Environments. J. Environ Management, 171: 80-94; http://dx.doi.org/10.1016/j.jenvman.2016.05.065

McWatters,R.S., Rowe, R.K., Wilkins, D., Spedding, T., Hince, G., Richardson, J., and Snape, J. 2019. Modelling of vapour intrusion into a building impacted by a fuel spill in Antarctica. Journal of Environmental Management, 231 2019): 467-482. 10.1016/j.jenvman.2018.07.092.

Maillard, R. and Serota, S. 1963. Screen grouting of alluvium by the E.T.F. process, Institution of Civil Engineers Symposium on Grouts and Drilling Muds in Engineering Practice, Butterworths.

Manassero, M. 1994. Slurry wall systems - TC5 report. In: Proceedings of the First Int. Congress on Environmental Geotechnics: July 10-15, 1994. Edmonton, Alberta, Canada. Vancouver:Bi-Tech Publisher Ltd, ISBN: 0921095325, Edmonton (Canada), July, 10-15, 1994.

Manassero M. 1997. Pollutants containment via passive barriers. Opening Lecture at the Discussion Session 6.1. In: Proceedings of the 14th Int. Conf. on Soil Mechanics and Foundation Engineering, Hamburg, 6-12 September 1997. Rotterdam: A.A. Balkema, ISBN: 9789054108917, Hamburg (Germany), September, 6-12.

Manassero M., Benson C. H., Bouazza A. 2000. Solid waste containment systems - Key-note Lecture. In: GeoEng 2000: Invited Papers. vol. 1, 520-642, Lancaster: Technomic Publishing Company Inc., ISBN: 1587160676, Melbourne, Australia, November, 19-24, 2000.

Manassero M., Fratalocchi E., Pasqualini E., Spanna C., Verga F., 1995. Containment with vertical cut-off walls. ASCE Geotechnical Special Publication, (46 /2), 1142–1172.

Manassero, M., Pasqualini, E. 1992. Ground pollutant containment barriers. In: Environmental geotechnology: proceedings of the Mediterranean Conf. on Environmental Geotechnology, Cesme, Turkey, 25-27 May, 1992. A.A. Balkema, Rotterdam. ISBN: 9054100559, Cesme (Turkey), May, 25-27.

Manassero M. and Shackelford C. D. 1994. The Role of Diffusion in Contaminant Migration through Soil Barriers / Il ruolo della diffusione molecolare nella migrazione degli inquinanti attraverso le barriere minerali. Rivista Italiana di Geotecnica, vol. 1, ISSN: 0557-1405.

Manassero M., Van Impe W.F., Bouazza A. 1996. Waste disposal and containment - State of the art lecture. In: Environmental Geotechnics. A.A. Balkema, Rotterdam. ISBN: 9054108487, Osaka (Japan), November, 5-8, vol. Vol. 3, 193-242.

Manassero, M., Viola C. 1992. Innovative aspects of leachate containment with composite slurry walls; a case history. In: Slurry Walls: Design, Construction and Quality Control ASTM-STP 1129, 181-193, Philadelphia: ASTM, ISBN: 9780803114272, Atlantic City (USA), June, 27-28.

Mazur, A. 1990. A Hazardous Inquiry: The Rashomon Effect at Love Canal. Harvard University Press.

Meer, S., and Benson, C. 2007. Hydraulic conductivity of geosynthetic clay liners exhumed from landfill final covers. Journal of Geotechnical and Geoenvironmental Engineering 133(5), 550-563.

Meyer, W., Meyer, P., and Gundle, C. 2014. Expanding containment barrier boundaries. The 10th International Conference on Geosynthetics (10ICG), 21–25 September, Berlin, Germany.

Mitchell, J.K. 1991. Conduction phenomena: from theory to geotechnical practice, Géotechnique, 41(3):299-340.

Michell, J., and Soga, K. 2005. Fundamentals of soil behaviour, 3rd edition, John Wiley and Sons, Inc., New York.

Mitchell, J.K., Hooper, D.R. and Campanella, R.G., 1965. Permeabþ of compacted clay. Soil Mechanics and Foundations Division, ASCE, 91(S4):41-65.

Michen, B., and Graule, T. 2010. Isoelectric points of viruses. Journal of Applied Microbiology 109(2), 388-397.

Montell Polyolefins Brochure, 1997. Astryn FPA high performance materials for geomembranes.

Millet, R.A., Perez, J.Y. and Davidson, R.R. 1992. USA practice slurry wall specifications 10 years later. In Slurry walls: Design, construction, and quality control. ASTM STP, Slurry walls design, construction and quality control, 1129, 42-66

Moore, R.S., Taylor, D.H., Sturman, L.S., Reddy, M.M., and Fuhs, G.W. 1981. Poliovirus adsorption by 34 minerals and soils. Applied and Environmental Microbiology 42, 963-975.

Moraes F. and Gardoni, M. 2020. Geotextile tubes to dewater and confine gold tailings. 4th Pan American Conference on Geosynthetics, Rio de Janeiro, Brazil, (in press).

Morais, F. 2020. Performance of a drained stacking with geotextile tubes - New proposal for disposal of mining fine waste, MSc. Thesis. Federal University of Minas Gerais, Dept. of Transport and Geotechnical Engineering, Belo Horizonte, Brazil. (in progress) (in Portuguese).

Moreira, T. 2011. Experimental evaluation of drainage systems with geosynthetics to decrease iron ore moisture content of the Carajás mining complex, MSc. Thesis, Federal University of Minas Gerais, Dept. of Transportation and Geotechnical Engineering, Brazil (in Portuguese).

Morgenstern, N., Vick, S. and Van Zyl, D. 2015. Report on Mount Polley Tailings Storage Facility Breach, Independent Expert Engineering Investigation and Review Panel, British Columbia, 30 January 2015, unpublished.

Morsy, M., and Rowe, R.K. 2017. Performance of blended polyolefin geomembrane in various incubation media based on Std-OIT. Proc., GeoFrontiers, ASCE, Reston, Virginia, USA, 1–10.

Msiza, J., 2020. Email Regulatory Standards in Africa for Pollution Control Barrier Systems confirming little progress with since request to IGS Technical Committee on Barriers in 2014, dated 22 August 2020.

Mukunoki, T., Nakano, T., Otani, J., and Gourc, J., 2014. Study of cracking process of clay cap barrier in landfill using x-ray CT. Applied Clay Science 101(10), 558–566.

Musso, G., Cosentini, R., Dominijanni, A., Guarena, N., Manassero, M. 2017. Laboratory characterization of the chemo-hydro-mechanical behaviour of chemically sensitive clays. Rivista Italiana di Geotecnica 51(3), 22-47.

Musso, G., Cosentini, R.M., Dominijanni, A., Guarena, N., and Manassero, M. 2017. Laboratory characterization of the chemo-hydro-mechanical behaviour of chemically sensitive clays. Rivista Italiana di Geotecnica 51(3), 22-47.

National Environmental Management Waste Act (NEMWA) 2013, Act 59 of 2008, Regulation 636, (2013. Norms and Standards for Disposal of Waste to Landfill, 23 August 2013, South Africa).

Ng, C., Chen, Z., Coo, J., Chen, R., and Zhou, C. 2015d. Gas breakthrough and emission through unsaturated compacted clay in landfill final cover. Waste Management 44, 155-163.

Ng, C., Chen, R., Coo, J., Liu, J., Ni, J., Chen, Y., and Lu, B. 2019. A novel vegetated three-layer landfill cover system using recycled construction wastes without geomembrane. Canadian Geotechnical Journal 56(12), 1863-1875.

Ng, C., Coo, J., Chen, Z., and Chen, R. 2016. Water infiltration into a new three-layer landfill cover system. Journal of Environmental Engineering 142(5), 04016007.

Ng, C., Liu, J., and Chen, R. 2015a. Numerical investigation on gas emission from three landfill soil covers under dry weather conditions. Vadose Zone Journal 14(8).

Ng, C., Liu, J., Chen, R., and Coo, J. 2015b. Numerical parametric study of an alternative three-layer capillary barrier cover system. Environmental Earth Sciences 74(5), 4419-4429.

Ng, C., Liu, J., Chen, R., and Xu, J. 2015c. Physical and numerical modeling of an inclined three-layer (silt/gravelly sand/clay) capillary barrier cover system under extreme rainfall. Waste Management 38, 210-221.

Norris, A. 2021. Mechanisms of interaction between montmorillonite and anionic polymer amendments in geosynthetic clay liners, Ph.D. dissertation, Colorado State University, Fort Collins, Colorado, USA.

Norris, A., Aghazamani, N., Conzelmann, J., Scalia, J., and Shackelford, C. 2020. Hydraulic conductivity of geosynthetic clay liners to synthetic mine waste leachates. Tailings and Mine Waste 2020, UBC Studios, University of British Columbia, 1102329 West Mall, Vancouver, British Columbia V6T 1Z4, Canada.

Norris, A., Scalia, J., and Shackelford, C. 2022. Polymer quantification methods for geosynthetic clay liners enhanced with anionic polymers. Geotechnical Testing Journal 45(2), GTJ20210134..

Norrish, X. 1954. Manner of swelling of montmorillonite. Nature 173, 256-257.

Olsen, S., and Kemper, W. 1968. Movement of nutrients to plant roots. Advances in Agronomy 20, 91-151.

Onikata, M., Kondo, M., Hayashi, N., and Yamanaka, S. 1996. Development and characterization of multiswellable bentonite. 2nd International Congress on Environmental Geotechnics, IS-Osaka '96, M. Kamon, Ed., Nov. 5-8, 1996, Osaka, Japan, Balkema, Rotterdam, Vol. 1, 587-590.

Onikata, M., Kondo, M., Hayashi, N., and Yamanaka, S. 1999. Complex formation of cation-exchanged montmorillonites with propylene carbonate: Osmotic swelling in aqueous electrolyte solutions. Clays and Clay Minerals 47(5), 672-677.

Opdyke S. M., Evans J. C. 2005. Slag-cement-bentonite slurry walls, Journal of Geotechnical and Geoenvironmental Engineering, 131(6): 673-681.

Ozhan, H. 2018a. Effects of temperature increase in 0.5 M MgCl2 solution on hydraulic capability of anionic polymer-treated geosynthetic clay liners used as barriers. Journal of Environmental Engineering 144(10), 04018100.

Ozhan, H. 2018b. Hydraulic capability of polymer-treated GCLs in saline solutions at elevated temperatures. Applied Clay Science 161, 364-373.

Paleologos, E.K., O'Kelly, B.C., Tang, C.-S., Cornell, K., Rodríguez-Chueca, J., Abuel-Naga, H., Koda, E., Farid, A., Vaverková, M.D., Kostarelos, K., Goli, V.S.N.S., Guerra-Rodríguez, S., Leong, E.C., Jayanthi, P., Shashank, B.S., Sharma, S., Shreedhar, S., Mohammad, A., Jha, B., Kuntikana, G., Bo, M.W., Mohamed, A.M.O. and Singh, D.N. 2021. Post COVID-19 water and wastewater management to protect public health and geoenvironment. Environmental Geotechnics 8(3), 193-207.

Palmeira, E., Beirigo, E., and Gardoni, M. 2010. Tailings-nonwoven geotextile filter compatibility in mining applications. Geotextiles and Geomembranes 28, 136-148.

Palmeira, E., Fannin, R., and Vaid, Y. 1996. A study on the behaviour of soil-geotextile systems in filtration tests. Canadian Geotechnical Journal 33(4), 899-912.

Palmeira, E., and Gardoni, M. 2000. The influence of partial clogging and pressure on the behaviour of geotextiles in drainage systems. Geosynthetics International 7(4–6), 403–431.

Palmeira, E., and Gardoni, M. 2002. Drainage and filtration properties of nonwoven geotextiles under confinement using different experimental techniques. Geotextiles and Geomembranes 20, 97-115.

Palmeira, E., Gardoni, M., and Bessa da Luz, D. 2005. Soil-geotextile filter interaction under high stress levels in the gradient ratio test. Geosynthetics International 12(4), 162-175.

Palmeira, E., and Trejos Galvis, H. 2017. Opening sizes and filtration behaviour of nonwoven geotextiles under confined and partial clogging conditions. Geosynthetics International 24(2), 125-138.

Parra D., César C., and Mendoza, J. 2014. Geomembrane and pipe design issues in deeper heap leach pads. Proc., Heap Leach Solutions 2014, Lima, Peru, 167-179.

Pavanello, P, Carrubba, P., and Moraci, N. 2018. Dynamic friction and the seismic performance of geosynthetic interfaces. Geotextiles and Geomembranes 46, 715–725.

Peggs, I. 2008. Prefabricated bituminous geomembrane: a candidate for exposed geomembrane caps for landfill closures. Proc., First Pan American Geosynthetics Conference and Exhibition, Cancun, Mexico, 191-197.

Peggs, I., Schmucker, B. and Carey, P. 2005. Assessment of maximum allowable strains in polypropylene geomembranes. Proc., Geofrontiers 2005, ASCE, Reston, Virginia, USA.

Petrov, R., Rowe, R.K., and Quigley, R. 1997a. Comparison of laboratory measured GCL hydraulic conductivity based on three permeameter types. Geotechnical Testing Journal 20(1), 49-62.

Petrov, R. Rowe, R.K., and Quigley, R. 1997b. Selected factors influencing GCL hydraulic conductivity. Journal of Geotechnical and Geoenvironmental Engineering 123(8), 683-695.

Petrov, R., and Rowe, R.K. 1997. Geosynthetic clay liner (GCL) – chemical compatibility by hydraulic conductivity testing and factors impacting its performance. Canadian Geotechnical Journal 34(6), 863-885.

Plaut, R., and Suherman, S. 1998. Two-dimensional analysis of geosynthetic tube. Acta Mechanica 3(4), 207-218.

Priyanto, D., Whitelaw, B., Rowe, R.K., Barone, F., Abdelaal, F., Zafari, M., Buckley, J. 2019. Implementation of Research and Development (R&D) Results in the Design of Liner System for the Near Surface Disposal Facility (NSDF) – 19089, WM2019 Conference, March 3 – 7, 2019, Phoenix, Arizona, USA.

Prongmanee, N., and Chai, J. 2019. Performance of geosynthetic clay liner with polymerized bentonite in highly acidic or alkaline solutions. International Journal of Geosynthetics and Ground Engineering 5(3), Article 26.

Prongmanee, N., Chai, J., and Shrestha, S. 2018a. Effects of cations on consolidation and permeability of polymerized bentonite. Lowland Technology International 20(3), 297-304.

Prongmanee, N., Chai, J., and Shen, S. 2018b. Hydraulic properties of polymerized bentonites. Journal of Materials in Civil Engineering 30(10), 04018247.

Qiu, H., and Yu, J. 2008. Polyacrylate/(carboxymethylcellulose modified montmorillonite) superabsorbent nanocomposite: preparation and water absorbency. Journal of Applied Polymer Science 107(1), 118-123.

Quigley, R.M. and Rowe, R.K. 1986. Leachate migration through clay below a domestic waste landfill, Sarnia, Ontario, Canada: Chemical interpretation and modelling philosophies. Hazardous and Industrial Solid Waste Testing and Disposal: Sixth Volume, ASTM STP 933:93-103 .

Quigley, R.M., Fernandez, F. and Rowe, R.K. 1988. "Clayey barrier assessment for impoundment of domestic waste leachate (southern Ontario) including clay-leachate compatibility by hydraulic conductivity testing. Canadian Geotechnical Journal, 25(3):574-581.

Quigley, R.M., Gwyn, Q.H.J., White, O.L., Rowe, R.K., Haynes, J.E. and Bohdanowicz, A. 1983. "Leda clay from deep boreholes at Hawkesbury, Ontario, Part I, Geology and Geotechnique. Canadian Geotechnical Journal, 20(2):288-298.

Rabideau, A., and Khandelwal, A. 1998. Boundary conditions for modeling transport in vertical barriers. Journal of Environmental Engineering 124(11), 1135-1139.

Ratkievicius, L., Da Cunha Filho, F., De Barros Neto, E., and Santanna, V. 2016. Modification of bentonite clay by a cationic surfactant to be used as a viscosity enhancer in vegetable-oil-based drilling fluid. Applied Clay Science 135, 307-312.

Razakamanantsoa, A., Barast, G., and Djeran-maigre, I. 2012. Hydraulic performance of activated calcium bentonite treated by polyionic charged polymer. Applied Clay Science 59-60, 103-114.

Reddy, K.R., Kumar, G., and Du, Y.-J. 2019. Risk, Sustainability and Resiliency Consideration in Polluted Site Remediation, Proc. 8th International Congress on Environmental Geotechnics, Springer, Singapore, Vol. 1, 145-163.

Redfearn, A., and Roberts, D. 2004. Ecological risk-assessment methodology: a UK case study for landfills, Water and Environment Journal 18(3), 139-143.

Renken, K., Mchaina, D., and Yanful, E. 2005. Geosynthetics research and applications in the mining and mineral processing environment. North American Geosynthetics Society (NAGS) -Geosynthetic Institute (GSI) Conference, Las Vegas, Nevada. December 14-16.

Rentz, A., Take W., Brachman, R., and Rowe, R.K. 2016. Effect of geomembrane colour and cover soil on solar-driven down slope bentonite erosion from a GCL. Geosynthetics International 23(4), 257–270.

Rentz, A., Brachman, R., Take, W.A., and Rowe, R.K. 2017. Comparison of wrinkles in white and black HDPE geomembranes. Journal of Geotechnical and Geoenvironmental Engineering 143(8), 04017033.

Robertson, A. 2011. Mine waste management in the 21st century: challenges and solutions beiynd incremental changes. Proc. Tailings and Mine Waste, Vancouver, British Columbia, Canada.

Rouf, M., Bouazza, A., Singh, R., Gates W., and Rowe, R.K. 2016a. Water vapour adsorption and desorption in GCLs. Geosynthetics International 23(2), 86-99

Rouf, M., Bouazza, A., Singh, R., Gates W., and Rowe, R.K. 2016b. A gas flow unified measurement system for measuring sequentially gas diffusion and gas permeability of partially hydrated geosynthetic clay liners. Canadian Geotechnical Journal 53(6), 1000-1012

Rouf, M., Singh, R., Bouazza, A. Rowe, R.K., and Gates W. 2016c. Gas permeability of partially hydrated geosynthetic clay liner under two stress conditions. Journal of Environmental Geotechnics 3(5), 325-333

Rowe, R.K. 1987. Pollutant transport through barriers. Proceedings of ASCE Specialty Conference, Geotechnical Practice for Waste Disposal '87, Ann Arbor, 159-181.

Rowe, R.K. 1988. Contaminant migration through groundwater: The role of modelling in the design of barriers. Canadian Geotechnical Journal, 25(4):778-798.

Rowe, R.K. 1992. Integration of hydrogeology and engineering in the design of waste management sites. Proceedings of the International Association of Hydrogeologists Conference on "Modern Trends in Hydrogeology. Hamilton, pp. 7-21.

Rowe, R.K. 1998. Geosynthetics and the minimization of contaminant migration through barrier systems beneath solid waste. 6th International Conference on Geosynthetics, IFAI, Roseville, Minnesota, USA, Vol. 1, 27-103.

Rowe, R.K. 2005. Long-term performance of contaminant barrier systems. Géotechnique 55(9), 631-678.

Rowe, R.K. 2009. Systems engineering the design and operations of municipal solid waste landfills to minimize leakage of contaminants to groundwater. Proc. 3rd Zeng Gou-Xi Lecture, Geosyntethics International 16(6), 391-404.

Rowe, R.K. 2011, Geosynthetics in bottom liners and covers for use in lagoons, secondary containment, landfill and mining applications, GIGSA Seminar, 6-7 September, Stone Cradle, Gauteng, South Africa.

Rowe, R.K. 2012. Short and long-term leakage through composite liners (7th Arthur Casagrande Lecture). Canadian Geotechnical Journal 49(2), 141–169.

Rowe, R.K. 2018. Environmental geotechnics: looking back, looking forward (16th Croce Lecture). Italian Geotechnical Journal 2018(4), 8-40.

Rowe, R.K. 2020a. Geosynthetic clay liners: perceptions and mis-conceptions. Geotextiles and Geomembranes 48(2), 137–156.

Rowe, R.K. 2020b. Protecting the environment with geosynthetics - The 53rd Karl Terzaghi Lecture. Journal of Geotechnical and Geoenvironmental Engineering 146(9), 04020081.

Rowe, R.K., and Abdelatty, K. 2011. Effect of calcium-rich soil on the performance of an overlying GCL. Journal of Geotechnical and Geoenvironmental Engineering 138(4): 423-431.

Rowe, R.K., and Booker, J.R. 1985a. 1-D pollutant migration in soils of finite depth. Journal of Geotechnical Engineering 111(4), 479-499.

Rowe, R.K., and Booker, J.R. 1985b. Two-dimensional pollutant migration in soils of finite depth. Canadian Geotechnical Journal 22(4), 429–436.

Rowe, R.K. and Booker, J.R. 2000. Theoretical solutions for calculating leakage through composite liner systems. in Developments in Theoretical Geomechanics - The John Booker Memorial Symposium, Sydney, November, 580-602.

Rowe, R.K., and Booker, J.R. 2005. POLLUTEv7: Pollutant migration through a nonhomogeneous soil, © 1983–2005. Distributed by GAEA Environmental Engineering Ltd, 87 Garden Street, Whitby, Ontario, Canada L1N 9E7.

Rowe, R.K., and Brachman, R.W.I. 2004. Assessment of equivalency of composite liners, Geosynthetics International 11(4), 273-286.

Rowe, R.K., and Ewais, A. 2014. Degradation behaviour of HDPE geomembrane with high and low initial high-pressure oxidative induction time. Geotextile and Geomembranes 42(2), 111–126.

Rowe, R.K., and Ewais, A. 2015. Ageing of exposed geomembranes at locations with different climatological conditions. Canadian Geotechnical Journal 52 (3), 326-343.

Rowe, R. K., Fan, J. (2021). Effect of geomembrane hole geometry on leakage overlain by saturated tailings. Geotextiles and Geomembranes, 49(6), 1506-1518.

Rowe, R.K. and Fraser, M.J. 1995. Effect of uncertainty in the assessment of the potential impact of waste disposal facilities, Proceedings ASCE Specialty Conference, New Orleans, pp. 270-284.

Rowe, R.K., and Hamdan, S. 2021a. Effect of wet-dry cycles on standard and polymer modified GCLs in covers subjected to flow over the GCL. Geotextiles and Geomembranes 49(4),1155-1165.

Rowe, R.K., and Hamdan, S. 2021b. Performance of GCLs after long-term wet-dry cycles under a defect in GMB. Geosynthetics International (in press).

Rowe, R.K., and Hosney, M. 2013. Laboratory investigation of GCL performance for covering arsenic contaminated mine wastes. Geotextiles and Geomembranes 39, 63-77.

Rowe, R.K., and Li, T. 2020. Self-healing of circular and slit defects in GCLs upon hydration from silty sand under applied stress. Geotextiles and Geomembranes 48, 667-683.

Rowe R.K., and Li, T. 2021. Influence of pore water chemistry on GCL self-healing with hydration from silica sand. Geotextiles and Geomembranes 49(4), 871-894.

Rowe, R.K. and Nadarajah, P. 1996. Estimating leachate drawdown due to pumping wells in landfills. Canadian Geotechnical Journal, 33(1):1-10.

Rowe, R.K., and Van Gulck, J. 2004. Filtering and drainage of contaminated water. Geofilters 4th International Conference, Stellenbosch, RSA, 1–63.

Rowe, R.K., and Verge, A. 2013. Prediction of geosynthetic clay liner desiccation in low-stress applications Geosynthetics International 20(5), 301-315.

Rowe, R.K., and Yu, Y. 2010. Factors affecting the clogging of leachate collection systems in MSW landfills. 6th International Conference on Environmental Geotechnics, November 2010, New Delhi, India, 3-23.

Rowe, R.K., and Yu, Y. 2013. A practical technique for estimating service life of MSW leachate collection systems. Canadian Geotechnical Journal 50(2), 165-178.

Rowe, R.K., and Yu, Y. 2018. Tensile strains in geomembrane landfill liners. Keynote Lecture GeoShanghai 2018, Shanghai, China, 1-10.

Rowe, R.K., and Yu, Y. 2019. Magnitude and significance of tensile strains in geomembrane landfill liners. Geotextiles and Geomembranes 47(3), 439-458.

Rowe, R.K., Caers, C.J. and Chan, C. 1993. Evaluation of a compacted till liner test pad constructed over a granular subliner contingency layer, Canadian Geotechnical Journal, 30(4):667-689.

Rowe, R.K., Quigley, R., Brachman, R., and Booker, J. 2004. Barrier systems for waste disposal facilities, 2nd edition, Taylor and Francis Books Ltd., London.

Rowe, R.K., Bostwick, L., Take, W.A. 2011a. Effect of GCL properties on shrinkage when subjected to Wet-Dry Cycles. Journal of Geotechnical and Geoenvironmental Engineering 137(11), 1019-1027.

Rowe, R.K., Rayhani, M., Take, W., Siemens, G., and Brachman, R. 2011b. GCL Hydration under simulated daily thermal cycles. Geosynthetics International 18(4), 196-205.

Rowe, R.K., Chappel, M., Brachman, R., and Take, W.A. 2012a. Field monitoring of geomembrane wrinkles at a composite liner test site. Canadian Geotechnical Journal 49(10), 1196-1211.

Rowe, R.K., Yang, P., Chappel, M., Brachman, R., and Take, W.A 2012b. Wrinkling of a geomembrane on a compacted clay liner on a slope. Geotechnical Engineering, Journal of the South East Asian Geotechnical Society 43(3), 11-18.

Rowe, R.K., Brachman, R., Irfan, H., Smith, M., and Thiel, R. 2013a. Effect of underliner on geomembrane strains in heap leach applications. Geotextiles and Geomembranes 40, 37-47.

Rowe, R.K., Rayhani, M., Take, W.A, Siemens, G. and Brachman, R.W.I 2013b. Physical modelling of nonwoven-nonwoven GCL shrinkage under simulated field Conditions", Geotextiles and Geomembranes, 40: 12-19.

Rowe, R.K., Abdelaal, F., and Brachman, R. 2013c. Antioxidant depletion from an HDPE geomembrane with a sand protection layer. Geosynthetics International 20(2), 73-89.

Rowe, R.K., Ashe, L, Take W.A., and Brachman, R. 2014. Factors affecting the downslope erosion of bentonite in a GCL. Geotextiles and Geomembranes 42(5), 445-456

Rowe, R.K., Brachman, R., Take, W.A., Rentz, A. and Ashe, L. 2016a. Field and laboratory observations of downslope bentonite migration in exposed composite liners. Geotextiles and Geomembranes 44(5), 686-706

Rowe, R.K., Rentz, A., Brachman, R., and Take W.A. 2016b. Effect of GCL type on downslope bentonite erosion in an exposed liner. Journal of Geotechnical and Geoenvironmental Engineering 142(12), 4016074.

Rowe, R.K., Joshi, P., Brachman, R.W.I and McLeod, H. 2017. Leakage through holes in geomembranes below saturated tailings. ASCE Journal of Geotechnical and Geoenvironmental Engineering, 143(2):4016099-1 to 10; DOI: 10.1061/(ASCE)GT.1943-5606.0001606.

Rowe, R.K., Brachman, R.W.I. and Take, W.A 2018 Field measurements of overlap reductions for two reinforced fabric-encased GCLs. Canadian Geotechnical Journal, 55(5): 631-639. https://doi.org/10.1139/cgj-2017-0375

Rowe, R.K., Brachman, R., Hosney, M., Take, W.A., and Arnepalli, D. 2017. Insight into hydraulic conductivity testing of GCLs exhumed after 5 and 7 years in a cover. Canadian Geotechnical Journal 54(8), 1118-1138.

Rowe, R.K., Morsy, M.S. and Ewais, A.M.R. 2019a. A Representative Stress Crack Resistance for Polyolefin Geomembranes Used in Waste Management, Waste Management, 100: 18-27. 10.1016/j.wasman.2019.08.028

Rowe, R.K., Garcia, J., Brachman, R., and Hosney, M. 2019b. Hydraulic and chemical performance of geosynthetic clay liners isothermally hydrated from silty sand subgrade. Geotextiles and Geomembranes 47(6), 740-754.

Rowe, R.K., Priyanto, D. and Poonan, R. 2019c. Factors affecting the design life of HDPE geomembranes in an LLW disposal facility, WM2019 Conference, March 3 – 7, 2019, Phoenix, Arizona, USA, 15p.

Rowe, R.K., Abdelaal, F., Zafari, M. Morsy, M., and Priyanto, D. 2020. An approach to geomembrane selection for challenging design requirements. Canadian Geotechnical Journal 57(10), 1550-1565.

Rowe, R.K., Garcia, J., Brachman, R., and Hosney, M. 2021. Moisture uptake and loss of GCLs subjected to daily thermal cycles from a silty sand subgrade. Geosynthetics International (in press).

Ruffing, D.G. and Evans, J.C. 2022,. Slurry trenching, (in prep.).

Ruffing, D.G., Evans, J.C. and Coughenour, N. 2018. Soil-Bentonite Slurry Trench Cut-off Wall Longevity. Int. Foundations Congress and Equipment Expo, March 5-10, 2018 214-223.

Ryan,C.R., Ruffing, D, and Evans, J. C. 2022. Soil Bentonite Slurry Trench Cutoff Walls: History, Design, and Construction Practices. In Geo-Congress: State of the Art and Practice on Geotechnical Engineering. Reston, VA: ASCE.

Sadeghi, G., Behrends, T., Schijven, J.F., and Hassanizadeh, S.M. 2013. Effect of dissolved calcium on the removal of bacteriophage PRD1 during soil passage: the role of double-layer interactions. Journal of Contaminant Hydrology 144(1), 78-87.

Sadeghi, G., Schijven, J.F., Behrends, T., Hassanizadeh, S.M., Gerritse, J., and Kleingeld, P.J. 2011. Systematic study of effects of pH and ionic strength on attachment of phage PRD1. Ground Water 49(1), 12-19.

Salles, F., Douillard, J., Denoyel, R., Bildstein, O., Jullien, M., Beurroies, I., and Damme, H. 2009. Hydration sequence of swelling clays: evolutions of specific surface area and hydration energy. Journal of Colloid and Interface Science 333, 510-522.

Samea, A., and Abdelaal, F. 2019. Chemical durability of bituminous geomembranes in heap leaching applications at 55oC. Geosynthetics 2019 Conference, Houston, Texas, USA.

Sampaio S., Gardoni M., Palmeira E. 2015. Interface and mechanical damage tests on geosynthetics used in gold tailings dams in Brazil. Proc., 2a Conferência Internacional Dam World, LNEC, Lisboa, Portugal, 112-116.

Sampaio S., Gardoni M., Palmeira E., and Park, J. 2014. Stability analysis of Jacobina's tailings dam, based on interface parameters of geomembrane-tailings obtained from laboratory tests, Proc., 10th International Conference on Geosynthetics, Berlin, Germany, 1022-1028.

Sampaio, S., Pimentel K., Halabi, A. and Gardoni, M. 2017. Stability Analysis of a Gold Tailings Dam Lined with HDPE Geomembrane, Proc., 1st International Conference on Technology and Applications of Geosynthetics, Santiago, Chile, 212-220.

Sample-Lord, K., Bohnhoff, G., and Tong, S. 2017. Diffusion of calcium chloride through polymerized bentonite. Proc., GeoFrontiers, ASCE, Reston, Virginia, USA, 200–208.

Santos, L. and Gardoni M. 2014. Study of the durability of geomembranes for waterproofing of reservoirs of gold tailings dams in Brazil. Proc., 10th International Conference on Geosynthetics, Berlin, Germany, 214-220.

Santos, L. and Gardoni, M. 2016. Evaluation of geomembrane degradation aged in laboratory and exposed to weathering. Proc., 3rd Pan American Conference on Geosynthetics, Miami Beach, USA, 156-164.

Sarsby, R.W. 2019. Environmental Geotechnics in Practice, Institution of Civil Engineers (ICE) Publishing, United Kingdom.

Sari, K., and Chai, J. 2013. Self healing capacity of geosynthetic clay liners and influencing factors. Geotextiles and Geomembranes 41, 64-71.

Scalia, J. 2012. Bentonite-polymer composites for containment applications, Ph.D. dissertation, University of Wisconsin-Madison, Madison, Wisconsin, USA.

Scalia, J., Bareither, C., and Shackelford, C. 2018b. Advancing the use of geosynthetic clay liners as barriers. Geotechnical Engineering Journal of the SEAGS and AGSSEA 49(4), 100-114.

Scalia, J and Benson, C. 2011. Hydraulic conductivity of geosynthetic clay liners exhumed from landfill final covers with composite barriers. Journal of Geotechnical and Geoenvironmental Engineering 137(1), 1-13.

Scalia, J., and Benson, C. 2011. Hydraulic conductivity of geosynthetic clay liners exhumed from landfill final covers with composite barriers. Journal of Geotechnical and Geoenvironmental Engineering 137(1), 1-13.

Scalia, J., and Benson, C. 2016. Evaluation of Na-bentonite-polyacrylate mixtures to enhance the chemical resistance of geosynthetic clay liners. Proc., Geo-Chicago 2016, GSP No. 271, ASCE, Reston, Virginia, USA, 388-397.

Scalia, J., and Benson, C. 2017. Polymer fouling and hydraulic conductivity of mixtures of sodium bentonite and a bentonite-polymer composite. Journal of Geotechnical and Geoenvironmental Engineering 143(4), 04016112.

Scalia, J., Benson, C., Bohnhoff, G., Edil, T., and Shackelford, C. 2014. Long-term hydraulic conductivity of a bentonite-polymer composite permeated with aggressive inorganic solutions. Journal of Geotechnical and Geoenvironmental Engineering 140(3), 04013025.

Scalia, J., Benson, C., Edil, T., Bohnhoff, G., and Shackelford, C. 2011. Geosynthetic clay liners containing bentonite polymer nanocomposite. GeoFrontiers 2011 Advances in Geotechnical Engineering, J. Han and D. Alazamora, Eds., ASCE, Reston, Virginia, USA, 2001-2009.

Scalia, J., Bohnhoff, G., Shackelford, C., Benson, C., Sample-Lord, K., Malusis, M., and Likos, W. 2018a. Enhanced bentonites for containment of inorganic wastes by GCLs. Geosynthetics International 25(4), 392-411.

Scheirs, J. 2009. A guide to polymeric geomembranes: a practical approach, John Wiley and Sons, Inc.

Scheirs, J., Pospisil, J., O'Connor, M.J., and Bigger, S. W. 1996. Characterization of conversion products formed during degradation of processing antioxidants. Polymer Durability, 359-374. (https://pubs.acs.org/doi/abs/10.1021/ba-1996-0249.ch024)

Scheller, C., Krebs, F., Minkner, R., Astner, I., Gil-Moles, M. and Wätzig, H. 2020. Physicochemical properties of SARS-CoV-2 for drug targeting, virus inactivation and attenuation, vaccine formulation and quality control. Electrophoresis 41(13-14), 1137-1151.

Schluchter B., Soyez B., Jessberger H. L., Manassero, M., Puthaar T., Street A. 1991. Geotechnics of landfills and contaminated land: technical recommendations, Berlin: Ernst and Sohn, ISBN: 3433012148, 1-76,.

Schluchter C., Soyez B. Jessberger H. L., Manassero, M., Ruardi P., Street A. 1993. Geotechnics of landfill design and remedial works: technical recommendations, Berlin: Ernst and Sohn, ISBN: 3433012733, 1-158,

Sethi, R., and Di Molfetta, A. 2019. Groundwater Engineering. A Technical Approach to Hydrogeology, Contaminant Transport and Groundwater Remediation, Springer, Switzerland.

Shackelford, C. 2008. Selected issues affecting the use and performance of GCLs in waste containment applications. Geosynthetics and Environment, Proceedings of the Geotechnical Engineering Conference of Torino (XXI Edition), M. Manassero and A. Dominijanni, Eds., Politecnico di Torino, Torino, Italy, Nov. 27-28, 2007, Pàtron Editore, Bologna, Italy.

Shackelford, C.D. 1990. Transit-time design of earthen barriers. Engineering Geology 29(1), 79-94.

Shackelford, C.D. 2005. Environmental issues in geotechnical engineering. Proc. 16th International Conference on Soil Mechanics and Geotechnical Engineering, Millpress, Rotterdam, The Netherlands, Vol. 1, 95-122.

Shackelford, C.D. 2014. The ISSMGE Kerry Rowe Lecture: The role of diffusion in environmental geotechnics. Canadian Geotechnical Journal 51(11), 1219-1242.

Shackelford, C., and Daniel, D. 1991. Diffusion in saturated soil: I. background. Journal of Geotechnical Engineering 117(3), 467-484.

Shackelford, C., and Moore, S. 2013. Fickian diffusion of radionuclides for engineered containment barriers: Diffusion coefficients, porosities, and complicating issues. Engineering Geology 152(1), 133-147.

Shackelford, C., and Scalia IV, J. 2016. Semipermeable membrane behaviour in bentonite-based barriers: past, present, and future. GEOVANCOUVER 2016, 69th Canadian Geotechnical Conference, Oct. 2-5, 2016, Vancouver, Canada, Canadian Geotechnical Society, Richmond, British Columbia, Canada, paper 4173.

Shackelford, C., Benson, C., Katsumi, T., Edil, T., and Lin, L. 2000. Evaluating the hydraulic conductivity of GCLs permeated with non-standard liquids. Geotextiles and Geomembranes 18(2-4), 133-161.

Shackelford, C., Meier, A., and Sample-Lord, K. 2016. Limiting membrane and diffusion behaviour of a geosynthetic clay liner. Geotextiles and Geomembranes 44(5), 707-718.

Shackelford, C., Sevick, G., and Eykholt, G. 2010. Hydraulic conductivity of geosynthetic clay liners to tailings impoundment solutions. Geotextiles and Geomembranes 28(2), 149-162.

Shamrock, J., and Msiza, J. 2015. HDPE geomembrane specification and performance implications. Western Cape LIG Seminar, Tulbagh, 15–16 September 2015.

Sherard, J., and Dunnigan, L. 1989. Critical filters for impervious soils. Journal of Geotechnical Engineering 115(7), 927-947.

Shercliff, D. 1998. Designing with the cylinder test. Proc. of the Polluted and Marginal Land Conference, Brunel University, London.

Shukla, S. 2012. Handbook of geosynthetic engineering, 2nd edition, ICE Publishing, London, UK, ISBN 978-0-7277-4175-2.

Silva, L. 2017. Geotextile tubes to dewater, confine, and stack finegold ore tailings, M.Sc Thesis, Federal University of Minas Gerais, Dept. of Transportation and Geotechnical Engineering, Brazil, Department of Transportation and Geotechnical Engineering. Belo Horizonte, Brazil (in Portuguese).

Silva, V. 2019. Analysis of the behaviour of geotextile pipes for containment of fine mining waste through numerical modeling, MSc. Thesis, Federal University of Minas Gerais, Dept. of Transportation and Geotechnical Engineering, Brazil, 168 p. (in Portuguese).

Silva V., Gardoni, M., and Maia, K. 2020. Numerical modeling of geotextile tubes filling process with gold mine tailings. Geosynthetics International (in press).

Simeral, L., and Amey, R. 1970. Dielectric properties of liquid propylene carbonate. Journal of Physical Chemistry 74(7), 1443-1446.

Singh, A., 2016. Confirmation letter to the Chamber of Mines SA, Risk Based Approach for Assessment Water Use License Applications in Relation of Facilities for Sction 21 G Water Uses in the Mining Sector, reference WULA/1/2016 dated 29/06/2016.

Singh, R. and Bouazza, A. 2013. Thermal conductivity of geosynthetics. Geotextiles and Geomembranes 39, 1–8.

Singh, M., Kijko, A. and van den Berg, L. 2010. Seismic risk ranking for large dams in South Africa. Acta Geophysica, Institute of Geophysics, Polish Academy of Sciences.

Smith, M. 2004. Drainage pipe deflection for high heaps. The Mining Record, 4th Quarter, 15-19. 2017c). Field measurements of water storage capacity in a loess–gravel capillary barrier cover using rainfall simulation tests. Canadian Geotechnical Journal 54(11), 1523-1536.

Soga, K., Ewais, A., Fern, J., and Park, J. 2019. Advances in Geotechnical Sensors and Monitoring. In: Lu, N., and Mitchell, J.K. (Eds.), Geotechnical Fundamentals for Addressing New World Challenges, Springer, Switzerland, 29-65.

Soong, T.-Y., and Koerner, R. 1998. Laboratory study of high density polyethylene geomembrane waves. Proc., 6th Int. Conf. on Geosynthetics, Austin, Texas, International Geosynthetics Society, 1, 301-306.

Soule, N., and Burns, S. 2001. Effects of organic cation structure on behaviour of organobentonites. Journal of Geotechnical and Geoenvironmental Engineering 127(4), 363-370.

Southen, J., and Rowe, R.K. 2004. Investigation of the behaviour of geosynthetic clay liners subjected to thermal gradients in basal liner applications. Journal of ASTM International 1(2) ID JAI11470, Online; Available: Hwww.astm.orgH; 1 February 2004, 13p. This was also published by ASTM in hardcopy in Advances in Geosynthetic Clay Liner Technology", Mackey, R.E. and von Maubeuge, K. (Eds), pp. 121-133.

Southen, J., and Rowe, R.K. 2005. Laboratory investigation of geosynthetic clay liner desiccation in a composite liner subjected to thermal gradients. Journal of Geotechnical and Geoenvironmental Engineering 131(7), 925-935.

Southen, J., and Rowe, R.K. 2007. Evaluation of the soil-water characteristic curve for geosynthetic clay liners. Geotextiles and Geomembranes 25(1), 2-9.

Southen, J., and Rowe, R.K. 2011. Numerical modelling of thermally induced desiccation of geosynthetic clay liners observed in laboratory experiments. Geosynthetics International 18 (5), 289-303.

Stone, J. 1984. Leakage monitoring of the geomembrane for proton decay experiment. Proc., International Conference on Geomembranes, IFAI, St. Paul, Minnesota, USA, Vol. 2, 475–480.

Syngouna, V.I., and Chrysikopoulos, C.V. 2010. Interaction between viruses and clays in static and dynamic batch systems. Environmental Science and Technology 44(12), 4539-4544.

Szczerba, M., and Kalinichev, A. 2016. Intercalation of ethylene glycol in smectites: several molecular simulation models verified by x-ray diffraction data. Clays and Clay Minerals 64(4), 488-502.

Take, W.A., Brachman, R., Rowe, R.K., and Rentz, A. 2014. Temperature measurements of exposed GMB/GCL composite liners. 10th International Conference on Geosynthetics (10ICG), 21–25 September, Berlin, Germany.

Take, W.A., Brachman, R., and Rowe, R.K. 2015. Observations of bentonite erosion from solar-driven moisture migration in GCLs covered only by a black geomembrane. Geosynthetics International 22(1),78–92.

Tallard, G. 1984a. Slurry Trenches and Hazardous Waste. ASCE Civil Engineering Magazine, February.

Tallard, G. 1984b. Acuavoir/Enhanced Aquifers, The Military Engineer Magazine Vol.76#492, March.

Tallard, G. 1992. New Trenching Method using synthetic polymers. ASTM publ. STP 1129.

Tallard G. 1992. Hazwaste Barriers, update for the 90's, Canadian Geotechnical Society 45th conference, October.

Tallard, G. 1995. From Cement Bentonite to IMPERMIX. D.O.E. barriers workshop, Denver CO, August.

Tallard, G. 1997a. Very Low Conductivity self-hardening slurry for permanent enclosures. Proc. Intl Containment Technology Conference, St Petersburg, Florida. 9-12 February.

Tallard, G. 1997b. Beyond cement-bentonite: Impermix self-hardening slurry. USCOLD annual conf.

Tang, C., Shi, B., Liu, C., Suo, W., and Gao, L., 2011. Experimental characterization of shrinkage and desiccation cracking in thin clay layer. Applied Clay Science 52(2), 69-77.

Tang, C.-S., Paleologos, E.K., Vitone, C., Du, Y.J., Li, J.S., Jiang, N.J., Deng, Y.F., Chu, J., Shen, Z., Koda, E., Dominijanni, A., Fei, X., Vaverková, M.D., Osiński, P., Chen, X., Asadi, A., Takeuchi, M.R.H., Bo, M.W., Abuel-Naga, H., Leong, E.C., Farid, A., Baser, T., O'Kelly, B.C., Jha, B., Goli, V.S.N.S. and Singh, D.N. 2021. Environmental geotechnics: challenges and opportunities in the post COVID-19 world. Environmental Geotechnics 8(3), 172-192.

Tang, H.S., Haynes, R.D., and Houzeaux, G. 2021. A Review of Domain Decomposition Methods for Simulation of Fluid Flows: Concepts, Algorithms, and Applications. Archives of Computational Methods in Engineering 28(3), 841-873.

Tedd, P., Holton, I.R., Butcher, A.P., Wallace, S. and Daly, P. 1997. Investigation of the performance of cement-bentonite cut-off walls in aggressive ground at a disused gasworks site. Proc. Intl Containment Technology Conf., St Petersburg, Florida.

Theng, B. 2012. Formation and properties of clay-polymer complexes. Developments in Clay Science 4, 526.

Thiel, R., and Criley, K. 2005. Hydraulic conductivity of partially prehydrated GCLs under high effective confining stress for three real leachates. Waste Containment and Remediation, GSP 142, GeoFrontiers 2005, ASCE, Reston, Virginia, USA.

Thiel, R., and Richardson, G. 2005. Concern for GCL shrinkage when installed on slopes. GRI-18 at GeoFrontiers, Folsom, Pennsylvania, USA.

Thiel, R., and Smith, M., 2004. State of the practice review of heap leach design issues. Geotextiles and Geomembranes 22, 555-568.

Thiel, R., Giroud, J., Erickson, R., Criley, K., and Bryk, J. 2006. Laboratory measurements of GCL shrinkage under cyclic changes in temperature and hydration conditions. Proc. Eighth International Conference on Geosynthetics, Millpress, Rotterdam, 157-162.

Tian, K., and Benson, C. 2019. Containing bauxite liquor using bentonite-polymer composite geosynthetic clay liners. 8th International Congress on Environmental Geotechnics, L. Zhan, Y. Chen, and A. Bouazza, Eds., Springer Nature Singapore Pte Ltd., Vol. 2, 672-678.

Tian, K., Benson, C., and Likos, W. 2016a. Hydraulic conductivity of geosynthetic clay liners to low-level radioactive waste leachate. Journal of Geotechnical and Geoenvironmental Engineering 142(8), 04016037.

Tian, K., Benson, C., and Likos, W. 2017. Effect of anion ratio on the hydraulic conductivity of a bentonite-polymer geosynthetic clay liner. Proc., GeoFrontiers, ASCE, Reston, Virginia, USA,180–189.

Tian, K., Likos, W., and Benson, C. 2016b. Pore-scale Imaging of polymer-modified bentonite in saline solutions. Proc., Geo-Chicago 2016, GSP No. 271, ASCE, Reston, Virginia, USA, 468-477.

Tian, K., Likos, W., and Benson, C. 2019. Polymer elution and hydraulic conductivity of bentonite-polymer composite geosynthetic clay liners. Journal of Geotechnical and Geoenvironmental Engineering 145(10), 04019071.

Tincopa, M., Bouazza, A., Rowe, R.K., and Rahardjo, H. 2020. Back-analysis of the water retention curve of a GCL on the wetting path. Geosynthetics International 27(5), 523-537.

Tognon, A., Rowe, R.K., and Moore, I. 2000. Geomembrane strain observed in large scale testing of protection layers. Journal of Geotechnical and Geoenvironmental Engineering 126(12), 1194-1208.

Tong X, Li Y-C, Ke H, Li Y, Pan Q. 2020. In situ stress states and lateral deformations of soil-bentonite cut-off walls during consolidation process. Canadian Geotechnical Journal, 57(1):139-148.

Touze-Foltz, N., and Farcas, F. 2017. Long-term performance and binder chemical structure evolution of elastomeric bituminous geomembranes. Geotextiles and Geomembranes 45(2), 121-130.

Trauger, R., and Darlington, J. 2000. Next-generation geosynthetic clay liners for improved durability and performance, TR-220, Colloidal Environmental Technologies Company, Arlington Heights, Illinois, USA.

US EPA 1989. Risk assessment guidance for superfund (RAGS): part A. Office of Emergency and Remedial Response, U.S. Environmental Protection Agency, Washington, D.C., USA.

US EPA 2010. Bisphenol A Action Plan, U.S. Environmental Protection Agency

US EPA 2015. Update of Human Health Ambient Water Quality Criteria: 2,4-Dimethylphenol 105-67-9, Office of Science and Technology, Office of Water, U.S. Environmental Protection Agency Washington, DC 20460

US HHS 1999. Toxicological profile for chlorophenols, U.S. Department of Health and Human Services, Public Health Service, Agency for Toxic Substances and Disease Registry

US HHS 2001. Toxicological profile for pentachlorophenol, U.S. Department of Health and Human Services, Public Health Service, Agency for Toxic Substances and Disease Registry

US HHS 2008a. Toxicological profile for cresols, U.S. Department of Health and Human Services, Public Health Service, Agency for Toxic Substances and Disease Registry

US HHS 2008b. Toxicological profile for phenols, U.S. Department of Health and Human Services, Public Health Service, Agency for Toxic Substances and Disease RegistryVandenberg, L. N., Hauser, R., Marcus, M., Olea, N., Welshons, W. V. 2007. Human exposure to bisphenol A (BPA. Reproductive Toxicology, 24(2), pp. 139–177.

Van Loon, L., Glaus, M., and Müller, W. 2007. Anion exclusion effects in compacted bentonites: towards a better understanding of anion diffusion. Applied Geochemistry 22(11), 2536-2552.

Vaverková, M.D., Paleologos, E.K., Dominijanni, A., Koda, E., Tang, C.S., Małgorzata, W., Li, Q., Guarena, N., Mohamed, A.M.O., Vieira, C.S., Manassero, M., O'Kelly, B.C., Xie, Q., Bo, M.W., Adamcová, D., Podlasek, A., Anand, U.M., Mohammad, A., Goli, V.S.N.S., Kuntikana, G., Palmeira, E.M., Pathak, S. and Singh, D.N. 2021. Municipal solid waste management under COVID-19: challenges and recommendations. Environmental Geotechnics 8(3), 217-232.

Vryzas, Z., Kelessidis, V., Nalbantian, L., Zaspalis, V., Gerogiorgis, D., and Wubulikasimu, Y. 2017. Effect of temperature on the rheological properties of neat aqueous Wyoming sodium bentonite dispersions. Applied Clay Science 136, 26-36.

Wang Y, Chen Y, Xie H, Zhang C and Zhan LT. 2016. Lead adsorption and transport in loess-amended soil-bentonite cut-off wall. Engineering geology, 215: 69-80.

Wang, Y., Ren, H., Yan, Y., He, S., Wu, S., and Zhao, Q. 2020. Hindered phenolic antioxidants as heat-oxygen stabilizers for HDPE. Polymers and Polymer Composites 29(9), 1403-1411.

Wichterle, O., and Lím, D. 1960. Hydrophilic gels for biological use. Nature 185, 117-118.

World Resources Institute 2015. Extreme water shortages are expected to hit these countries by 2040, article by Jeff Desjardins, August 31, 2015, www.visualcapitalist.com.

Xanthakos, P., 1979. Slurry Walls, McGraw-Hill Book Co.

Xu, X., Liu, X., Oh, M., and Park, J. 2018. Swelling capacity and hydraulic conductivity of polymer-modified bentonite under saline water conditions. Applied Sciences 8, 1025.

Xu, H., Qiu H., Zhu G., Zhan L., Zhang Z., Xu X., Chen Y., and Wang Y. 2019. Comparison of settlement behaviours of high-food-waste-content (HFWC) and low-food-waste-content (LFWC) MSWs and assessment of their prediction models. SCIENCE CHINA Technological Sciences 62(12), 2271-2292.

Xu, H., Wang J., Zhan L., Zhang Z., Xu X., Chen Y., and Yao K. 2020. Characterization of compression behaviours of high food waste content (HFWC) MSW and no food waste content (NFWC) MSW in China. Waste Management 103, 305-313.

Yamamoto, T. and Yasuhara, A. 1999. Quantities of Bisphenol A leached from plastic waste samples, Chemosphere, 38(11), 2569-2576.

Yeo, S. S., Shackelford, C. D., and Evans, J. C. 2005). Consolidation and hydraulic conductivity of nine model soil-bentonite backfills. Journal of Geotechnical and Geoenvironmental Engineering, ASCE, 131, No. 10, 1189-1198.

Yong, R.N., and Mulligan, C.N. 2019. Natural and Enhanced Attenuation of Contaminants in Soils. Second Edition. CRC Press, USA.

Yu, B., and El-Zein, A. 2019. Experimental investigation of the effect of airgaps in preventing desiccation of bentonite in geosynthetic clay liners exposed to high temperatures. Geotextiles and Geomembranes 47, 142-153.

Yu, B., El-Zein, A., and Rowe, R.K. 2020. Effect of added polymer on the desiccation and healing of a geosynthetic clay liner subject to thermal gradients. Geotextiles and Geomembranes 48(6), 928-939.

Yu, C., Liao, R., Cai, X., and Yu, X. 2019. Sodium polyacrylate modification method to improve the permeant performance of bentonite in chemical resistance. Journal of Cleaner Production 213, 242-250.

Zainab, B., and Tian, K. 2020. Hydraulic conductivity of bentonite-polymer geosynthetic clay liners to coal combustion product leachates. Geo-Congress 2020, GSP 316, ASCE, Reston, Virginia, USA.

Zhan, T., Xu, X., Chen, Y., Ma, X., and Lan, J. 2015. Dependence of gas collection efficiency on leachate level at wet municipal solid waste landfills and its improvement methods in China. Journal of Geotechnical and Geoenvironmental Engineering 141(4), 04015002.

Zhan, L., Qiu, Q., Xu, W., and Chen, Y. 2016. Field measurement of gas permeability of compacted loess used as an earthen final cover for a municipal solid waste

Zhan L., Xu, H., Chen Y., et al. 2017a. Biochemical, hydrological and mechanical behaviours of high food waste content MSW landfill: Preliminary findings from a large-scale experiment. Waste Management 63, 27-40.

Zhan L., Xu, H., Chen Y., et al. 2017b. Biochemical, hydrological and mechanical behaviours of high food waste content MSW landfill: Liquid-gas interactions observed from a large-scale experiment. Waste Management 68, 307-318.

Zhan, L., Xu, H., Jiang, X., Lan, J., Chen, Y., and Zhang, Z. 2019. Use of electrical resistivity tomography for detecting the distribution of leachate and gas in a large-scale MSW landfill cell. Environmental Science and Pollution Research 26(20), 20325-20343.

Zhan LT, You YQ, Zhao R Chen C and Chen YM. 2020. Retarding the lead(II) migration in soil-bentonite cut-off wall by loess amendment: centrifuge and numerical modeling. Submitted to International Journal of Physical Modeling in Geotechnics.

Zhang, W., and Sun, C. 2014. Parametric analyses of evapotranspiration landfill covers in humid regions. Journal of Rock Mechanics and Geotechnical Engineering 6(4), 356-365.

Zhang, W., Sun, C., and Qiu, Q. 2016. Characterizing of a capillary barrier evapotranspirative cover under high precipitation conditions. Environmental Earth Sciences 75(6), 513.

Zhan, L., Xu, X., Chen, Y., Ma, X., and Lan, J. 2015. Dependence of gas collection efficiency on leachate level at wet municipal solid waste landfills and its improvement methods in China. Journal of Geotechnical and Geoenvironmental Engineering 141(4), 04015002.

Zhan, L., Li, G., Jiao, W., Wu, T., Lan, J., and Chen, Y. 2017c. Field measurements of water storage capacity in a loess–gravel capillary barrier cover using rainfall simulation tests. Canadian Geotechnical Journal 54(11), pp.1523-153

Zhan, L., Wu, T., Feng, S., Li, G., He, H., Lan, J., and Chen, Y. 2020a. Full-scale experimental study of methane emission in a loess-gravel capillary barrier cover under different seasons. Waste Management 107, 54-65.

Zhan, L., Li, G., Jiao, W., Lan, J., Chen, Y., and Shi, W. 2020b. Performance of a compacted loess/gravel cover as a capillary barrier and landfill gas emissions controller in Northwest China. Science of The Total Environment 718, 137195.

Zheng, Q-T, Rowe, R.K. and Feng, S-J. 2018. Design of Vertical Landfill Gas Collection Wells Considering Non-homogeneity with depth. Waste Management, 82: 26-36. /doi.org/10.1016/j.wasman.2018.10.012

Zheng, Q-T, Rowe, R.K. and Feng, S-J. 2019a. Recovery Response of Vertical Gas Wells in Non-homogeneous Landfills. Waste Management, 83: 33-45. doi.org/10.1016/j.wasman.2018.10.043

Zheng, Q-T, Rowe, R.K. and Feng, S-J. 2019b. Design of Horizontal Landfill Gas Collection Wells in Non-homogeneous Landfills. Waste Management, 98: 102-112. https://doi.org/10.1016/j.wasman.2019.08.017

Zheng, Q-T, Rowe, R.K. and Feng, S-J. 2020. Control and Estimation of Maximum Gas Pressure below Landfill Cover with Horizontal Gas wells. Waste Management,114: 33–42, https://doi.org/10.1016/j.wasman.2020.06.033